

Characterization of the electron-accepting part of the  
organohalide respiration chain of *Dehalobacter* and  
*Desulfitobacterium*

Présentée le 17 juin 2022

Faculté de l'environnement naturel, architectural et construit  
Laboratoire de biotechnologie environnementale  
Programme doctoral en chimie et génie chimique

pour l'obtention du grade de Docteur ès Sciences

par

**Lorenzo CIMMINO**

Acceptée sur proposition du jury

Prof. C. Heinis, président du jury  
Prof. C. Holliger, Dr J. Maillard, directeurs de thèse  
Prof. J. Simon, rapporteur  
Prof. L. Adrian, rapporteur  
Dr M. Pavlou, rapporteuse



Chase your passion  
not your pension.  
— *Denis Waitley*

To my parents...

# Acknowledgements

*Ph.D is not a linear path and it is mainly blood, sweat and tears.* This is what most of my colleagues kept telling me during this journey and undoubtedly, after these four years, I can confirm it. Nevertheless, the accomplishment of the Ph.D. degree could not be possible without the support of my colleagues, friends and, most importantly, my family.

First, I would like to thank my thesis director, **Prof. Christof Holliger**, for accepting me in your laboratory in a very difficult moment of my professional career and for giving me the chance to prove my value in the research.

Furthermore, I would like to thank my thesis co-director, **Dr. Julien Maillard**, for being a comprehensive supervisor, collaborator and in some cases also a "psychologist". Our frank and sincere (sometimes too much) discussions and your precious advice are things that I will always remember and treasure for my future.

This four-years journey gifted me with one of the best professional (but also personal) experiences of my life. For this I would like to truly thank **Prof. Inês Cardoso Pereira** and the researchers working in the "Bacterial Energy Metabolism" Lab at Universidade Nova de Lisboa (ITQB) for welcoming me and for making me feel part of it from day one. However, this collaboration could not be so special (and successful) without the enormous support and great supervision of **Dr. Americo Duarte**. His incredible passion for the research together with his exceptional enthusiasm helped me to reach results that nobody could even imagine at the beginning of my Ph.D.

I would also like to take the opportunity to thank all the scientists who have composed the jury of this thesis: **Prof. Lorenz Adrian**, **Prof. Jörg Simon**, **Dr. Maria Pavlou**, and **Prof. Christian Heinis**, for reviewing the manuscript, providing me with helpful comments, and mostly, for fostering a very interesting scientific discussion during my Ph.D. defense.

This achievement would not have been possible without the constant help and support that I received from the amazing (present and former) members of the LBE family. First, I would like to thank the technical team, the "senior" technicians as well as the young apprentices, for constantly supporting my work during these years. Among them, a special thank goes to **Stéphane Marquis**, my "personal" french teacher and companion of great laughs, and to **Emmy Oppliger** who actively contributed to the success of this project working hard in



cultivating our tidious-to-grow bacteria. I would like to deeply thank **Filomena Jacquier**, "La mia seconda mamma svizzera", for comforting me in the difficult moments of my Ph.D. as well as for sincerely rejoicing in my personal and professional achievements. I always considered your office a little "italian enclave" where I could enter and chat with you about everything and without any filter. Last but not least, I also want to deeply thank the people who have shared my Ph.D. at 360°: audience of my loud and sometimes "theatrical" complaints, but also of my stupid (but I hope also funny) jokes. In particular, I would like to deeply thank the "old guard" of the second floor offices: **Dr. Aline Adler**, rigorous eater of mini panettone and great office mate for the the first half of my Ph.D.; **Dr. Mathilde Willemin** the extrovert "pink unicorn" of the office with whom I shared the pain of working with the anaerobic bacteria but also great laughs, beers and conferences (among all, the proteomic conference was undoubtedly the funniest one) and **Arnaud Gelb**, "the custodian of CH building" for his crazy working hours, always supportive and keen to help me in every single aspect of my life in Switzerland; you have been simply too nice to be real. Furthermore I would like to thank so much the researchers that lately joined our lab and brought the enthusiasm that, due to Covid, was quietened. In particular, I would like to thank **Dr. Laetitia Cardona**, for showing me pure friendship and sincere support in this last and particularly stressful period; **Natalia Rodilla Ramirez**, la "chica latina" that was missing in our lab and has finally arrived, with her enthusiasm and very particular sense of humour, made my last two years very lively.

A special thank goes to my friends who I had the luck to meet in Lausanne: the colleagues from our neighbour labs (EML and Ludwig group): **Tobias Borgmeyer**, **Simiao Wang**, **Dr. Margaux Molinas**, **Dr. Eduard Vico Oton** and **Colin Volet** with whom I shared pressure-releasing and funny coffee-breaks and apero; **François Tilmant**, my kind-hearted giant friend; **Diego Francescangeli**, loyal friend and best companion of "misadventures" since the first day I arrived in Lausanne; **Veronica Leccese**, my "Happiness" during the last year of my Ph.D. and an incredible "IT master and commander"; **Kevin Kaser** and **Rana Hosseini** adorable friends who helped me to make feel integrated in the Swiss society; **Julia** and **Agustin**, thanks to the shared passion for watches and classic music we found quickly a great synchronicity; and **Laure**, with whom I shared great weekends and memorable music and sport events.

Furthermore, I would like to deeply thank the "Belgian family" I had the luck to meet in Gent and with whom I have fantastic memories: **Chiara**, **Racha**, **Nayaret**, **Mohammad**, **Federico** and **Viviana**. Despite the distance and the pandemic you have always supported me and showed me true love and friendship. I will be forever grateful to you for this.

I would like to acknowledge the "Italian fan club" that always stands with me as a unique giant family. A first special thank goes to **Lorenzo**, he embodies the "faithful friend", from kindergarten until now he has been always close to me in the highlights of my life. In addition, I would like to thank **Ilaria** and **Daniele**, probably the owners of the card n.1 of this crazy fan club, first ones to drink to my achievements as well as to encourage me in the difficult moments of this journey; **Stefano**, my rowing-partner with whom I shared many boat capsized in the Tevere river but also countless laughs and great time together; **Beatrice**, my "female

## Acknowledgements

---

alter ego", great and loyal friend with whom I share the "radical chic" attitude; **Tiago**, my Portuguese brother, and **Henrique**, with whom it was like "love at first sight" in Trondheim and since then we are connected by a great friendship; **Maurizio**, **Enrico**, **Federico**, **Fabio** and **Erica** for being supportive in numerous situations and for taking care of me when I was in Rome helping me to relax and to have pure good time.

A special thank goes to **Annalucia**, my "*deus ex machina*", my muse, my best partner in jokes, arguments, crying and in all the other aspects of my life. I won't be able to thank you enough for what you did for me in these years, you have been simply essential for the success of this incredible journey. I also would like to truly thank your family, which become my Abruzzo family: **Francesca**, **Levino**, **Marcello**, **Angela**, and the baby boss **Christopher**, who welcomed me long time ago making me feel part of it and (apparently) they are not fed up with me yet.

Lastly, I would like to thank my family because without them I could never reach all of this. In particular, I would like to thank: **Cristina**, my beloved aunt, the strongest and most resolute person that I have ever met in my life, from whom I learned the importance of commitment and professionalism to be successful in life; **Carlo**, the "thinker" of the family, the embodiment of pure love, who taught me the respect and the acceptance of the others and for "the different"; **Guido**, my cousin, "the brother I never had", with whom I shared every joys and sorrows of our family; **Filippo**, the artist of our family from whom I learned the importance to have dreams in life and pursue them despite the adversities; **Assunta** and **Annita**, the pillars of my family, my old "grandmothers-sisters" who have been accompanying me for my entire life, being always my best allies.

Talking of family, I would like to acknowledge and give the warmest thanks to my beloved parents, Mamma **Zina** and Papà **Maurizio**, for teaching me how to live in this World, showing me always the right things to do without ever failing in the principles of fairness and loyalty. Papà **Maurizio**, you have been and always will be my superhero, the man I hope to become one day and also look forward to meeting again. Mamma **Zina**, my mother but also my best friend who represents the best mix of strength, love and kindness (together with other thousands more qualities). Your enthusiasm and optimism always give me the energy to welcome and face everything occurs in my life. Achieved this, it is time now to welcome the next challenge..but always together!

*Lausanne, 17<sup>th</sup> June 2022*

Lorenzo Cimmino



# Abstract

Halogenated organic compounds (so-called organohalides) represent one of the major class of groundwater pollutants. The exploration of how organohalides are used as energy source is important in terms of ecosystem remediation but is also essential for the complete understanding of microbial metabolic interactions in the environment. Organohalide respiration (OHR) is a bacterial anaerobic process that use halogenated compounds, e.g. tetrachloroethene (PCE), as terminal electron acceptors. Our model organisms, *Dehalobacter restrictus* strain PER-K23, an obligate OHR bacterium (OHRB), and *Desulfitobacterium hafniense* strain TCE1, a bacterium with a versatile metabolism, harbour the *pceABCT* gene cluster, which represents one model system for the study of PCE respiration. To date, the function of PceA, the key enzyme in the process, and PceT, the dedicated molecular chaperone for PceA maturation, are well defined. However, the role of PceB and PceC are still not elucidated and the biochemistry of OHR electron transfer is still relatively elusive. Based on the genetic composition of the *pce* gene cluster, the hypothesis that PceB and PceC may play a role in electron transfer in the metabolism of organohalide respiration is tempting but the question remains largely unanswered. In the present Ph.D. thesis, a multilevel study aiming at characterizing the electron-accepting part of the respiratory chain of OHRB will be presented. The investigation was assessed at molecular level by the deciphering of the stoichiometry of *pceABCT* individual gene products, and at physiological and biochemical levels, where the characterization of the membrane PceA-containing protein complex of both obligate and facultative OHRB was the main focus. The stoichiometry analysis at RNA level revealed that the *pce* gene cluster is an operon with, however, a level of transcription that differs for individual genes, an observation that could be explained by post-transcriptional events. At proteomic level, an apparent 2:1 stoichiometry of PceA and PceB was obtained in the membrane fraction, while a low abundance of PceC in comparison to the other two proteins was observed. In the soluble fraction, a 1:1 stoichiometry of PceA and PceT was identified. Furthermore, a combination of Clear-Native (CN)PAGE gel and a herein developed in-gel PceA enzymatic activity assay were applied to identify the RDH complex from the membrane of *D. restrictus* and *D. hafniense* strain TCE1. The results revealed an active RDH complex in the membrane extract of both organisms with an estimated molecular mass of 180 kDa, while no RDH activity could be detected in the soluble fraction. Furthermore, Western blot analysis for PceA on CN-PAGE gel revealed the presence of a sec-

ond, however inactive, PceA-containing complex with a molecular mass of 670 kDa, which was confirmed by MS analysis to be largely dominated by the molecular chaperone GroEL alongside with PceA and likely representing the tetradecameric GroEL maturation complex. The RDH complex was tentatively purified from the membrane extract by chromatography. The obtained fractions were analysed by LC-MS/MS showing unambiguously the presence of PceA and PceB. Furthermore, preliminary cryogenic electron microscopy (cryo-EM) analysis led to propose a 3D reconstruction of the RDH complex, revealing the likely presence of a Pce(AB)<sub>2</sub> complex. In summary, this study represents a road-map for the identification of RDH complexes from OHRB. The identification of PceA associated with the GroEL maturation complex raised new questions about the biosynthetic pathway of PceA and invites to consider the involvement of GroEL, but also PceT and other possible molecular chaperones into the maturation of the key enzyme in organohalide respiration. Finally the preliminary results obtained via cryo-EM analysis set the basis for further investigation on the structure of the RDH complex and open new horizons towards the elucidation of the electron transfer chain involved in the reduction of PCE.

Key words: Organohalogenes, anaerobic respiration, Firmicutes (Bacillota), gene product stoichiometry, *rdh* gene clusters, parallel reaction monitoring quantitative proteomics, reductive dehalogenase (RDH) complex, in-gel PceA enzymatic activity assay, cryo-EM analysis.

## Sommario

I composti organici alogenati, detti anche organo-alogenati, rappresentano una delle principali classi di inquinanti delle falde acquifere. Lo studio sulla modalità con cui i batteri utilizzano i composti alogenati come fonte di energia è importante ai fini del risanamento ambientale, ma è anche essenziale per la completa comprensione del metabolismo microbico. La respirazione dei composti alogenati (OHR) è un processo batterico anaerobico che utilizza i composti alogenati, ad esempio il tetracloroetilene (PCE), come accettori terminali di elettroni. I batteri di riferimento per questo studio sono *Dehalobacter restrictus* ceppo PER-K23, che cresce solo in presenza di PCE, e *Desulfitobacterium hafniense* ceppo TCE1, caratterizzato invece da un metabolismo più versatile. Entrambi ospitano nel loro genoma il cluster genico *pceABCT*, che consente loro di "respirare" PCE. Ad oggi, la funzione di PceA, l'enzima chiave del processo, e di PceT, il chaperone molecolare dedicato alla maturazione di PceA, sono ben definite. Tuttavia, il ruolo di PceB e PceC non è ancora stato chiarito e la biochimica della catena di trasporto degli elettroni che avviene durante il processo di respirazione dei composti organo-alogenati rimane ancora relativamente elusiva. Sulla base della composizione genetica del cluster genico *pce*, l'ipotesi che PceB e PceC possano avere un ruolo nel trasferimento di elettroni è suggestiva, ma tuttavia ad oggi priva di risposta. Lo studio qui di seguito presentato ha come obiettivo la caratterizzazione della porzione terminale della catena di trasporto che culmina con la dealogenazione riduttiva del composto PCE. Tale ricerca è stata eseguita a livello molecolare, con la definizione della stechiometria dei prodotti genici di *pceABCT*, e a livello fisiologico e biochimico, con la caratterizzazione del complesso proteico di membrana contenente PceA (detto anche complesso dealogenasi riduttiva, o complesso RDH) in *Dehalobacter restrictus* e *Desulfitobacterium hafniense* ceppo TCE1. L'analisi stechiometrica a livello trascrizionale ha dimostrato che il cluster genico *pce* viene trascritto come singolo RNA messaggero policistronico con, tuttavia, livelli di trascrizione diversi per i singoli geni, fenomeno che potrebbe essere dovuto a eventi post-trascrizionali. Inoltre, è stato osservato un rapporto stechiometrico di 2:1 tra le proteine PceA e PceB a livello della membrana citoplasmatica, mentre è stata riscontrata una quantità notevolmente più bassa di PceC. Nel citoplasma, è stato osservato un rapporto stechiometrico di 1:1 tra PceA e PceT. D'altro canto, l'identificazione del complesso di membrana dealogenasi riduttiva è stata ottenuta mediante una combinazione di tecniche come l'elettroforesi su gel di poliacrilammide in condizioni native (Clear-Native PAGE) e un innovativo saggio enzimatico per l'attività di PceA applicato

direttamente su gel elettroforetico, ideato e ottimizzato nei nostri laboratori. I risultati hanno permesso l'identificazione del complesso RDH attivo nell'estratto di membrana di entrambi gli organismi con una massa molecolare stimata di 180 kDa, mentre nessuna attività enzimatica è stata rilevata nella frazione solubile. Inoltre, l'applicazione della tecnica Western blot su gel nativo ha rivelato la presenza di un secondo complesso contenente PceA, tuttavia inattivo, con una massa molecolare di 670 kDa. L'analisi mediante spettrometria di massa (LC-MS/MS) di tale complesso ha confermato la presenza del chaperone molecolare GroEL e di PceA, lasciando intendere che si tratti del complesso di maturazione tetradecamerico di GroEL. Successivamente, il complesso RDH è stato purificato mediante cromatografia. Le frazioni ottenute sono state analizzate mediante LC-MS/MS mostrando inequivocabilmente la presenza di PceA e PceB. La successiva analisi mediante microscopia crioelettronica (cryo-EM) ha permesso di ottenere una ricostruzione 3D del complesso RDH, caratterizzato dalla presenza di un complesso Pce(AB)<sub>2</sub>. In conclusione, questo studio rappresenta una road map per l'identificazione dei complessi dealogenasi riduttiva nei batteri in grado di respirare composti organo-alogenati. In aggiunta, l'identificazione di PceA associato al complesso di maturazione GroEL ha sollevato nuovi interrogativi sulla via biosintetica di PceA e invita a considerare il coinvolgimento di GroEL, ma anche di PceT e di altri possibili chaperoni molecolari nella maturazione dell'enzima chiave nella respirazione dei composti organoalogenati. Infine, i risultati preliminari ottenuti mediante microscopia crioelettronica pongono le basi per ulteriori indagini sulla struttura del complesso RDH e aprono nuovi orizzonti verso la delucidazione della catena di trasferimento degli elettroni coinvolta nella respirazione del composto organo-alogenato PCE.

**Parole chiave:** Organo-alogenati, respirazione anaerobica, Firmicutes (Bacillota), stechiometria dei prodotti genici, cluster di geni *rdh*, proteomica quantitativa, dealogenasi riduttiva (RDH), saggio di attività enzimatica per dealogenasi riduttiva su gel elettroforetico, analisi di microscopia crioelettronica.

## Résumé

Les composés organiques halogénés, également appelés organohalogénés, constituent l'une des principales classes de polluants des eaux souterraines. L'étude de la manière dont les bactéries utilisent les composés halogénés comme source d'énergie est importante pour l'assainissement de l'environnement, mais elle est également essentielle pour la compréhension complète de ce métabolisme microbien en particulier. La respiration des composés organohalogénés (abrégée en anglais OHR) est un processus bactérien anaérobie qui utilise des composés halogénés, par exemple le tétrachloroéthylène (PCE), comme accepteurs d'électrons terminaux. Les bactéries modèles utilisées pour cette étude sont *Dehalobacter restrictus* PER-K23, qui se développe uniquement en présence de PCE, et *Desulfitobacterium hafniense* TCE1, qui se caractérise par un métabolisme énergétique plus polyvalent. Ces deux bactéries hébergent dans leur génome le groupe de gènes *pceABCT*, qui représente un système modèle pour l'étude de la respiration du PCE. A ce jour, les fonctions de PceA, l'enzyme-clé du processus OHR, et de PceT, le chaperon moléculaire dédié à la maturation de PceA, sont bien définies. Cependant, le rôle de PceB et PceC n'a pas encore été clarifié, et la biochimie de la chaîne de transport d'électrons qui se produit au cours du processus de respiration reste encore relativement peu élucidée. Sur la base de la composition génétique du groupe de gènes *pce*, l'hypothèse selon laquelle PceB et PceC pourraient jouer un rôle dans le transfert d'électrons a été proposée, mais reste néanmoins sans réponse à ce jour. L'étude présentée ici vise à caractériser la partie terminale de la chaîne de transport des électrons qui aboutit à la déshalogénation du PCE. Ces recherches ont été menées au niveau moléculaire, avec la définition de la stoechiométrie des produits géniques de *pceABCT*, et au niveaux physiologique et biochimique, avec la caractérisation du complexe de protéines membranaires contenant PceA (également connu sous le nom de complexe de déshalogénase réductive, abrégé en anglais RDH complex pour 'reductive dehalogenase'). Ce travail a été effectué pour les deux bactéries modèles. L'analyse stoechiométrique au niveau transcriptionnel a montré que le groupe de gènes *pce* est transcrit comme sous la forme d'un seul ARN messager polycistronique avec, cependant, des niveaux différents de transcription pour les gènes individuels, un phénomène qui pourrait être dû à des événements post-transcriptionnels. De plus, un rapport stoechiométrique de 2 :1 a été mesuré entre les protéines PceA et PceB au niveau de la membrane cytoplasmique, alors qu'une quantité significativement plus faible de PceC



a été détectée. Dans le cytoplasme, un rapport stœchiométrique de 1 :1 entre PceA et PceT a été observé. D'autre part, l'identification du complexe membranaire de la déshalogénase réductrice a été réalisée par une combinaison de techniques telles que l'électrophorèse sur gel de polyacrylamide en conditions natives (Clear-Native PAGE) et par le développement d'un test enzymatique innovant pour mesurer l'activité de l'enzyme PceA directement dans les gels natifs. Les résultats ont permis d'identifier le complexe RDH sous sa forme active dans l'extrait membranaire des deux bactéries avec une masse moléculaire estimée à 180 kDa, alors qu'aucune activité enzymatique n'a été détectée dans la fraction soluble. En outre, l'application de la technique du Western blot sur des gels natifs a révélé la présence d'un second complexe contenant l'enzyme PceA, mais inactif celui-là, dont la masse moléculaire est d'environ 670 kDa. L'analyse par spectrométrie de masse (LC-MS/MS) de ce complexe a confirmé la présence du chaperon moléculaire GroEL et de PceA, suggérant qu'il s'agit du complexe tétradécamérique de maturation GroEL. Par la suite, le complexe RDH de 180 kDa a été purifié par chromatographie. Les fractions obtenues ont été analysées par LC-MS/MS montrant sans équivoque la présence de PceA et PceB. Une analyse ultérieure par cryo-microscopie électronique (cryo-EM) a permis de reconstruire en 3D le complexe RDH sous la forme d'un complexe Pce(AB)<sub>2</sub>. En conclusion, cette étude présente une feuille de route pour l'identification des complexes de déshalogénases réductrices chez les bactéries capables de respirer les composés organohalogénés. De plus, l'identification de PceA associée au complexe de maturation GroEL a soulevé de nouvelles questions sur la voie de biosynthèse de PceA et invite à considérer l'implication de GroEL, mais aussi de PceT et d'autres chaperons moléculaires possibles dans la maturation de l'enzyme-clé de la respiration des organohalogénés. Enfin, les résultats préliminaires obtenus par cryo-microscopie électronique jettent les bases d'une investigation plus avancée de la structure du complexe RDH et ouvrent de nouveaux horizons vers l'élucidation de la chaîne de transfert d'électrons impliquée dans la respiration du PCE.

Mots clefs : Composés organohalogénés, respiration anaérobie, Firmicutes (Bacillota), stœchiométrie des produits géniques, groupes de gènes *pce*, protéomique quantitative, complexe de déshalogénase réductrice (RDH), test d'activité enzymatique de PceA en gel, analyse cryo-EM.

# Contents

<b>Acknowledgements</b>	<b>i</b>
<b>Abstract (English/Italiano/Français)</b>	<b>v</b>
<b>List of figures</b>	<b>xv</b>
<b>List of tables</b>	<b>xix</b>
<b>1 Introduction</b>	<b>1</b>
1.1 Environmental issues regarding chloroethene . . . . .	1
1.2 Organohalide respiration (OHR) . . . . .	3
1.2.1 Organohalide-respiring bacteria (OHRB) . . . . .	3
1.2.2 OHRB Firmicutes . . . . .	5
1.3 Electron transport chain in OHR . . . . .	7
1.3.1 Quinones in OHR . . . . .	7
1.4 Reductive dehalogenase and accessory genes . . . . .	10
1.4.1 RdhB, a membrane anchor for RdhA? . . . . .	10
1.4.2 Diversity of <i>rdh</i> gene clusters in OHRB . . . . .	11
1.4.3 The conserved <i>pceABCT</i> gene cluster . . . . .	12
1.5 Thesis objectives . . . . .	13
1.5.1 Outline of the thesis . . . . .	14
<b>2 Quantitative proteomics approach</b>	<b>17</b>
2.1 Introduction . . . . .	17
2.1.1 Earlier findings . . . . .	17
2.1.2 Rationale behind the development of a quantitative proteomics approach	19
2.2 Materials and methods . . . . .	20
2.2.1 Bacterial strains and growth conditions . . . . .	20
2.2.2 Cell harvest, fractionation and protein extraction . . . . .	20
2.2.3 Protein quantification . . . . .	21
2.2.4 SDS-PAGE . . . . .	21
2.2.5 Coomassie gel staining . . . . .	21
2.2.6 In-gel sample digestion . . . . .	21
2.2.7 Shotgun LC-MS/MS analysis . . . . .	22

2.2.8	Data processing and database searches . . . . .	22
2.3	Results and discussion . . . . .	23
2.3.1	Preliminary in-gel shotgun LC-MS/MS analysis . . . . .	23
2.3.2	Effect of detergent on protease activities and optimization of digestion conditions . . . . .	25
2.3.3	Validation of proteotypic peptides via SRM . . . . .	28
2.3.4	Definition of the peptide signatures for Pce proteins . . . . .	30
2.3.5	Qualitative and quantitative validation of heavy-labelled peptides . . . . .	31
2.3.6	Validation of the unique PceB reference peptide . . . . .	34
2.3.7	Definition of limit of detection (LoD) and limit of quantification (LoQ) of heavy and light peptides . . . . .	36
2.3.8	Optimized sample preparation protocol . . . . .	37
2.3.9	Application of the optimized protocol to <i>D. hafniense</i> strain TCE1 . . . . .	38
2.4	Conclusions . . . . .	39
<b>3</b>	<b>Stoichiometry of <i>pce</i> gene products</b>	<b>41</b>
3.1	Introduction . . . . .	41
3.2	Materials and methods . . . . .	42
3.2.1	Spike experiment . . . . .	42
3.2.2	RNA extraction . . . . .	43
3.2.3	Reverse transcription, PCR and quantitative PCR . . . . .	43
3.2.4	In-solution sample digestion . . . . .	44
3.2.5	Shotgun LC-MS/MS analysis . . . . .	44
3.2.6	Selection of signature peptides for parallel reaction monitoring proteomics . . . . .	44
3.2.7	PRM-based quantitative proteomics . . . . .	45
3.2.8	Data processing and database searches . . . . .	45
3.3	Results and Discussion . . . . .	46
3.3.1	The <i>pceABCT</i> genes form an operon . . . . .	46
3.3.2	Stoichiometric relationships of <i>pceABCT</i> gene products at RNA level . . . . .	47
3.3.3	Stoichiometry of Pce proteins by quantitative proteomics . . . . .	48
3.4	Discussion . . . . .	55
3.4.1	Transcription pattern heterogeneity and stoichiometry of gene transcripts associated with <i>rdh</i> clusters in the Firmicutes . . . . .	55
3.4.2	Challenges in the detection of Rdh proteins from Firmicutes . . . . .	56
3.4.3	PceA and PceB - but not PceC - appear with a similar concentration in the membrane fraction . . . . .	56
3.5	Conclusions . . . . .	57
<b>4</b>	<b>Extraction and identification of the RDH complex</b>	<b>59</b>
4.1	Introduction . . . . .	59
4.2	Materials and Methods . . . . .	60
4.2.1	Bacterial strains and cultivation . . . . .	60
4.2.2	Cell harvest and fractionation . . . . .	60

## CONTENTS

---

4.2.3	Protein quantification . . . . .	61
4.2.4	Blue Native and Clear Native -PAGE . . . . .	61
4.2.5	SDS-PAGE and two dimensional (2D) Native/SDS-PAGE gels . . . . .	62
4.2.6	Silver staining of gels . . . . .	62
4.2.7	Western blot analysis . . . . .	62
4.2.8	In-gel PCE reductive dehalogenase enzymatic assay . . . . .	63
4.2.9	LC-MS/MS analysis . . . . .	63
4.3	Results and discussion . . . . .	63
4.3.1	Optimization of the membrane extraction and protein identification for the RDH complex . . . . .	64
4.3.2	Identification of the RDH complex from <i>D. restrictus</i> and <i>D. hafniense</i> strain TCE1 . . . . .	75
4.3.3	Conclusions . . . . .	78
<b>5</b>	<b>Characterization of the RDH complex</b>	<b>79</b>
5.1	Introduction . . . . .	79
5.2	Materials and methods . . . . .	80
5.2.1	Protein purification . . . . .	80
5.2.2	Quinol-based PceA enzymatic assay . . . . .	81
5.2.3	Cryogenic electron microscopy analysis . . . . .	81
5.3	Results and discussion . . . . .	82
5.3.1	Purification attempts of the RDH complex . . . . .	83
5.3.2	Quinol-based PceA enzymatic assay . . . . .	90
5.3.3	Cryogenic electron microscopy of the RDH complex . . . . .	91
5.4	Conclusions . . . . .	95
<b>6</b>	<b>Concluding remarks and perspectives</b>	<b>97</b>
<b>A</b>	<b>Supplementary material Chapter 3</b>	<b>101</b>
A.1	quantitative PCR analysis . . . . .	101
A.2	PRM-based quantitative proteomics . . . . .	104
<b>B</b>	<b>Supplementary material Chapter 4</b>	<b>109</b>
	<b>Bibliography</b>	<b>120</b>
	<b>Curriculum Vitae</b>	



# List of Figures

1.1	Model of chloroethene-contaminated aquifer . . . . .	2
1.2	Phylogenetic tree of OHRB based on bacterial 16S rRNA sequences . . . . .	4
1.3	Reductive dechlorination pathways for chloroethenes by OHRB . . . . .	5
1.4	Tentative model of the respiration chain of <i>Dehalobacter restrictus</i> . . . . .	8
1.5	Hypothetical model of the organohalide complex in <i>Dehalococcoides mccartyi</i> strain CBDB1 . . . . .	9
1.6	Genetic map of Tn-Dha1 and <i>pceABCT</i> gene cluster from <i>D. hafniense</i> strain TCE1	11
1.7	Ph.D. thesis workflow . . . . .	13
2.1	PceC prediction in <i>D. hafniense</i> strain TCE1 . . . . .	18
2.2	Pce proteins sequence coverage in <i>D. restrictus</i> strain PER-K23 . . . . .	18
2.3	SDS-PAGE gel of subcellular fractions of <i>D. restrictus</i> . . . . .	23
2.4	Examples of MS/MS spectra of PceA and PceC peptides with SRM method . . .	25
2.5	SDS-PAGE gel for PceB in-gel MS analysis . . . . .	26
2.6	Validation of PceB peptide via SRM method . . . . .	27
2.7	Validation of proteotypic peptides via SRM . . . . .	28
2.8	Validation of heavy-labelled peptides . . . . .	31
2.9	Fine-tuning ratio between endogenous and heavy-labelled peptides signal . . .	32
2.10	SRM analysis of logarithmic vs stationary cell-free extract of <i>D. restrictus</i> . . . .	33
2.11	Quantification of two peptides of PceA belonging to logarithmic cell-free extract of <i>D. restrictus</i> . . . . .	34
2.12	Validation of the unique PceB heavy-labelled peptide via PRM method . . . . .	35
2.13	Detection of heavy-labelled peptides against identical amounts of the endogenous sample . . . . .	36
2.14	Quantification of Pce proteins in <i>D. hafniense</i> strain TCE1 via PRM method . .	38
2.15	Quantification of Pce proteins of cell-free extract of <i>D. hafniense</i> strain TCE1 at logarithmic vs stationary growth phases . . . . .	39
3.1	Co-transcription of <i>pce</i> genes in <i>D. restrictus</i> and <i>D. hafniense</i> strain TCE1 . . .	46
3.2	Quantitative analysis of the individual <i>pce</i> transcripts in <i>D. restrictus</i> and <i>D. hafniense</i> strain TCE1 . . . . .	47
3.3	Graphical representation of sequence coverage of Pce proteins and F1 $\alpha$ -subunit of ATP synthase by shotgun MS analysis . . . . .	50

3.4	PRM chromatograms and transitions of selected heavy-labelled peptides . . . . .	51
3.5	LC-MS/MS analysis of the PceB synthetic fragment . . . . .	52
3.6	Quantitative proteomics analysis of Pce proteins in cell-free extracts . . . . .	53
3.7	Quantitative proteomics analysis of Pce proteins in in sub-cellular compartments	54
4.1	BN-PAGE analysis of protein fractions from <i>D. restrictus</i> - effects of different detergents used for membrane extraction . . . . .	64
4.2	BN-PAGE and SDS-PAGE gel testing different detergents and amounts of membrane extracts . . . . .	65
4.3	CN-PAGE gel and PCE in-gel assay in <i>D. restrictus</i> . . . . .	66
4.4	Evaluation of different cell lysis techniques applied on <i>D. restrictus</i> on CN-PAGE gel . . . . .	67
4.5	CN-PAGE gel and Western blot of <i>D. restrictus</i> sub-cellular fractions . . . . .	68
4.6	SDS-PAGE gel and Western blot of <i>D. restrictus</i> sub-cellular fractions . . . . .	69
4.7	Effect of membrane extract concentration in CN-PAGE migration pattern and resulting 2D-Native/SDS-PAGE gel . . . . .	70
4.8	CN-PAGE of <i>D. restrictus</i> and respective western blot for PceA . . . . .	71
4.9	2D-Native/SDS-PAGE gel of <i>D. restrictus</i> and respective western blot for PceA .	72
4.10	SDS-PAGE gel of <i>D. restrictus</i> fractions and respective western blot for PceA and PceC . . . . .	72
4.11	In-gel PCE enzymatic assay on cell-free extract of <i>D. restrictus</i> . . . . .	73
4.12	CN-PAGE stained with Coomassie staining and PCE in-gel assay . . . . .	74
4.13	CN-PAGE gel, in-gel PCE assay and 2D-SDS/CN-PAGE gel of membrane extract gel lane . . . . .	75
4.14	List of proteins detected by LC-MS/MS analysis of the 140 and 180 kDa gel bands	76
4.15	In-gel PCE assay applied to <i>D. restrictus</i> and <i>D. hafniense</i> strain TCE1 . . . . .	76
4.16	2D-Native/SDS-PAGE gel of CN-PAGE 180 kDa gel band of <i>D. restrictus</i> . . . . .	77
4.17	2D-Native/SDS-PAGE gel of CN-PAGE 180 kDa gel band of <i>D. hafniense</i> strain TCE1 . . . . .	77
5.1	Anion-Exchange Chromatography on membrane extract of <i>D. restrictus</i> . . . . .	83
5.2	CN-PAGE and SDS-PAGE gels resulting from the anions-exchange chromatography of ME of <i>D. restrictus</i> . . . . .	84
5.3	SDS-PAGE gel and Western blot for PceA and PceC of the fractions obtained from anions-exchange chromatography . . . . .	85
5.4	Anion-exchange chromatogram of the membrane extract of <i>D. restrictus</i> . . . . .	86
5.5	Western blot analysis of selected purification fractions using anti-PceA antibodies.	86
5.6	MS analysis of AEC fractions loaded on CN-PAGE gel . . . . .	87
5.7	Chromatogram of the cation exchange chromatography of the membrane extract from <i>D. restrictus</i> . . . . .	88
5.8	CN-PAGE gel of fractions obtained from cations-exchange chromatography . .	89
5.9	SDS-PAGE analysis of the fractions obtained from cations-exchange chromatography . . . . .	89

## LIST OF FIGURES

---

5.10 Sample preparation and cryo-EM imaging of the RDH complex . . . . .	92
5.11 3D Density map reconstruction of the RDH complex using cryo-EM . . . . .	93
5.12 3D reconstruction of the RDH complex using cryo-EM . . . . .	94
A.1 qPCR reaction melting curves . . . . .	102
A.2 Prediction of a putative hairpin loop structure in the <i>pceBC</i> intergenic region .	107
B.1 LC-MS/MS analysis of 670 kDa native gel piece . . . . .	110
B.2 2D-Native/SDS-PAGE gel and LC-MS/MS analysis of the gel spots . . . . .	111





## List of Tables

2.1	List of detected peptides of Pce proteins after in-gel LC-MS/MS analysis. . . . .	24
2.2	MS sequence coverage of PceB under different experimental conditions. . . . .	27
2.3	Effect of protease inhibitor on sequence coverage of Pce proteins in CFE and MF samples . . . . .	29
2.4	List of heavy-labelled peptides. . . . .	30
3.1	Discovery MS analysis on cell-free extracts, soluble and membrane fractions of <i>D. restrictus</i> and of <i>D. hafniense</i> strain TCE1 . . . . .	49
5.1	In-solution quinol-based PceA activity assay . . . . .	91
A.1	Primers used in the quantitative PCR analysis . . . . .	101
A.2	Quantitative PCR raw data . . . . .	103
A.3	Statistical analysis output of qPCR analysis . . . . .	103
A.4	Sample list for PRM proteomic analysis . . . . .	104
A.5	Raw data of PRM proteomics analysis. . . . .	105
A.6	Data analysis of PRM quantitative proteomics analysis . . . . .	105
A.7	Calculated stoichiometric relationships obtained via PRM quantitative proteomics analysis . . . . .	106
A.8	Identification of RdhA, B, C and T proteins from Firmicutes OHRB by proteomic analyses . . . . .	106
B.1	CN-PAGE gel preparation . . . . .	109



# 1 Introduction

## 1.1 Environmental issues regarding chloroethene

Halogenated compounds, so called organohalogens or organohalides, are a class of organic molecules that contain one or more covalently bound halogen atoms. To date, over five thousands natural halogenated compounds have been identified on Earth and the majority of them are naturally produced by a plethora of biotic and abiotic processes [1]. Diverse natural enzymatic and abiotic reactions account for the halogenation and dehalogenation of natural organohalogen metabolites [2]. For example, PCE and TCE are known to be naturally present in the environment as a result of abiotic reactions like volcanic activities or from biological production by marine algae [3, 4]. Within this class of compounds, chlorinated and brominated compounds represent the most abundant ones that are naturally produced [5]. Chlorinated compounds are known to be produced by higher plants, algae, fungi and bacteria and their concentration in pristine soil ranges from 0.01 to 0.1 mg chlorine equivalent per g of soil (dry weight) [6]. However, over the last 80 years, the natural cycle of chlorine was disrupted by an extensive anthropogenic production of chlorinated compounds. One important group are the chlorinated ethenes (or chloroethenes, CEs), the halogenated compounds of interest in this Ph.D. thesis. They are characterized by a carbon-carbon double bond linked to one or more chlorine atoms. Based on the number of chlorines present, the compounds are named tetrachloroethene or perchloroethene (PCE,  $C_2Cl_4$ ), trichloroethene (TCE,  $C_2HCl_3$ ), dichloroethene (DCE,  $C_2H_2Cl_2$ ) and vinyl chloride (VC,  $C_2H_3Cl$ ) [7]. PCE was first synthesized in 1821 by Michael Faraday, however, the commercial use in Europe started in the 1920's. Since then, the production of organohalides has dramatically increased [8]. PCE and TCE have been extensively used as industrial solvents and cleaning agents in a wide range of fields, with industrial, agricultural and military applications. The mismanagement of the compounds along with careless storage represent the direct cause of their spreading in and contamination of the environment [9]. Due to their toxic properties and persistence in the environment, CEs belong to the most frequently found organic contaminants posing serious environmental concerns. PCE and TCE are hydrophobic and have relatively low solubility; moreover, because of their higher density and viscosity than that of water, they form dense non-aqueous phase

liquids (DNAPLs) that do not mix easily with water [10] (**Figure 1.1**). In the last decades, this has prompted intensive remediation activity along with research on natural microbial communities able to degrade chloroethenes into less harmful compounds. While PCE and TCE in contaminated aquifers originate from human activities, *cis*-1,2-DCE (cDCE) and VC have been identified as degradation products deriving from microbial activity [11, 12]. Both cDCE and VC are more toxic than the parental compounds and tend to accumulate in the aquifers [6]. This is of particular concern, as VC is the most carcinogenic of the chloroethenes and thus, has the lowest regulatory limit in drinking water, i.e. 2 ppb in the United States compared with 5 ppb for PCE and TCE [6]. The transformation of PCE and TCE into cDCE and VC is due to microbial reductive dechlorination reactions [13, 14]. The anaerobic reduction of both PCE and TCE by microorganisms takes place through a series of steps, each consisting of progressively removing one chlorine and replacing it by a hydrogen thus producing less chlorinated ethenes. The end product of the stepwise reductive dechlorination is ethene, a harmless compound. Other microbial pathways have been shown as possible alternatives for the transformation of chloroethenes (**Figure 1.1**). Microbial anaerobic oxidation of cDCE and VC have been observed in environmental samples in the presence of strong oxidizers, such as Fe(III)- or Mn(IV)-reducing conditions [14–16]. Chloroethenes are also known to be dechlorinated by methanogens and homoacetogens via co-metabolic activities, however the majority of the reductive dechlorination is likely to be catalysed by bacteria that utilize chloroethenes as a terminal electron acceptors in a process called organohalide respiration (OHR) [17].

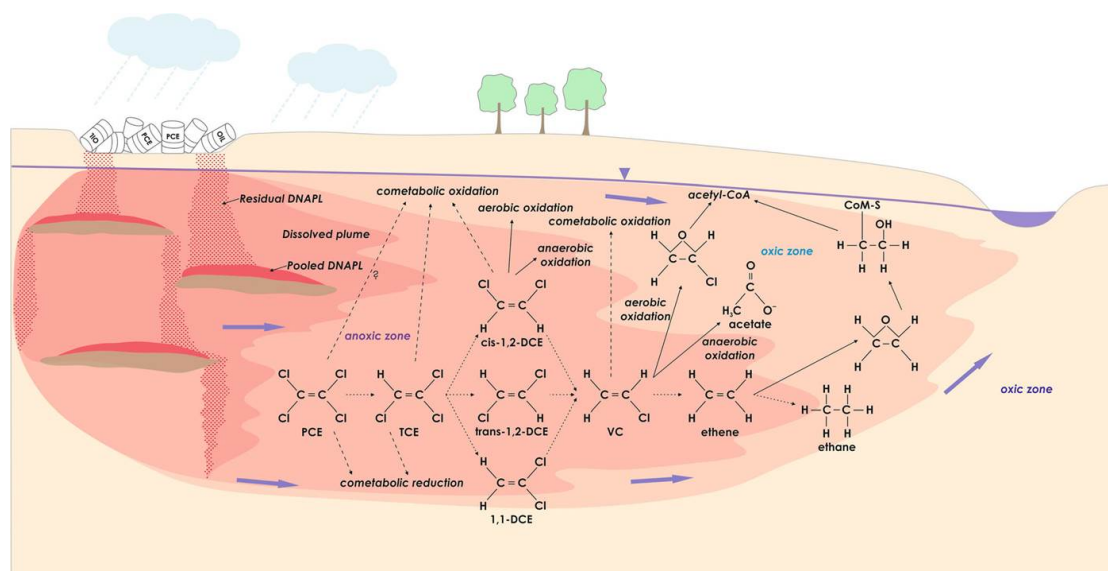


Figure 1.1: Conceptual model of a chloroethene-contaminated aquifer with the relevant biological degradation pathways. Dotted arrows reductive reactions, solid arrows oxidative reactions, dashed arrows co-metabolic reactions. Taken from [14].

## 1.2 Organohalide respiration (OHR)

Biodegradation is known as the chemical breakdown of compounds by organisms and their associated metabolic processes [18]. Initially, highly chlorinated CEs were considered as resistant to microbial degradation due to their persistence in aerobic environments and their presence in the environment was considered to be due entirely to anthropogenic activities [18]. Nowadays, it is known that practically all CEs are degradable when certain chemical and redox conditions are met. CEs biodegradation can also occur in contaminated sites but the success depends on many factors which are usually difficult to understand, thus leading to very slow or incomplete remediation. It is known that lower chlorinated compounds can be biologically transformed under aerobic conditions via co-metabolic processes or as sources of carbon and energy [6, 19]. Anaerobic biodegradation of highly chlorinated ethenes occurs through reductive dechlorination.

OHR represents a major pathway for CEs reductive dechlorination in anaerobic environments [20]. During OHR, CEs are used as electron acceptors and energy conserved from exergonic dehalogenation reactions is used for growth. The complete anaerobic reduction of CEs is a process where chlorine atoms are sequentially replaced by hydrogen atoms until the production of the environmentally harmless ethene. PCE and TCE are stronger oxidants than many naturally occurring electron accepting compounds found in anoxic groundwater systems. Therefore these compounds are thermodynamically favourable electron acceptors in the absence of dissolved oxygen [17]. The OHR metabolism was initially described for a mixed culture capable of reductive dechlorination of PCE [21]. This represented the first step towards the discovery of diverse bacteria capable of using organohalides as electron acceptors and conserving energy during the reductive dehalogenation, so called organohalide-respiring bacteria (OHRB).

### 1.2.1 Organohalide-respiring bacteria (OHRB)

To date, phylogenetically diverse bacteria, including members of Chloroflexi, Firmicutes (newly named as Bacillota [22]), Beta-, Delta- and Epsilonproteobacteria have been identified that conserve energy using OHR [23] (**Figure 1.2**). The first described anaerobic bacterium, which was capable to couple reductive dehalogenation of an organohalide (3-chlorobenzoate) to energy conservation, was *Desulfomonile tiedjei* strain DCB-1 [24]. Later, CEs were also shown to be used as terminal electron acceptors by OHRB [21, 25, 26]. Nowadays, more than seventy strains capable of OHR have been isolated from different polluted environments [27]. These isolates can be divided into facultative and obligate OHRB based on whether OHR is the only energy-conserving metabolism, or whether they have alternative energy metabolisms.

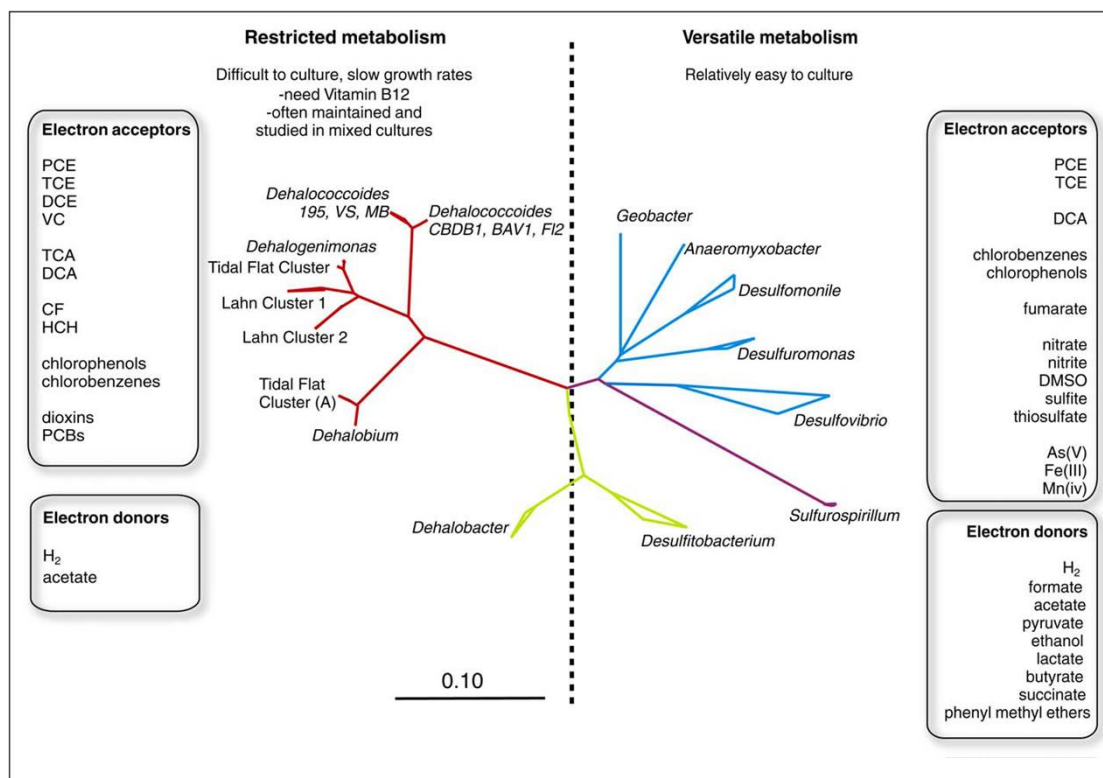


Figure 1.2: Phylogenetic tree of OHRB based on bacterial 16S rRNA sequences. The reference bar at the bottom centre indicates the branch length that represents 10% of sequence divergence. Electron donors and acceptors are listed in the flanking text boxes, and are grouped according to their chemical nature and complexity. Color key: Chloroflexi (red), Deltaproteobacteria (blue), Epsilonproteobacteria (purple), Firmicutes (green). Taken from [23].

Facultative OHRB are able to use nitrate, sulfite, thiosulfate, iron, and many more compounds as electron acceptors, beside organohalides. They are also characterized by a more versatile metabolism regarding the electron donor they can oxidize (formate, lactate, pyruvate, acetate, butyrate, fumarate etc.) [28] (**Figure 1.2**). Isolates belonging to the genera *Desulfitobacterium* [29], *Desulfoluna* [30], *Sulfurospirillum* [29], *Desulfomonile* [24], *Desulfovibrio* [31], *Desulfuromonas* [26], *Geobacter* [32] and *Shewanella* [33] are such energetically versatile OHRB. *Sulfurospirillum* is the only organohalide-respiring Epsilonproteobacteria, and is phylogenetically distinct from other OHRB (Purple line in **Figure 1.2**). The genus *Sulfurospirillum* takes the name from its ability to reduce and oxidize sulfur compounds. However, several strains, although not all, can reductively dechlorinate chloroethenes (PCE and TCE) and also dehalogenate brominated ethenes and chloropropenes. Their versatile metabolism allowed them to use various non-chlorinated electron acceptors such as fumarate, sulfur, polysulfide, thiosulfate, sulfite, DMSO, TMAO, nitrate, nitrite, arsenate, selenate and manganate [34]. Obligate OHRB strictly require organohalides as terminal electron acceptors to support their growth, among which *Dehalobacter* [35], *Dehalococcoides* [36] and *Dehalogenimonas* [37] are the best representative genera. *Dehalobacter* spp. from the Firmicutes has first been shown

to reductively dechlorinate PCE and TCE to *cis*-DCE [35, 38, 39] (**Figure 1.3**). Cultivation and environmental studies also revealed an increasing number of halogenated compounds that can be used by *Dehalobacter* spp. [35].

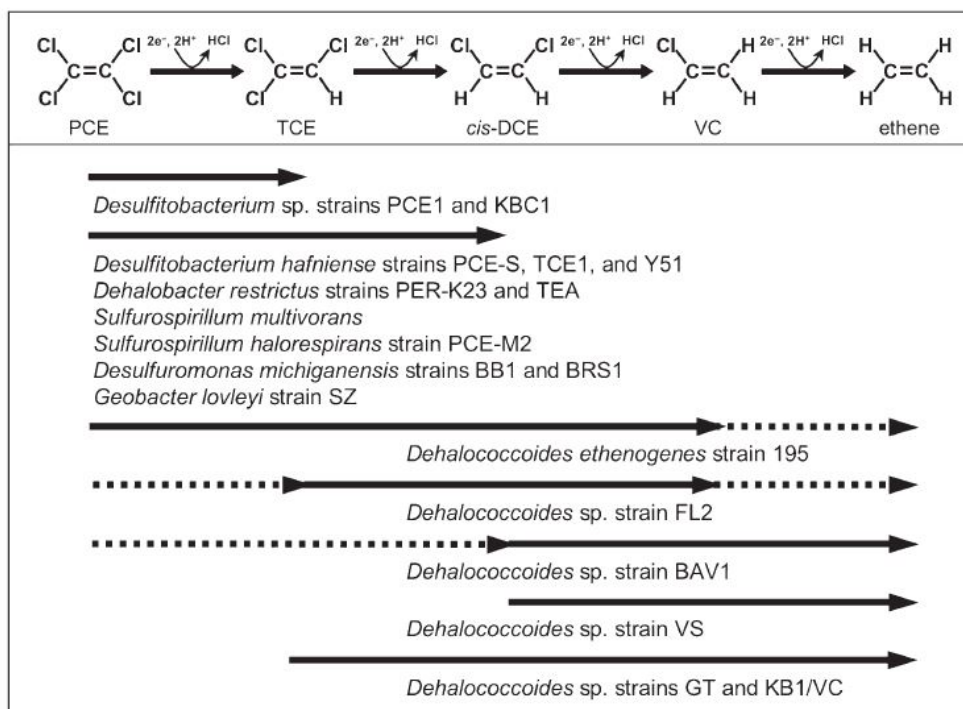


Figure 1.3: Reductive dechlorination pathways for chloroethenes by the organohalide-respiring bacteria. The dashed arrow shows the co-metabolic dechlorination reactions. Taken from [13].

The *Dehalococcoidia* class from the Chloroflexi contains the highest number of obligate OHRB isolates. To date, *Dehalococcoides mccartyi* strain 195 is the only bacterium known that can completely dechlorinate PCE to ethene, although the last step does not conserve energy [25]. The range of CE dechlorination by *Dehalococcoides* spp. is varying considerably depending on the isolates [36] (**Figure 1.3**). More recently, *Dehalogenimonas lykanthroporepellens* [40] and *Dehalogenimonas alkenigignens* strain IP3-3T [41], also from the Chloroflexi, have been shown to reductively dehalogenate chlorinated alkanes such as 1,2-dichloroethane, 1,2-dichloropropane and 1,1,2-trichloroethane.

### 1.2.2 OHRB Firmicutes

The Firmicutes phylum contains facultative organohalide-respiring *Desulfitobacterium* spp. as well as metabolically restricted *Dehalobacter* spp. *Dehalobacter restrictus* strain PER-K23 and *Desulfitobacterium hafniense* strain TCE1, are considered as model organisms in the present Ph.D. thesis.



The genus *Dehalobacter* has been first described in 1998 [42]. To date, several members of the genus *Dehalobacter* have been isolated and seven genomes are publicly available. The majority of these genomes are between 2.6 to 3.1 Mbp in size with the exception of strain FTH1 (with a draft genome of 6,3 Mbp) [43]. All isolates of *Dehalobacter* spp. are obligate organohalide-respiring bacteria that strictly rely on the use of H<sub>2</sub> as the sole electron donor, acetate as carbon source and halogenated compound as terminal electron acceptor (except for two reports on fermentative growth by one *Dehalobacter* sp. in an enrichment culture with chloromethane [44, 45]). In particular, *Dehalobacter restrictus* strain PER-K23 is the first isolate and type strain of this genus and was isolated from an anaerobic PCE-dechlorinating packed-bed column [42]. Since then, several studies have investigated various aspects of that particular strain directly [46–50] and in 2013, its genome has been sequenced [51]. It grows by coupling the oxidation of H<sub>2</sub> to the reduction of PCE or TCE and no growth has been observed with any other electron donor or acceptor, nor fermentative growth has been shown [51]. The 2.9 Mb genome of *D. restrictus* strain PER-K23 revealed the unexpected presence of twenty-five reductive dehalogenase (*rdhA*) genes, eight hydrogenases, and the complete biosynthetic pathway of corrinoids, the cofactor present in reductive dehalogenase enzymes (RDases). The eight different hydrogenases and the large number of putative reductive dehalogenase genes underscore the central role of hydrogen and halogenated compounds in its energy metabolism [51].

The *Desulfitobacterium* genus also belongs to the Firmicutes and comprises bacteria, the majority of which are facultative OHRB [29]. They have a versatile metabolism, carrying out fermentation and anaerobic respiration with a wide range of compounds as electron donors and acceptors. Most of them have been described to couple reductive dehalogenation of organohalides with energy conservation. The first member of the genus *Desulfitobacterium* was isolated in 1992 and named strain DCB-2 [52]. In the recent years, a large number of strains belonging to *Desulfitobacterium* spp. have been isolated: *D. hafniense* strains PCP-1, TCE1, DP7, TCP-A and G2, *D. dehalogenans* strains JW/IU-DC1 and PCE1, *D. dichloroeliminans* strain DCA1. The average size of the genome is around 5.3 Mbp and in contrast to the 25 *rdhA* genes from *D. restrictus* strain PER-K23, the genomes of *Desulfitobacterium* spp. only encode one to seven *rdhA* genes, with strain TCE1 displaying a unique *rdhA* gene, which encodes the PCE reductive dehalogenase (PceA). *D. hafniense* strain TCE1 was isolated in 1999 by a selective enrichment from a chloroethene-contaminated aquifer and was reported to dechlorinate PCE and TCE [53]. Growth with H<sub>2</sub>, formate, lactate, butyrate, crotonate, or ethanol as the electron donor depends on the availability of an external electron acceptor. When lactate is the electron donor and carbon source, strain TCE1 can use the following electron acceptors: PCE and TCE (to produce cDCE), sulfite and thiosulfate (to produce sulfide), nitrate (to produce nitrite), and fumarate (to produce succinate).

### 1.3 Electron transport chain in OHR

Respiration is a catabolic process where the electrons are extracted from different organic or inorganic substrates, namely the electron donors, and are passed via freely diffusible carriers (such as NADH and FADH<sub>2</sub> or quinones for the anaerobic respiration), into a multi-protein electron transport pathway, which constitutes the respiratory chain. The electrons entering the electron transport chain have a low electrochemical potential, while the electron acceptor is usually featured with high mid-point redox potential, making it a strong oxidant. Thus, the electrons flow from low electrochemical potential substrate to the one with high redox potential and the free energy released during this electron transfer is used to drive the translocation of protons across the membrane, which in turn generates a trans-membrane electrochemical proton motive force (*pmf*). The resulting electrical potential across the membrane is used by the ATP synthase to transform adenosine diphosphate (ADP) into adenosine triphosphate (ATP), which constitutes the energy reservoir for the cells [54]. Regarding reductive dehalogenation by OHRB, electrons are transferred from H<sub>2</sub> or other electron donors to organohalides via a membrane-associated electron transport chain [55, 56]. This process is coupled with oxidative phosphorylation to support the growth of OHRB. OHR is composed of hydrogenases or dehydrogenases and reductive dehalogenases. The quinone pool, which shuttles electrons from the electron-donating enzymes to the electron-accepting enzymes, is not always present in OHRB respiratory systems.

#### 1.3.1 Quinones in OHR

Quinones are small, diffusible, lipophilic, membrane-embedded organic molecules that can carry two electrons and two protons when fully reduced. This is the quinol state. Different kinds of quinones have different electrochemical potentials and many bacteria can synthesize more than one type of quinones: namely ubiquinones [ $E^0$  ' (UQ/UQH<sub>2</sub>) = +40 mV] and menaquinones [ $E^0$  ' (MK/MKH<sub>2</sub>) = -74 mV] [57]. The detailed mechanism how quinones contribute to the shuttling of electrons between the electron-donating and -accepting enzymes in the respiratory chain was described by “the redox loop mechanism” [58]. Conceptually, it consists of two quinone-interacting membrane proteins, a quinone-reducing and a quinol-oxidizing enzyme system, organized in the cytoplasmic membrane. Nine different structural architectures, differentiated on the basis of the localization of the active sites for the electron donor and acceptor on the positive (P-side, out) or negative (N-side, in) sides of the membrane, the localization of the quinone/quinol-binding site on the P- or N-sides and the direction of electron transfer, have been proposed for bacteria [54]. In recent years, redox loops were commonly found in different anaerobic respiratory chains where the free energy of the redox reactions is smaller than in aerobic respiration, and where, consequently, shorter respiratory chains and few proton-translocating enzymes are employed [54]. Strong evidence showed that menaquinones play an important role in the cytoplasmic membrane of different obligate and facultative OHRB. For example, *D. restrictus* was shown to contain different menaquinones (MK; mainly MK-7 and MK-8) [42]. Comparative spectral analysis of *D. restrictus* membranes

reduced by  $H_2$  and oxidized with PCE revealed a clear change in the absorbance spectrum of the menaquinone pool, indicating its participation in the PCE respiratory chain. Moreover, the addition of HQNO, a quinone antagonist, resulted in the complete disruption of PCE reduction [46] (**Figure 1.4**). Other facultative and obligate OHRB contain menaquinones: *S. multivorans* [59], *D. dehalogenans* [60], *D. tiedjei* [61] and *D. hafniense* strain TCE1 [62].

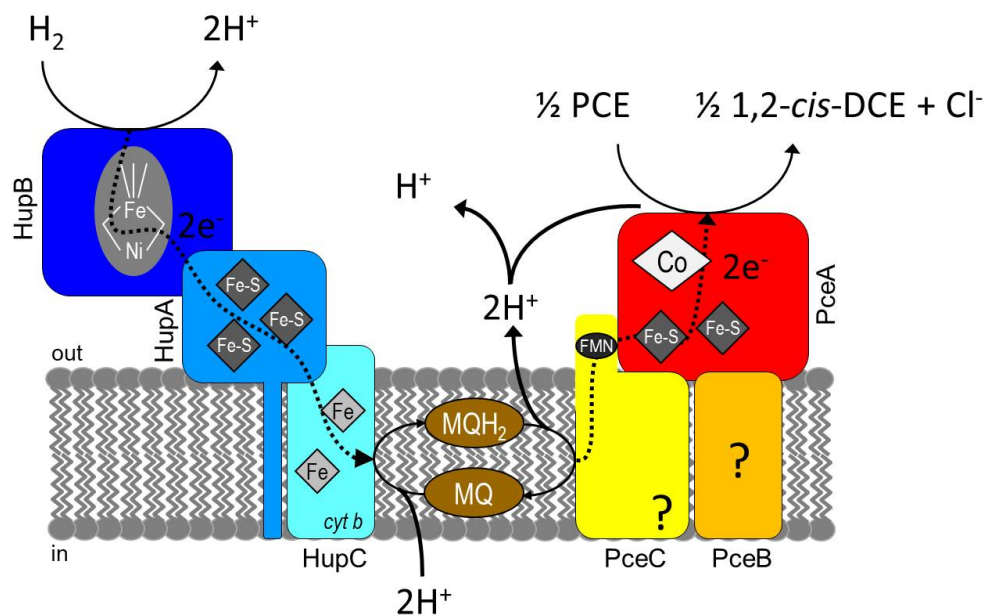


Figure 1.4: Tentative model of the respiration chain of *Dehalobacter restrictus* involving hydrogen oxidation by a Ni-Fe hydrogenase (HupB), transfer of electrons via menaquinones (MQ) from the cytochrome b subunit (HupC) of the hydrogenase to PceC, and finally to PceA that reductively dechlorinates PCE to *cis*-1,2-DCE. Adapted from [35].

Collectively, these observations confirm the involvement of quinones in the respiratory chain of certain OHRB. However, this raises the still unresolved question of how electrons from quinol, with a well-accepted mid-point redox potential of  $E^0' = -74$  mV [57], allow the reduction of PCE to TCE (mid-point redox potential of  $E^0' = 580$  mV [63]) via PceA which features cofactors which display midpoint redox potentials of -480 mV (FeS clusters) and -350 mV (cobalamin). So far, two possible routes to solve this have been proposed: the reverse electron flow as in the case of *S. multivorans* [64] that depends on the proton-motive force across the membrane, and electron bifurcation [65], where the recently discovered flavin-based complex combines the endergonic activation of electrons by a concomitant exergonic redox reaction. However, none of these hypotheses have been yet clearly addressed in OHR. The electron flow scheme for quinone-dependent reductive dehalogenation was found in other electron transport chains in anaerobic bacteria. For example, a similar electron flow exists for menaquinol oxidation by the NrfA nitrite reductase in *Wolinella succinogenes* and *Desulfovibrio vulgaris* [54]. In this mechanism, the periplasmic formate (or  $H_2$ ) oxidation is

coupled to nitrate reduction, thus producing nitrite, which is further reduced to ammonium. The quinol pool is oxidised by the Nap and Nrf systems in order to catalyse electroneutral nitrate reduction to nitrite and nitrite reduction to ammonium, respectively. Consequently, the whole respiratory nitrate ammonification system depends on *pmf* generation at the level of electron input (electron-donating part) into the quinone pool, rather than at the level of electron output (electron-accepting part). Hence, the role of the Nap and Nrf systems is to serve turnover of the quinol pool to ensure a continued supply of oxidised quinone for the quinone-reducing electron input components.

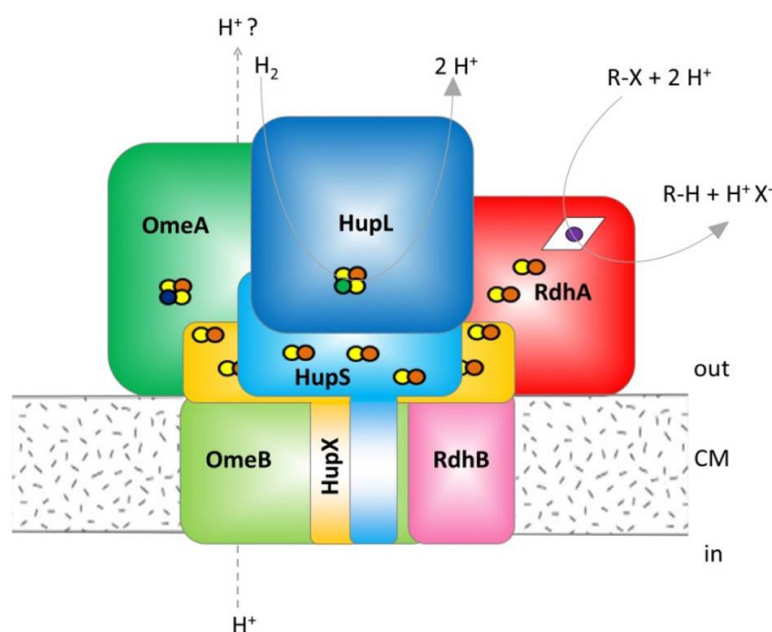


Figure 1.5: Hypothetical model of the organohalide complex in *Dehalococcoides mccartyi* strain CBDB1, representing multiple interactions between subunits. HupL, hydrogenase large subunit; HupS, hydrogenase small subunit; HupX, iron/sulfur protein; OmeA, organohalide respiration involved molybdoenzyme subunit A; OmeB, organohalide respiration involved molybdoenzyme subunit B; RdhA, reductive dehalogenase homologous protein catalytic subunit A; RdhB, reductive dehalogenase homologous anchoring subunit B. Taken from [66].

In contrast to the quinone-dependent electron transfer, *Dehalococcoides* spp. and *Dehalogenimonas* spp. are characterized by the absence of quinones, thus, with an alternative organization in the electron transfer to the terminal RdhA enzymes. The first evidence of this alternative strategy has been shown in *D. mccartyi* strain CBDB1 for which OHR was not inhibited by HQNO [67] neither driven by reduced quinone analogues (i.e. DMNH<sub>2</sub>) [56]. In the absence of quinones, the alternative is protein-mediated electron transfer from a hydrogenase to the RdhA enzyme [56]. To date, only for *D. mccartyi* strain CBDB1, a quinone-independent electron transfer was proposed featuring a large protein complex able to catalyse the reduction of organohalides as a standalone enzyme complex [66, 68].

The studies on *D. mccartyi* strain CBDB1 using Blue-Native polyacrylamide gel-electrophoresis

(BN-PAGE) revealed that the dehalogenating activity was associated with a high molecular mass protein complex (250 kDa) (**Figure 1.5**). The presence of three different modules constituting the protein complex was revealed: *i*) a reductive dehalogenase (RdhA) together with RdhB, which is the putative membrane anchor of RdhA; *ii*) a complex iron-sulphur molybdoenzyme (CISM) characterized by the catalytic subunit, OmeA, and its related membrane anchor OmeB, and *iii*) the hydrogen uptake hydrogenase module composed by three different subunits, HupL, HupS and HupX. RdhB and OmeB are predicted to be membrane integral proteins, while HupX and HupS may be membrane-associated with one trans-membrane domain each. As shown in **Figure 1.5**, the electron transfer is proposed to begin with the oxidation of the dihydrogen molecule catalysed by HupL and the following separation of charges. Protons are released outside of the cell, while the electrons are transferred via the iron-sulphur cluster in HupS, HupX and OmeA to RdhA, which is known to catalyse the reduction of the organohalides [68].

## 1.4 Reductive dehalogenase and accessory genes

Reductive dehalogenase (*rdh*) genes are typically organized in an operon composed of *rdhA*, the gene encoding the catalytically active enzyme, and *rdhB*, a gene encoding the putative membrane anchor protein for RdhA [49, 69]. The *rdhAB* genes represent the minimal *rdh* operon so far detected [70], with the exception of a few strains of *Dehalogenimonas* spp. and *Dehalococcoides* spp., which display some orphan *rdhA* genes [71]. However, at proteomic level, none of these RdhA enzymes have been detected [72]. One or more accessory genes may also be present in the direct genetic proximity of *rdhAB* genes, the gene products of which have been shown to be involved in transcriptional regulation and enzyme maturation. An exemplifying case is the chlorophenol reductive dehalogenase (*cpr*) gene cluster from *D. dehalogenans*, which harbours six additional genes in close proximity to the *cprA* and *cprB* genes (*cprTKZEBACD*) [73].

### 1.4.1 RdhB, a membrane anchor for RdhA?

The genetic vicinity of *rdhB* and a robust reductive dehalogenase activity associated with the membrane fraction during purification [74, 75] corroborate the hypothesis that RDases consist of the catalytic RdhA enzymes bound to the outer face of the cytoplasmic membrane via RdhB, a short integral membrane protein of ~100 amino acids. A recent transcriptomic and proteomic study has revealed a similar up-regulation of *tmrA* and *tmrB* in the trichloromethane-respiring *Dehalobacter* sp. strain UNSWDHB [76]. In addition, the presence of the B subunit was detected in the respiratory complex of *D. mccartyi* [68]. The topology prediction of RdhB proteins shows in most cases three trans-membrane  $\alpha$ -helices, an exoplasmic N-terminus and a slightly conserved short exoplasmic loop between helices 2 and 3 [56]. The predicted topology of RdhB, together with the assumption that RdhA proteins do not display any integral membrane segment invites to consider the direct interaction between the two proteins. This

interaction could likely occur at the level of the exoplasmic loop of RdhB protruding outside of the membrane. Although the loops of different PceB proteins displayed low sequence identity, two conserved glutamic acid residues have been proposed as possible binding sites for RdhA [56]. However, no evidence has been yet obtained for the interaction between RdhA and RdhB proteins.

### 1.4.2 Diversity of *rdh* gene clusters in OHRB

The reductive dehalogenase encoding genes are located in the *rdh* gene clusters. The diversity of *rdh* gene clusters in OHRB is present at different levels. There are evidences of different gene composition and organization in *rdh* gene clusters across different OHR genera. However, the diversity in *rdh* gene clusters is also shown across members belonging to the same genus, as illustrated in *Desulfitobacterium* spp. [77]. For example, in *D. restrictus* strain PER-K23 three *rdh* genes organizations can be considered [49]. The genome of strain PER-K23 harbours twenty-five *rdh* gene clusters in total, one of which is truncated (*rdh25*). Two gene clusters (*rdh20* and -22) are sharing the same genetic organization as *rdh24*, which is the characterized *pceABCT* gene cluster. Seven gene clusters are lacking the *rdhT* gene, five of them are in the *rdhABC* orientation and two as *rdhBAC* clusters, while the remaining *rdhA* are accompanied only by their respective B subunit, exclusively in the *rdhBA* orientation. Rupakula *et al.* showed that RdhA proteins, which are encoded by gene clusters sharing the same organization, are also more closely related at the sequence level, suggesting that gene duplication events might have occurred [49]. Even though PCE and TCE are the only substrates known to be used as electron acceptors by *D. restrictus*, the high *rdhA* gene diversity in this bacterium suggests a greater OHR potential. In contrast with obligate OHRB (i.e. *Dehalococcoides* spp. and *Dehalobacter* spp.), which display up to 36 genes coding for RdhA enzymes [35], only up to seven *rdhA* genes were identified in the genomes of *Desulfitobacterium* spp. [77].

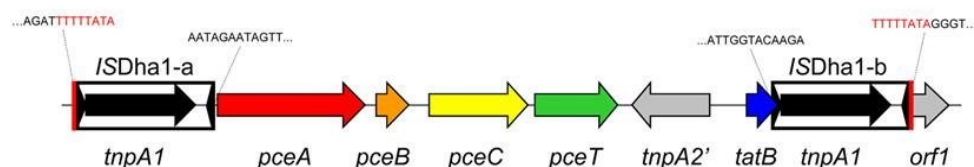


Figure 1.6: Genetic map of *Tn-Dha1* from *D. hafniense* strain TCE1 and related genetic structures. *Tn-Dha1* contains 6 ORFs, including the conserved *pceABCT* gene cluster, and is flanked by two identical copies of the insertion sequence *ISDha1*. Above the map are the sequences of each IS site (with *Tn-Dha1* direct repeats in red). Taken from [78].

As shown in the comparative analysis by Kruse *et al.*, and despite the fact that the *rdh* gene cluster composition varies among different *Desulfitobacterium* strains, it was possible to define seven different “super clusters” which are highly conserved across the strains [77]. In particular, *D. hafniense* strain TCE1 harbours only one *rdh* gene cluster which is *pceABCT* (**Figure 1.6**). This gene cluster is flanked by two identical transposase genes. This cluster has been shown to be part of an active transposon that is able to excise itself from the genome in different forms [78, 79]. It does not encode any predicted transcriptional regulator and has been shown to be constitutively expressed [80].

### 1.4.3 The conserved *pceABCT* gene cluster

In *Dehalobacter* and *Desulfitobacterium* spp., the *pceABCT* gene cluster encodes for the enzyme catalysing the reductive dehalogenation of PCE and for other accessory proteins that are likely relevant for OHR. Despite the fact that *pceABCT* represents one of the paradigmatic genetic systems in OHR, only scarce biochemical knowledge is available on the gene products with the exception of PceA [13, 46, 48]. *D. restrictus* strain PER-K23 and *D. hafniense* strain TCE1 display in their genome the *pceABCT* gene cluster, which codes for the proteins that might form the electron-accepting part of the OHR pathway. Besides the production of PceA, the gene cluster also codes for two putative integral membrane proteins, PceB and PceC [81], for which no function has been assigned yet, and PceT, which is a molecular chaperone involved in the folding process of PceA [82, 83]. So far, only PceA (encoding for *rdhA24*) has been biochemically characterized. Transcriptional analysis and proteomic data suggested that other RdhA proteins are also expressed in *D. restrictus*, but this now awaits further biochemical investigation [49]. PceC represents the most enigmatic protein encoded by the *D. restrictus* gene cluster. Based on sequence similarity with its homologous protein CprC of *D. dehalogenans* [73] and NosR, PceC was originally suggested to be a putative transcriptional regulator [79]. NosR is an FeS cluster containing protein harbouring a flavin cofactor facing the periplasm and redox centres located on the cytoplasmic side of the membrane [84]. Since then, NosR was considered as a transcriptional regulator [85]. Recently, different studies demonstrated that it rather plays a role in the activation as well as in the electron transfer to the nitrous oxide reductase (NosZ) [84, 86]. In our laboratory, this led to reconsider the role of PceC in electron transfer between menaquinol and PceA. Indeed, preliminary proteomic analyses from membrane extracts of *D. hafniense* strain TCE1 and *D. restrictus* strain PER-K23 allowed the detection of PceC, and the proteomic data further suggested that it may be as abundant as PceB (G. Buttet and J. Maillard, unpublished data). In addition, sequence prediction and experimental work revealed that PceC harbours a covalently-bound FMN cofactor allocated in the part of the protein facing the outside of the cytoplasmic membrane, named as the FMN-binding domain (FBD). Recently, a study also led to the development of a reconstitution protocol to produce the redox-active FMN-binding domain of PceC in *E. coli* [81]. The *in silico* prediction of PceC highlighted the presence of two conserved CX<sub>3</sub>CP towards the cytoplasmic face of PceC in the trans-membrane helices 5 and 6, as also found in NosR, for which no role has been yet assigned. PceT is a molecular chaperone most likely assisting in correct folding of PceA.

It was shown to bind to the N-terminal Twin-arginine translocation (Tat) signal sequence of PceA [83]. In proteomic studies on *D. hafniense* strain TCE1 [80] or *D. restrictus* strain PER-K23 [49] actively growing with PCE, PceT was detected. For a long time attempts to produce active recombinant RdhA enzymes failed. Only in recent years, new findings on the maturation of RdhA enzymes and selection of new hosts have led to *in vivo* production of the first active recombinant RdhA enzyme [87]. *In vitro* reconstitution of an active RdhA has also been recently achieved. This was feasible using *Escherichia coli* expression system where the overexpression of *E. coli*'s cobamide transport system, *btu*, and anaerobic expression conditions were found to be essential for production of active RDases from *Dehalobacter restrictus* [88].

## 1.5 Thesis objectives

The membrane-associated reductive dehalogenase plays a key role in the energy metabolism of OHRB. Most of biochemical studies on OHR focused essentially on the catalytic enzyme, RdhA, but little is known about the global energy metabolism of OHRB and about the role of accessory enzymes involved in this respiratory metabolism. The present Ph.D. thesis aims at elucidating the electron-accepting moiety of Firmicutes OHRB by investigating the stoichiometric relationships between the proteins encoded in the *pceABCT* gene cluster and by isolating and characterizing the membrane-bound reductive dehalogenase (RDH) protein complex (Figure 1.7).

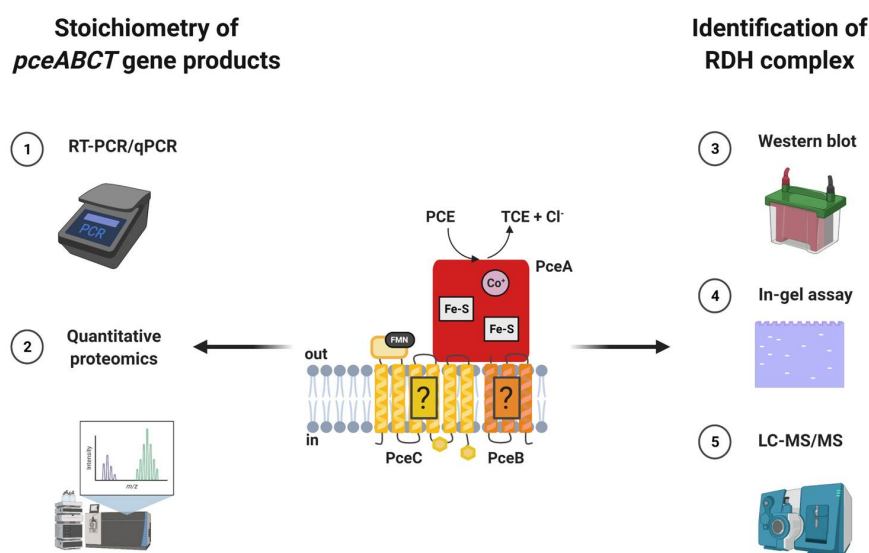


Figure 1.7: Graphical representation of the main objectives of the present Ph.D. thesis and the respective techniques applied throughout the study.



For both aspects, the obligate OHRB *Dehalobacter restrictus* strain PER-K23 and the facultative OHRB *Desulfitobacterium hafniense* strain TCE1 were considered as model organisms. The investigation of both obligate and facultative OHRB are tackled at two different levels, namely the physiological level by the characterization of the membrane PceA-containing protein complex of both obligate and facultative OHRB, and the RNA and protein levels where the accessory proteins PceB and PceC likely involved in the OHR metabolism will be the main focus. This will permit to explore the use of the *pceABCT* gene cluster across different genera and the role of the corresponding proteins in the composition of the OHR electron transfer chain.

### 1.5.1 Outline of the thesis

In **Chapter 1**, an introductory overview of the OHR metabolism and the key bacterial players in the field is presented.

In **Chapter 2**, the hypothesis of a possible PceABC protein complex was specifically addressed via quantitative proteomics. In collaboration with the Proteomic Core Facility (PCF) at EPFL, the parallel reaction monitoring (PRM) technology was defined as the most suitable strategy to answer the question of the stoichiometry of PceA, PceB, PceC and PceT in *D. restrictus* and *D. hafniense* strain TCE1. However, the different nature of the targeted proteins (a rather soluble PceA and very hydrophobic PceB and PceC proteins) represents the major difficulty in addressing this question and it requires a very careful sample preparation prior to MS analysis. In this chapter, the tedious work leading to the development and optimization of a defined protocol for quantitative proteomics is presented in detail.

**Chapter 3** presents the results obtained from the investigation of the *pceABCT* gene cluster in OHRB harbouring diverse metabolic strategies, i.e. the obligate *D. restrictus* strain PER-K23 and the versatile *D. hafniense* strain TCE1. In this chapter, the investigation on the stoichiometry of the *pceABCT* individual gene products at RNA and protein level is discussed.

In **Chapter 4**, the identification of the reductive dehalogenase (RDH) protein complex is described. In collaboration with Professor I. Pereira Laboratory at the Universidade Nova de Lisboa (Portugal), the combination of different techniques and the development of an in-gel enzymatic assay for the detection of PceA are presented. With the application of Clear-Native PAGE (CN-PAGE) technology on membrane fractions of *D. restrictus*, the question of possible PceA-containing complexes is addressed, while the in-gel PceA enzymatic activity assay offers a way to localize PceA in the gel and determine the size of the RDH complex. Furthermore, the optimization process for the sample preparation protocol, which represented a crucial pre-requisite for their applicability, is therein presented.

In **Chapter 5**, the experiments aimed at purifying and characterizing the RDH complex. A combined use of chromatography and Mass Spectrometry (MS) analysis was considered to address the question of the possible protein partner(s) associated with PceA in the RDH

complex. Additionally, the development of an in-solution enzymatic assay investigating the electron shuttling to the RDH complex is presented.

Finally, in **Chapter 6**, the main findings presented in this thesis are discussed and evaluated in respect to the present knowledge on organohalide respiration.



## 2 Development and optimization of quantitative proteomics approach

### 2.1 Introduction

#### 2.1.1 Earlier findings

The *rdhABCT* gene operon involved in PCE respiration can be found in members of the genera *Desulfitobacterium* and *Dehalobacter*, and can be considered as one of the model gene clusters for studying OHR. To date, the function of RdhA, the key catalytic enzyme in the process, and RdhT, the dedicated molecular chaperone for RdhA maturation, are well defined. However, the role of RdhB and RdhC proteins are still not elucidated and the biochemistry of OHR electron transfer remains elusive. Based on sequence information, the hypothesis that RdhC may play a role in the electron transfer chain to RdhA is tempting but the question remains largely unanswered. In the framework of G. Buttet PhD thesis [89] two proteomics analyses were conducted on *Dehalobacter restrictus* and *Desulfitobacterium hafniense* strain TCE1 with the aim to investigate the presence of *pceABCT* encoded proteins in cell extract as well as their relative abundance in the sub-cellular compartments.

Firstly, urea (6 M) was added to the cell extracts in order to extract membrane proteins. After centrifugation, the resulting soluble fraction (SF) and the insoluble fraction (IF) containing the membranes were analyzed via a shotgun MS approach. The analysis revealed that for many predicted membrane-bound enzyme complexes, mainly the non-membrane subunits were detected. Focusing on the *pceABCT* gene cluster, all its encoded proteins were identified, however PceB and PceC resulted in a much lower sequence coverage than PceA and PceT. **Figure 2.1** shows the predicted topology of PceC and PceB highlighting the detected peptides. Interestingly, the analysis of IF revealed a similar abundance of PceB and PceC while the loosely membrane-bound PceA was 15 times more abundant than PceB and PceC in this protein fraction.

In the second experiment, the membrane fraction of *D. restrictus* obtained by centrifugation of cell-free extract was analyzed via shotgun MS. Strikingly, according to *in-silico* topology prediction, the peptides detected for PceB and PceC belonged to the portion of proteins

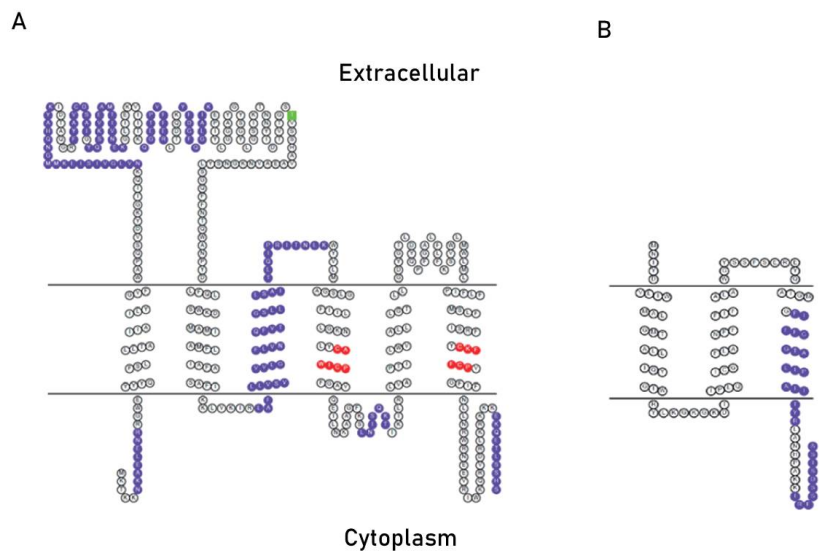


Figure 2.1: Representation of the predicted membrane topology of PceC and PceB proteins of *D. hafniense* strain TCE1. For PceC, the predicted FMN-binding threonine residue is shown in green and the conserved cysteine motifs in red. For PceC and PceB, purple amino acid stretches indicate the peptides detected in proteomic analysis. Taken from [89].

protruding outside the lipid bilayer, and thus likely more accessible to tryptic digestion and MS detection (Figure 2.2). Furthermore, MS data confirmed the presence of a covalently-bound FMN cofactor in a peripheral domain of PceC facing the outside of the cytoplasmic membrane [81], and suggested comparable abundance of PceB and PceC at membrane level. Overall, these findings corroborated the hypothesis that PceC might play a role in the electron transfer.

Dehre 2398 (PceA) - 364/551 amino acids (66% sequence coverage)											
MGEINRRNFL	KASMLGAAAA	AVASASAVKQ	MSPLVADAA	DIVAPITETS	EFYKVDAY	GRYNSLKNFF	EKTFDPEANK				
TPIKFHYDDV	SKITGRKDTG	KDLPTLNAER	LGIKGRPATH	TETSILFHTQ	HLGAMLTORH	NETGWTGLDE	ALNAGAWAVE				
FQYSGFNAAQ	GGPGSVILPY	PINPHNEIA	NEPMVPGYV	NWDNIDVESV	RQGGQWKFE	SKEEAKSLK	KATRLGADL				
VGIAPYDERW	TYSTWGRKIL	KPKCMFNGRT	KYLPWDLPKM	LSGGGVEVFG	HAKFEPDWEK	YAGFKPKSVI	VFVLEEDYEA				
IRTSFVSISS	ATVGKSYSNM	AEVAYIAVAF	LRKLGYYAAP	CGNDTGISVP	MAVQAGLGEA	GRNGLLITQK	FGPRHRIAKV				
YTOLELAPDK	PRKFGVREFC	PLCKKEADAC	PAQAISHEKD	PKVLQPEDCE	VAENPYTEKW	HLDSNRQSP	WAYNGSPCAN				
GVAVCSWNKV	ETWNHDVARI	ATQIPLLQDA	ARKFDEWFQV	NGFVNPERDL	ESGYVQNMVK	DFWNNPESIK	Q				
Dehre 2397 (PceB) - 18/105 amino acids (17% sequence coverage)											
MNIYDVLIM	ALQMTALLIQ	YGIWRYLKGG	GKDTIPLQIC	GFLANFFIF	ALAWGYSSFS	EREYQAIGMG	FIFFGGTALI				
PAIITYRLAN	HPAKKIRESS	DTISA									
Dehre 2396 (PceC) - 140/428 amino acids (33% sequence coverage)											
VKTKKNKAEL	ENRRGWEYYY	QFSLLTAAI	AILYGVFWAP	OSVDYKGLIQ	KNVLGVISIE	KMMGNQHAYK	IDTAGGRFYA				
VCDSAIGYQS	KVEAMTIVNE	KGLIEKVIIT	KQGETPVFFE	RLTDQKYFDG	FQGLAIKEPI	YLGGAIGYSQ	YLGSIKTNNY				
IDRVTVGSFVS	SHAVAAEAVNK	GNSYLSGOFF	NTOWANPYDL	FQLSWKDMAM	IAMFLIAFAS	AFIKKLVKIR	LAFLLVSVVV				
LGFLVMQFVT	GSLLLSAITL	OIPRITNLKW	YVLMAGSLGF	IILLGKNLYC	AWICPPGAVQ	EILNKAAGFK	SLNISQKTIK				
ILFLVAPTIL	WYALLLGTLL	GDYGTLDYQP	FGALFLFKSV	WLMWMLPIF	LFMSLFISRF	YCKFFCPVGF	IYNLLNRWRN				
EEVRIWKQRV	DRLKRRKKKEE	QETWSSHS									
Dehre 2395 (PceT) - 171/316 amino acids (54% sequence coverage)											
MKPELGGYK	GLNVKRFDDT	VQEEELQOAL	DYIIOSFDEI	EEKRNNEPIK	TNDYVIVDID	GYEKDATVPV	IRNIDTKLIV				
QSEGVFREVY	ANLLLGKMOD	TYTTFESVIQF	DAPLQPRWGG	SVPVVKPEL	TEELIRKVEP	DLKHLKDLKN					
MLALKITHEK	EGKEREANIL	LIFOALVKQC	KYEFDEEELD	SAAEOLYKFF	TEELKIVDDM	ELMEYLIHRK	ITADQLLAEC				
KEEASRRILW	ELMINSVIEK	EEINLTPEEI	KYLEKRINES	RONGQLPEEF	MDINFLASY	LRKKTIDYLL	KINLAS				

Figure 2.2: Graphical representation of sequence coverage of Pce proteins of *D. restrictus* strain PER-K23 by shotgun MS analysis performed in the framework of G. Buttet Ph.D. thesis (2017). The peptides that were detected via discovery MS analysis are shaded in yellow. Amino acids with post-translational modifications (PTMs) are shaded in green.

### 2.1.2 Rationale behind the development of a quantitative proteomics approach

The preliminary studies performed on *D. hafniense* strain TCE1 and *D. restrictus* revealed that the integral membrane proteins PceB and PceC were detected with substantially lower frequency than the membrane-associated PceA. However, the interpretation of this result needed caution as the shotgun MS method does not provide *per se* any quantitative estimate of proteins. In addition, the relatively low abundance of PceB and PceC was likely due to the difficulty to detect integral membrane proteins fully embedded in the lipid environment. This aspect still constitutes an analytical bottleneck for MS analysis of membrane proteins despite numerous MS-based methods have been proposed to improve their detection [90, 91]. For these reasons, the necessity of a tailor-made solubilization protocol and a defined proteomics approach represented the main objectives for the quantification of Pce proteins. This work was performed in collaboration with the Proteomic Core Facility of EPFL.

Initially, targeted proteomics technology was considered as the most suitable quantification strategy to answer the question of the stoichiometry of PceA, PceB, PceC and PceT in *D. restrictus* and *D. hafniense* strain TCE1. This powerful technique allows to overcome the limitations of shotgun MS approach and offers a route to determine absolute abundance of specific proteins. In the targeted proteomics approach, either in the selected reaction monitoring (SRM) [92, 93] or in its more recently implemented "cousin" parallel reaction monitoring (PRM) [94], the quantification is achieved by comparing the mass spectrometry signal intensity of the peptides of interest to that of accurately quantified, isotope-labelled reference peptides, which are used as internal standards. Theoretically a targeted proteomics method constitutes three main steps: 1) selection of peptide signatures for each of the proteins of interest 2) qualitative and quantitative validation of the heavy-labelled peptide surrogates, and 3) the application of the method to the biological samples.

One of the major challenges in the quantification of *pceABCT* encoded proteins derives from the different nature of the proteins of interest. In MS-based proteomic studies, most digestion conditions were optimized for soluble proteins. However, here the highly hydrophobic nature of PceB and PceC in contrast to the rather high hydrophilicity of PceA make sample preparation and membrane extraction a crucial step. Furthermore, the extraction protocol plays a fundamental role in the definition of the reference peptides as well as for the quantitative analysis. For this reason, prior to the selection of peptides for quantitative proteomics, the development of a suitable solubilization protocol of the membrane fraction of *D. restrictus* and *D. hafniense* strain TCE1 is crucial for the success of the approach. The first phase of the development required that the analytical limitations and detection of the *pceABCT* encoded proteins were defined. In this context, an unpolished sample preparation protocol was applied on *D. restrictus*. In the following "Materials and Methods" section, the initial strategies are described while all the improvements leading to the defined protocols will be thoroughly presented in "Results and discussion" section of the present chapter.

## 2.2 Materials and methods

### 2.2.1 Bacterial strains and growth conditions

*Dehalobacter restrictus* strain PER-K23 (DSM 9455) and *Desulfitobacterium hafniense* strain TCE1 (DSM 12704) were cultivated anaerobically at 30°C under agitation (100 rpm). Volumes of 40 and 200 mL (in 100 and 500-mL serum flasks, respectively) of medium were prepared where the head space was replaced by a mixture of N<sub>2</sub>/CO<sub>2</sub> (80%/20%) as described earlier [95] with the modifications that cyanocobalamin was supplemented at 50 µM (final concentration) and that dicyanocobinamide was used instead of cyanocobalamin for the cultivation of *D. restrictus* strain PER-K23. Dicyanocobinamide was used here to allow *D. restrictus* to complement the corrinoid cofactor with the lower ligand of its choice, likely with purine as suggested earlier [96], and in studies on *Desulfitobacterium* [97, 98]. Completed medium was supplemented with acetic acid (5 mM) as carbon source, the head space replaced by a gas mixture of H<sub>2</sub>/CO<sub>2</sub> (80%/20%) to provide H<sub>2</sub> as electron donor, and inoculated with 5% (v/v) of a preculture. To study OHR metabolism, cultures were supplemented with PCE as electron acceptor (nominal concentration of 10 mM) in a biphasic system [21]. For *D. hafniense* strain TCE1 1% (v/v) of a 2 M PCE stock solution in hexadecane was used (with an estimated aqueous concentration of 0.4 mM), while for *D. restrictus* it was 4% (v/v) of a 500 mM PCE stock solution, thus keeping a lower aqueous PCE concentration (0.1 mM). Indeed, we have observed that a high PCE concentration had a slight toxic effect on the growth of *D. restrictus*. The cultures were routinely transferred to fresh medium after 10 days of cultivation.

### 2.2.2 Cell harvest, fractionation and protein extraction

For proteomic analysis, *D. restrictus* and *D. hafniense* strain TCE1 were cultivated anaerobically in duplicates as described above. The growth was monitored at OD<sub>600</sub> and the biomass was collected after three days of incubation corresponding to exponential growth. After removal of the PCE-containing organic phase from the culture, the liquid was transferred in 1-L plastic bottles (Beckman Coulter, Switzerland) and the biomass was collected by 20 min of centrifugation (9000 × g) at 4°C. The resulting biomass pellets were washed three times in 10 ml of 50 mM Tris-HCl (pH 7.5), and the cell pellets stored at -80°C until use. The biomass pellets were resuspended in 50 mM Tris-HCl buffer supplemented with the protease inhibitor (Sigma) and with a few crystals of DNase I (Merck) at a ratio of 5 mL per g of cells (wet weight). The cells were lysed with five rounds of sonication at 60% amplitude on the Sonic Dismembrator FB120 (Fisher Scientific, Reinach, Switzerland). After 15 min of a mild centrifugation (500 × g, 4°C), the supernatant corresponded to the cell-free extract (CFE) whereas the pellet of unbroken cells was discarded. Soluble and membrane fractions were obtained by ultracentrifugation (30'000 × g, 4°C, and 30 min) of the cell-free extract. The resulting supernatant was collected and represented the soluble fraction (SF) sample. The pellet obtained with ultracentrifugation was resuspended in 500 µl of 50 mM Tris-HCl buffer containing the protease inhibitor and 2% of SDS and transferred in a new ultracentrifugation tube. After 30 minutes of solubilization

under constant stirring at 4° C, ultracentrifugation was applied. The resulting supernatant was collected in a new Eppendorf tube and represented the membrane fraction after first treatment with 2% SDS (MF1) while the membrane pellet was resuspended with 50 mM Tris-HCl buffer supplemented with the protease inhibitor and 4% SDS under continuous stirring for 2 h at RT. Later, ultracentrifugation was applied and the resulting supernatant was transferred to a new Eppendorf. This sample represented the membrane fraction after the second treatment with SDS (MF2). Despite the two subsequent SDS treatments of the membrane fractions, a pellet representing the fraction not solubilized by SDS was still present on the wall of the tube. This required an additional treatment of the remaining pellet with 2% formic acid (MF3) to fully dissolve the remaining membrane aggregates. Later, 10  $\mu$ l aliquots of each of the fractions collected throughout the experiments, namely CFE, SF and MF samples (MF1, MF2 and MF3), were transferred in new Eppendorf tubes and stored at 80 °C until use.

### 2.2.3 Protein quantification

Protein quantification in crude extracts was performed with a Pierce bicinchoninic acid (BCA) protein assay kit (Thermo Fisher Scientific, Lausanne, Switzerland) according to the manufacturer's instructions. A calibration curve using BSA was established in the same buffer conditions as the analyzed samples to calculate the concentrations of proteins.

### 2.2.4 SDS-PAGE

SDS-polyacrylamide gel electrophoresis (PAGE) was performed with gels containing 12% acrylamide using the MiniProtean 3 system (Bio-Rad). Samples containing 50  $\mu$ g protein were mixed with 2 x loading buffer (100 mM Tris-HCl (pH 6.8), 200 mM dithiothreitol, 4% SDS, 0.2% Bromophenol Blue and 20% glycerol) and incubated for 5 min at 95°C before loading into the gel.

### 2.2.5 Coomassie gel staining

After electrophoresis, the lanes designated for staining were cut from the rest of the gel with a scalpel and stored for 2 h at room temperature in a Coomassie staining solution (20% (v/v) methanol, 10% (v/v) acetic acid, and 0.1% (w/v) Coomassie Brilliant Blue R) and then destained for 2 h at room temperature in destaining solution (25% (v/v) ethanol and 7.5% (v/v) acetic acid).

### 2.2.6 In-gel sample digestion

For proteomic identification, aliquots of samples were mixed with 2x loading buffer (100 mM Tris-HCl (pH 6.8), 200 mM dithiothreitol, 4% SDS, 0.2% Bromophenol Blue and 20% glycerol) and incubated for 5 min at 95 °C before loading into SDS-polyacrylamide gel electrophoresis



(PAGE) and stained after run with Coomassie blue. Gel pieces were cut at the migration level of interest and proteins were in-gel digested. Briefly, samples were reduced in 10 mM dithioerythritol (DTE) alkylated in 55 mM iodoacetamide (IAA), and gel pieces were dried. Digestion was performed overnight at 37 °C using mass spectrometry grade trypsin and LysC protease (Thermo Fisher Scientific) at a concentration of 12.5 ng/ $\mu$ l in 50 mM Ammonium Bicarbonate (AB) and 10 mM CaCl<sub>2</sub>. The resulting peptides were extracted in 70% ethanol and 5% formic acid. Samples were dried by vacuum centrifugation followed by a re-solubilization in a 0.1% TFA / water solution and then cleared with home-made C18 stage desalting tips followed by a drying step and storage at 20 °C.

### 2.2.7 Shotgun LC-MS/MS analysis

Shotgun mass spectrometry (MS) analysis was performed on an Orbitrap Exploris 480 mass spectrometer (Thermo Fisher Scientific) coupled to a nano-UPLC Dionex pump. For liquid chromatography (LC)-MS/MS analysis, Trypsin/LysC digested samples were resuspended in 30-60  $\mu$ L of a mobile phase (solvent A: 2% acetonitrile (ACN) in water, 0.1% formic acid (FA)) and then separated by reversed-phase chromatography using a Dionex Ultimate 3000 RSLC nanoUPLC system on a home-made 75  $\mu$ m ID  $\times$  50 cm C18 capillary column (Reprosil-Pur AQ 120 Å, 1.9  $\mu$ m) in-line connected with the MS instrument. Peptides were separated by applying a non-linear 150 min gradient ranging from 99% solvent A to 90% solvent B (90% ACN and 0.1% FA) at a flow rate of 250 nl/min. For spectral library and charge state determination of the peptides from PceA, PceB, PceC, PceT and the F1  $\alpha$ -subunit of the ATP synthase, the MS instrument was operated in data-dependent mode (DDA). Full scan MS spectra (300-1500 m/z) were acquired at a resolution of 120'000 at 200 m/z. Data-dependent MS/MS spectra were recorded followed by HCD (higher-energy collision dissociation) fragmentation on the ten most intense signals per cycle (2 s), using an isolation window of 1.4 m/z. HCD spectra were acquired at a resolution of 60'000 using a normalized collision energy of 32 and a maximum injection time of 100 ms. The automatic gain control (AGC) was set to 100'000 ions. Charge state screening was enabled such that unassigned and charge states higher than six were rejected. Precursors intensity threshold was set at 5'000. Precursor masses previously selected for MS/MS measurement were excluded from further selection for a duration of 20 s, and the mass exclusion window was set at 10 ppm.

### 2.2.8 Data processing and database searches

PEAKS Studio X+ Pro software (Bioinformatics Solutions Inc.) was used for data processing. The raw MS data files were imported into PEAKS Studio software using the following parameters for the database search. For protein identification, the UniProt/Swiss-Prot *Dehalobacter restrictus* database (Proteome ID UP000018934) combined with a decoy database was used.

## 2.3 Results and discussion

The protocol, as described in the Materials and methods section, was further subjected to numerous changes leading to the definition of a fine-tuned proteomics protocol tailored for Pce proteins absolute quantification. These improvements with the corresponding results are thoroughly discussed in this section.

### 2.3.1 Preliminary in-gel shotgun LC-MS/MS analysis

To confirm the earlier findings, a preliminary in-gel shotgun analysis on cell-free extract and subcellular fractions of *D. restrictus* was performed (**Figure 2.3**). This was mainly required because of the difference in detection normally due to the use of distinct MS instruments. For this experiment the denaturing ionic detergent SDS was chosen, as it was commonly used to solubilize membrane proteins in complex sample matrix [99].

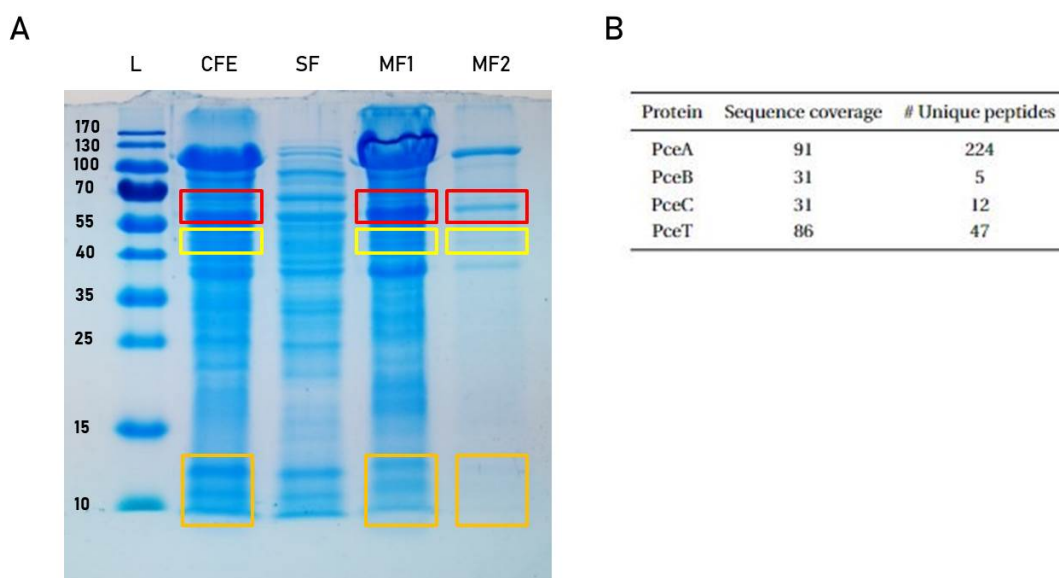


Figure 2.3: SDS-PAGE gel of subcellular fractions of *D. restrictus*. A) SDS-PAGE gel prior the excision of the different gel slices. The coloured boxes represented the portions of the gel excised and subjected to LC-MS/MS analysis. In red the boxes corresponding to the area where PceA is likely to migrate, while the yellow and orange boxes are referred to PceC and PceB, respectively. B) Sequence coverage of Pce proteins of *D. restrictus* from in-gel LC-MS/MS analysis of membrane fraction after solubilization with 2% SDS (MF1).

The MS shotgun analysis on the different SDS-PAGE gel lanes confirmed a high sequence coverage for PceA and PceT in the membrane fraction after first treatment with 2% SDS (MF1), 91% and 86% respectively, while for both PceB and PceC only 31% of the sequences was detected (**Table 2.1**). If compared with the earlier findings [89], a significant improvement in sequence coverage was achieved for most of the proteins of interest except for PceC.

Table 2.1: List of detected peptides belonging to each of the Pce protein targets after the in-gel LC-MS/MS (see **Figure 2.3**).

Protein	Sequence	Mass [m/z]
PceA	TFDPEANK (light)	461.219257
PceA	FHYDDVSK (light)	505.732531
PceA	DLPTLNAER (light)	514.772188
PceA	LLGADLVGIAPYDER (light)	801.430312
PceA	WTYSTWGR (light)	528.748516
PceA	ILKPCK (light)	351.22256
PceA	YLPWDLPK (light)	516.28166
PceA	FEPDWEK (light)	475.71635
PceA	YAGFKPK (light)	405.729063
PceA	SVIVFVLEEDYEAIR (light)	891.469634
PceA	TSPSVISSATVGK (light)	617.337892
PceA	NGLLITQK (light)	443.77146
PceA	VLQPEDCEVAENPYTEK (light)	982.451313
PceA	WHLDSNR (light)	464.225208
PceA	VETWNHDVAR (light)	613.799268
PceA	IATQIPLLQDAAR (light)	705.409183
PceA	FDEWFGYNGPVNPDER (light)	971.423747
PceA	DFWNNPESIK (light)	625.296027
PceB	GGTALIPAIITYR (light)	673.395544
PceB	LANHPAK (light)	375.716487
PceB	ESSDTISA (light)	405.179797
PceC	AELENR (light)	366.18776
PceC	NVLGVISIEK (light)	536.324056
PceC	IDTAQGR (light)	380.701034
PceC	QGETPVFFER (light)	605.29857
PceC	YFDGFQGLAIK (light)	629.826963
PceC	EPIYLGGAYGYSGYLGSIK (light)	1004.50675
PceC	TNNYIDR (light)	448.217048
PceC	VTGSTVSSHAAEAVNK (light)	828.931208
PceC	SLNISQK (light)	395.226885
PceC	EEQETWSSHS (light)	610.246731
PceT	TNDYVIVDIDGYEK (light)	822.393592
PceT	DATVPVIR (light)	435.755809
PceT	LIVGSEGVFR (light)	538.808573
PceT	EVSANLLGK (light)	465.766374
PceT	WWGSEFTFTVK (light)	694.337695
PceT	SVFVVK (light)	339.712882
PceT	KPELTEELIR (light)	614.350802
PceT	EANILLIFQALVK (light)	736.447777
PceT	YEFDEEELDSAAEDLYK (light)	1033.44167
PceT	FTEELK (light)	383.702711
PceT	EEINLTPDEIK (light)	650.835182
PceT	TIDYLLK (light)	433.255111

Furthermore, it appeared that 2% SDS sample preparation resulted in high recovery of the proteins of interest, although all proteins were also detected in the soluble fraction and in MF2. This led to conclude that no difference in MS detection was observed between 2% and 4% SDS sample preparations and also confirmed that the treatment with 2% SDS ensured a good level of membrane solubilization. From this analysis a preliminary list of all detected peptides belonging to each of the protein targets was compiled (**Table 2.1**).

To confirm the usefulness of these peptides for the quantitative approach, the resulting peptides were targeted by a further selected reaction monitoring (SRM) analysis. For this experiment, in-gel samples of the last round of experiment were analyzed.

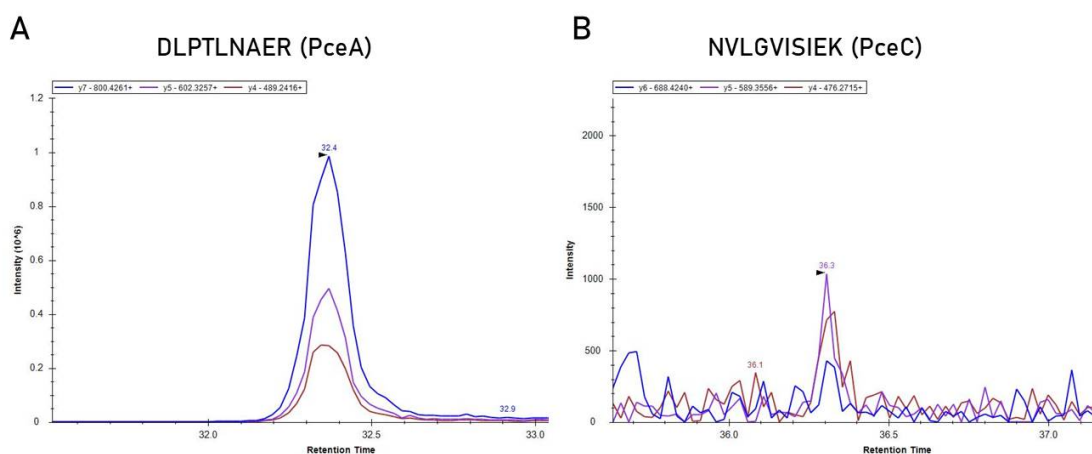


Figure 2.4: Examples of MS/MS spectra using SRM method of two peptides belonging to PceA and PceC, respectively. The peaks show the intensity of the different product ions derived from the target peptide. A) The MS fragmentation of DLPTLNAER belonging to PceA generate a neat spectrum while B) the intensity of the product ions of the PceC peptide NVLGVISIEK are not measurable.

From the generated spectra, two to three best peptides for each protein were selected. The resulting data allowed to select only the best suited peptides, which were again analysed by SRM using also the best 2-3 transitions (fragments) of these peptides for the future quantitative use (**Figure 2.4**).

### 2.3.2 Effect of detergent on protease activities and optimization of digestion conditions

Prior to finalize the list of peptides, further improvement and validation in the detection of the candidate peptides for PceB was required. To achieve this, several changes in the solubilization protocol were proposed in the next experiment. As defined in earlier studies, the use of high concentration of SDS is detrimental for an efficient MS analysis since it precludes enzymatic digestion and dominates mass spectra due to its ready ionizability and great abundance compared to individual peptides [100]. To overcome this issue, a mass spectrometry-compatible

detergent, namely RapiGest, supporting enzymatic cleavage of the membrane proteins, was proposed as alternative solubilizing agent. In addition, in-solution proteolysis was also proposed to compare the results with in-gel MS analysis and the use of different proteolytic enzymes, namely Chymotrypsin and Glu-C, were also suggested to evaluate any improvement of sequence coverage.

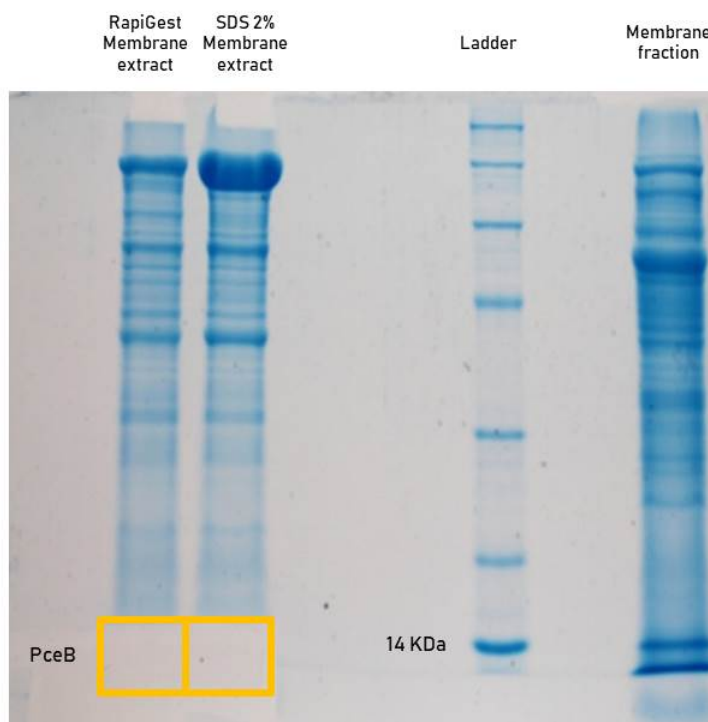


Figure 2.5: SDS-PAGE gel loaded with 10  $\mu$ l of membrane extract treated with 0.2% RapiGest or 2% SDS respectively. 10  $\mu$ l Membrane fraction suspension prior the addition of solubilizing agents was also loaded. The yellow boxes represent the portions of gel used for in-gel MS analysis.

In summary, the proposed experiment aimed at comparing the recovery of the proteins of interest by testing alternative solubilizing agents (RapiGest *vs* SDS), digestion procedures (in-gel *vs* in-solution) and alternative proteolytic enzymes (Chymotrypsin *vs* Glu-C). For this experiment, 300 mg of wet biomass of *D. restrictus* was resuspended with 50 mM Tris-HCl buffer supplemented with the protease inhibitor cocktail and successively split into two equal fractions. After ultracentrifugation, the solubilization of the pellet was performed with either 0.2% RapiGest or 2% SDS. An aliquot was taken for SDS-PAGE (**Figure 2.5**) and the rest of the in-solution samples was digested either with chymotrypsin or Glu-C in-solution.

The results showed that no substantial difference in sample processing (in-gel *vs* in-solution) and digestion (Glu-C *vs* chymotrypsin) was observed between samples prepared with RapiGest or SDS. Furthermore, increased sequence coverage of all the proteins of interest was achieved

Table 2.2: Comparison of MS sequence coverage of PceB by testing alternative solubilizing agents (RapiGest and SDS), digestion procedures (in-gel and in-solution) and alternative proteolytic enzymes (trypsin, chymotrypsin and Glu-C).

Protease	Digestion	Solubilizing agent	Sequence coverage
Trypsin	in-gel	SDS	31% (from Tab 2.1)
Trypsin	in-gel	RapiGest	26%
Glu-c	in-gel	RapiGest	40%
Glu-c	in-solution	RapiGest	24%
Chymotrypsin	in-solution	RapiGest	62%
Chymotrypsin	in-solution	SDS	54%

using chymotrypsin. In particular, PceB sequence coverage was significantly improved (62%) using chymotrypsin as compared to Glu-C and the earlier used trypsin. Strikingly, the results showed the presence of peptides featuring tryptic cleavage in samples digested exclusively with chymotrypsin (see **Table 2.2**).

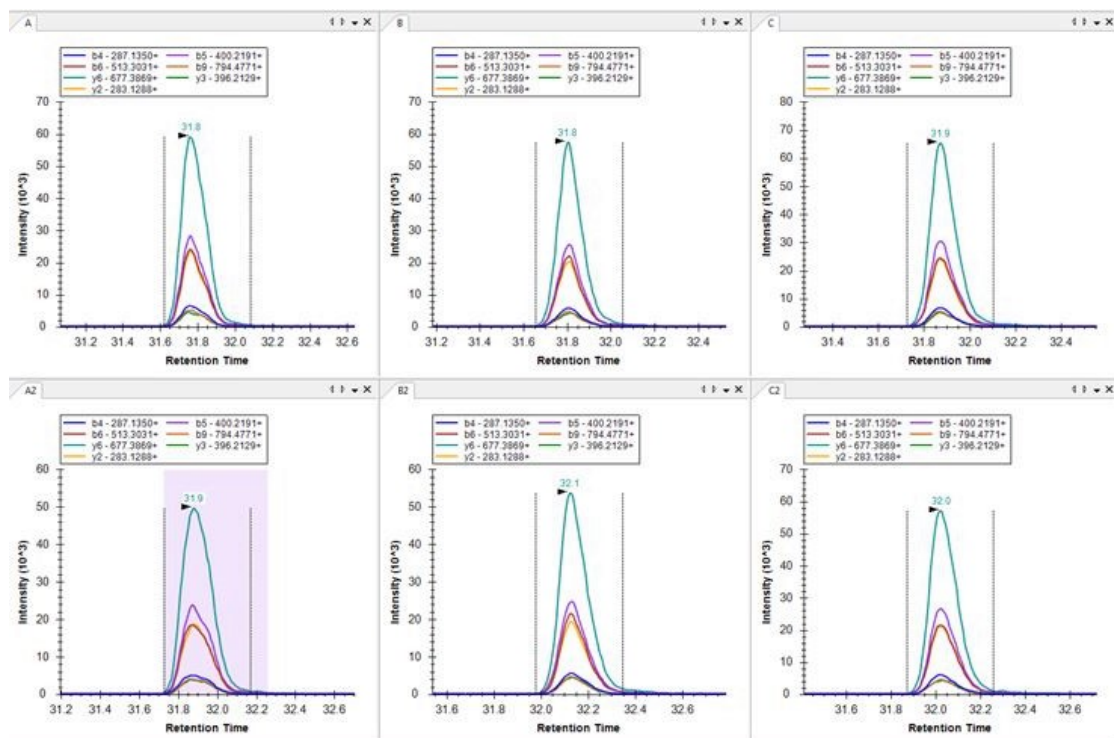


Figure 2.6: Validation via SRM of the only one PceB detected: GGTALIPAIITY. The analysis was performed in biological duplicates and technical triplicates (series from A to C).

Chymotrypsin is a protease that has alternative cleavage specificity to trypsin. It primarily cleaves at the hydrophobic aromatic amino acid residues of tryptophan, tyrosine, and phenylalanine. However, additional cleavage at other sites such as leucine, histidine, and methionine

might occur but with a lower level of specific activity. The unspecific cleavage properties of chymotrypsin may introduce experimental variation in sample preparations and thus bias in peptides quantification.

This aspect was further evaluated by analyzing the different cleavage products of PceB in technical triplicates using SRM. The results showed that only one peptide (EGGTALIPAIITY.R) was successfully validated (**Figure 2.6**). Furthermore, we observed that PceB cleavage by chymotrypsin is reproducible between replicates but the selection of ideal target peptides for absolute quantitative purposes remains challenging for this short protein.

### 2.3.3 Validation of proteotypic peptides via SRM

As validation and confirmation of the best peptides for quantitative MS, in-solution sample in presence of RapiGest was digested with trypsin and later analyzed via SRM. The analysis permitted to validate for PceA and PceT at least two tryptic peptides while for PceC one peptide (NVLGVISIEK) was validated showing good transitions whereas the other one (YFDGQGLAIK) did not show a good spectrum and could be replaced by a chymotryptic peptide if needed (**Figure 2.7**). For PceB, only one semi-tryptic peptide (F.GGTALIPAIITYR.L) was successfully validated via SRM and it covered almost the same sequence of the one previously defined with chymotrypsin digestion except that the semi-tryptic fragment has a C-term arginine (R) residue. However, this peptide does not reflect the predicted cleavage map by trypsin and it represents a truncated version of its full expected length (R.EYQAIGMGFIFFGGTALIPAIITYR.L). The SRM analysis confirmed the predominantly presence of the form cleaved after residue F74 as well as the absence of the full-length tryptic fragment of this sequence indicating that the truncated form is predominant in the sample.

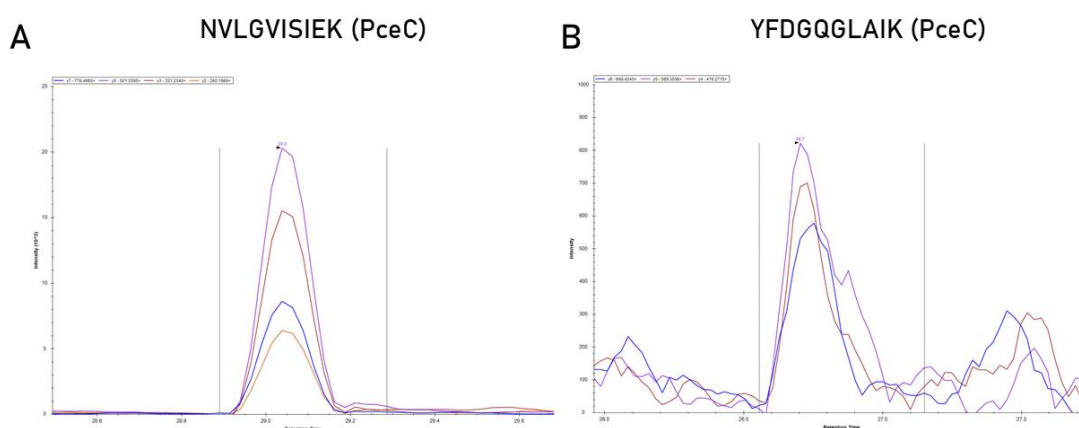


Figure 2.7: Examples of MS spectra of two peptides belonging to PceC protein. A) The spectrum of NVLGVISIEK peptide shows a well-defined product ions peaks pattern, B) MS spectrum of YFDGQGLAIK peptide displays not optimal product ions pattern.

Several hypothesis were postulated to explain the detection of a truncated form of an expected tryptic peptide. One possibility accounted for the presence of endogenous proteolytic enzymes which were released upon cell lysis and eventually resulted in the cleavage at residue F. Otherwise, the hypothesis of autocleavage rather than proteolytic cleavage was also considered. This could result from the in-solution sample preparation and the presence of RapiGest that have possibly induced some conformational changes of the protein resulting in spontaneous backbone cleavage through nucleophilic attack. To rule out these hypotheses, a validation of the tryptic and chymotryptic cleavage products of PceB was performed in a further analysis. In this experiment, additional improvements during sample preparation were applied. First, an alternative and high-performance protease inhibitor, the complete EDTA-free protease inhibitor cocktail, was tested. In addition, to overcome the hypothesis of in-solution protein degradation or modification due to over-exposure in the sample matrix, the enzymatic digestion of the sample was carried out immediately after RapiGest solubilization. Cell-free extract and membrane fraction of *D. restrictus* were resuspended in parallel in Tris-HCl buffer, DNase I and protease inhibitor, as well as in buffer depleted in the protease inhibitor. To enhance the membrane solubilization RapiGest concentration was also increased and it was added to the samples at a final concentration of 1%, the highest possible concentration according to the manufacturer's instructions.

Table 2.3: Sequence coverage of Pce proteins in cell-free extract and membrane fraction samples. All the samples were treated with RapiGest prior to MS analysis. The effect of High performance Protease inhibitor (PI) on in-solution protein degradation was evaluated.

Digestion	Protein	Coverage (%) CFE + PI	Coverage (%) CFE w/o PI	Coverage (%) MF + PI	Coverage (%) MF w/o PI
Chymotrypsin	PceA	66	91	93	88
	PceB	30	44	32	56
	PceC	4	26	27	37
	PceT	19	66	53	86
Trypsin	PceA	81	81	73	84
	PceB	30	23	15	20
	PceC	25	29	12	25
	PceT	67	64	52	67

The results showed in **Table 2.3** revealed that under trypsin digestion the truncated peptide (EGGTALIPAITYR.L) was detected in spite of the presence of protease inhibitor. This allowed us to conclude that the hypothesis of endogenous proteolytic digestion was unlikely. Interestingly, under chymotrypsin digestion the peptide (EGGTALIPAITYR) was shown only in samples without protease inhibitor. Overall, the experiment confirmed the difficulty to detect this specific peptide and the alternative use of chymotrypsin or trypsin did not bring any improvement. However, an additional test was performed on in-gel trypsin digestion to evaluate if the detection of the truncated fragment was reproducible also in this experimental condition. For this experiment, 45  $\mu$ g of cell-free extract sample was loaded into a gradient (4-12%) NuPAGE gel, which ensured good resolution at low molecular weight level. After migration, five gel pieces, numbered from the lowest to the highest molecular weight,



targeting the region between 3 and 13 kDa were cut and analyzed via LC-MS/MS analysis. Gel band #2 revealed the highest sequence coverage of PceB with 58% and the presence of the truncated peptide was still observed. Furthermore, PceB was also detected in other gel bands, however with lower sequence coverage. This is likely due to carryover contamination during the LC-MS analysis or trailing of the protein during gel migration. Overall, the analysis confirmed that the presence of the truncated form might be true and biologically relevant since it was also clearly detected in the gel band #1 which corresponds to the lowest molecular weight migration point. However, further experiments would be required to investigate this hypothesis.

### 2.3.4 Definition of the peptide signatures for Pce proteins

As result of the validation of the tryptic peptides via LC-MS/MS and via SRM, a list of the best 2 or 3 peptides for each protein of interest was compiled. At this stage, alongside with the *pce-ABCT* encoded proteins, the F1  $\alpha$ -subunit of the ATP synthase was included as housekeeping protein, since it was detected with a high sequence coverage and reproducible signal intensity in a preliminary MS analysis performed on cell-free extracts and membrane fraction of *D. restrictus*.

Table 2.4: List of heavy-labelled peptides. For each peptide, the labelled amino acid is marked in red. All the indicated mass-to-charge (m/z) ratios are given for a peptide charge state of 2. Reference peptides used for PRM analysis are indicated in bold. Indicated with a star (\*) is the peptide used for *D. hafniense* strain TCE1, while (\*\*) indicates is the alternative peptide used for *D. restrictus*.

Peptide #	Species	Sequence	Mass [m/z] Light / Heavy
1 *	PceA	YLPWDL <b>P</b> K	516.28166 / 520.28876
2 **	PceA	TSPSVISSAT <b>V</b> G <b>K</b>	617.33789 / 621.34499
3	PceA	IATQIPLLQDA <b>A</b> R	705.40918 / 710.41332
4	PceA	LLGADLVGIAPY <b>D</b> E <b>R</b>	801.43031 / 806.43445
5	PceB	GGTALIPAIIT <b>Y</b> R	673.39554 / 678.39968
6	PceB	LANHP <b>A</b> K	375.71649 / 379.72359
7	PceC	NVLGVISIE <b>K</b>	536.32406 / 540.33116
8	PceC	QGETPVFF <b>E</b> R	605.29857 / 610.3027
9	PceC	EPIYLGGAYGYSGYLGS <b>I</b> K	1004.50675 / 1008.51385
10	PceC	YFDGFQGLAI <b>K</b>	629.82696 / 633.83406
11	PceT	EV <b>S</b> ANLLG <b>K</b>	465.76637 / 469.77347
12	PceT	WWGSEFTFT <b>V</b> K	694.3377 / 698.34479
13	PceT	DATVPV <b>I</b> R	435.75581 / 440.75994
14	ATP synthase	ELIIG <b>D</b> R	408.2377 / 413.2388
15	ATP synthase	ELSLLL <b>K</b>	408.2655 / 412.2726
16	ATP synthase	QVAGQL <b>R</b>	386.2272 / 391.2314

The selection of the peptides was based on unique proteotypic peptide sequences and features that enhance chemical stability as indicated in the next sentences. Priority was given to those peptides that were previously identified in the discovery dataset with high MS/MS spectral quality and validated by SRM analysis.

Peptides containing cysteine or methionine residues were excluded. Peptide uniqueness was confirmed by searching against the *D. restrictus* proteome database. Furthermore, an additional criterion was that the selected peptides display a fully conserved amino acid sequence in the protein homologues from both *D. restrictus* and *D. hafniense* strain TCE1. The screening resulted in a selection of 16 peptides, accounting for 2 or 3 peptides for each protein of interest (**Table 2.4**). Therefrom the synthetic, accurately quantified heavy-isotope labelled reference peptides, with either C-terminal heavy lysine (K) or arginine (R) were purchased from JPT Peptide Technologies GmbH (Berlin, Germany).

### 2.3.5 Qualitative and quantitative validation of heavy-labelled peptides

After the development of the solubilization protocol and the definition of the reference peptides, the following step in the quantitative proteomics approach was a qualitative and quantitative validation of the heavy-labelled peptides. The first experiment was performed on cell-free extracts of *D. restrictus* to validate the behaviour of the labelled peptide surrogates in presence of an endogenous sample.

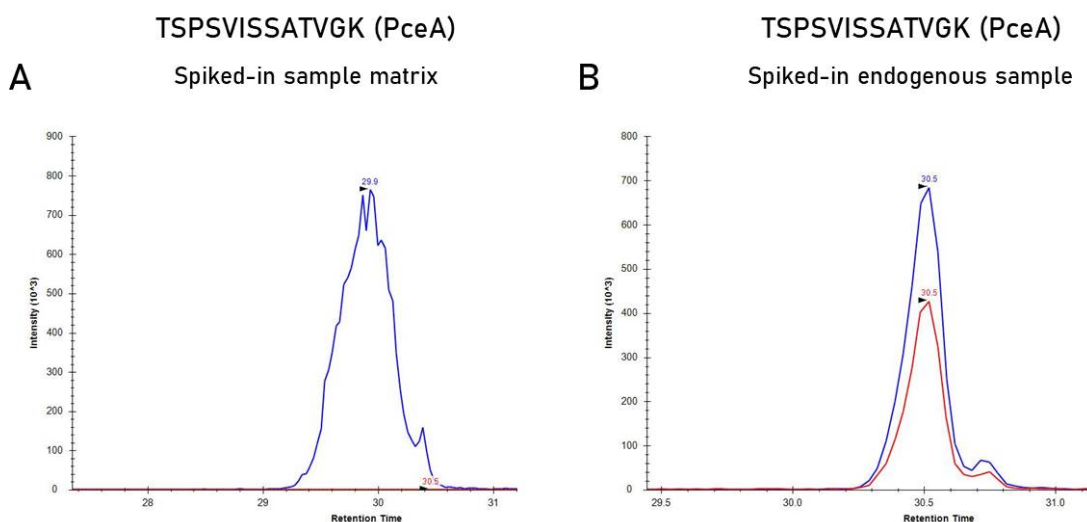


Figure 2.8: Validation of heavy-labelled peptides via SRM method. The blue line represents the intensity of the heavy labelled peptide while the red line is the intensity of the endogenous peptide. TSPSVISSATVGK peptide belonging to PceA was taken as an example for this analysis. A) Heavy labelled peptide spiked in absence of endogenous sample. B) heavy labelled peptide analysed in presence of 2  $\mu$ g cell-free extract sample of *D. restrictus*

An aliquot of 2  $\mu$ g of digest proteins was spiked-in with 125 fmol of heavy-labelled peptides and analyzed. In parallel, 250 fmol of heavy peptides resuspended in only Tris-HCl, protease inhibitor and 1% RapiGest were analyzed to assess their detection in presence of the sole sample matrix. The results showed that, for most of the peptides, the heavy form largely exceeded the amount of the endogenous form and this required an adjustment in concentration. In addition, strong variability was observed in the signal of some of the heavy-labelled peptides likely due to solubilization issues.

These aspects were further investigated in an additional test experiment where the amount of endogenous sample of *D.restrictus* was fine-tuned in relation with the spiked heavy-labelled peptides. In the experiment, 5  $\mu$ g of sample were digested in presence of spiked-in heavy peptides (2 pmol) and injected at different volumes (2-8  $\mu$ l). As shown in **Figure 2.9**, overall a good ratio between endogenous and heavy-labelled peptides, and a good linearity between the sample volume injected and the detected signal were observed.

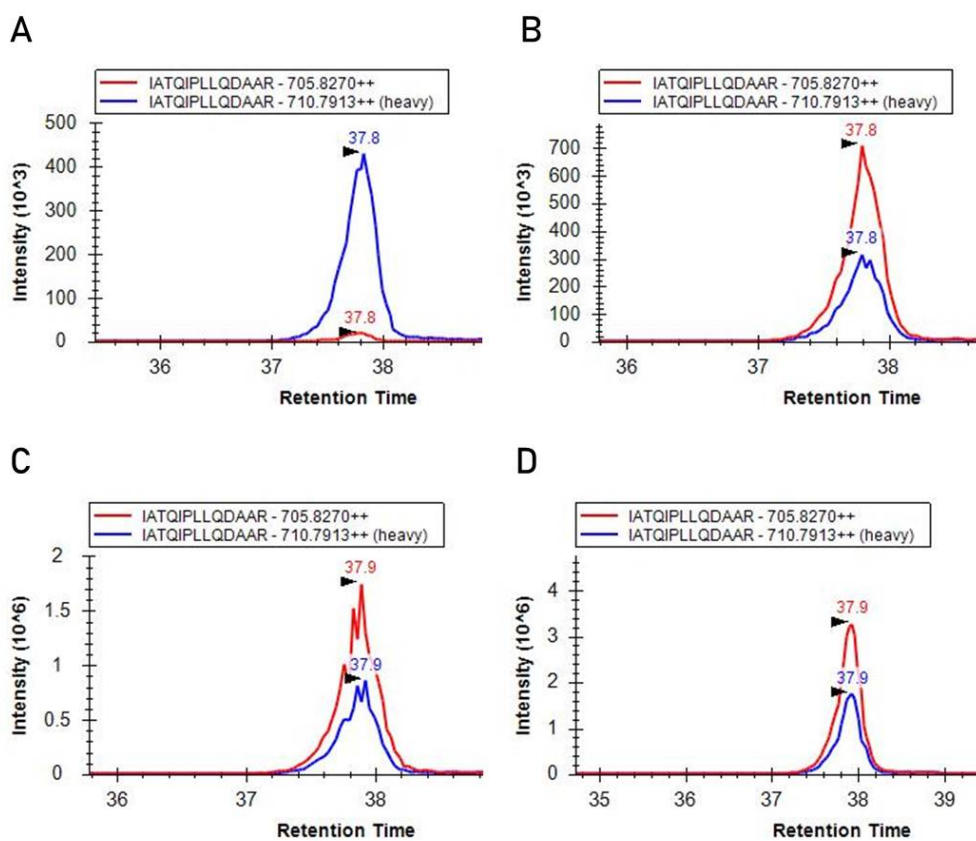


Figure 2.9: Fine-tuning ratio between endogenous (red line) and heavy-labelled (blue line) peptides signal. IATQIPLLQDAAR peptide belonging to PceA was taken as example for this analysis. A) heavy-labelled peptide in absence of endogenous sample. B) Analysis of 2  $\mu$ l of heavy-labelled peptide and endogenous sample mixture. C) 4  $\mu$ l of heavy-labelled peptide and endogenous sample mixture. D) 8  $\mu$ l of heavy-labelled peptide and endogenous sample mixture.

To test the reproducibility of the ratio between light and heavy peptides in technical replicates, the biomass of *D. restrictus* collected at different growth phases, namely logarithmic and stationary phase, were used as initial samples. Each sample was diluted to a final concentration of 2 mg/ml. Later, 10  $\mu$ l of 2 mg/ml cell-free extract samples were transferred in a new Eppendorf tube and supplemented with 10  $\mu$ l of 1% RapiGest. Three technical replicates for each biological replicate were analyzed via SRM (**Figure 2.10**).

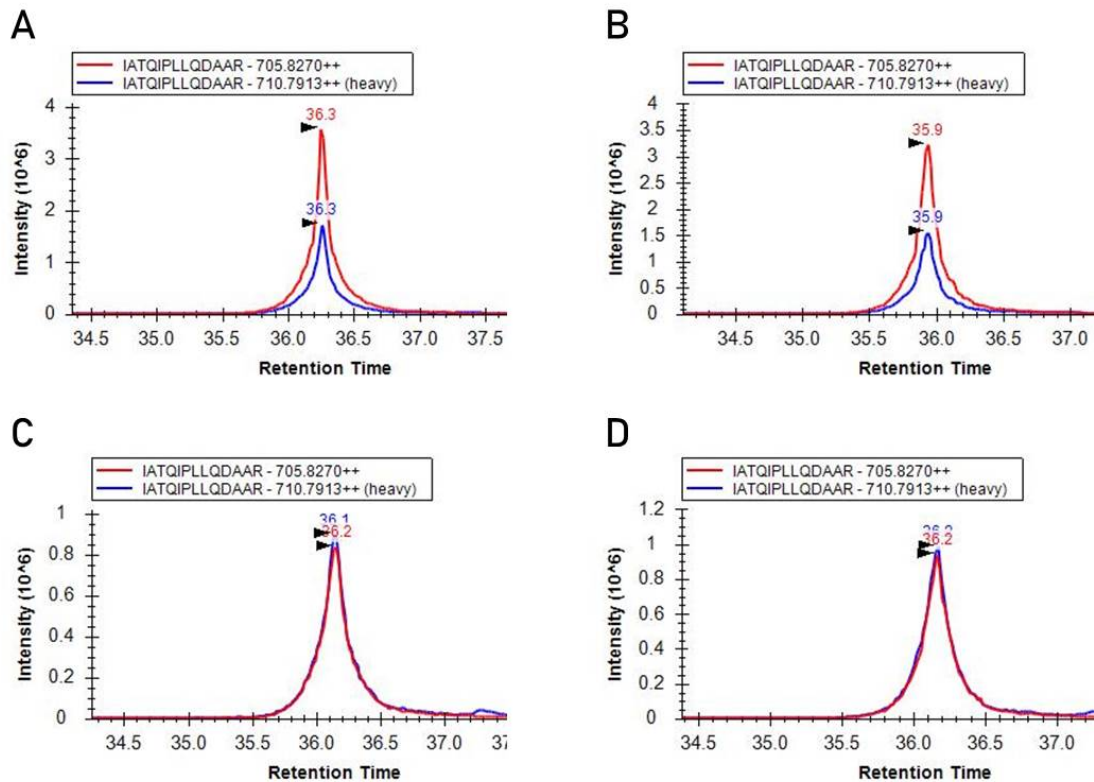


Figure 2.10: SRM analysis of logarithmic vs stationary cell-free extract of *D. restrictus*. IATQIPLLQDAAR peptide belonging to PceA was taken as example for this analysis. A) and B) two technical replicate of cell-free extract of *D. restrictus* collected at logarithmic growth phase. C) and D) duplicates of cell-free extract of *D. restrictus* collected at stationary growth phase.

The results showed a higher concentration of proteins in the logarithmic phase if compared with that of the stationary phase for all the proteins of interest, while similar amounts of ATP synthase were observed in both phases. This latter result confirmed the reliability of ATP synthase as housekeeping protein and further showed equal protein extractions for both types of sample. However, high variability in absolute quantification was observed for different peptides belonging to the same protein (**Figure 2.11**). This was due to the experimental approach chosen. Indeed, some endogenous peptides belonging to the same protein are cleaved only partially or less efficiently resulting in different ratios of light and heavy peptides in the same protein.

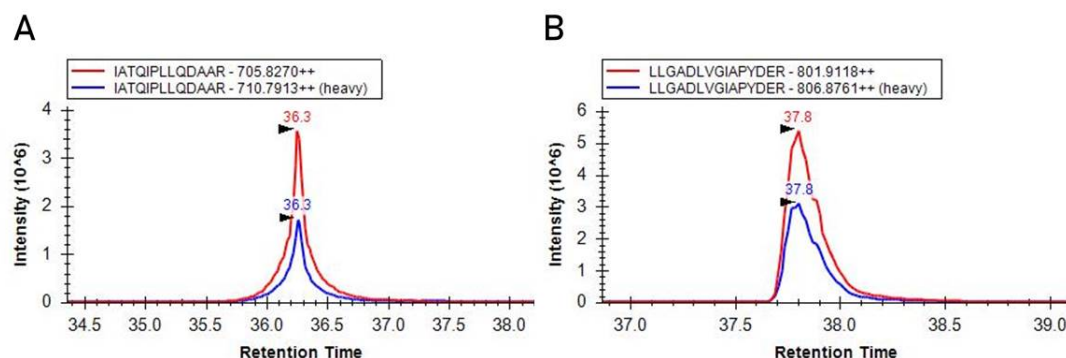


Figure 2.11: Quantification of two peptides of PceA belonging to logarithmic cell-free extract of *D. restrictus* via SRM method. The results showed strong intra-sample variability in quantification of two different peptides belonging to the same protein. PceA peptides: IATQIPLLQDAAR and LLGADLVGIAPYDER were taken as examples for this analysis.

Theoretically, if a specific peptide is efficiently cleaved from a whole protein sequence, the derived values/ratios with its relative heavy surrogate should be more reproducible. This is a clear limitation of this experimental approach and the ultimate way to improve this bias would be to use of a full-length, heavy-labelled protein standard for quantitative studies, as the protein standard mimic the *in-vitro* digestion efficiency of the endogenous (light) protein. This option was not pursued due to the elevated costs and the time constraints required for the purchase and the shipment of heavy-labelled protein. However, the synthetic polypeptide corresponding to the C-terminal of PceB and including the single target PceB peptide was considered as alternative strategy to gain more confidence on the applicability of the unique PceB peptide for quantitative purpose. This experiment is thoroughly discussed in the following section.

### 2.3.6 Validation of the unique PceB reference peptide

For PceB, due to the overall scarcity and low solubility of its peptides, it was sought to validate the reproducible quantification of the single PceB tryptic peptide LANHPAK by assessing the digestibility and recovery of this peptide, using a synthetic, quantified form of the C-terminal part of PceB spanning the sequence of amino acid residues from 63 to 105 (ProteoGenix, Schiltigheim, France). The sequence included the complete third transmembrane helix of PceB together with the C-terminal hydrophilic end (EYQAIGMGFIFFGGTALIPAITTYRLANHPAKKIRESSDTISA). The cleavage fingerprint of the synthetic PceB protein obtained after tryptic digestion indicated that the sole peptide used for PRM (LANHPAK) was representative of the whole protein and thus gave the necessary confidence in using only one peptide for PceB protein quantification. This conclusion was based on LC-MS analysis of all the fragment fingerprints generated post-trypt/LysC digestion, where the reference peptide LANHPAK was the most abundant cleavage product found. Other miss-cleaved (-KK) forms or truncated

forms of PceB represented <1% (relative LC-MS peaks area) of the main proteolytic products. Furthermore, digestion of different amounts (50 ng and 1.25  $\mu$ g) of the quantified synthetic PceB protein standard were tested in 5 technical replicates. In each of the tubes, heavy-labelled peptide standards were spiked-in and PRM analysis was performed (**Figure 2.12**).

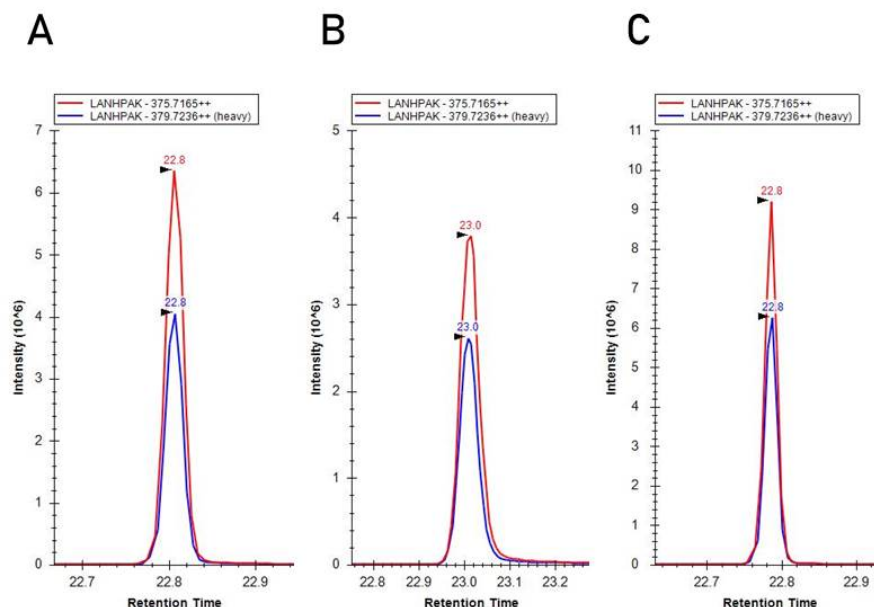


Figure 2.12: Validation of the unique PceB heavy-labelled peptide (LANHPAK) of PceB via PRM method. Different amounts (from 50 ng to 1.25  $\mu$ g) of the quantified synthetic PceB protein standard were tested in 5 technical replicates. MS spectra of three technical replicates (A, B and C) of 1.25  $\mu$ g amount of synthetic PceB protein are shown.

The concentration of the synthetic PceB protein standard was measured by BCA at 850 fmol per injection, while the spiked-in heavy peptide standard accounted for 480 fmol per injection. The ratio of light/heavy (L/H) PceB peptides was calculated to be 1.3, 1.51 and 1.59 in the replicates 1-3, respectively, which resulted in a measured light PceB value of approximately 1,47 (mean ratio)  $\times$  480 fmol= 704 fmol. The replicates 4 and 5 were significantly higher as compared to replicates 1-3. Solubility issues associated with this PceB peptide as well as delay in the sample processing may have contributed to this variation. Therefore only replicates 1-3 were used for the calculations. For the 50 ng sample aliquots, large analytical variability was observed likely due to the relative loss and overall poor solubility of PceB at low concentrations. Therefore, only the 1.25  $\mu$ g aliquots were used for calculations. Overall, quantitative analysis by PRM revealed a difference of 19% in PceB concentrations, which was taken as acceptable considering the analytical variation as well as quantification using the BCA assay. The overall coefficient of variation (CV) was calculated at 13.5% using five technical replicates (heavy PceB peptide standard) and was therefore within the acceptable range for these types of assays (MRM and PRM).



### 2.3.7 Definition of limit of detection (LoD) and limit of quantification (LoQ) of heavy and light peptides

In parallel with a qualitative and quantitative validation of the heavy peptides, it was also important to define a calibration curve of each heavy-labelled peptide against identical amounts of the endogenous sample. Thus, the following experiment aimed at defining the limit of detection as well as the linearity of each heavy peptide at increasing concentrations against fixed concentrations of endogenous proteins.

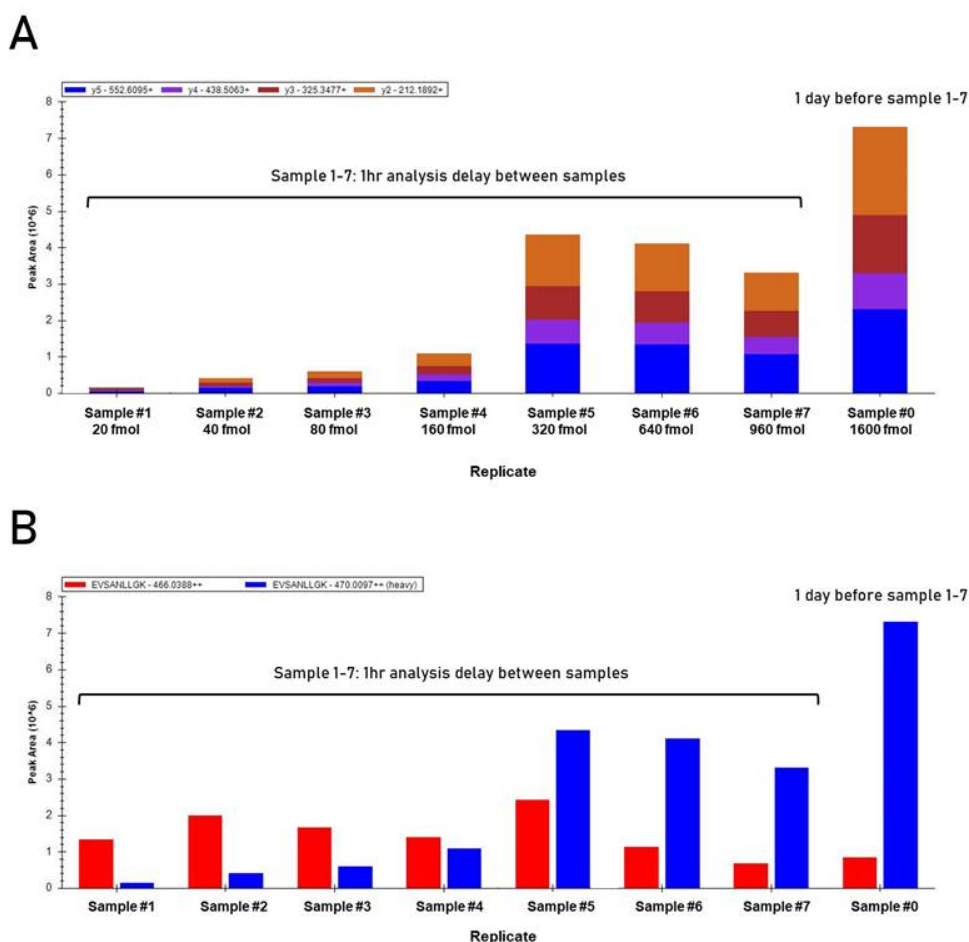


Figure 2.13: Detection of heavy-labelled peptides against identical amounts of the endogenous cell-free extract sample of *D. restrictus* via SRM method. The peptide EVSANLLGK belonging to PceT protein was taken as example for this analysis. A) Graphical representation of the signal intensity of the heavy labelled peptide EVSANLLGK measured in different dilutions of cell-free extract sample. Each bar accounts for the signal intensity of product ions generated by the ionization of heavy labelled peptide EVSANLLGK. B) Graphical representation of the signal intensity of the heavy labelled (blue bar) and endogenous (red bar) peptide EVSANLLGK measured in different dilutions of cell-free extract sample.

For this experiment, no technical replicates were required as a single 10  $\mu$ g sample aliquot was adequate to perform 2-3 injections that were used for determining the analytical CV. The analysis showed strong signals for all peptides. However, time-dependent loss of the target peptides was observed (**Figure 2.13**). This was initially attributed to the delay between two subsequent sample analyses (approximately 1 h), which may cause precipitation and therefore strong variability in peptide detection. To overcome this issue, it was decided to improve the protocol by solubilizing each sample individually shortly before MS analysis. However, despite the strict respect of the solubilization time prior to MS analysis, an absence of linearity between different sample dilutions was observed (**Figure 2.13A**). This issue was also noted for the endogenous light peptides (**Figure 2.13B**). Overall, this analysis led to conclude that the precipitation issue was mainly due to the intrinsic insolubility of membrane proteins. Nevertheless, the ratios between heavy and light peptides showed linearity in the different replicates meaning that the solubility issues observed did not affect absolute quantification since the heavy spike-in peptide varied in a similar manner as the endogenous peptides. To further corroborate the SRM data, the samples were also analyzed by PRM on the Q-Exactive orbitrap MS. The advantage of using PRM lies in the fact that the fragment ions are monitored on a Orbitrap and therefore have high confidence in the identification of the peptides. Furthermore, the PRM method permitted to analyze all peptides in a single run, whereas with the SRM each precursor ion/product ion transition is monitored at a time. Another analytical bottleneck for SRM was represented by the fact that chromatographic separation of peptides led to the co-elution of peptides at similar retention time.

The analysis showed a strong correlation between SRM and PRM data (data not shown), meaning that the ratios and therefore quantification were reproducible on two different LC-MS instruments. Overall, this result gave confidence in providing absolute values in spite of the solubility issues associated with these proteins. The experiment confirmed also that PRM permitted a more accurate quantification of the heavy/light ratio of the proteins of interest and for this reason was defined as the reference technique for the PceABCT quantitative proteomics approach.

### 2.3.8 Optimized sample preparation protocol

Based on the results obtained with shotgun and SRM/PRM approaches, the protocol for quantitative proteomics analysis was finalized. To summarize, in the sample matrix, a high-performance protease inhibitor was required to exclude endogenous proteolytic activity, while RapiGest was preferred over SDS as it was tested as a MS-compatible detergent achieving a high solubilization of membrane proteins. Furthermore, in-solution sample preparation was preferred over in-gel sample preparation as it ensured a higher protein detection and less time investment, while Trypsin was chosen over chymotryptic or Glu-C as it gave a high sequence coverage and required a standard labelling on arginine (R) or lysine (K) at the C-terminal end of the heavy peptide surrogates. Moreover, to normalize the protein amount prior MS analysis, each sample was diluted up to 2 mg/ml and therefrom 10  $\mu$ l (20  $\mu$ g of total protein) were



transferred in a new tube and mixed with 10  $\mu$ l of 2% RapiGest.

### 2.3.9 Application of the optimized protocol to *D. hafniense* strain TCE1

An additional experiment was performed with the aim to validate the developed protocol with cell-free extract of *D. hafniense* strain TCE1, since only *D. restrictus* was tested so far. Two biological duplicates, namely CFE from cultures collected at the logarithmic phase and stationary phases, and technical triplicates were considered for this analysis. Surprisingly, the samples were clearly much more difficult to solubilize when compared with the ones of *D. restrictus*. Some technical replicates had to be excluded because it was not possible to inject them in the current insoluble state while for others repeated centrifugation steps were required to be able to analyze the samples. Moreover, some peptides were not detected or the MS signal was too noisy due to the bad sample quality (**Figure 2.14** and therefore had to be excluded.

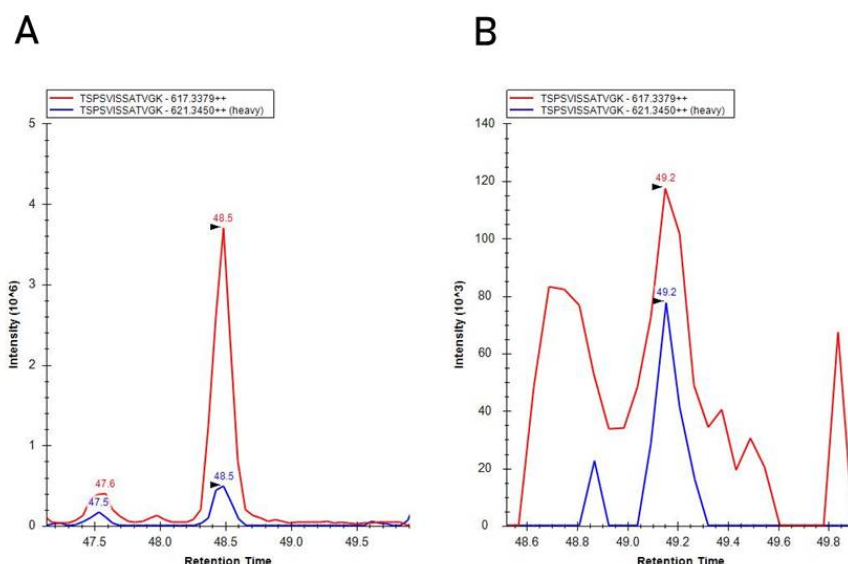


Figure 2.14: Quantification of Pce proteins in *D. hafniense* strain TCE1 via PRM method. The peptide TSPSVISSATVGK belonging to PceA was taken as example for this analysis. A) Technical replicate showing good MS signal of the endogenous and the heavy labelled peptide. B) Technical replicate showing noisy MS signal of the endogenous peptide.

The graph shows only a comparison between biological duplicates **Figure 2.15**, each one represented by one technical replicate. Theoretically, the technical and biological replicates need to be combined together to plot the graph. However, due to the high variation observed it was not possible to consider the different replicates of this data set. Strikingly, the ATP synthase peptides were the only reproducible ones across all experiments.

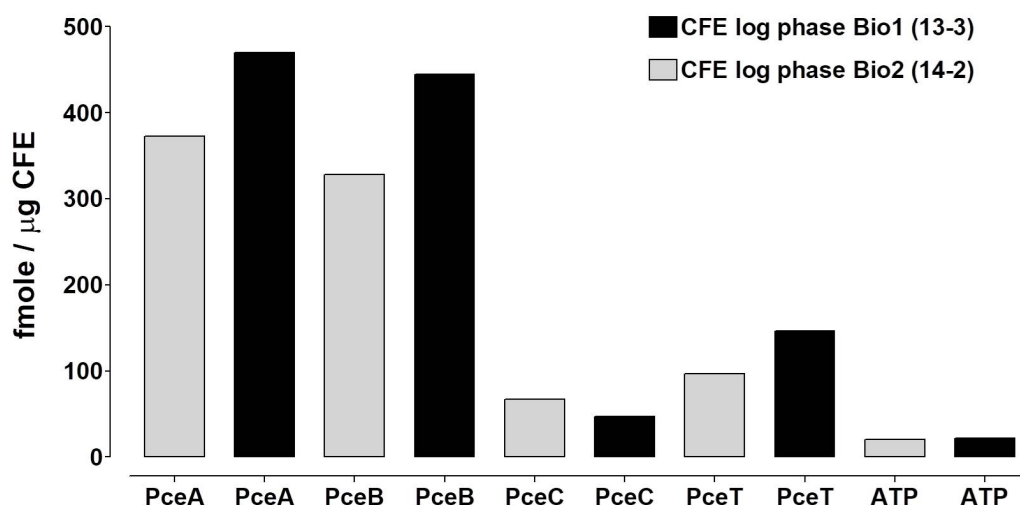


Figure 2.15: Quantification of Pce proteins of cell-free extract of *D. hafniense* strain TCE1 at logarithmic vs stationary growth phases. Only one biological replicate per each growth phase was used to build the graph.

In order to enhance the sample quality for MS analysis, further improvements were proposed at the level of sample collection after each centrifugation step. In detail, the top 80% of the supernatant obtained after mild centrifugation was collected (and considered as CFE), while the remaining 20% of volume close to the pellet was discarded. Furthermore, soluble and membrane fractions were obtained by ultracentrifugation ( $90'000 \times g$ ,  $4^\circ \text{C}$  and 30 min) of the CFE sample. At this step, the top half of the resulting supernatant was transferred to a new tube and subjected to an additional ultracentrifugation where from the top 80% of the supernatant was collected and represented the soluble fraction (SF) sample. On the other hand, the pellet obtained from the first ultracentrifugation step was resuspended in 50 mM Tris-HCl buffer containing the protease inhibitor and transferred in a new tube. Ultracentrifugation was applied again and the resulting membrane pellet was resuspended with 50 mM Tris-HCl buffer supplemented with the protease inhibitor cocktail to produce the membrane fraction (MF).

## 2.4 Conclusions

With the last improvements, the development of a final protocol for quantitative proteomics analysis, from biomass collection to the sample preparation, reached its final configuration. The tedious work discussed so far represented a crucial step to investigate and compare the relative abundance of Pce proteins in *D. restrictus* and *D. hafniense* strain TCE1. The stoichiometry of the *pceABCT* gene products at transcriptional and protein levels are presented in the following chapter with the aim to address the question of the possible function of the accessory proteins PceB and PceC in OHR.



## 3 Stoichiometry of the *pce* gene products in *D. restrictus* and *D. hafniense* strain TCE1

This chapter corresponds to a modified version of the following publication :  
**Cimmino, L.**; Schmid, A. W.; Holliger, C.; Maillard, J. *Frontiers in Microbiology* **2022**, 13:838026.

### 3.1 Introduction

The sequenced genomes of *D. restrictus* strain PER-K23 and *D. hafniense* strains TCE1 share the highly conserved (99% amino acid sequence identity) and well-characterized PCE reductive dehalogenase, which is encoded by the *pceA* gene [48] and is part of a four-gene cluster (*pceABCT*), that also displays 99% DNA sequence identity between the two organisms [79]. The conserved *pceABCT* gene cluster, and more generally, *rdhABCT* gene clusters, have been found in the genera *Dehalobacter* and *Desulfitobacterium* exclusively [78]. A variant of this gene cluster that displays a different gene order and duplicated genes, and that shares a low sequence homology with *rdhABCT*, was identified on a genomic island in the chromosome of *Geobacter lovleyi* strain SZ [101], and was therefore not considered as part of the conserved *rdhABCT* gene clusters. At genomic level, the *pce* gene cluster in *D. hafniense* strain TCE1 is located on the active composite transposon *Tn-Dha1* [78, 79], a structure that has been found with some variations in other *Desulfitobacterium* spp. [78, 102, 103]. In *D. hafniense* strain TCE1, the presence of the transposon flanking the *pceABCT* gene cluster resulted in the constitutive expression of the *pce* genes, while a gradual loss of the entire *pce* gene cluster was confirmed during serial sub-cultivation of strain TCE1 under growth conditions devoid of PCE [78]. By contrast, no transposon structure is found around the *pceABCT* gene cluster of *D. restrictus*.

Respiratory reductive dehalogenase genes are typically organized in gene clusters composed of *rdhA*, the gene encoding the catalytic enzyme, and at minimum *rdhB*, coding for the putative membrane anchor protein that attaches RdhA at the cytoplasmic membrane. The *rdhAB* or *rdhBA* genes represent the minimal *rdh* gene sets so far detected [70], with the exception

of a few strains of *Dehalogenimonas* spp. that display some isolated *rdhA* genes [71]. The operon nature of *rdhAB* or *rdhBA* genes has been revealed for several gene clusters [73, 79, 104, 105]. A robust reductive dehalogenase activity associated with the membrane fraction of selected OHRB [46, 48, 74] corroborate the hypothesis that respiratory RdhA enzymes are bound to the cytoplasmic membrane, although they do not display any transmembrane helix in the matured form, as demonstrated by the crystal structure of the dimeric PceA in *Sulfurospirillum multivorans* [106]. The genetic vicinity of *rdhB*, the sequence of which was predicted to form a short integral membrane protein of approximately 100 amino acids with two or three transmembrane helices [56], invites considering the RdhB protein as the membrane anchor of their cognate RdhA. However, so far only indirect evidence has been obtained for their interaction [66]. Additional accessory proteins are often encoded adjacently to *rdhAB* or *rdhBA* operons (for reviews, see [77, 107]).

For the two accessory genes present in the *pceABCT* gene cluster, a function has only been clearly established for the gene product of *pceT*. PceT and other RdhT proteins are molecular chaperones most likely assisting in the correct folding of the catalytic subunit. It has been shown to bind to the Twin-arginine translocation (Tat) signal sequence of PceA [82, 83]. Moreover, in proteomic analyses conducted on *D. hafniense* strain TCE1 [80] and strain Y51 [108], or on *D. restrictus* strain PER-K23 [49], PceT has been clearly detected. PceC (and more generally RdhC proteins) encodes a predicted integral membrane protein (with six transmembrane helices) harbouring a flavin mononucleotide (FMN)-binding domain and two conserved CX<sub>3</sub>CP amino acid motifs. Experimental work has confirmed the presence of a covalently-bound FMN cofactor in the protein domain of PceC that faces the outside of the cytoplasmic membrane [81]. These data suggested that RdhC proteins could play a role in electron transfer and form a membrane-bound protein complex with RdhA and RdhB [35], although there is no experimental evidence to support this hypothesis.

In the present study, OHRB harbouring diverse metabolic strategies, i.e. the obligate *D. restrictus* strain PER-K23 and the versatile *Desulfitobacterium hafniense* strain TCE1, were investigated to elucidate the stoichiometry of the *pceABCT* individual gene products at RNA and protein levels.

## 3.2 Materials and methods

### 3.2.1 Spike experiment

*D. hafniense* strain TCE1 was cultivated in anaerobic flasks containing 40-mL of medium with 40 mM sodium pyruvate as carbon and energy source (thus replacing acetic acid, H<sub>2</sub> and PCE). This culture set-up was used for an experiment where PCE was spiked in after 24 h of growth on pyruvate (at an optical density at 600 nm (OD<sub>600</sub>) of 0.08). Upon PCE addition, four replicate culture flasks were incubated for 5 h before biomass collection. The experiment conducted on *D. restrictus* cells growing with H<sub>2</sub> and PCE was performed slightly differently as no spike

nor alternative growth conditions are possible. There, the transcription of the *pce* genes was compared to the corresponding DNA gene copy number from sample aliquots obtained during the RNA extraction procedure. For harvesting, the cultures were transferred to 50-mL Falcon tubes, centrifuged for 5 min at  $4000 \times g$  and the biomass pellets were quickly resuspended in 0.5 mL of RNAprotect Bacteria Reagent (Qiagen AG, Hombrechtikon, Switzerland) and transferred to 1.5-mL Eppendorf tubes. After 3 min of incubation at room temperature, the biomass was pelleted again by 3 min of centrifugation at  $10'000 \times g$ , and stored at  $-80^{\circ}\text{C}$  until use.

### 3.2.2 RNA extraction

Biomass pellets resulting from 40-mL cultures were resuspended by pipetting in 0.5 mL of TRIzol reagent (Thermo Fisher Scientific SARL, Ecublens, Switzerland) and incubated for 5 min at room temperature. A volume of 0.1 mL of chloroform was added and the mixture was vortexed vigorously for 15 s, incubated for 2 min and centrifuged at  $10'000 \times g$  for 15 min. The supernatant was carefully collected, mixed with an equal volume of 100% ethanol and purified using the Direct-zol RNA MiniPrep kit (Zymo Research, Lucerna-Chem AG, Luzern, Switzerland), following the manufacturer's instructions with the following modifications. The nucleic acids were eluted in 50  $\mu\text{L}$  of water and a 5- $\mu\text{L}$  aliquot was withdrawn to be used as DNA reference sample in quantitative PCR. The remaining elution was then supplemented with 5  $\mu\text{L}$  of DNase buffer and 1  $\mu\text{L}$  of DNase I enzyme (DNase Max Kit, Qiagen), and incubated for 30 min at  $37^{\circ}\text{C}$ . The DNase I enzyme was then removed with 5  $\mu\text{L}$  of DNase Removal Resin according to the instructions. RNA samples were quantified using the Qubit RNA HS Assay Kit (Thermo Fisher Scientific) and stored at  $-80^{\circ}\text{C}$  until further use.

### 3.2.3 Reverse transcription, PCR and quantitative PCR

Depending on the RNA samples, between 250 and 1000 ng of RNA were transcribed to complementary DNA (cDNA) using the GoScript<sup>TM</sup> Reverse Transcriptase Kit with random primers (Promega AG, Dübendorf, Switzerland) following the manufacturer's instructions. The resulting cDNA was diluted  $10 \times$  with ddH<sub>2</sub>O and either subjected to PCR or quantitative PCR (qPCR). A typical mixture for PCR in 20  $\mu\text{L}$  contained the following: 4  $\mu\text{L}$  of MyTaq Reaction Buffer, 1  $\mu\text{L}$  of each of the 10  $\mu\text{M}$  primers (see **Supplementary Table A.1**), 0.4  $\mu\text{L}$  of MyTaq DNA Polymerase (Meridian Bioscience, LABGENE Scientific SA, Châtel-St-Denis, Switzerland), and 1  $\mu\text{L}$  of cDNA template. The PCR program was: 1 min at  $95^{\circ}\text{C}$ , then 30 cycles of 15 s at  $95^{\circ}\text{C}$ , 15 s at  $52^{\circ}\text{C}$  and 10 s at  $72^{\circ}\text{C}$ , followed by 5 min at  $72^{\circ}\text{C}$ . PCR products were visualised on 2% agarose gels following standard procedures. For qPCR, technical duplicates were run from three to four biological replicates of each strain and each growth condition considered. Ten  $\mu\text{L}$  reactions were prepared on the Myra Pipetting Robot (Bio Molecular Systems, LABGENE Scientific SA) with the following composition: 5  $\mu\text{L}$  of SensiFAST SYBR No-ROX reagent (Meridian Bioscience), 0.2  $\mu\text{L}$  of each primer at 10  $\mu\text{M}$ , 2.1  $\mu\text{L}$  of ddH<sub>2</sub>O and 2.5  $\mu\text{L}$  of cDNA template. The qPCR was run on a MIC Real-Time PCR System (Bio Molecular Systems) with

the following program: 2 min at 95°C, 40 cycles of 5 s at 95°C, 15 s at 60-62°C (depending on the target gene), 20 s at 72°C, followed by a 4 min denaturation ramp from 72 to 95°C. Data analysis was performed with the in-built MIC software using the relative quantification REST mode and *rpoB* as reference gene. In case of spike experiments, the samples obtained from the non-spiked cultures (with pyruvate) were used as control. Raw data, qPCR melting curves and statistical analysis output are given in **Supplementary Figure A.1**.

### 3.2.4 In-solution sample digestion

Cell-free extract, soluble and membrane samples were reduced and alkylated as outlined below followed by in-solution overnight digestion at 37°C with Trypsin/LysC proteases (Thermo Fisher Scientific). RapiGest-treated samples were generally prepared according the manufacturer's instructions. Protein digests were then subjected to C18 stage tip cleaning, dried in a speed-vacuum and stored at -20°C.

### 3.2.5 Shotgun LC-MS/MS analysis

As described in Chapter 2 (see section 2.2.7). Furthermore, the mass spectrometry proteomics discovery data have been deposited to the ProteomeXchange Consortium via the PRIDE partner repository [109], with the dataset identifiers PXD030941 and 10.6019/PXD030941. (The access to the database by using the following account and password to connect to PRIDE: username: reviewer\_pxd030941@ebi.ac.uk; password: ACwpi3iC.)

### 3.2.6 Selection of signature peptides for parallel reaction monitoring proteomics

For parallel reaction monitoring (PRM)-based quantitative proteomics, alongside with the *pceABCT* encoded proteins, the F1  $\alpha$ -subunit of the ATP synthase was included as house-keeping protein, since it was detected with a high sequence coverage and reproducible signal intensity in a preliminary MS analysis performed on cell-free extracts of *D. restrictus* and in the discovery MS analysis (**Figure 3.3**). The selection of signature peptides was based on unique proteotypic peptide sequences and features that enhance chemical stability. Priority was given to those peptides that were previously identified in the discovery dataset with high MS/MS spectral quality. Peptides containing cysteine or methionine residues were excluded. Peptide uniqueness was confirmed by searching against the *D. restrictus* proteome database. An additional criterion was that the selected peptides display a fully conserved amino acid sequence in the protein homologues from both *D. restrictus* and *D. hafniense* strain TCE1. Synthetic, accurately quantified heavy-isotope labelled reference peptides, with either C-terminal heavy lysine (K) or arginine (R) for PceA, PceB, PceC, PceT and the  $\alpha$ -F1 subunit of ATP synthase were purchased from JPT Peptide Technologies GmbH (Berlin, Germany).

### 3.2.7 PRM-based quantitative proteomics

PRM-based proteomics was conducted on biological duplicates of samples from *D. restrictus* and *D. hafniense* strain TCE1. Each sample (CFE, SE, MF) was analysed as technical triplicates. PRM analysis was performed using a Q-Exactive hybrid quadrupole-orbitrap mass spectrometer (Q-OT, Thermo Scientific). The MS/MS resolution was set at 17'500 (at  $m/z$  200). The maximum fill time was set at 75 ms. A precursor target isolation window of 1.4  $m/z$  was applied and a normalized collision energy of 35 was employed for fragmentation. Digested samples were resuspended in 30-60  $\mu\text{L}$  of the mobile phase solvent A and then separated by reversed-phase chromatography using a Dionex Ultimate 3000 RSLC nanoUPLC system on a home-made 75  $\mu\text{m}$  ID  $\times$  50 cm C18 capillary column (Reprosil-Pur AQ 120 Å, 1.9  $\mu\text{m}$ ). Peptides were separated by applying a non-linear 90 min gradient ranging from 99% of solvent A to 90% of solvent B (as above) at a flow rate of 250 nl/min. For quantitative analysis, digested samples were spiked with a known amount of heavy-labelled surrogate peptide standards (Table 2.4), ranging from 20-100 fmol/ $\mu\text{L}$  (final concentration). Typically, 4-8  $\mu\text{L}$  of sample volumes were injected containing 160-800 fmol of heavy-labelled peptide standards. The amount of spiked heavy-labelled peptide corresponded to 20-50% of the relative abundance of the light endogenous peptides, as determined by preliminary PRM analyses. A single *vs* multiple spike-in heavy peptide standard concentration was used to calculate absolute levels of PceB protein. For all PRM analyses, samples were processed and analyzed using a single spike-in reference standard at the concentration mentioned above. A PRM validation experiment was performed for PceB using a synthetic fragment of PceB (ProteoGenix, Schiltigheim, France) that was quantified with the BCA assay and digested as described in section 2.3.6.

### 3.2.8 Data processing and database searches

For peptide identification, the following settings were used: enzyme: Trypsin; missed cleavages: 2; precursor mass tolerance: 10 ppm; fragment mass tolerance: 0.2 Da; minimum charge: 2; maximum charge: 5; fixed modifications: Carbamidomethyl (C); variable modifications: Oxidation (M). False discovery rate (FDR) was calculated based on the target/decoy database and peptides as well as proteins with FDR threshold of  $\leq 1\%$  were chosen as true positive hits. Quantitative data analyses were performed using Skyline (version 21.1.0.278, MacCoss lab, University of Washington, USA), an open source software tool application for quantitative data processing and proteomic analysis. All integrated peaks were manually inspected to ensure correct peak detection and integration. Protein concentrations were calculated using peaks area ratios (light/heavy) derived from accurately quantified and spiked-in heavy-isotope labelled peptide standards. The concentration of each protein of interest was calculated from the average of the concentrations of its quantified peptides in the technical triplicates. The standard deviation was calculated using the STDEV.S method in Excel.



### 3.3 Results and Discussion

The present study investigates the electron-accepting moiety of organohalide respiration in *D. restrictus* and *D. hafniense* strain TCE1 by defining the stoichiometric relationships of the *pceABCT* individual gene products at RNA and protein levels. The investigation of our model organisms allowed us to explore the use of the *pceABCT* gene cluster in two different bacterial genera and to question the participation of the encoded proteins in the composition of the electron transfer chain involved in PCE reductive dechlorination. The transcription and co-transcription of individual genes from the *pceABCT* gene clusters were elucidated via a combination of reverse transcription (RT)-PCR and quantitative RT-PCR. At protein level, the stoichiometric relationships between the *pceABCT* encoded proteins was addressed via PRM quantitative proteomics.

#### 3.3.1 The *pceABCT* genes form an operon

The co-transcription of *pceABCT* individual genes was investigated in *D. restrictus* and *D. hafniense* strain TCE1 via RT-PCR. PCR primers targeting individual genes and also the 3'-end and 5'-end of successive gene pairs were applied to complementary DNA obtained from both strains cultivated in OHR conditions. It resulted in the transcription of the *pceABCT* individual genes as well as that of the different intergenic regions (**Figure 3.1**), revealing the operon nature of *pceABCT* gene clusters. A differential intensity of the PCR products was observed in *D. restrictus*, which was mostly evident in the lower abundance of the *pceBC* and *pceCT* intergenic regions (**Figure 3.1A**). This was not the case for *D. hafniense* strain TCE1 as all PCR products displayed a similar level of amplification (**Figure 3.1B**).

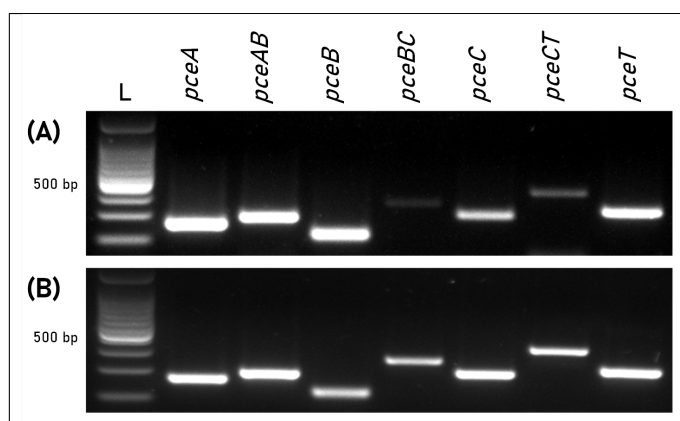


Figure 3.1: Co-transcription of *pce* genes in *D. restrictus* and *D. hafniense* strain TCE1. Individual genes and gene junctions were targeted by RT-PCR on RNA from (A) *D. restrictus* and (B) *D. hafniense* strain TCE1 cultivated with H<sub>2</sub> and PCE as electron donor and acceptor, respectively.

### 3.3.2 Stoichiometric relationships of *pceABCT* gene products at RNA level

The versatile energy metabolism of *D. hafniense* strain TCE1, in contrast to *D. restrictus*, allowed us to evaluate the transcription levels of the *pceABCT* genes in different growth conditions. To address the question of the stoichiometry of individual gene products at RNA level, fermentation with pyruvate and OHR metabolism were considered here. A spike of PCE to *D. hafniense* strain TCE1 cells growing fermentatively on pyruvate did not show any regulation of the *pce* genes when compared to non-spiked cells. The relative stoichiometry of the *pceABCT* genes was calculated to 1.0:1.0:1.2:1.1, after normalization of the data to the transcription level of *pceA* (**Figure 3.2A**).

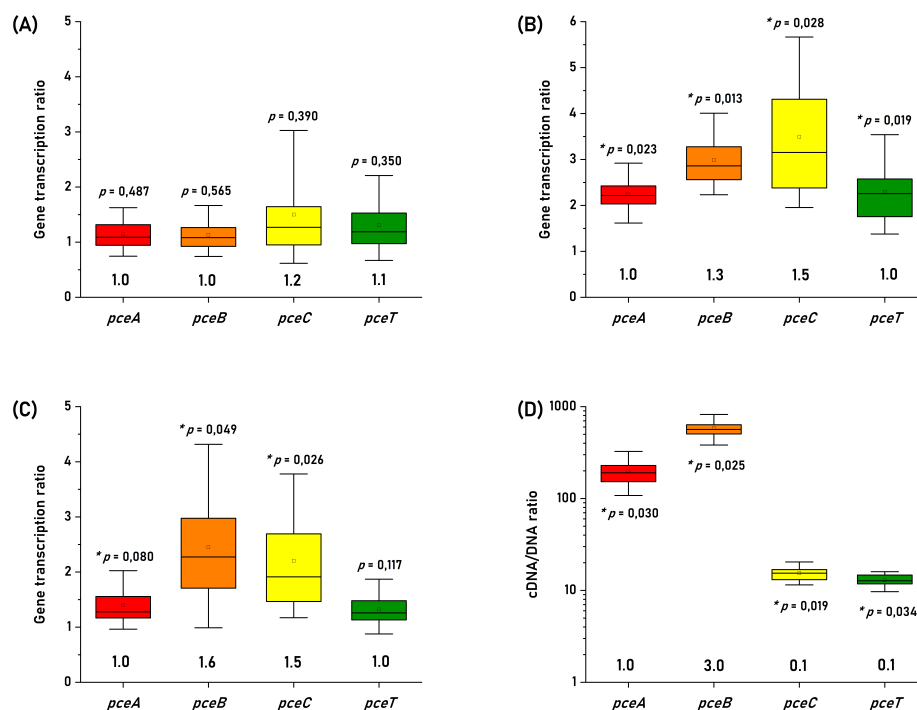


Figure 3.2: Quantitative analysis of the individual *pce* transcripts in (A) *D. hafniense* strain TCE1 cultivated on pyruvate and spiked with PCE; (B) *D. hafniense* strain TCE1 routinely cultivated with H<sub>2</sub> and PCE; (C) *D. hafniense* strain TCE1 routinely cultivated with pyruvate and PCE; and (D) *D. restrictus* routinely cultivated with H<sub>2</sub> and PCE. Please note that the transcriptional data of *D. hafniense* strain TCE1 were compared to transcripts obtained from cells routinely cultivated with pyruvate, while the gene transcription ratio of *D. restrictus* was calculated using DNA as reference.

Then, the analysis was conducted on strain TCE1 cells routinely growing with hydrogen and PCE (H<sub>2</sub>-PCE), which revealed a slight, however significant, increase in the transcription level of all *pce* genes in comparison to fermentatively growing cells (**Figure 3.2B**) and revealed a normalized stoichiometry of 1.0:1.3:1.5:1.0. Similarly, a slight increase in the transcription

level was also obtained mainly for *pceB* and *pceC* in cells routinely cultivated with pyruvate and PCE as electron donor and acceptor (Pyr-PCE), respectively, revealing a stoichiometry of 1.0:1.5:1.6:1.0 (**Figure 3.2C**). The RT-qPCR analysis conducted on *D. restrictus* cells was performed slightly differently as no spike nor alternative growth conditions could be applied (**Figure 3.2B**). There, the level of transcription of the *pce* genes was compared to the gene copy number in DNA obtained from the same samples during the RNA extraction procedure. The analysis of the transcription pattern of the *pce* genes revealed a clearly higher transcription level for *pceA* and *pceB* than that of *pceC* and *pceT* with a normalized relative stoichiometry of approximately 1.0:3.0:0.1:0.1 (**Figure 3.2D**).

### 3.3.3 Stoichiometry of Pce proteins by quantitative proteomics

The analysis of *pceABCT* encoded proteins consisted of a combination of discovery proteome analysis (shotgun LC-MS/MS) and a quantitative proteomic analysis with heavy-labelled peptide standards. Both approaches were applied to the same samples, namely cell-free extracts and sub-cellular fractions of *D. restrictus* and *D. hafniense* strain TCE1. The discovery analysis was performed to evaluate the overall proteome and to define which specific peptides from the Pce proteins were best suited for the quantitative analysis with heavy-labelled reference peptides. The discovery analysis identified 1433 proteins in total for *D. restrictus* across the different samples (corresponding to 50% of the genome-derived proteome), while 1751 proteins were detected in the proteome of *D. hafniense* strain TCE1 (35% of the genome-derived proteome). As showed in **Table 3.1**, this analysis allowed us the identification of the complete set of Pce proteins in both *D. restrictus* and *D. hafniense* strain TCE1, however with different outcome depending on the nature of the proteins and the type of samples. Furthermore, as example for *D. restrictus*, the analysis revealed a high level of detection of PceA which was characterized by a high sequence coverage (between 74% and 81%) and its position within the top 6 best identified proteins across the different samples when considering the total number of MS spectra (data not shown). A similar trend was observed for PceT, which displayed a sequence coverage in the range between 68% and 75% in the different fractions. However, overall PceT ranked slightly lower than PceA in the number of detected MS spectra. By contrast, the results on the two integral membrane proteins, namely PceB and PceC, were characterized by a generally lower detection level in the samples. For PceB, the highest sequence coverage (31%) was observed in the cell-free extract. Only two MS spectra identified PceB in the soluble fraction, possibly due to a slight cross-contamination during the fractionation of cell-free extracts. Finally, PceC was not detected in the soluble fraction, and showed only a limited sequence coverage (as shown in **Figure 3.3**) and low numbers of MS spectra in both the cell-free extract and the membrane fraction. Overall, a similar pattern was observed for the detection and distribution of the PceA, B, C and T proteins in the discovery analysis of *D. hafniense* strain TCE1. Despite the known limitations in the detection of integral membrane proteins in general, and of PceB and PceC in particular, this dataset helped us to define several peptide candidates to be targeted by the quantitative analysis.

Table 3.1: Discovery MS analysis on cell-free extracts, soluble and membrane fractions of *D. restrictus* and of *D. hafniense* strain TCE1

<i>D. restrictus</i> / <i>D. hafniense</i> strain TCE1 <sup>a</sup>				
<i>Protein</i>	<i>Sample</i>	<i>Coverage (%)</i>	<i># MS spectra</i> <sup>b</sup>	<i>Area</i> <sup>c</sup>
PceA	Cell-free extract	81 / 69	436 / 294	2·10 <sup>10</sup> / 3·10 <sup>9</sup>
	Soluble fraction	74 / 74	259 / 182	7·10 <sup>9</sup> / 6·10 <sup>9</sup>
	Membrane fraction	78 / 85	418 / 487	2·10 <sup>10</sup> / 2·10 <sup>10</sup>
PceB	Cell-free extract	41 / 34	28 / 40	6·10 <sup>8</sup> / 1·10 <sup>9</sup>
	Soluble fraction	19 / -	2 / -	2·10 <sup>6</sup> / -
	Membrane fraction	32 / 41	34 / 27	4·10 <sup>8</sup> / 5·10 <sup>8</sup>
PceC	Cell-free extract	24 / 16	15 / 9	1·10 <sup>8</sup> / 3·10 <sup>7</sup>
	Soluble fraction	- / 2	- / 1	- / 2·10 <sup>6</sup>
	Membrane fraction	22 / 25	14 / 22	1·10 <sup>8</sup> / 2·10 <sup>8</sup>
PceT	Cell-free extract	72 / 68	100 / 72	6·10 <sup>9</sup> / 4·10 <sup>8</sup>
	Soluble fraction	75 / 90	122 / 233	6·10 <sup>9</sup> / 1·10 <sup>10</sup>
	Membrane fraction	62 / 82	56 / 60	2·10 <sup>9</sup> / 8·10 <sup>8</sup>
ATP synthase	Cell-free extract	74 / 29	119 / 23	7·10 <sup>9</sup> / 1·10 <sup>8</sup>
	Soluble fraction	68 / 39	83 / 29	2·10 <sup>9</sup> / 6·10 <sup>8</sup>
	Membrane fraction	76 / 57	146 / 50	6·10 <sup>9</sup> / 8·10 <sup>8</sup>

<sup>a</sup>For each data entry, the first value corresponds to the proteomic analysis of *D. restrictus* and the second to that of *D. hafniense* strain TCE1.

<sup>b</sup># MS spectra correspond to the total number of spectra identified that support the given protein.

<sup>c</sup>Area is the total area or intensity of peptide features from unique supporting peptides of the corresponding protein. This can be used as an indicator of the abundance of the protein.

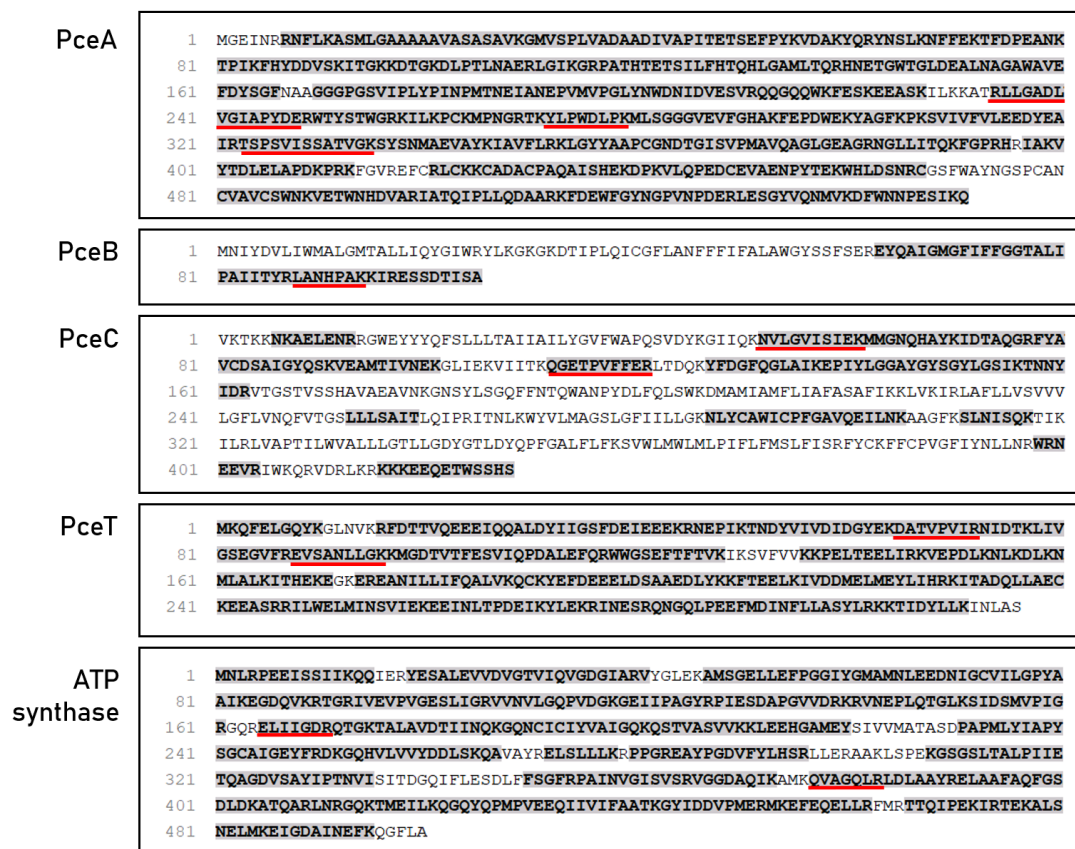


Figure 3.3: Graphical representation of sequence coverage of Pce proteins and F1  $\alpha$ -subunit of ATP synthase by shotgun MS analysis. The peptides that were detected via discovery MS analysis (i.e. sequence coverage) are shaded in grey. Red underlines indicate the peptides which were used in the PRM quantitative proteomic analysis.

The investigation of stoichiometry was conducted on cell-free extracts from biomass harvested at exponential phase. In addition, to define the relative abundance of the targeted proteins in the sub-cellular compartments, the quantification was also performed on the soluble and membrane fractions issued from cell-free extracts following a protocol that minimized protein extraction biases. RapiGest-based extraction was applied to whole membrane fractions without separating the proteins from the membrane particles. Although we cannot exclude that some of the proteins would remain embedded in the membrane lipids upon extraction, we hypothesize that the solvent-exposed fragments of these proteins are likely accessible to and digested by trypsin, thus minimizing their loss during PRM analysis. The selection of signature peptides based on the criteria reported in the Material and Methods section resulted in the definition of a total of 16 unique peptides (Table 2.4). Based on first results, a shorter selection of 10 labelled peptides was established (indicated in bold in Table 2.4), corresponding to a minimum of two peptides for each protein of interest, with the exception of PceB that could only be targeted by one peptide due to the small size and hydrophobic

nature of the protein and due to discrepancies in the detection of the second peptide in the preliminary analyses. An example of the obtained PRM spectra is given in **Figure 3.4**.

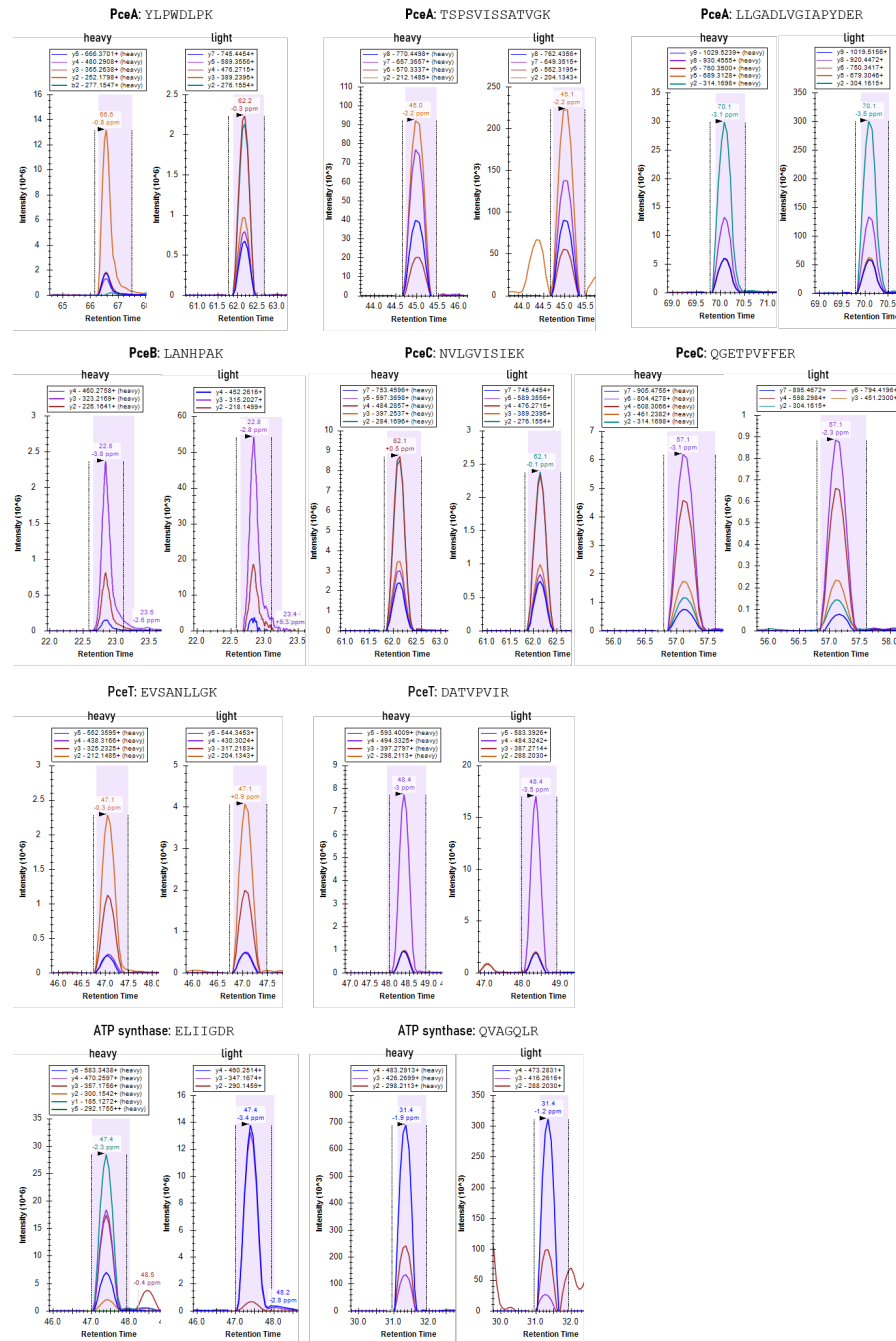


Figure 3.4: Representative examples of PRM chromatogram of selected transitions of all heavy-labelled peptides used in the quantification analysis.

For PceB, due to the overall scarcity and low solubility of its peptides, we sought to validate the reproducible quantification of the single PceB tryptic peptide LANHPAK by assessing the digestibility and recovery of this peptide, using a synthetic, quantified form of the C-terminal part of PceB, spanning the sequence of amino acid residues from 63 to 105. We show that this peptide is indeed a reproducible cleavage product of the PceB protein and therefore serves a surrogate reference peptide for the quantification of PceB in biological samples. PRM applied to the synthetic PceB protein fragment with spike-in heavy-labelled peptide revealed a 19% difference in PceB concentration. This value seems acceptable considering the experimental variation of the PRM analysis, as well as that of the initial quantification of the synthetic PceB protein. In addition, LC-MS/MS analysis on the synthetic PceB fragment confirmed that the selected peptide was the most abundant cleavage product found, with other mis-cleaved forms (-KK) or truncated forms of PceB representing less than 1% (relative peak area) of the main proteolytic product (**Figure 3.5**). Moreover, this peptide has been predicted to protrude out of the cytoplasmic membrane [56], and is likely to be relatively accessible for trypsin digestion. The quantification of PceA, B, C and T proteins from the cell-free extract of *D. restrictus*

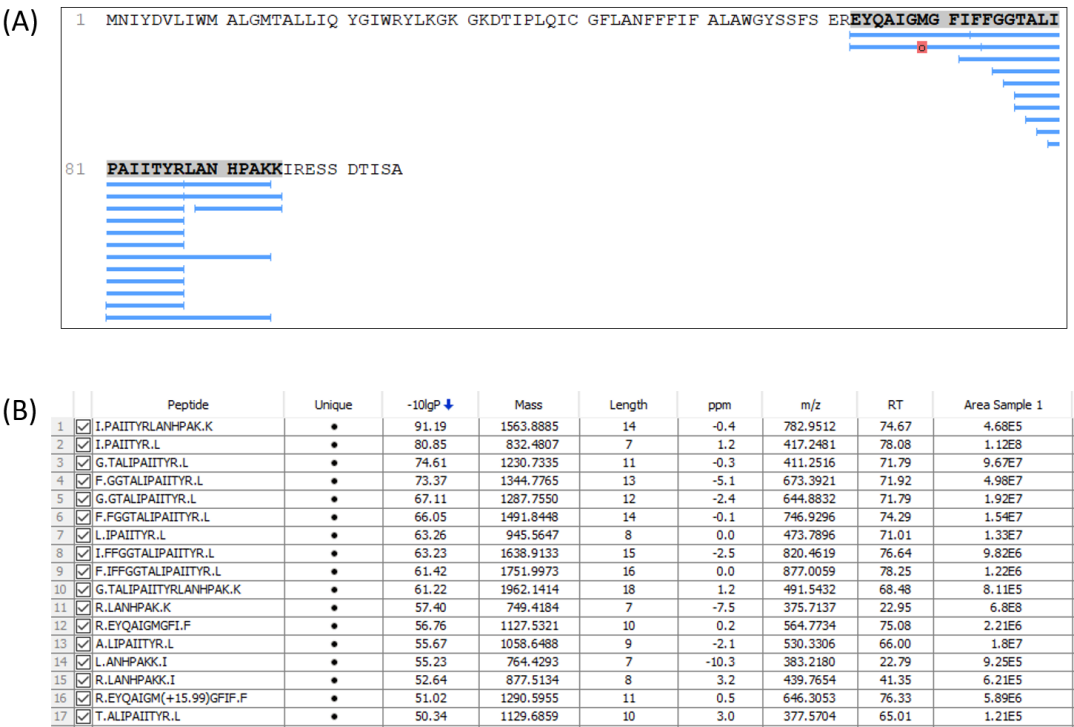


Figure 3.5: LC-MS/MS analysis of the PceB synthetic fragment. (A) Peptide coverage. (B) List of PceB peptides identified and their relative abundance (peak area) found. The peptide LANHPAK (11) represents a major cleavage product, whereas some minor, miss-cleaved forms such as LANHPAKK (15) could be still identified, which, however, represented less than 1% of the overall abundance of the major fully cleaved fragment.

resulted in a relative stoichiometry normalized to PceA of 1.0:0.5:0.02:0.2, showing a likely 2:1 stoichiometry between PceA and PceB, while PceC and PceT resulted approximately in fifty- and five-fold lower abundance than PceA, respectively (**Figure 3.6**).

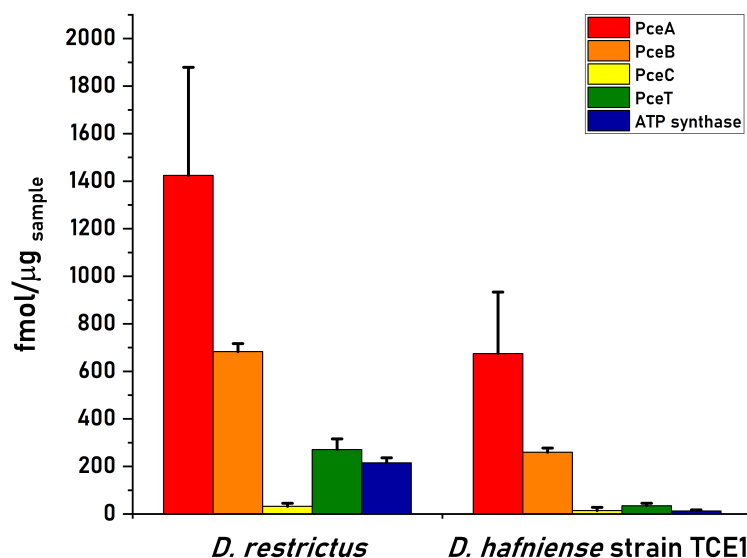


Figure 3.6: Quantitative proteomics analysis of Pce proteins and the F1  $\alpha$ -subunit of the ATP synthase in cell-free extracts (CFE) from *D. restrictus* and *D. hafniense* strain TCE1. This graph shows the results of one biological replicate and is representative of the trend also observed for the second replicate (data not shown). The concentration of each protein was calculated by averaging the values obtained for the selected peptides in technical triplicates. Error bars indicate the calculated standard deviation.

In *D. hafniense* strain TCE1, the cell-free extract displayed a slightly different ratio (1:0.38:0.02:0.05) with a calculated PceA/PceB ratio of approximately 3:1. PceC and PceT resulted in a fifty- and twenty-fold lower abundance than PceA, respectively, similarly to *D. restrictus* (**Figure 3.6**). In the soluble fraction of *D. restrictus*, PceA and PceT were largely present while PceB and PceC could not be detected. The data thus revealed a 1.0:0.8 stoichiometry between PceA and PceT (**Figure 3.7A**). A similar trend was also observed in the soluble fraction of *D. hafniense* strain TCE1, displaying a PceA:PceT stoichiometry of 1.0:1.0 (**Figure 3.7B**). In the membrane fraction, the analysis showed a stoichiometry of 1.0:0.57:0.02:0.07 across the Pce proteins in *D. restrictus* (**Figure 3.7A**), while *D. hafniense* strain TCE1 displayed a ratio of 1.0:0.5:0.03:0.04 (**Figure 3.7B**). Overall, the results revealed a similar trend in the membrane fraction of both strains, with PceA and PceB resulting as predominant subunits and exhibiting a relative stoichiometry of 2:1 in favour of PceA. As observed in cell-free extracts, both PceC and PceT resulted as many times less abundant proteins than PceA. The results shown in **Figures 3.6** and **3.7** are derived from data of one biological replicate for each strain and is representative of the trend also



observed for the second biological replicate (see **Supplementary Figure A.6**). The nature of integral membrane proteins and their challenging quantification invite us to consider these results with care and to propose a physiological and biochemical interpretation which may require additional evidence in the future.

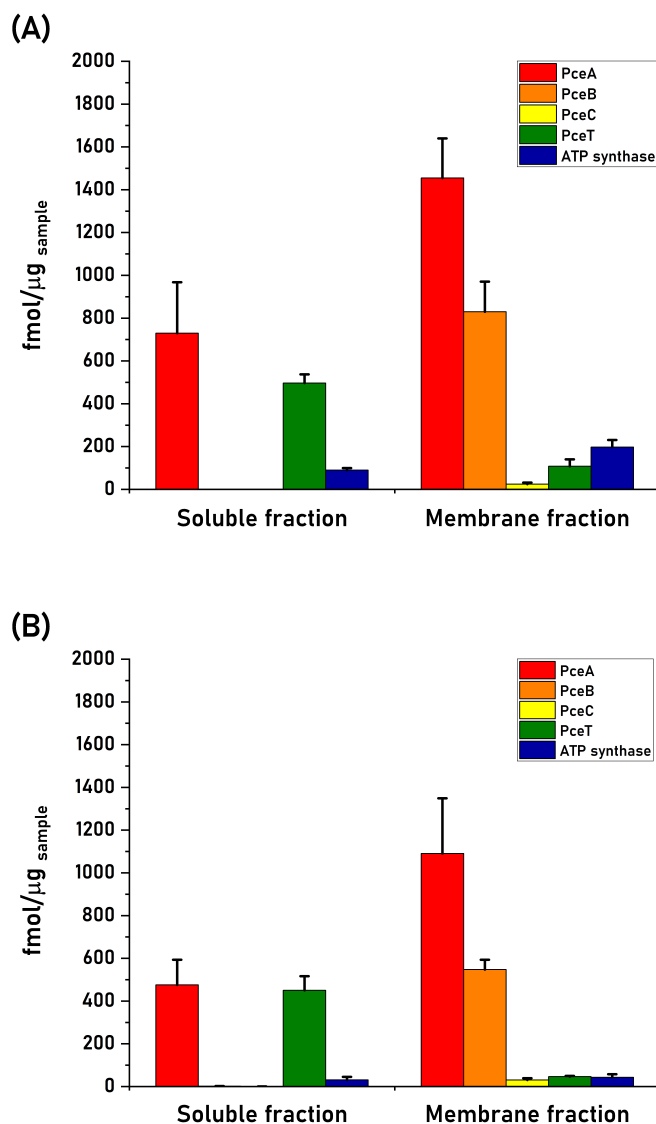


Figure 3.7: Quantitative proteomics of the Pce proteins and the F1  $\alpha$ -subunit of the ATP synthase in sub-cellular compartments obtained from cell-free extracts of (A) *D. restrictus* and (B) *D. hafniense* strain TCE1. These graphs show the results of one biological replicate and are representative of the trend also observed for the second replicate (data not shown). The concentration of each protein was calculated by averaging the values obtained for the selected peptides in technical triplicates. Error bars indicate the calculated standard deviation.

### 3.4 Discussion

Reductive dehalogenase (*rdh*) genes are typically organized in clusters composed of at least *rdhA*, the gene encoding the key catalytic enzyme, and *rdhB*, a gene encoding the putative membrane anchor protein for RdhA. This minimal gene set, however, is frequently accompanied by a variable set of accessory genes, for most of which the exact function is still unknown [107]. In the present study, the global expression of the *pce* genes from the conserved *pceABCT* gene clusters was investigated via a multilevel approach on RNA and proteins.

#### 3.4.1 Transcription pattern heterogeneity and stoichiometry of gene transcripts associated with *rdh* clusters in the Firmicutes

During the last two decades many studies have addressed the transcription of *rdh* genes in OHRB by applying a large variety of methodologies [43]. Among them, only a few studies have reported on the transcription of *rdhA*-associated genes. The co-transcription of *rdhAB* or *rdhBA* gene pairs has been reported for *S. multivorans* [104], *Dehalococcoides* spp. [110, 111] and *D. dichloroeliminans* [112], while only three studies have been conducted on *rdh* accessory genes, namely the *cprTKZEBACD* gene cluster of *D. dehalogenans*, the *pceABCT* gene cluster of *D. hafniense* strain Y51, and the OHR gene region in *S. multivorans* [73, 102, 113]. In *D. dehalogenans* a combination of Northern blot and RT-PCR has revealed a strong regulation of the *cpr* gene cluster in presence of the organohalogen 3-chloro-4-hydroxyphenylacetate, resulting in the transcription of bicistronic units, i.e. *cprZE*, *cprBA* and *cprCD*, along with occasional formation of the polycistronic *cprBACD* transcript [73]. In the work on the *pce* cluster harboured by *D. hafniense* strain Y51, Northern blot analysis has shown the co-transcription of *pceABC*, while *pceT* was transcribed as a monocistronic transcript. RT-PCR analysis, on the other hand, has suggested a co-transcription of *pceC* and *pceT*, thus challenging the Northern blot results [102]. Finally, the transcriptomic analysis of the OHR region in *S. multivorans* has confirmed the co-transcription of *pceA* and *pceB* genes and also revealed the PCE-dependent up-regulation of several transcriptional units among which a 29-gene transcript including the putative quinol dehydrogenase *pceMN* genes and the corrinoid biosynthesis genes [113]. In the present work, the transcription pattern of *rdh* genes observed in *D. restrictus* showed the co-transcription of all four of the *pce* gene targets, which led us to consider *pceABCT* as an operon. However, the stoichiometry analysis of *pce* individual gene transcripts in *D. restrictus* displayed a significantly higher level of transcription of *pceA* and *pceB*, as it appeared ten- and thirty-fold more abundant than that of *pceC* and *pceT*, respectively. A different transcription pattern was observed for *D. hafniense* strain TCE1 cells growing fermentatively on pyruvate and subsequently spiked with PCE. Indeed, the quantitative analysis displayed a comparable abundance of all *pce* gene transcripts after the spike. Collectively, these results confirm the lack of transcriptional regulation of the *pce* gene cluster in *D. hafniense* strain TCE1, which is likely due to the presence of a constitutive strong promoter upstream of *pceA* that is encoded in the right inverted repeat of the *ISDha1* insertion sequence, as already proposed in previous studies [78, 79]. In addition, the higher level of transcription of *pceAB* observed in *D. restrictus*,

but not in *D. hafniense* strain TCE1, raises new questions on possible post-transcriptional events occurring in the operon, such as RNA processing and differential RNA stability [114]. This is possibly corroborated by sequence analysis of the *pceABCT* operons from *D. restrictus* and *D. hafniense* strain TCE1, revealing a predicted hairpin loop structure in the *pceBC* intergenic region (see **Supplementary Figure A.2**). One possible scenario is that the hairpin loop may protect the 3'-end of the *pceAB* transcript from degradation by 3'-exoribonucleases once the *pceABCT* mRNA is processed into two or more fragments, while the *pceCT* transcript is partially degraded by exoribonucleases. The data obtained for *D. hafniense* strain TCE1 contrast with this hypothesis, but one explanation for this difference might be found in specific pools of RNA processing enzymes in *D. restrictus* and *D. hafniense*. The abundance of *pce* gene transcripts, however, cannot be used as proxy for the abundance of the cognate proteins (for a review see [115]).

### 3.4.2 Challenges in the detection of Rdh proteins from Firmicutes

Focusing exclusively on OHRB belonging to the Firmicutes, proteomic analyses of Rdh proteins were reported in twelve studies [49, 50, 80, 116–124]. The different methodologies that were applied in those studies (1 or 2D native or denaturing gels, and in-solution LC-MS/MS analyses) render their comparison very difficult. Nevertheless, one common feature is the challenge to detect integral membrane proteins as their extraction often results in low abundance. Indeed, they are (at least partially) embedded in membrane lipids, and their hydrophobic transmembrane helices are known to be relatively poor in the trypsin-targeted arginine and lysine residues. From these studies, it is clear that the integral membrane proteins RdhB and RdhC were less frequently detected than the membrane-associated RdhA proteins (**Supplementary Table A.8**). On the one hand, the small and highly hydrophobic RdhB was only detected in one third of these studies, while RdhC, that displays an exposed peripheral domain [81], was identified in half of the relevant studies (4 out of 8). The cytoplasmic RdhT molecular chaperone was identified in two-thirds of the relevant studies (4 out of 6), the two missing cases can be explained by the methodology applied (selected in-gel analysis). The results of our discovery proteomic analysis seem to be in line with these considerations since PceA and PceT were detected with a higher coverage, as well as a higher number of MS spectra and their derived total area, than PceB and PceC (**Table 3.1**). Whether the issue regarding the detection of integral membrane proteins precludes, or at least, bias the comparison of proteins of very different nature needs to be carefully addressed. This issue was also the reason why we decided to apply a quantitative approach with selected heavy-labelled reference peptides.

### 3.4.3 PceA and PceB - but not PceC - appear with a similar concentration in the membrane fraction

Based on physiological data and sequence information reported for the *pceABCT* operon, a tentative model of the electron transfer chain involved in OHR has been proposed previously, where PceA, B and C could form a membrane-bound protein complex [35]. There, PceC was

suggested to play a role in electron transfer in agreement with the redox activity of the FMN-binding domain [81]. In this context, the elucidation of the stoichiometry of the Pce proteins present in membrane fractions constitutes an important information. The application of PRM-based quantitative proteomics succeeded to detect all Pce proteins and to quantify them in *D. restrictus* and *D. hafniense* strain TCE1, thus offering a new and presumably more accurate vision of the biochemical premise for the terminal reductase involved in (at least some) OHRB. The analysis of cell-free extracts revealed an apparent stoichiometry of PceA to PceB of 2:1 or 3:1, while PceC and PceT were less abundant. It was especially pronounced for PceC, which is in agreement with recent studies on the *rdhABC* gene cluster of *Desulfoluna* sp., where the C subunit was not detected at all [122, 123]. The soluble fraction, a 1:1 ratio between PceA and PceT suggests that most of the PceA that is not yet associated with the membrane is likely accompanied by PceT, giving additional evidence of the role of PceT as a molecular chaperone specifically dedicated to the maturation of PceA [82, 83]. At the membrane, an apparent stoichiometry of 2:1 between PceA and PceB was identified in both strains, while again PceC and PceT were largely under-represented. In spite of the challenges that integral membrane proteins pose to their quantification, we think that the measured stoichiometry of the Pce proteins better reflects the physiological state than any previous analysis based on non-quantitative proteomics. The PceA:PceB ratio in the membrane fraction is clearly improved in favour of PceB when compared to the ratio estimated from our discovery MS analysis (**Table 3.1**) and to that of a previous study [49]. The possibility that, due to its hydrophobic nature, PceB remains largely undetected in our quantitative analysis has no clear support. Although we cannot unambiguously exclude this possibility, the observed PceA:PceB stoichiometry is rather in agreement with the well-accepted function of PceB as membrane anchor for PceA and the proposed 1:1 interaction of both proteins in the membrane [106, 125]. Moreover, the targeted PceB peptide is predicted to protrude outside the cytoplasmic membrane and, thus, should be exposed to trypsin digestion. Taken together, and beyond possible limitations in the detection of integral membrane proteins, the stoichiometry results strengthen the mutual link between RdhA and RdhB proteins, thus corroborating the role of the B subunit in anchoring the catalytic subunit at the membrane, as already proposed in previous studies [73, 104]. The elucidation of the crystal structure of PceA from *S. multivorans* has identified PceA as a homodimer, which led to the proposition of a Pce(AB)<sub>2</sub> complex associated with the cytoplasmic membrane [106]. In agreement with the dimeric structure of PceA, the observed 2:1 stoichiometry between PceA and PceB identified here rather suggests that the dimeric PceA is attached to the membrane by only one copy of PceB in a possible PceA<sub>2</sub>B protein complex.

### 3.5 Conclusions

Overall, the present study showed a strong relationship between *pceA* and *pceB* gene products, both at RNA and protein levels, thus demonstrating the mutual importance of these two subunits for the OHR metabolism. For the first time, a quantitative proteomics approach

targeting the key proteins in OHR helped us to challenge the model for the electron-accepting moiety in some Firmicutes [35] and to propose a new putative PceA<sub>2</sub>B reductive dehalogenase complex associated with the cytoplasmic membrane, thus excluding PceC from the complex. Further biochemical investigation is needed to unambiguously confirm our results and to elucidate the exact composition of the electron-transfer chain involved in PCE dechlorination in *D. restrictus* and *D. hafniense* strain TCE1.

## 4 Extraction and identification of the reductive dehalogenase (RDH) complex

### 4.1 Introduction

One of the key features to understand the energy metabolism of OHRB is to identify membrane protein complexes that are likely playing a role in the transfer of electrons and in the establishment of the proton motive force. The biochemistry studies conducted so far on OHRB among the Firmicutes have focused only on PceA (for a review, see [72]). However, the genetic composition of the *pce* gene cluster in *D. restrictus* and *D. hafniense* strain TCE1 and a robust reductive dehalogenase activity in the membrane fraction during purification [74, 75] corroborate the hypothesis that PceA enzyme is bound to the outer face of the cytoplasmic membrane via PceB. The earlier findings drive to consider the organization of PceA at the membrane and investigate the presence of a possible PceA-containing protein complex.

Since it was originally developed [126], Blue Native PAGE (BN-PAGE) and its derived techniques has become a very useful tool to extract, separate and identify membrane protein complexes. Complete respiratory complexes have been isolated from bacteria, yeast, and mitochondria over the past years [127], and several well-established protocols have been proposed [116, 128]. Furthermore, BN-PAGE was also used in earlier studies conducted on the OHRB *Dehalococcoides mccartyi* strain CBDB1 which permitted the identification of the multi-subunit protein complex [66, 68]. In this context, the use of BN-PAGE was considered as a key tool for the detection of possible protein complexes from the membrane of *D. restrictus*. However, sample preparation represented a fundamental step for the applicability of BN-PAGE. Theoretically the sample preparation for membrane proteins isolation constitutes of two main steps: cell fractionation and solubilization of the membrane fraction. Tailor each of these stage to *D. restrictus* represented one of the main challenges towards the RDH complex identification and required a meticulous work of refinement. The necessity to fine-tune the sample preparation protocol and the perspective to fully characterize the RDH complex implies the production of large amounts of biomass. In this context, the slow growth rate of *D. restrictus* and its low yield of biomass (<1 g of wet weight per liter of culture) represented important bottlenecks. Moreover, the application of a downstream in-gel PceA enzymatic assay

required avoiding any oxygen contamination from biomass harvest until the sample preparation and Clear Native PAGE (CN-PAGE). All the above-mentioned considerations highlighted the need of a careful procedure for biomass collection and cell fractionation. Furthermore, the solubilization of the membrane fraction requires a meticulous choice of detergents, or a combination thereof. The optimisation of this step aimed at minimizing the disruption of the proteins forming complexes and at maximizing the detection of the proteins. Furthermore, the application of BN-PAGE and its derived CN-PAGE technology on membrane fractions of *D. restrictus* was sought to address the question of a possible PceA-containing complex. In parallel, the development of in-gel PCE RDase activity assay offered a way to localize PceA and determine the size of the RDH complex on native gel. Moreover, the analysis of the resulting PceA-containing gel band via LC-MS/MS analysis also allowed broadening the horizon of the research by addressing the question of other possible proteins besides Pce proteins that may also interact with PceA and contribute to the RDH complex. The development of a tailor-made solubilization protocol for Pce proteins as well as the BN-PAGE and the associated techniques were carried out in collaboration with the laboratory of Prof. I. A. Pereira in Lisbon, Portugal.

In the following "Materials and Methods" section, the developed methods applied for the RDH complex isolation are described. All steps towards the optimization of the sample preparation protocol as well as the development of the in-gel assay procedure are illustrated in the "Results" section of the present chapter.

## 4.2 Materials and Methods

### 4.2.1 Bacterial strains and cultivation

*Dehalobacter restrictus* strain PER-K23 (DSM 9455) and *Desulfitobacterium hafniense* strain TCE1 (DSM 12704) were cultivated anaerobically at 30 °C under agitation (100 rpm). The medium was prepared as described in Chapter 2 (see Section 2.2.1). Anaerobic 1-L serum flasks containing 600 ml of medium were supplemented with acetate (2 mM) as carbon source, inoculated with 5% (v/v) inoculum and hydrogen (80% H<sub>2</sub>/20% CO<sub>2</sub>) as electron donor. For *D. hafniense* strain TCE1, 1% of the culture volume from a 2 M PCE in hexadecane was added as electron acceptor, while it was 4% of the culture volume from a 500 mM PCE solution in hexadecane to *D. restrictus*, respectively.

### 4.2.2 Cell harvest and fractionation

For all the subsequent steps, the use of an anaerobic glove box (Coy Laboratory) and anaerobic solutions were requested if the PCE reductive dehalogenase enzymatic activity assay was performed. The biomass (from approximately 2.5 L of culture for each experiment) was harvested after 3-4 days, thus corresponding to the late logarithmic phase. After removal of the PCE-containing organic phase from the culture, the liquid was transferred in 1-L plastic bottles (Beckman Coulter, Switzerland) and the biomass was collected by 20 min of centrifuga-

tion (9000 x g) at 4 °C. During the development protocol process, the use of 800-mL plastic Harvestline System liners (Beckman Coulter, Switzerland) was introduced to maintain strictly anaerobic conditions during the biomass harvest. An approximate yield of 0.4 g (wet weight) of biomass per liter culture was typically obtained. The pellet was washed in 50 mM Tris-HCl (pH 7.5), then transferred into cryotubes and pelleted again by 3 min of centrifugation at 10000 x g. Pellets were immediately stored at -80 °C until further use. For protein extraction, the pellet was resuspended in 50 mM Tris-HCl (pH 7.5) supplemented with few crystals of DNase I (Roche) and protease inhibitors (cOmplete mini, EDTA-free, Roche). In case of protein extraction under anaerobic conditions, the chamber of the French press was also flushed with oxygen-free 50mM Tris-HCl (pH 7.5) buffer. Furthermore, the addition in the sample preparation buffer of 10 to 100 mM of the reducing agent dithiothreitol (DTT) was introduced during the optimization of the fractionation protocol. After the cells were disrupted, the suspensions were immediately transferred into tubes previously flushed with N<sub>2</sub>, and then the tubes were placed in the anaerobic chamber. The cells were disrupted by the French press by 3 rounds at 1000 psi and 4 °C. Unbroken cells were removed by centrifugation (1000 x g, 20 min, 4 °C), and the supernatant (cell-free extract, CFE) was centrifuged at 90000 x g for 1h30 at 4 °C, yielding the soluble fraction (SF) and the membrane fraction (MF). Following, as result of the optimization process, an additional membrane wash step using 50 mM Tris-HCl (pH 7.5) supplemented with 300 mM KCl and protease inhibitors was introduced. After further ultracentrifugation (90000 x g, 1h30, 4 °C) the resulting pellet was finally resuspended in 500  $\mu$ L of 50 mM Tris-HCl (pH 7.5) supplemented with specific concentration of detergent for the protein extraction. During the optimization of the protocol, the ratio of 1:10 between concentration of protein and detergent was considered for the extraction mixture. Proteins were extracted by stirring the solution overnight at 4 °C. After ultracentrifugation, the resulting supernatant, corresponding to the membrane extract (ME), was concentrated when needed, using 2-mL centrifugal filters (50 kDa MW cut-off membrane, Amicon).

### 4.2.3 Protein quantification

The protein concentration of all samples was measured either with the NanoDrop apparatus (NanoDrop ND-1000, ThermoFisher) or with the BCA protein assay kit (ThermoFisher), according to the manufacturer's instructions.

### 4.2.4 Blue Native and Clear Native -PAGE

Electrophoresis was performed under anaerobic conditions in the glove box only if the downstream in-gel enzymatic assay was carried out. A hand-cast gradient Bis-Tris gel (5 to 15% (w/v) acrylamide/Bis-acrylamide, 1.0 mm thick, Hoefer Inc) was used in the SE260 Mighty Small II Deluxe Mini Vertical system (Hoefer Inc) (see **Supplementary Table B.1** for the preparation of the CN-PAGE gel preparation). The protein standard (Amersham high molecular weight standard, GE Healthcare) was used for the analysis while 20-50  $\mu$ g of protein of each sample were loaded into the gel. Each sample was loaded in replicate if downstream analysis, i.e.



Coomassie staining, in-gel enzymatic assay and Western blot, were performed in parallel. The samples, including the protein standards, were mixed at a 1:1 ratio with loading buffer (37.5 mM Tris-HCl (pH 6.8), 0.05% (v/v) Bromophenol Blue, 10% (v/v) Glycerol) supplemented with 0.05% (w/v) sodium deoxycholic acid. Addition of 0.02% (w/v) of detergent was required only for the protein samples that were not previously exposed to the detergent. Samples were incubated at 37 °C for 20 min before loading into the gel. The preparation of anode and cathode buffers differed depending if Blue Native (BN-PAGE) or Clear Native (CN-PAGE) were run. The buffers were prepared as described earlier [126, 129] and were pre-chilled to 4 °C prior to use. Samples migrated by imposing a constant current of 4 mA per gel and voltage limited to 350 V for 3 h.

#### 4.2.5 SDS-PAGE and two dimensional (2D) Native/SDS-PAGE gels

SDS-PAGE gel was previously described in Chapter 2 (see Section 2.2.4). Two dimensional SDS-PAGE was performed after CN-PAGE. The native gel pieces were first treated with a 5% SDS and 5% (v/v) of  $\beta$ -mercaptoethanol solutions and incubated at 45 °C for 30 min. Later, they were washed twice with ddH<sub>2</sub>O and incubated in presence of a solution containing 4.5% (w/v) iodoacetamide for 30 min at 45 °C. After a further wash with ddH<sub>2</sub>O the gel pieces were placed in-between the glass plates before casting the gel.

#### 4.2.6 Silver staining of gels

If silver staining was performed after Coomassie staining, PAGE gels were treated with 50% methanol solution and incubated at room temperature for 20 min. However, if the gel was unstained only 10 min incubation with a solution of 50% methanol was sufficient. This step led to the complete destaining and fixation of the gel. After a wash with ddH<sub>2</sub>O, the gel was treated with the sensitizing solution of 0.02% sodium thiosulfate (Sigma-Aldrich) and incubated for 1 min. The gel was washed twice with ddH<sub>2</sub>O and incubated in presence of a solution containing 0.1% (v/v) silver nitrate (Sigma-Aldrich) for 20 min at 4 °C. After the incubation, the solution was discarded and replaced with a basic developer solution of 3% sodium carbonate (Na<sub>2</sub>CO<sub>3</sub>) supplemented with 50  $\mu$ l of a 40% formaldehyde solution. Upon shaking of the gel-containing box, the bands or the spots appeared within 5 min. Once the adequate staining was reached, the development was stopped by adding a solution of 5% acetic acid in the gel-containing box. Within one minute the development reaction was stopped and the the solution was discarded. After rinsing with ddH<sub>2</sub>O, the gel was ready to be analyzed.

#### 4.2.7 Western blot analysis

For the immunological detection, purified anti-PceA antibodies were diluted 1:1000 in PBS-T solution (phosphate-buffered saline supplemented with 0.1 % of Tween 20), while purified anti-PceC antibodies (M. Willemin, unpublished data) were diluted 1:500 in PBS-T. The goat

anti-rabbit antibody conjugated with horseradish peroxidase (HRP) (Bio-Rad) was finally used at a dilution of 1:5000 in PBS-T for the detection of primary antibodies. HRP activity was revealed using the ChemiDoc system (Bio-Rad) and the Image Lab software package was used to visualize the intensity of the signals.

#### 4.2.8 In-gel PCE reductive dehalogenase enzymatic assay

The activity of the PceA reductive dehalogenase was assayed in an anaerobic glove box (Coy Laboratory) at room temperature. After CN-PAGE, the portion of the gel assigned to the enzymatic assay was transferred to 50 mM Tris-HCl buffer (pH 7.5) solution. Methyl viologen (MV) and PCE, which was previously dissolved in ethanol, were used as electron mediator and acceptor respectively. Before starting the assay, 250 mM of MV was reduced to obtain a dark blue colour. Initially, sodium dithionite (Sigma-Aldrich) was used as reducing agent for MV but later was replaced by incubating MV with zinc powder (Sigma-Aldrich) prior to add it to the reaction. Approximately 1 mL of reduced MV was added drop-wise on the surface of the gel yielding a homogeneous blue staining. After a removal of the excess liquid, 200  $\mu$ L of a 100 mM PCE solution in ethanol (20 mM final concentration) were added drop-wise on the gel surface. The gel was incubated at room temperature until the bands with PceA activity appeared colourless (corresponding to oxidized MV). Once the bands were clearly visible, a 150 mM solution of 2,3,5-triphenyltetrazolium chloride was added to stop the enzymatic reaction and fix irreversibly the blue staining of the gel into a red color. The colourless tetrazolium solution turns to red upon reaction with the reduced form of MV yielding a homogeneous and irreversible red staining of the gel. As result, the colourless bands, corresponding to PceA, remain visible and stable in the gel.

#### 4.2.9 LC-MS/MS analysis

This method was already described in Chapter 2 (see section 2.2.7).

### 4.3 Results and discussion

One of the major and promising objectives of the present research is the isolation of the reductive dehalogenase (RDH) protein complex from *Dehalobacter restrictus*. The achievement of this objective implied the definition of a tailor-made extraction protocol in combination with the development of an in-gel enzymatic assay for the detection of PceA. However, the limiting factors of low biomass yield of *Dehalobacter restrictus* and the large amount of biomass needed to identify the RDH complex represented constraints that made this approach highly demanding and ambitious.

### 4.3.1 Optimization of the membrane extraction and protein identification for the RDH complex

In this section the main steps towards the development of the membrane extraction protocol and the in-gel PCE reductive dehalogenase (PceA) enzymatic assay are described. The establishment of a reproducible extraction protocol represented a crucial pre-requisite for the localization of the RDH complex via the in-gel PceA enzymatic assay. To this purpose, preliminary experiments were conducted in collaboration in the Professor I.A. Pereira Laboratory at Universidade Nova de Lisboa (Lisbon, Portugal) and aimed at defining the first protocol to apply to *D. restrictus*. Then, an extensive work was conducted to evaluate the application of alternative techniques as well as the introduction of intermediate steps throughout the protocol. Finally, specific aspects of the protocol were improved in order to propose a definitive tailor-made protocol for the RDH complex identification.

**Preliminary experiments.** In the first experiments, the protocol for membrane proteins extraction used in the Pereira Lab was applied to *D. restrictus* biomass. In this context, different detergents were tested in parallel to evaluate their efficiency in solubilizing the RDH complex from the membrane fraction (**Figure 4.1**). Cells of *D. restrictus* were lysed by French press (1000 psi, 4 °C) to obtain cell-free extract (CFE).

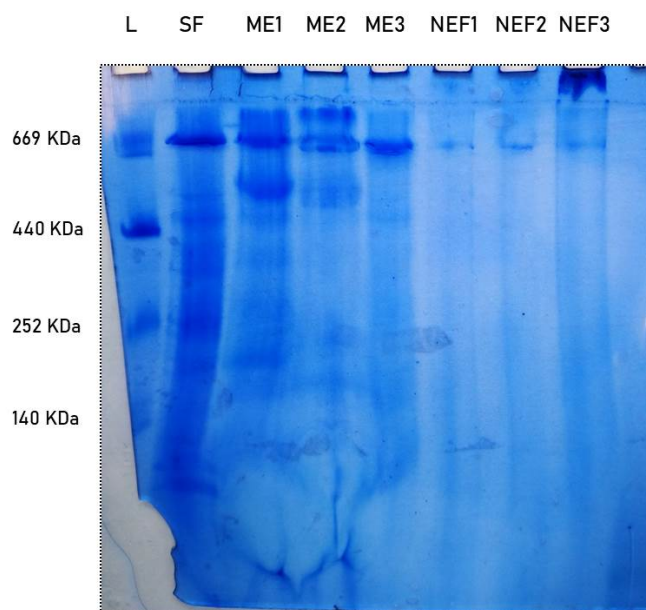


Figure 4.1: BN-PAGE analysis of protein fractions from *D. restrictus* - effects of different detergents used for membrane extraction. Aliquots of 50  $\mu$ g of the following samples were loaded on the gel: soluble fraction (SF), membrane extract after 3% DDM treatment (ME1), membrane extract after 1% digitonin treatment (ME2), membrane extract after 3% digitonin treatment (ME3), not-extracted fraction after 3% DDM treatment (NEF1), not-extracted fraction after 1% digitonin treatment (NEF2), not-extracted fraction after 1% Triton treatment (NEF3).

The membrane pellet was resuspended in Tris-HCl buffer supplied with 1% digitonin, 3% Triton and 3% *n*-dodecyl  $\beta$ -D-maltoside (DDM) in parallel. After overnight incubation at 4 °C the samples were centrifuged and the resulting supernatants corresponding to the different membrane extracts were collected. Following to protein quantification of the samples, 50  $\mu$ g of the fractions were analyzed by BN-PAGE gel. The gel revealed a very low resolution and irregular migration pattern of the membrane samples probably due to the high concentration of detergent. Despite these aspects, the ME1 sample, corresponding to the extract with DDM, showed a more resolved pattern than the other membrane extracts (**Figure 4.1**).

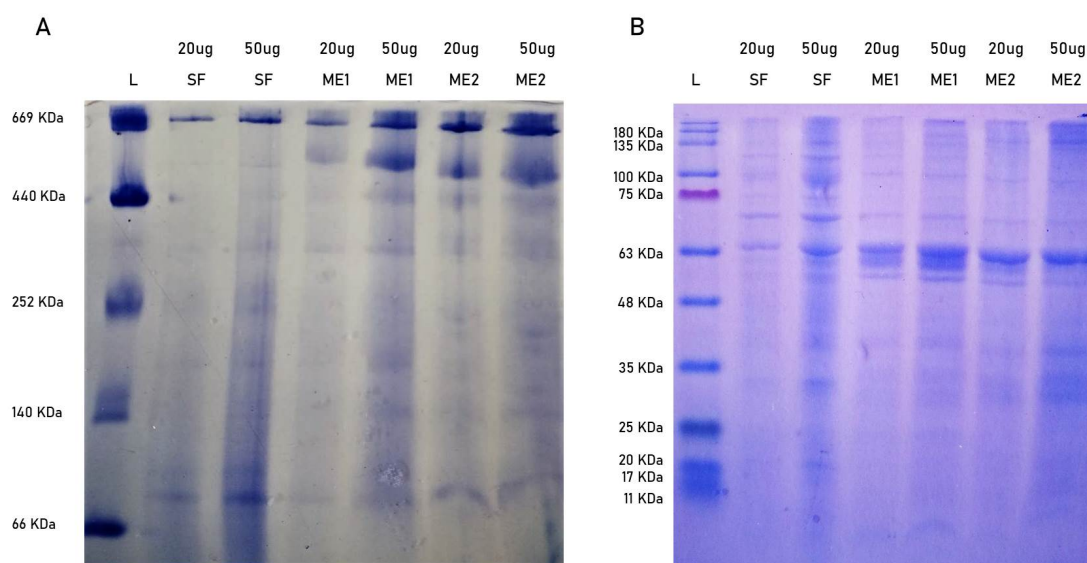


Figure 4.2: Effects of different amounts of sample loaded in the gel (20 or 50  $\mu$ g) and of different detergents (DDM and Triton-X-100) in native and denaturing gels. A) BN-PAGE gel loaded with the soluble fraction (SF), the membrane extract after treatment with 3% DDM (ME1) and with 1% Triton X-100 (ME2). B) SDS-PAGE gel loaded with the soluble fraction (SF), the membrane extract after treatment with 3% DDM (ME1) and with 1% Triton X-100 (ME2).

In addition, to overcome the irregular migration, the loading of a lower amount of samples was considered for the future experiments. In this context, 20 and 50  $\mu$ g of membrane extracts resulting from Triton X-100 and DDM extraction were analyzed by BN-PAGE and SDS-PAGE in parallel (**Figure 4.2**). Overall the migration pattern on the native gel still appeared as blurred and the detergent was dominant at the gel front impeding a good resolution of the bands around the area of 50 kDa of molecular weight (**Figure 4.2A**). However, a neater migration of the bands was obtained with DDM (ME1) and 50  $\mu$ g exhibited an increased resolution of the bands over 20  $\mu$ g. Furthermore, a higher protein recovery from the DDM extraction than that of Triton X-100 was observed by SDS-PAGE (**Figure 4.2B**). Taken together, these results convinced to choose DDM as solubilizing agent for the next experiments.

In the next round of experiments, several changes were proposed to improve the overall resolution of the native gel. In this framework, the application of centrifugal filter with 50 kDa cut-off prior to load the gel was sought to reduce the excess of DDM in the membrane extract. Furthermore, CN-PAGE was considered over BN-PAGE as it is milder, and as it has been shown to keep labile supra-molecular assemblies of membrane protein complexes that are otherwise dissociated under BN-PAGE conditions [128]. In addition, CN-PAGE offers an decisive advantage over BN-PAGE when Coomassie interferes with techniques required to further analyze the native complexes, as in the case of the downstream application of the in-gel PceA enzymatic assay. The results obtained with these modifications of the protocol showed an increased resolution of the migration pattern (**Figure 4.3**). Furthermore, two intense bands above 140 kDa showing PceA-activity were excised and analysed via MALDI-TOF/MS analysis. The sole presence of PceA was detected while PceB and PceC were not revealed (data not shown). This result was likely due to the presence of detergents that might have strongly inhibited proteases and thus severely decreased the detection of these proteins on MALDI spectra. For this reason, other experiments were considered to verify these preliminary results.

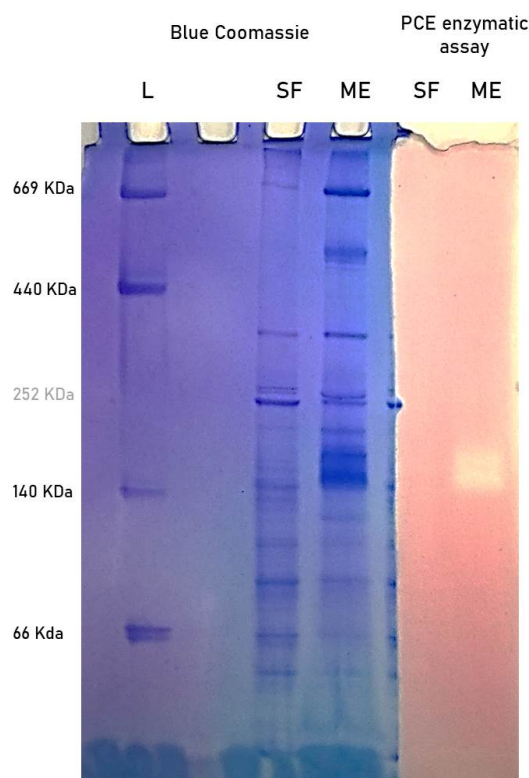


Figure 4.3: *D. restrictus* soluble and membrane extract analysis through CN-PAGE. Total protein was detected by Blue Coomassie staining (left) and PceA activity as described in the M&M section (right side). SF and ME stand for soluble fraction and membrane extract respectively.

**Optimization of the membrane extraction protocol.** The early-stage findings urged to exploit the expertise on sample preparation and native gel analysis learned from the Pereira laboratory with the aim to reproduce and further improve the results obtained in Lisbon. In this context, several changes in the sample preparation process were proposed. Firstly, different cell lysis techniques were tested in parallel and their effect on the resolution in native gels was evaluated. So far this step was performed via the French press placed outside the anaerobic chamber with the risk to expose the samples to oxygen contamination. Sonication or glass beads lysis were tested as possible alternatives to the French press as they could be easily performed in anaerobic conditions. This aspect appears to be crucial when PceA enzymatic activity is considered. Overall, a blurred migration of the bands was observed with the different lysis techniques. However, the membrane extract resulting from the French press displayed the best resolution around 140 kDa, where the RDH complex is likely to migrate in native conditions. These results exhorted to consider the French press as the standard cell lysis technique for the following experiments (**Figure 4.4**).

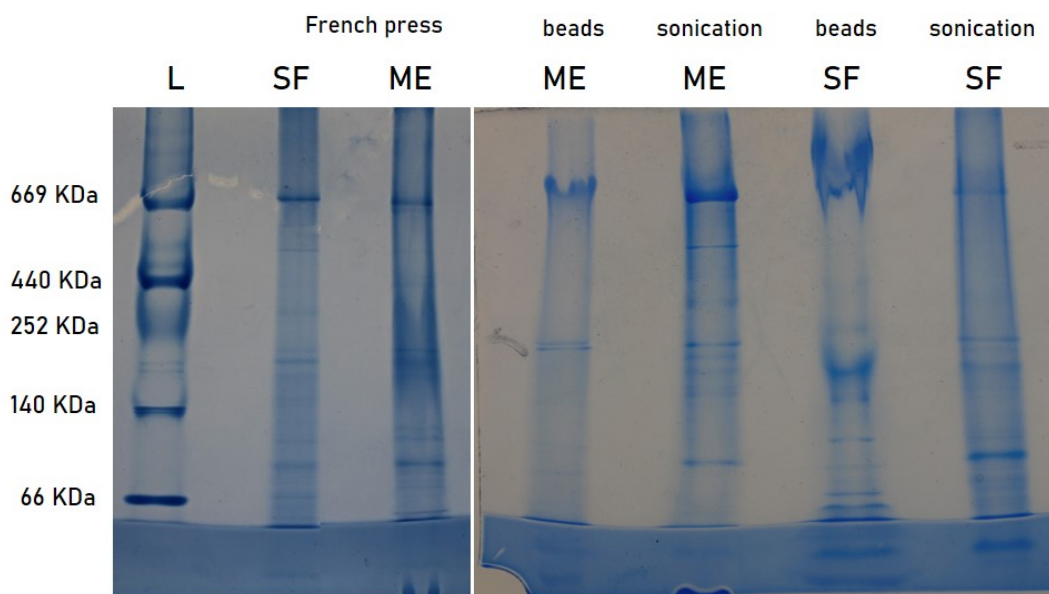


Figure 4.4: Effects of different cell lysis techniques applied on *D. restrictus* on the protein resolution in CN-PAGE analysis. In this experiment the French press, glass beads and sonication lysis techniques were tested in parallel. The evaluation of the lysis efficiency was made on the resulting migration pattern in CN-PAGE gels.

A new experiment was proposed to evaluate the effect of an additional wash of the membrane fraction with 300 mM KCl. This was sought to remove the loosely bound or soluble proteins contaminating the membrane fraction. The different fractions, namely soluble fraction, membrane extract (ME1, as before) and membrane fraction after KCl wash (ME2) were analyzed by SDS-PAGE and CN-PAGE, and immunoblotting for PceA and PceC was performed (**Figures 4.5 and 4.6**). The analysis using anti-PceA antibodies in native conditions confirmed the



presence of the antigen in two different bands with a molecular mass of ~150 kDa but also revealed the presence of a second PceA-containing complex at ~670 kDa in the soluble fraction (**Figure 4.5B**). Strikingly, in the membrane extract obtained with KCl wash (ME2), the two PceA-containing complexes coexisted and were detected with strong signal intensity, although the one of ~150 kDa band seems stronger. On the other hand, the membrane extract without KCl wash (ME1) showed mostly the signal of 150 kDa for the PceA-containing complex (**Figure 4.5B**).

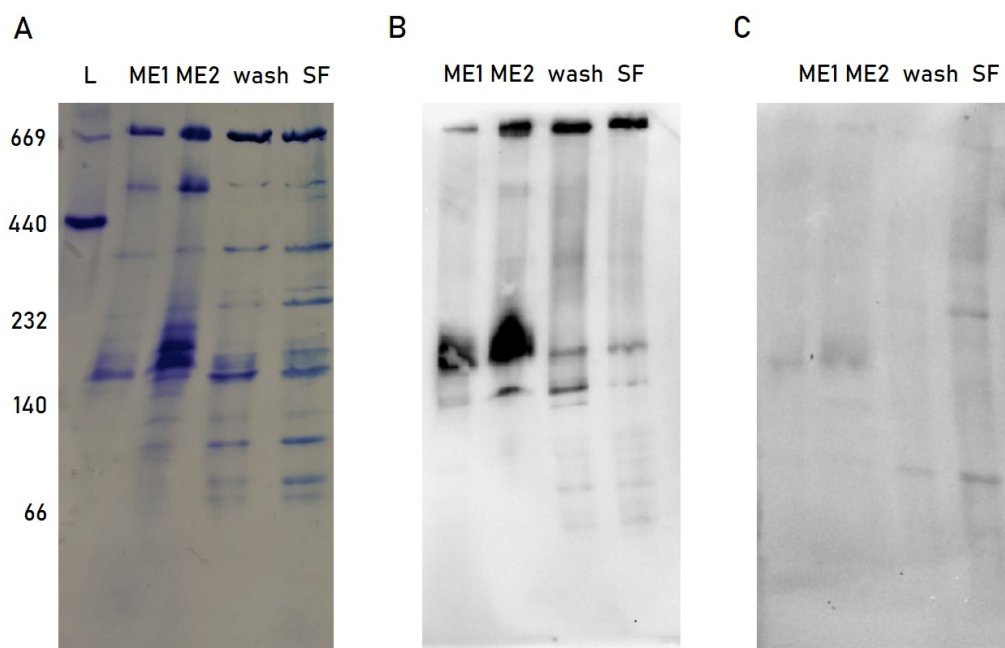


Figure 4.5: CN-PAGE analysis and PceA- and PceC- immunoblotting of *D. restrictus*. ME1: membrane extract without KCl treatment. ME2: membrane extract after KCl treatment. Wash: supernatant obtained from the membrane fraction washed with KCl. SF: soluble fraction. A) CN-PAGE gel stained with Coomassie blue. B) Western blot using anti-PceA antibodies. C) Western blot using anti-PceC antibodies.

Moreover, according to MS analysis, the 670 kDa complex was largely dominated by the molecular chaperone GroEL alongside with PceA and many other proteins (see **Supplementary Figure B.1**), which likely represents a maturation complex. This result was also confirmed on a 2D-Native/SDS-PAGE gel of the 670 kDa band, which revealed the presence of a major band at the molecular mass of ~63 kDa, corresponding to the effective molecular weight of the GroEL chaperone protein (see red arrow in **Figure 4.7B**). Furthermore, immunoblotting using anti-PceA antibody on SDS-PAGE gel revealed a relatively high intensity signal in each of the loaded fractions, suggesting the high abundance of PceA in the different sub-cellular compartments (**Figure 4.6B**). Moreover, the intense PceA signal in the wash sample confirmed the importance of KCl treatment in removing the portion of PceA loosely bound to the membrane or carried over during the separation after ultracentrifugation. Differently, Western blot analysis using the anti-PceC antibody was performed on CN-PAGE to detect and localize PceC.

The data showed a weak signal around 150 kDa in the membrane extract sample, however the detection of PceC signal in soluble and wash samples suggest the poor specificity of anti-PceC antibodies for their antigen (**Figure 4.5C**).

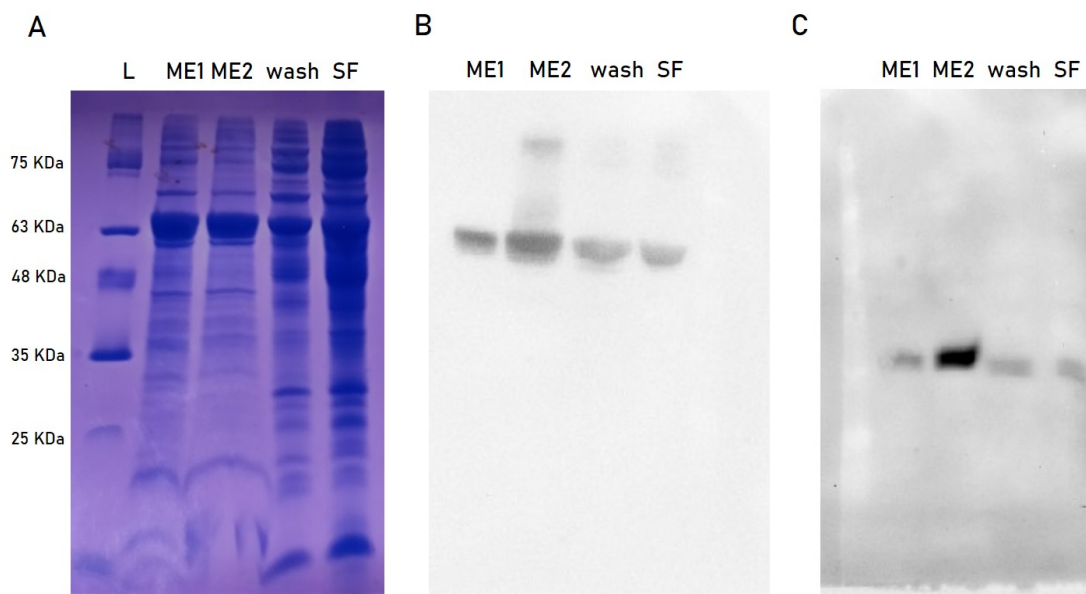


Figure 4.6: SDS-PAGE analysis and PceA- and PceC- immunoblotting of *D. restrictus*. ME1: membrane extract without KCl treatment. ME2: membrane extract after KCl treatment. Wash: supernatant obtained from the membrane fraction washed with KCl. SF: soluble fraction. A) SDS-PAGE gel stained with Coomassie blue. B) Western blot using anti-PceA antibodies. C) Western blot using anti-PceC antibodies.

On the other hand, the same analysis conducted on SDS-PAGE showed an intense signal in the membrane extract sample obtained after KCl wash (ME2), while faint signals were detected in the membrane sample without KCl wash (ME1) as well as in the soluble fraction (SF) (**Figure 4.6C**). Overall, the results highlighted the difficulty to localize PceC in native conditions and led to consider Western blot analysis as valuable tool for the localization of PceA only in native and denaturing gels.

**Towards the definition of the final sample preparation protocol.** The extensive work of optimization resulted in several improvements of the sample preparation protocol. However different technical issues concerning buffer preparation, acrylamide solution and electrophoresis gel system prevented to obtain a high resolution CN-PAGE which is crucial for the in-gel localization of the RDH complex. To overcome the resolution issue further changes on the protocol were applied. The first experiment aimed at fine-tuning the extraction step with DDM. So far, 3% DDM (W/v) was supplied to the membrane fraction suspension regardless of its protein concentration. This approach prevented the reproducibility of the extraction protocol as the ratio of detergent to membrane proteins as well as the extraction yield varied



from one experiment to the other. A previous study defined the 10:1 (w/w) detergent to protein ratio as the optimal threshold to obtain the complete delipidization of the membrane and individual detergent-protein complexes formation [130].

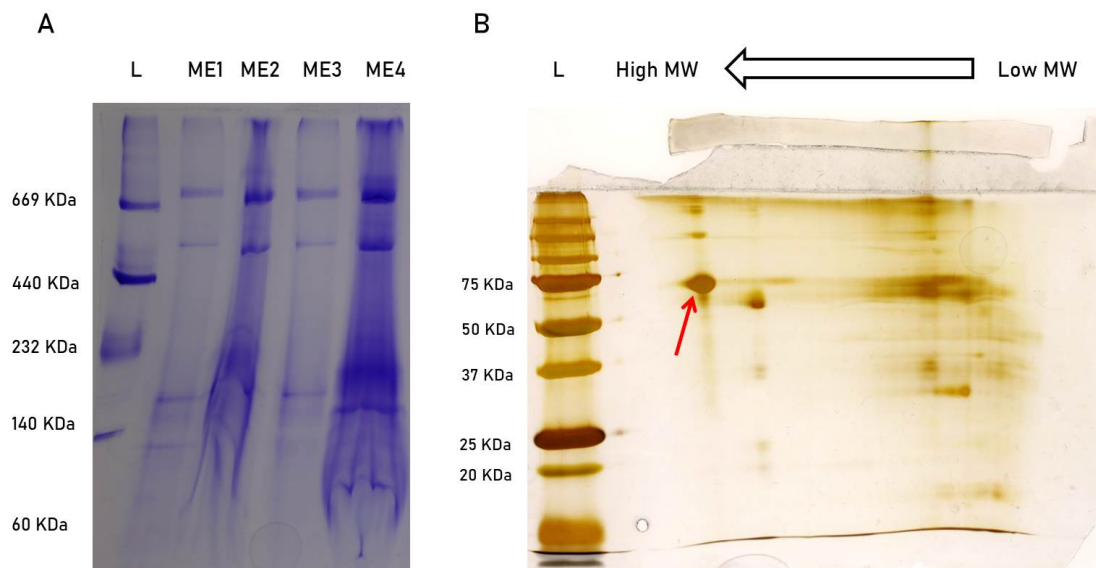


Figure 4.7: Effect of concentration step applied on membrane extract in CN-PAGE migration pattern and 2D-Native/SDS-PAGE gel performed using 10:1 DDM/protein CN-PAGE gel lane as starting material. Panel A) Different DDM to membrane protein ratios were tested in parallel. The figure shows only 5:1 and 2.5:1 DDM to protein ratios. To evaluate the effect of concentration step, 50  $\mu$ g of protein were loaded in each lane. ME1: 2.5:1 DDM to membrane protein ratio without concentration. ME2: 2.5:1 DDM to membrane protein ratio after concentration. ME3: 5:1 DDM to membrane protein ratio without concentration. ME4: 5:1 DDM to membrane protein ratio after concentration. Panel B) 2D-Native/SDS-PAGE gel performed using 10:1 DDM/protein concentrated membrane extract. The corresponding CN-PAGE gel lane was cut and used as starting material for the second dimension SDS-PAGE gel. the red arrow shows the 63 kDa GroEL chaperonin protein dominating the native 670 kDa band.

In this context, different DDM to membrane protein ratios, namely from 1.25:1 until 10:1 (w/w), were applied in parallel in the extraction mixture. Furthermore, the effect of the concentration with centrifugal filters (PM-50, Amicon) prior to gel loading was also tested for the different membrane extracts. The **Figure 4.7A** showed only two ratios tested, namely 5:1 and 2.5:1 DDM to protein ratio. The results showed that no substantial difference in migration pattern was observed between the different DDM extractions. Moreover, the native gel revealed that concentration of the sample led to an increase of DDM in the sample which resulted in an irregular migration pattern and blurred bands resolution on gel, despite same amount of protein of concentrated and not-concentrated samples was loaded (**Figure 4.7A**). The identification of the different proteins composing the bands around 140 kDa failed due to lack of neat resolution in that specific area of the native gel (**Figure 4.7B**). These result proved that the concentration step prevents to have a neat migration pattern in CN-PAGE,

thus compromising the downstream analysis of the resulting gel bands.

A further experiment was performed to improve the protein bands resolution in CN-PAGE and make possible the downstream analysis, such as the identification of single proteins in 2D-Native/SDS-PAGE gel and MS analysis. In this context, a 10:1 DDM to proteins ratio was applied, and no concentration step was applied to the membrane extract prior to electrophoresis. Multiple lanes of soluble fraction and membrane extract were loaded to perform Western blot for PceA on native condition (**Figure 4.8**), 2D-Native/SDS-PAGE gel (**Figure 4.9**) and on single dimension denaturing gel (**Figure 4.10**). The immunological assay on native gel confirmed the earlier findings by revealing the presence of PceA in two different complexes migrating at ~150 kDa and ~670 kDa in native gel (**Figure 4.8B**). Furthermore, Western blot analysis performed after one-dimensional SDS-PAGE showed that DDM was highly efficient to extract the membrane-bound PceA (**Figure 4.10B**). Additionally, MS analysis applied on protein spots of 2D-Native/SDS-PAGE gel (see **Supplementary Figure B.2**) allowed to identify the  $\alpha$  (MW: 55 kDa) and  $\beta$  (MW: 50 kDa)  $F_1$  subunits of the ATP synthase as the major proteins composing the complex migrating at ~540 kDa in CN-PAGE (**Figure 4.9A**) indicated with blue arrow). Earlier studies conducted on the  $F_0F_1$  ATP synthase complex of *E. coli* revealed a molecular weight of ~530 kDa [131]. Taken together, these results led to conclude that the complex identified in the native gel was likely the complete  $F_0F_1$  ATP synthase. In addition, from ATP synthase of *E. coli*, it appeared that the  $\alpha$  and  $\beta$   $F_1$  subunits are in 3:1 stoichiometry ratio with the other subunits of  $F_1$  subunit of the complex [131]. This might be the reason why these two subunits displayed an intense signal after silver staining, while the other subunits appeared with a lower intensity.

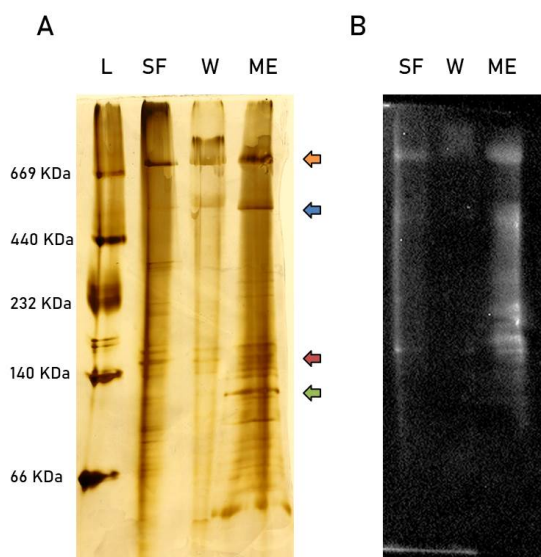


Figure 4.8: CN-PAGE of *D. restrictus* and Western blot for PceA. A) CN-PAGE gel stained with silver nitrate. The orange arrow corresponds to 670 kDa complex, the blue arrow indicates the  $F_0F_1$  ATP synthase complex and the red and green arrows correspond to 150 kDa and 120 kDa areas, respectively. The same annotation is used for Figure 4.9. B) Western blot for PceA applied on the CN-PAGE gel.

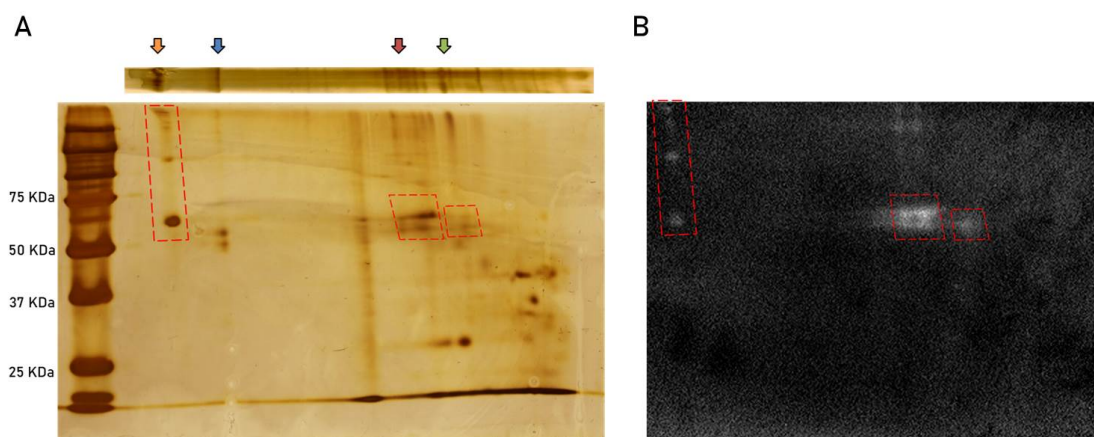


Figure 4.9: 2D Native/SDS-PAGE gel of *D. restrictus* and correspondent Western blot for PceA. A) 2D-Native/SDS-PAGE gel stained with silver nitrate. The orange arrow corresponds to the ~670 kDa complex, the blue one indicates the  $F_0F_1$  ATP synthase complex, while the red and green arrows correspond to the 150 kDa and 120 kDa gel areas, respectively. B) Western blot for PceA applied to the 2D-Native/SDS-PAGE gel.

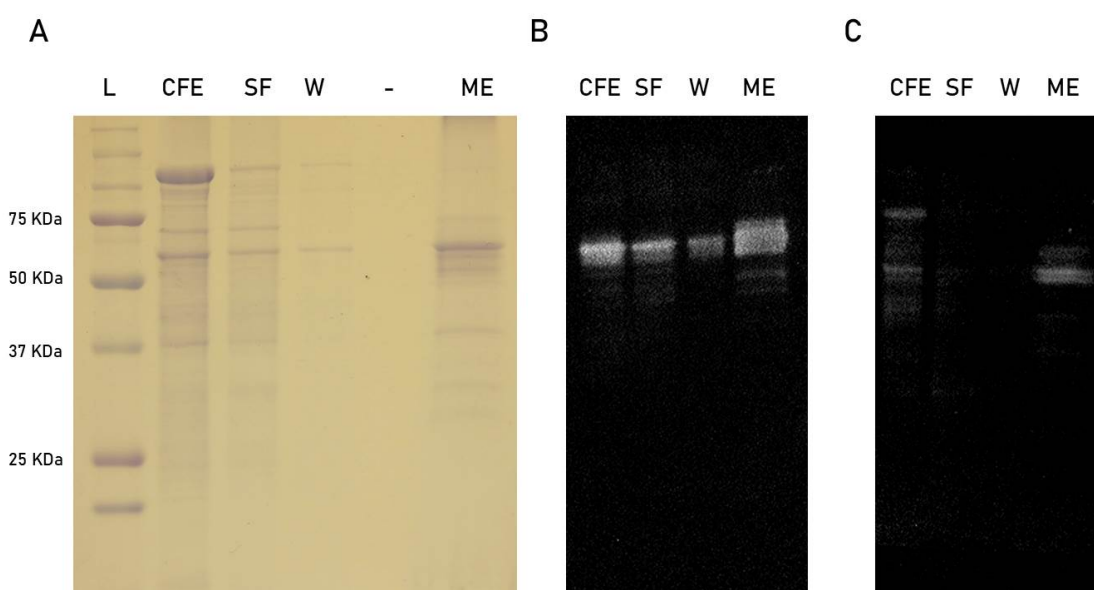


Figure 4.10: SDS-PAGE analysis of *D. restrictus* fractions and correspondent Western blot analysis for PceA and PceC. A) SDS-PAGE gel stained with Coomassie. B) Western blot for PceA performed with the SDS-PAGE gel. C) Western blot for PceC performed with the SDS-PAGE gel.

Interestingly, the second dimension Native/SDS-PAGE gel coupled with MS analysis revealed that the complex at ~120 kDa was mainly composed of a 28 kDa protein (Dehre\_1178) (**Figure 4.9A**), indicated with light green arrow), which is homologous to the cytoskeleton protein

RodZ of *E.coli* (see **Supplementary Figure B.2**). The above-described experiments represented the main steps that led to the establishment of protocols for cell fractionation and membrane solubilization. In the following section the development of the in-gel PceA enzymatic assay is thoroughly presented.

**Development of the in-gel PceA enzymatic assay** PceA is an enzyme sensitive to oxygen and for this reason the necessity to avoid any oxygen contamination throughout the process of biomass harvesting, cell fractionation and membrane protein complex extraction represents a prerequisite for a successful in-gel PceA enzymatic assay. To achieve this goal, airtight 1-L plastic Harvestline System liners (Beckman Coulter, Switzerland) were introduced to preserve the anaerobic conditions during the biomass harvest, while membrane extraction and following downstream analyses were performed inside the anaerobic chamber. The in-gel PceA activity assay is based on the ability of methyl viologen to turn from intense dark blue to colourless as a result of the change from its reduced state to the oxidized form. For the first tests, a cell-free extract of *D. restrictus* and a pre-cast NuPAGE gel (4%-15%) (Bio-Rad, Switzerland) were used to evaluate the feasibility of the in-gel assay (**Figure 4.11**).

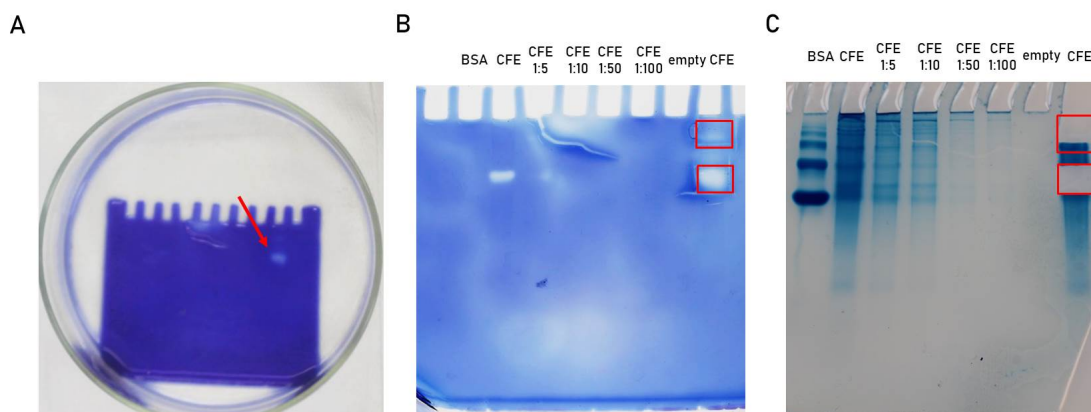


Figure 4.11: In-gel PceA enzymatic assay on cell-free extract of *D. restrictus*. Different dilutions of CFE were loaded on the gel to evaluate the intensity of PceA activity signal. A) Pre-cast NuPAGE gel (4%-15%) after the addition of reduced methyl viologen and PCE. The red arrow shows the white band corresponding to PceA activity. B) NuPAGE gel (4%-15%) at the end of in-gel PCE enzymatic assay. The red boxes indicate the portions of gel with more PceA activity. C) NuPAGE gel (4%-15%) stained with Coomassie blue after the in-gel enzymatic assay. The portion of gel corresponding to the red boxes were cut and analyzed via LC-MS/MS.

Alongside with the cell-free extract, BSA was also loaded as a negative control. After electrophoresis, the gel was transferred in a glass Petri dish containing Tris-HCl buffer and 250 mM of methyl viologen previously reduced with 100  $\mu$ L of 3% dithionite solution. The incubation with the reduced form of methyl viologen resulted in an intense dark blue staining of the gel. Later, the excess of liquid was removed and PCE was supplied onto the gel. Two bands with PceA enzymatic activity were observed as they appeared colourless after due to methyl

viologen oxidation (**Figure 4.11**). MS analysis on the two bands confirmed the presence of PceA with high sequence coverage, although many other proteins were detected together with it (data not shown).

After the achievement of a neat protein migration pattern in CN-PAGE gels, numerous attempts of the in-gel enzymatic assay were performed to unequivocally localize PceA-containing complexes in the native gel (**Figure 4.12**). Strikingly, the appearance of white bands in the soluble fraction were observed prior to the addition of PCE (data not shown). This was likely due to the presence of hydrogenase complexes responsible for the oxidation of methyl viologen by  $H_2$  that was present in the anaerobic chamber. To overcome this issue, the gel was transferred in a anaerobic serum flask and flushed with nitrogen to remove any trace of hydrogen. The different reagents for the in-gel enzymatic assay were later injected therein. Moreover, to fix the signal of oxidized methyl viologen after completion of the assay upon exposure to air, the gel was incubated with 2,3,5-triphenyltetrazolium chloride (Sigma-Aldrich). The tetrazolium salt reacts with methyl viologen in the gel which turned from blue to purple irreversibly (**Figure 4.12**).

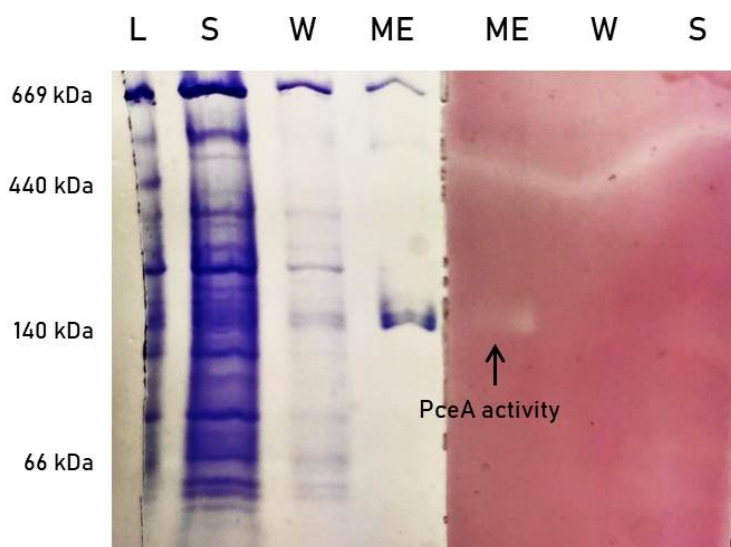


Figure 4.12: CN-PAGE analysis and in-gel PceA enzymatic assay. Half of the gel was stained with Coomassie (on the left), while the in-gel PceA assay was run with the other half (on the right). The pink colour is due to the addition of 2,3,5-triphenyltetrazolium chloride at the end of the assay to stably fix the methyl viologen signal.

The tedious work done in the RDH complex extraction and localization was then exploited in the form of an optimized protocol that was applied to biomass samples of *D. restrictus* and *D. hafniense* strain TCE1. This is presented in the following section.



### 4.3.2 Identification of the RDH complex from *D. restrictus* and *D. hafniense* strain TCE1

The optimized protocol for sample preparation was first applied to the biomass of *D. restrictus* in anaerobic conditions. To preserve the oxygen-depleting environment for cell lysis, the French press apparatus was flushed with anaerobic Tris-HCl buffer prior the use of biomass suspension. In addition, to prevent the exposure of sample to oxygen a system of tubing connecting the instrument to the oxygen-depleted tube was used. The obtained Coomassie-stained CN-PAGE gel revealed the presence of two major bands with apparent size of ~140 kDa and ~180 kDa in the membrane extract, as shown by the in-gel PceA enzymatic assay (**Figure 4.13A**). Furthermore, 2D-Native/SDS-PAGE (**Figure 4.13B**) together with MS analysis of the resulting bands were performed on the two PceA-containing bands that displayed activity to investigate the protein composition.

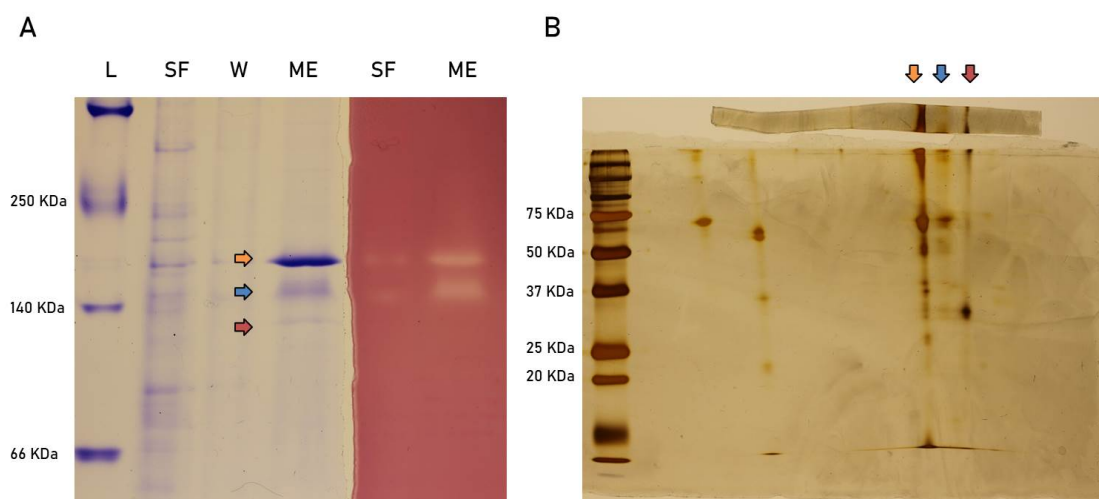


Figure 4.13: CN-PAGE analysis, in-gel enzymatic assay and SDS-PAGE analysis of protein fractions from *D. restrictus*. A) CN-PAGE gel of *D. restrictus* fractions stained with Coomassie blue (left part) and its corresponding in-gel PceA enzymatic assay (right part). The yellow, green and red arrows indicate the portions of gel corresponding to 180, 140 and 120 kDa, respectively. The same annotation was used B) SDS-PAGE analysis was applied to the CN-PAGE gel lane of the membrane extract.

PceA and PceB were detected by MS, however several other proteins were also identified revealing the limit of 2D-Native/SDS-PAGE to separate and define unequivocally the proteins forming the different complexes (**Figure 4.14**). To improve the anoxic environment throughout the sample preparation protocol, the chamber of french press was previously flushed with anaerobic Tris-HCl buffer supplemented with 10 mM dithiothreitol (DTT) (Thermo Scientific) prior to cell lysis and same amount of reducing agent was also added in the buffers used throughout the membrane extraction protocol.

Identified Proteins	Accession Number	MW (kDa)	140 kDa	140 kDa rank	180 kDa	180 kDa rank
Dehre_2398 reductive dehalogenase 2410979:2412634 reverse MW:61206	Dehre_2398	61	2339	1	1934	1
Dehre_2052 reductive dehalogenase 2066281:2067939 reverse MW:61546	Dehre_2052	62	74	4	71	2
Dehre_2397 hypothetical protein 2410599:2410916 reverse MW:11857	Dehre_2397	12	81	3	58	3
Dehre_2336 chaperonin GroL 2341504:2343138 reverse MW:57484	Dehre_2336	57	63	5	35	4
Dehre_2170 Uncharacterized protein conserved in bacteria 2185636:2186637 reverse MW:35463	Dehre_2170	35	22	9	31	5
Dehre_1488 nicotinate-nucleotide-dimethylbenzimidazole phosphoribosyltransferase 1479257:1480375 forward MW:38628	Dehre_1488	39	19	12	24	6
Dehre_2489 Uncharacterized protein conserved in bacteria 2503987:2505234 reverse MW:44869	Dehre_2489	45	26	7	18	7
Dehre_2800 proton translocating ATP synthase, F1 alpha subunit 2836817:2838319 reverse MW:54762	Dehre_2800	55	21	10	18	8
Dehre_0470 Integral membrane protein (PIN domain superfamily) 470575:471741 forward MW:42712	Dehre_0470	43	26	8	13	9
Dehre_2802 ATP synthase, F0 subunit b 2838890:2839447 reverse MW:21216	Dehre_2802	21	6	16	12	10
Dehre_2875 hypothetical protein 2914762:2915373 reverse MW:23380	Dehre_2875	23	20	11	10	11
Dehre_2395 FKBP-type peptidyl-prolyl cis-trans isomerase (trigger factor) 2408127:2409077 reverse MW:37037	Dehre_2395	37	10	14	9	12
Dehre_2396 FMN-binding domain. 2409205:2410491 reverse MW:48876	Dehre_2396	49	16	13	7	13
Dehre_2799 ATP synthase, F1 gamma subunit 2835950:2836798 reverse MW:31084	Dehre_2799	31	3	17	7	14
Dehre_2549 YeeE/YeeE family (DUF395). 2565547:2566623 reverse MW:37412	Dehre_2549	37	89	2	5	15
Dehre_2798 ATP synthase, F1 beta subunit 2834509:2835912 reverse MW:50789	Dehre_2798	51	7	15	5	16
Dehre_2710 Uncharacterized protein conserved in bacteria 2737504:2738403 reverse MW:33036	Dehre_2710	33	35	6	1	17

Figure 4.14: List of proteins detected by LC-MS/MS analysis of the 140 and 180 kDa bands. For each gel band of interest the first column accounts for the number of spectra of each protein detected while the second column indicate the rank of each protein from the most (position 1) to the less detected (position 17). The ranking was based on the number of spectra.

The results obtained for *D. restrictus* revealed the presence of a highly abundant PceA-containing complex at the apparent size of ~180 kDa, while scarce activity of RDH complex at 140 kDa was observed in *D. restrictus* (Figure 4.15). In contrast, for *D. hafniense* strain TCE1, two bands, at ~180 and ~140 kDa, showed PceA enzymatic activity with similar intensity, while Coomassie staining of the corresponding area revealed a dominant band at 180 kDa with the 140 kDa band much less intense (Figure 4.15B).

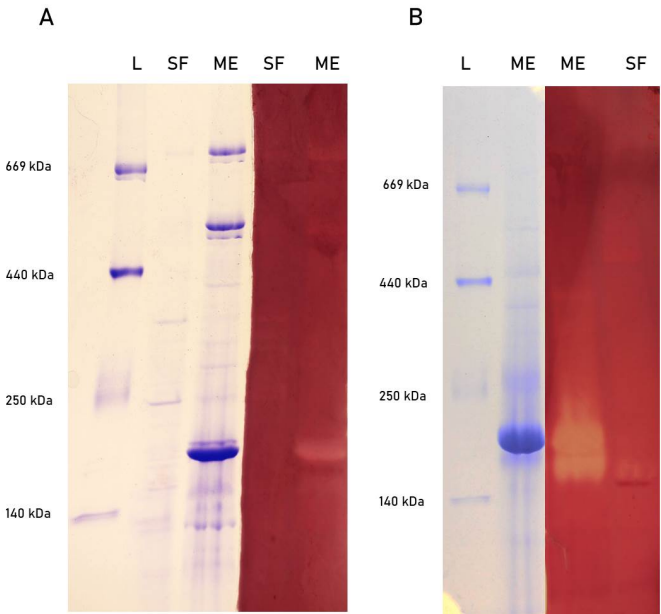


Figure 4.15: CN-PAGE analysis and in-gel PceA enzymatic assay of protein fractions from A) *D. restrictus* and B) *D. hafniense* strain TCE1.

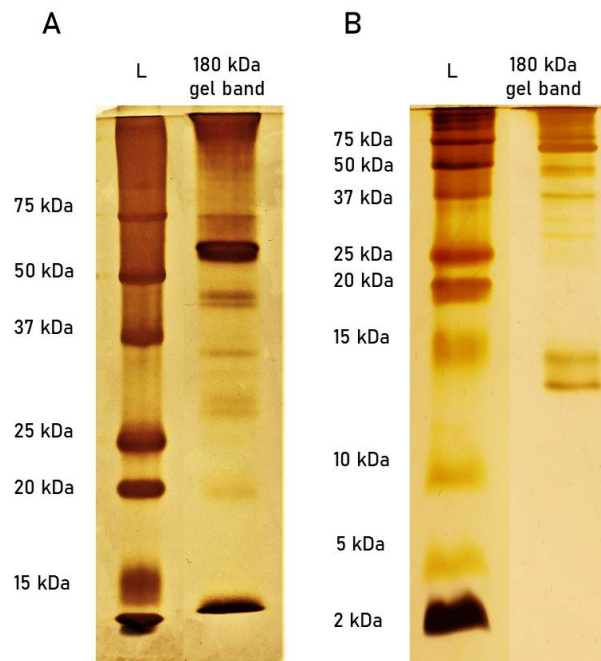


Figure 4.16: SDS-PAGE analysis of the 180 kDa gel band excised from the CN-PAGE gel of *D. restrictus* membrane extract. SDS-gels were made with A) 12% and B) 20% acrylamide in the resolving gel.

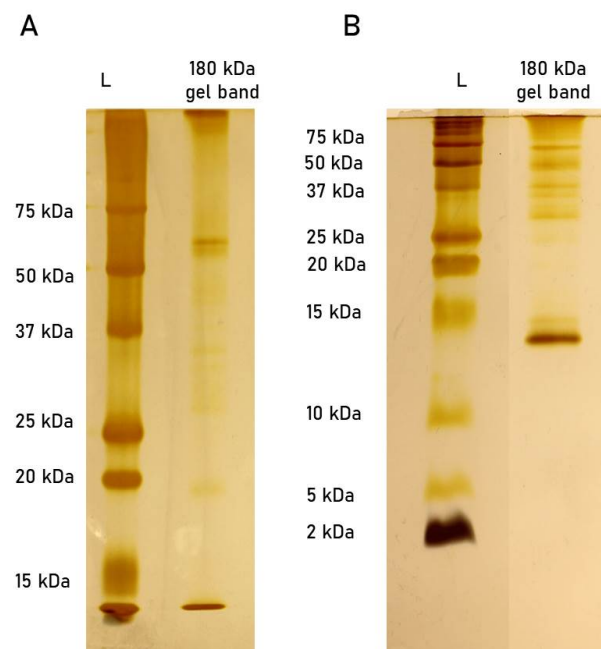


Figure 4.17: SDS-PAGE analysis of the 180 kDa gel band excised from the CN-PAGE gel of *D. hafniense* membrane extract. SDS-gels were made with A) 12% and B) 20% acrylamide in the resolving gel.



Overall, these results led to hypothesize that the reducing conditions in presence of DTT helped to preserve the integrity of the 180 kDa complex, while the 140 kDa complex is likely the result of its partial dismantlement (**Figure 4.15A**). Furthermore, SDS-PAGE analysis was performed with the 180 kDa band from both strains. In the case of *D. restrictus*, two major bands at 60 kDa and 13 kDa were revealed with silver staining, although other proteins were also present with a lower intensity (**Figure 4.16A**). A similar pattern was observed for *D. hafniense* strain TCE1 (**Figure 4.17**).

### 4.3.3 Conclusions

In the present chapter the tedious and time-consuming work on the optimization of sample preparation and in-gel enzymatic assay was presented in detail. The results obtained from the application of these two methods allowed the extraction of the RDH complex from the cytoplasmic membrane and its localization in native gels. Beside the Pce proteins, the defined solubilization protocol applied to membranes of *D. restrictus* and *D. hafniense* strain TCE1 coupled with 2D-CN/SDS-PAGE analysis helped also identifying other protein complexes, such as the GroEL maturation complex and F<sub>0</sub>F<sub>1</sub> ATP synthase. Likewise, the in-gel PceA enzymatic assay represented a substantial improvement in the identification and localization of the active RDH complex when compared to the existing literature. Earlier studies conducted on *Dehalococcoides mccartyi* strain CBDB1 revealed the presence of the multi-subunit protein complex using BN-PAGE analysis coupled to mass spectrometric label-free protein quantification [66, 68]. An extensive screening of the numerous gel slices with LC-MS/MS was required to identify the relative abundance of the different subunits of the complex. Furthermore, to assay the distribution of the reductive dehalogenase activity in unstained BN-PAGE gel lanes, individual gel slices were transferred in anaerobic vials supplied with methyl viologen and the chlorinated compounds, and were analyzed by gas chromatography. The development of the in-gel enzymatic assay in CN-PAGE gels proposed in the present work, represents an innovative way to localize the RDH complex in native gels. Its practicality and wide applicability constitute the main assets of the method, that could become a reference tool for the identification of other oxygen-sensitive protein complexes in the field of OHR and beyond.

Despite the improvement achieved in the resolution of CN-PAGE gels and in the localization of the RDH complex via the in-gel enzymatic assay, LC-MS/MS analysis performed on gel pieces corresponding to the complex failed to unambiguously identify the protein partners associated with PceA. The results revealed the presence of a band around 13 kDa, likely corresponding to PceB (see **Figure 4.16** and **Figure 4.17**). However, MS analysis could not confirm this hypothesis, as many other proteins were also detected together with the target protein. Furthermore, despite several attempts, any clear indication on the involvement of other protein partner(s) was obtained. This represents a major bottleneck of protein identification from in-gel MS analysis. For this reason, further investigation was attempted to better characterize the RDH complex. These aspects are discussed in the following chapter.

## 5 Characterization of the reductive dehalogenase complex

### 5.1 Introduction

The *pceABCT* gene operon represents one of the paradigmatic genetic systems in OHR, nonetheless, only scarce biochemical knowledge is available on the gene products except for PceA [13, 46, 48]. To date, most of the studies have revealed that reductive dehalogenases (RDases) are highly sensitive to oxygen and have been identified as a 46-65 kDa monomeric proteins [72]. However, the crystal structure of PceA from *S. multivorans* has been elucidated revealing a homodimer [106]. Regardless of the fact that the characterized RDases belong to phylogenetically diverse OHRB, the structural analysis of the enzymes confirmed the presence of common sequence features: a corrinoid cofactor, which is deeply buried in the protein, and two iron-sulfur clusters located close to the surface of the enzyme and in close proximity to the corrinoid cofactor [70]. Besides PceA, the gene cluster also codes for two putative integral membrane proteins, PceB and PceC, for which no unambiguous function has been assigned yet, and for PceT, which is a molecular chaperone involved in the folding process of PceA [82, 83].

As presented in the previous chapter, recent advances in the extraction and localization of the reductive dehalogenase complex have been made. However, numerous open questions on the 180 kDa complex harbouring PceA activity resulted as unanswered yet. The in-gel MS analysis confirmed the presence of PceA and likely PceB in the 180 kDa complex, however did not permit any conclusion on the complete protein composition of the RDH complex due to the high number of proteins detected together with PceA. Thus, at this stage the possibility that other protein(s) might be part of the complex has to be envisaged. Based on the hypothetical model presented by Maillard and Holliger [35] for the transfer across the membrane, the electrons are taken up by electron carrier(s), such as menaquinone that likely function as electron shuttle between the electron-donating and -accepting enzymes as described by the redox loop mechanism [58]. However, the involvement of menaquinone in electron transfer in *S. multivorans* was questioned due to its relatively high redox potential (-74 mV) resulting in its unlikely role in direct electron delivery to RDases [64]. Thus, the

involvement of additional unknown electron carriers to subsequently generate the proton motive force was considered. Recent studies have proposed a putative membrane bound quinol dehydrogenase as a potential candidate linking menaquinol and PceA in *S. multivorans* [34] or CprA in *D. dehalogenans* [117]. Moreover, in *D. restrictus* and *D. hafniense* strain TCE1, the flavoprotein PceC was also postulated to act as a protein linking menaquinol and PceA [81]. However, the quantitative proteomic analyses presented in Chapter 3 targeting the membrane fractions of *D. hafniense* strain TCE1 and *D. restrictus* revealed the presence of PceC in a much lower abundance than that of PceA and PceB [132]. This result seems to controvert the hypothesis of a PceABC complex, as proposed earlier. However, the quantification of Pce protein in membranes does not represent *per se* a proof that PceC does not play a role in the electron transfer chain. Additionally, the observed 2:1 ratio between PceA and PceB suggests that a PceA dimer is attached to the membrane by only one copy of PceB in a possible PceA<sub>2</sub>B protein complex. This is in agreement with the homodimeric crystal structure of PceA from *S. multivorans*, but on the other hand, it collides with the proposition made by the same authors of a Pce(AB)<sub>2</sub> complex associated with the cytoplasmic membrane [106].

In the present chapter, the characterization of the electron-accepting moiety of the respiratory chain in our model organisms is presented with the aim to elucidate the protein composition, the quinol-oxidizing activity and the structure of the membrane-bound PceA-containing protein complex identified in Chapter 4.

## 5.2 Materials and methods

In Chapter 4, the applied procedures starting from bacterial cultivation until the in-gel localization of the RDH complex was presented and discussed. Here, the methods applied for the characterization of the RDH complex are described.

### 5.2.1 Protein purification

**Anion exchange chromatography** This analysis was performed at Protein Production and Structure Core Facility at EPFL under the supervision of Dr. Kevin Lau. The membrane extract (ME) obtained as described in Chapter 4 was loaded with buffer QA (50 mM Tris-HCl buffer (pH 7.5), 0.01% (w/v) DDM and 10% (v/v) glycerol) on a 5-mL HiTrap Q HP anion exchange chromatography column (GE Healthcare) connected to the ÄKTA fast performance liquid chromatography (FPLC) system (GE healthcare). After 10 column volumes (CV) of washing in buffer QA, the proteins were eluted at a flow rate of 5 mL/min in buffer QA following an incremental 5% NaCl step gradient with buffer QB (buffer QA supplemented with 1 M NaCl). During the elution, the absorbance was set at 280 nm to monitor the presence of proteins. In parallel, the wavelengths of 450 and 540 nm were chosen to monitor the signals of the oxidized form of flavins and the corrinoid in Co(II) form, respectively. Fractions of 1 ml were collected in 96-wells plates. From each peak of the chromatogram, 10 µl of the fraction displaying the highest absorbance value at 280 nm was analysed by CN-PAGE, SDS-PAGE and Western blot to

detect the presence of PceA. The fractions of each peak containing PceA were pooled together and concentrated by ultrafiltration (PM-10 membrane, Amicon).

**Cation exchange chromatography** For cation exchange chromatography, the membrane extract was loaded with CA buffer (50 mM MES buffer (pH 5.5), 0.02% (w/v) DDM and 10% (v/v) glycerol) on a 5-ml HiTrap SP HP cation exchange chromatography column (GE Healthcare) connected to the ÄKTAPrime fast performance liquid chromatography (FPLC) system (GE healthcare). After 10 column volumes (CV) of washing in buffer QA, the proteins were eluted at a flow rate of 5 mL/min in buffer QA following a continuous gradient to 2 M of NaCl (buffer CB). For the elution, the absorbance was set at 280 nm to monitor the presence of proteins. One mL fractions were collected in Eppendorf tubes and from each peak of the chromatogram, 10  $\mu$ L of the fractions displaying the highest absorbance value at 280 nm were analysed by CN-PAGE and SDS-PAGE to detect the presence of PceA.

### 5.2.2 Quinol-based PceA enzymatic assay

All experimental steps, except for GC analysis, were carried out inside an anaerobic chamber (Coy Laboratory) at room temperature. The assay aimed at monitoring the activity of PceA using menadiol and PCE as electron donor and acceptor, respectively. Before starting the assay, 50 mM of menadione, a menaquinone analogue, were first dissolved in ethanol and reduced with zinc powder to obtain a transparent solution of menaquinol. Complete reduction was verified by UV/Vis spectroscopy. For the assay, in-solution samples, namely the membrane extract (ME) and the soluble fraction (SF), or excised CN-PAGE gel pieces corresponding to the RDH complex were used. The samples were transferred to 500  $\mu$ L of 50 mM Tris-HCl (pH 7.5) buffer supplemented with 0.1% DDM. Successively, 5 mM (v/v) of menadiol and 1 mM (v/v) of PCE (final concentration) were added in this order. For in-solution samples, the PceA enzymatic activity was monitored by measuring menadiol oxidation via UV-vis spectroscopy (Thermo Fisher) at a wavelength of 262 nm. Alternatively, if the excised gel pieces were used, the reduction of PCE to TCE and cDCE was run in 5-ml serum flasks, taken outside the anaerobic chamber and monitored via gas chromatography (FID-GC), as described earlier [133].

### 5.2.3 Cryogenic electron microscopy analysis

**Buffer screening and negative stain EM** RDH complex was obtained in form of a membrane extract (ME) from *D. hafniense* strain TCE1 using a buffer containing the detergent DDM with a 10-fold DDM/protein initial concentration ratio (w/v) and 10% glycerol. As such high detergent and glycerol concentrations are incompatible with cryogenic electron microscopy (cryo-EM) analysis, further sample optimization was necessary. To optimize the sample matrix for cryo-EM, the ME sample at 2.84 mg/mL in buffer containing 50 mM Tris-HCl pH7.5, 10% glycerol and an undefined concentration of DDM were diluted 20-fold in 4 different buffers

before analysis by negative stain EM: - Buffer 1: 25 mM HEPES-NaOH pH: 7.5, 150 mM NaCl, 0.1% DDM - Buffer 2: 25 mM HEPES-NaOH pH: 7.5, 0.1% DDM, 5% glycerol - Buffer 3: 25 mM HEPES-NaOH pH: 7.5, 150 mM NaCl, 0.005% Lauryl Maltose Neopentyl Glycol (LMNG) - Buffer 4: 25 mM HEPES-NaOH pH: 7.5, 0.005% LMNG, 5% glycerol For negative stain EM, 3  $\mu$ L of diluted sample was applied on glow discharged 400 mesh copper grids on carbon film. The grids were incubated with 2% (w/v) uranyl acetate for 30 s for staining. Grids were imaged on the Philips CM 100 transmission electron microscope (TEM). The results from screening showed that sample in Buffer 3 produced a homogeneous population of mono-dispersed particles suggesting that this buffer condition would be optimal for further EM analysis.

**Sample preparation for cryo-EM** To prepare sample for cryo-EM, an additional step of size exclusion chromatography using Buffer 3 (25 mM HEPES-NaOH pH 7.5, 150 mM NaCl, 0.005% LMNG) was performed. 400  $\mu$ L of ME sample was pre-equilibrated with Buffer 3, subsequently loaded onto Superose 6 Increase 10/300 GL column (Cytiva) at a flow rate of 0.5 ml/min on an ÄKTA Go FPLC system (Cytiva) performed. Fractions of the RDH complex peak (peak elution volume of 14.9 ml) as confirmed by SDS-PAGE were pooled and concentrated to 1 mg/ml using a 30 kDa cut-off centrifugal concentrator (Millipore).

**Cryo-EM data collection** Cryo-EM grids were prepared by applying 3.5  $\mu$ L of concentrated sample to glow discharged 400 mesh R1.2/1.3 UltrAuFoil grids (Quantifoil Micro Tools GmbH). The sample adsorbed for 30 s on the grids followed by plunge freezing in liquid ethane using a Vitrobot Mark IV plunge freezer (Thermo Fischer Scientific). Cryo-EM data were collected using the automated data acquisition software EPU on a Titan Krios G4 transmission electron microscope (Thermo Fischer Scientific) equipped with a cold-FEG and Falcon IV at an operating at 300 kV and physical pixel size of 0.51 Å. In total, 13,783 movies were collected from a round of data collection.

**Cryo-EM data processing** Data processing was performed using the data processing software cryoSPARC V3. Briefly, from a total 5,014,614 particles extracted from 9378 dose weighted micrographs, 110,862 particles were used obtain a final 3D map at less than 3 Å.

### 5.3 Results and discussion

CN-PAGE combined with the in-gel PceA enzymatic activity assay represents a powerful tool to identify and localize the RDH complex in native gels. However, the information obtained on the protein composition as well as the identification of the direct electron donor to the complex remain elusive. So far, MS analysis of the 180 kDa native gel band confirmed the presence of PceA and PceB, but several other proteins were also detected with a comparable number of spectra. Similarly, the application of 2D-Native/SDS-PAGE on the 180 kDa band revealed two major bands with an apparent molecular weight of 60 kDa and 13 kDa, most

likely PceA and PceB. However, and despite the neat resolution of the gel, the MS spectra revealed the detection of numerous proteins together with the Pce proteins, thus impeding any possibility to assess unequivocally their presence in the RDH complex (see **Figure 4.14** in Chapter 4).

### 5.3.1 Purification attempts of the RDH complex

The incomplete data obtained from in-gel MS analysis led to consider additional purification steps of the membrane extract with the aim to enrich the RDH complex proteins over the proteins not belonging to it. However, lack of knowledge on predicting the binding of RDH complex to a specific resin prevented any consideration on the best purification strategy to apply. For this reason, anion and cation exchange chromatography approaches were chosen as "exploratory" strategies to attempt purifying the RDH complex.

**Anion exchange chromatography.** The first attempt of anion exchange chromatography was performed in the laboratory of Prof. I. Pereira in Lisbon using the membrane extract from *D. restrictus* obtained in the early phase of the optimization of the protocol (see Chapter

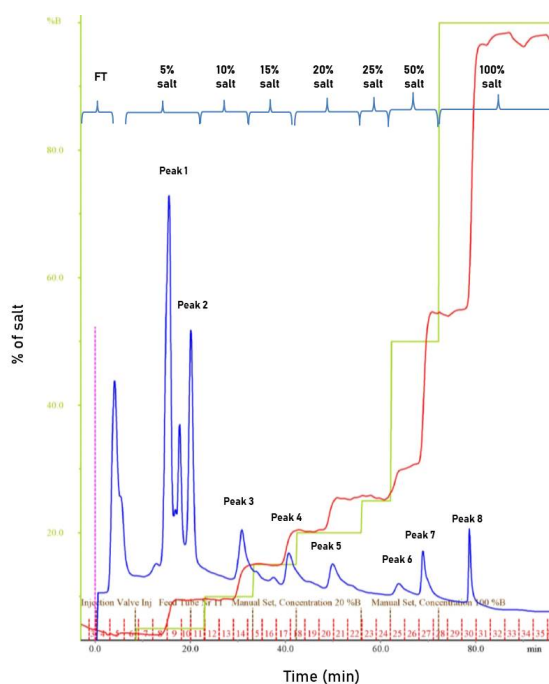


Figure 5.1: Anion-exchange chromatography of the membrane extract from *D. restrictus*. The blue line indicates the protein absorbance at 280 nm; the green and red lines indicate the theoretical and measured step-wise increment in NaCl concentration, respectively. The numbers on x-axis indicate the number of fractions collected throughout the purification process.

4). The ME sample was loaded on the anion exchange chromatography column and eluted by following a step-wise elution (**Figure 5.1**). Aliquots of 10  $\mu$ l of the fractions corresponding to the nine major peaks visible in the chromatogram were loaded on CN-PAGE and SDS-PAGE gels in parallel (**Figure 5.2**). The native gel shows a complex with an apparent above 140 kDa in fraction 4, which corresponds to a band at 66 kDa in denaturing condition, likely PceA, and two other major bands at 45 kDa, 30 kDa, respectively. Moreover, another band around 14 kDa was present with low resolution due to the effect of the detergent (as indicated with red asterisks in **Figure 5.2B**). However, with MALDI-TOF/MS analysis conducted on the CN-PAGE excised band (red box of **Figure 5.2A**) only PceA was detected, while PceB and PceC were not detected (data not shown). This result was in contrast with the established idea that PceA is a membrane-associated protein anchored to the integral membrane protein PceB. Furthermore, the presence of PceA in portions of the gel where it was not likely to migrate revealed that shotgun MS analysis allowed the identification of the easy-to-detect soluble proteins that are dominant in the spectra and likely covering the detection of less abundant ones, e.g. of the membrane proteins.

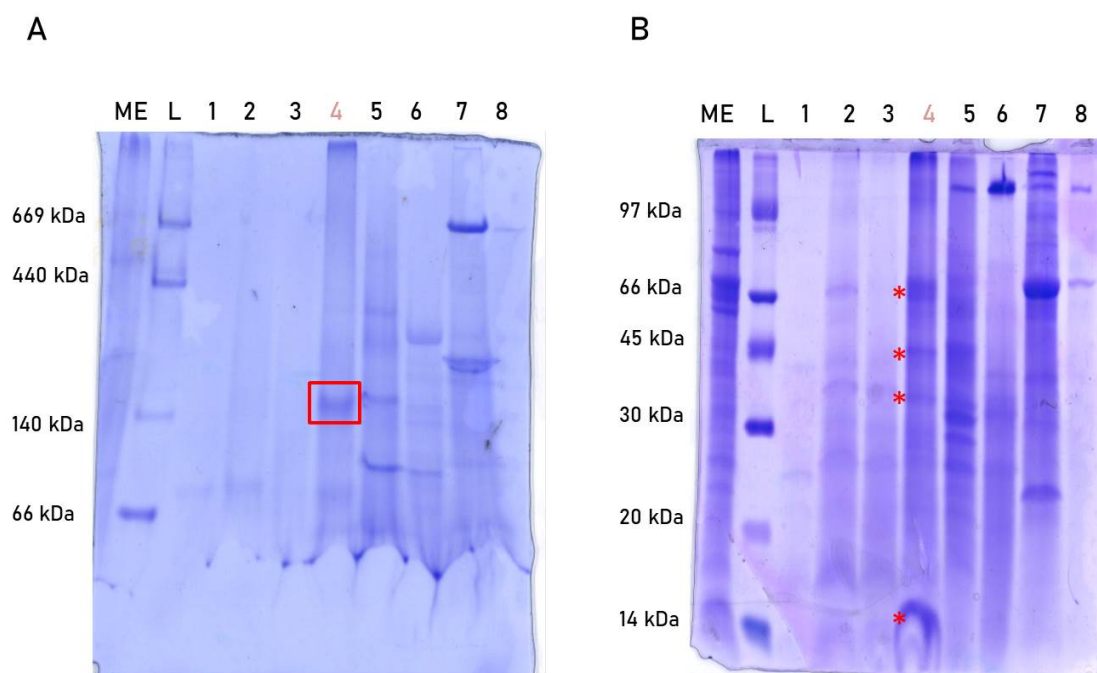


Figure 5.2: CN-PAGE (A) and SDS-PAGE (B) analysis of selected fractions resulting from the anion-exchange chromatography applied to the membrane extract of *D. restrictus*. ME: Membrane extract prior loading on the column. L: High-molecular weight ladder for native electrophoresis (Amersham). The major protein bands composing to 140 kDa CN-PAGE gel band are marked with red asterisks.

To overcome the issue of low detection of membrane proteins that usually occurs with MALDI-TOF or LC-MS/MS analysis, it was sought to repeat the anion exchange chromatography and to use Western blot to identify PceA and PceC. The use of immunoblot represented an alternative to MS analysis, thus permitting to address the question of the possible involvement of PceC in the RDH complex (**Figure 5.3**).

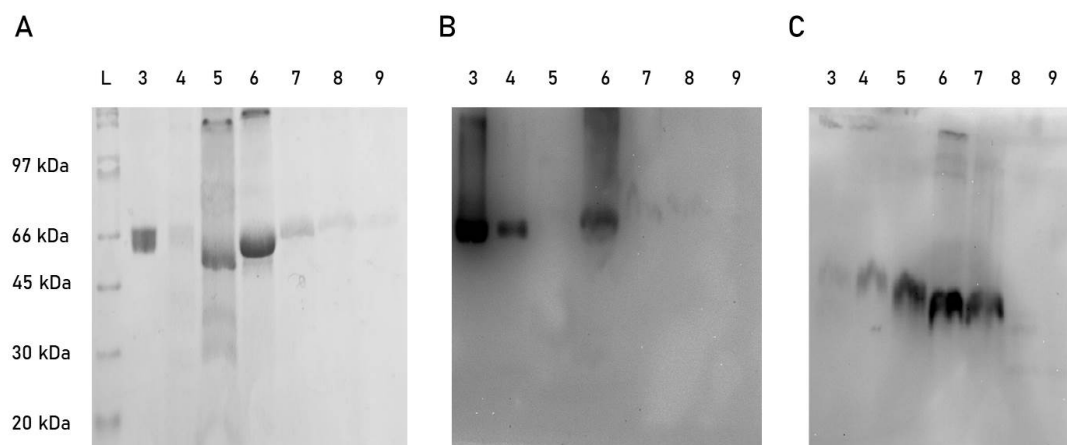


Figure 5.3: SDS-PAGE analysis and Western blot for PceA and PceC of the selected fractions obtained from anion-exchange chromatography. A) SDS-PAGE gel stained with Coomassie Blue. B) Western blot for PceA. C) Western blot for PceC.

Despite technical issues that occurred with the UV/vis detector in the second attempt and resulted in a bad quality chromatogram (data not shown), nine different fractions were run on a SDS-PAGE gel. Western blot for PceA revealed the presence of PceA mostly in fractions 3, 4 and 5, while anti-PceC antibodies gave signal for the antigen in fractions 4 to 7 with fraction 6 displaying the highest intensity. Overall, this analysis led to hypothesize a possible co-elution of PceA and PceC in fraction 6 (**Figure 5.3**). Although this result did not represent a proof that PceA and PceC were associated in the complex (unfortunately, no CN-PAGE analysis was performed for these samples), it constitutes an important result that would require further analysis for its validation. In this context, a third attempt of anion exchange chromatography was performed (**Figure 5.4**). This experiment was done in the PTPSP facility at EPFL with some improvements. Besides the absorbance at 280 nm to monitor the presence of proteins, the wavelengths of 450 nm and 540 nm were also chosen to monitor the absorbance of the oxidized form of flavins (of PceC) and the cobalt(II) form of the corrinoid (present in PceA), respectively. Thirteen different fractions, corresponding to each of the eluted peaks at 280 nm, were collected and loaded on SDS-PAGE gels. Western blot for PceA that was performed after SDS-PAGE showed the presence of PceA in the fractions 3 to 9 with fraction 8 displaying the highest signal (**Figure 5.5**).



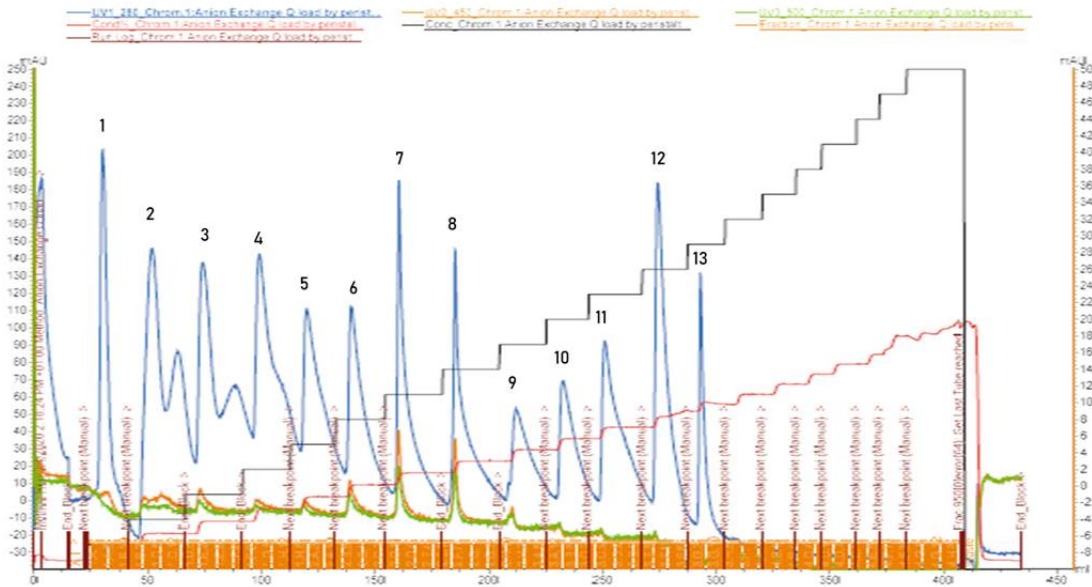


Figure 5.4: Anion-exchange chromatogram of the membrane extract of *D. restrictus*. In this third attempt, the elution was run with an extended 5% step gradient from 0 to 100% of NaCl (final concentration at 1 M). Moreover, the wavelength of corrinoid (540 nm, green line) and the oxidized FMN (450 nm, orange line) were monitored in addition to 280 nm for proteins (in blue).

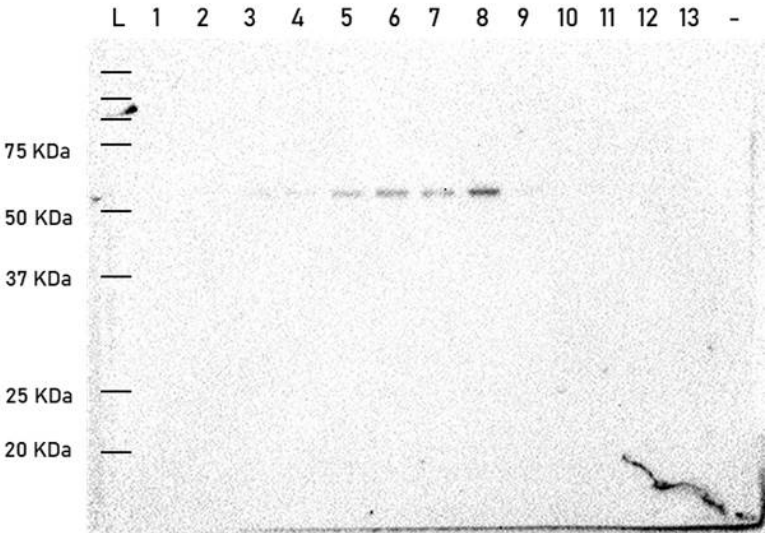
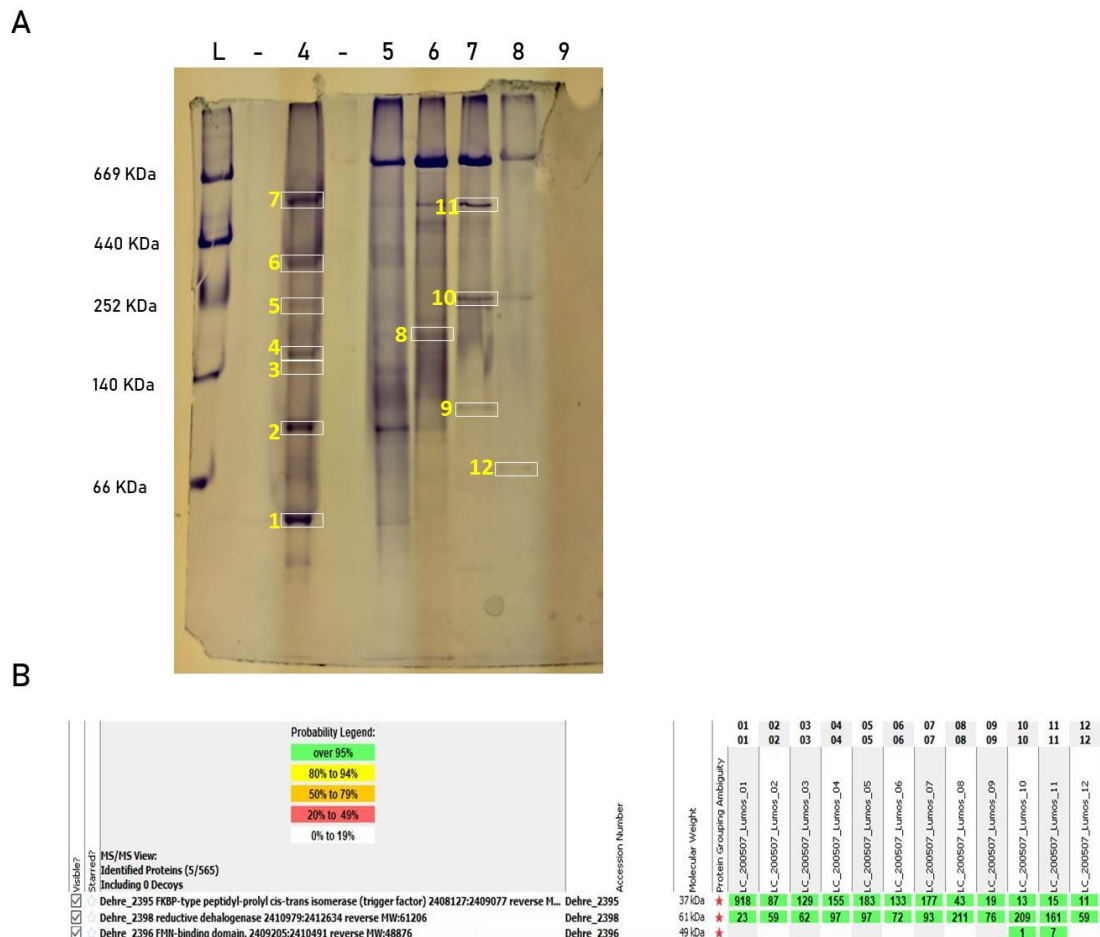


Figure 5.5: Western blot analysis of selected purification fractions (1-13) using anti-PceA antibodies from SDS-PAGE gel. The immunoblot showed PceA signal in fractions from 4 to 8, with fraction 8 owing the strongest signal.

This was in line with the data from the corrinoid monitoring, showing the highest absorbance value also in fraction 8. Fractions from 4 to 9 were loaded on a CN-PAGE gel and after

Coomassie Blue staining 12 gel pieces were analyzed via LC-MS/MS analysis (**Figure 5.6A**). The resulting spectra revealed a large number of proteins for each of the gel piece, while PceB was not detected and PceC was identified only in the gel pieces 10 and 11 with a very low number of spectra. This prevented to draw any solid conclusion on the composition of the RDH complex (see **Figure 5.6B**).



**Figure 5.6:** CN-PAGE analysis and LC-MS/MS analysis of selected gel pieces. **A)** Twelve gel pieces were excised from the native gel and analyzed with LC-MS/MS analysis. In yellow are indicated the selected proteins or protein complexes that were analyzed. **B)** Number of spectra belonging to each of the Pce proteins in the 12 selected gel pieces analyzed. PceA (Dehre\_2398) and PceT (Dehre\_2395) were well detected, while PceB (Dehre\_2397) was not detected and PceC (Dehre\_2396) was detected only with a few spectra in the gel pieces 10 and 11.

Focusing on Pce proteins, PceA and PceT were among the most dominant proteins in the gel bands. On the other hand, PceC was detected in only two gel bands with a low number of spectra while PceB was not observed. Theoretically, the binding of the proteins with an isoelectric point (pI) lower than the pH of the buffer is favoured to bind on an anion exchange column. Calculation of the isoelectric point (pI) of the Pce proteins revealed that

PceB and PceC display a pI of 9.17 and 9.56, while PceA and PceT present a pI of 6.58 and 4.79, respectively. Since the buffer used in anion exchange chromatography was set at pH 7.5, the binding of PceB and PceC to the column might have been hindered and this might be an explanation of the low abundance of these membrane proteins in the MS spectra. Additionally, the migration pattern of the native gel revealed the presence of several protein complexes in single gel lanes suggesting their co-elution in the fractions. Similarly, protein complexes with identical molecular weight appeared across different fractions, suggesting that the binding of the complexes to the column was loose and inefficient to enrich individual protein complexes. Overall, these results led to the conclusion that anion exchange chromatography was not an appropriate technique for the purification of the RDH complex. Instead, cation exchange chromatography was applied as an alternative purification strategy (**Figure 5.7**). For this experiment the elution buffer at pH of 5.5 was chosen allowing theoretically the binding of PceA, PceB and PceC proteins while PceT should not be retained by the column. The chromatogram of the cation exchange chromatography revealed the elution of only two peaks largely overlapping each other (**Figure 5.7**).

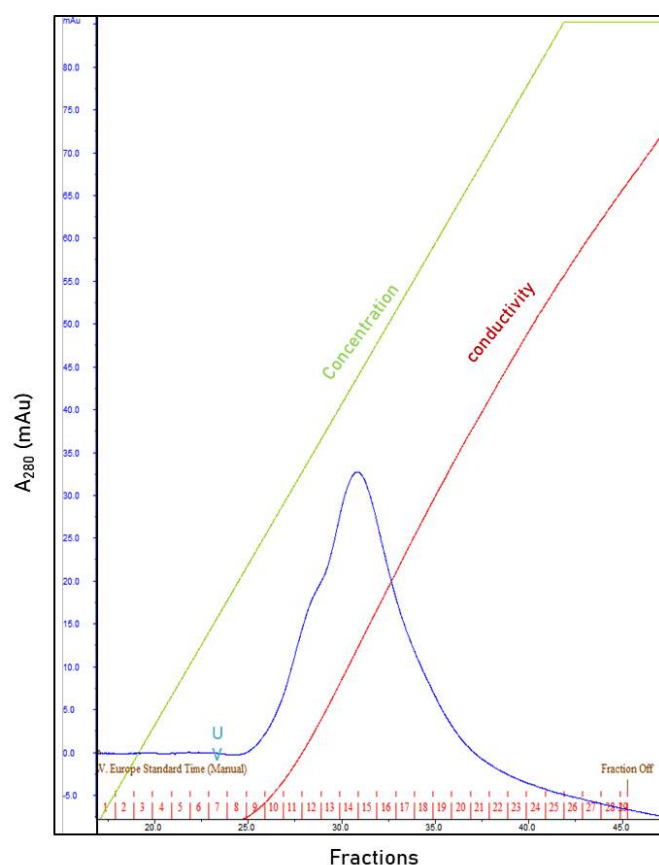


Figure 5.7: Cation exchange chromatography of membrane extract from *D. restrictus*. The blue line indicates the absorbance at 280 nm for protein monitoring, the green line the concentration of NaCl added (up to 2M final) while the red line indicates the conductivity.

Three different fractions spanning the amplitude of the peaks were analyzed via CN-PAGE (**Figure 5.8A**) while on SDS-PAGE (**Figure 5.9**) an aliquot of each fraction collected in cations exchange analysis was loaded in parallel. The native gel revealed the presence of a complex with an apparent size of 120 kDa, however only in fraction 15, which displayed the highest value of absorbance at 280nm, while no protein was observed in the other two fractions (**Figure 5.8**). Strikingly, the migration pattern of the membrane extract showed fade bands in the portion of the gel corresponding to RDH complex (**Figure 5.8B**). A similar pattern was

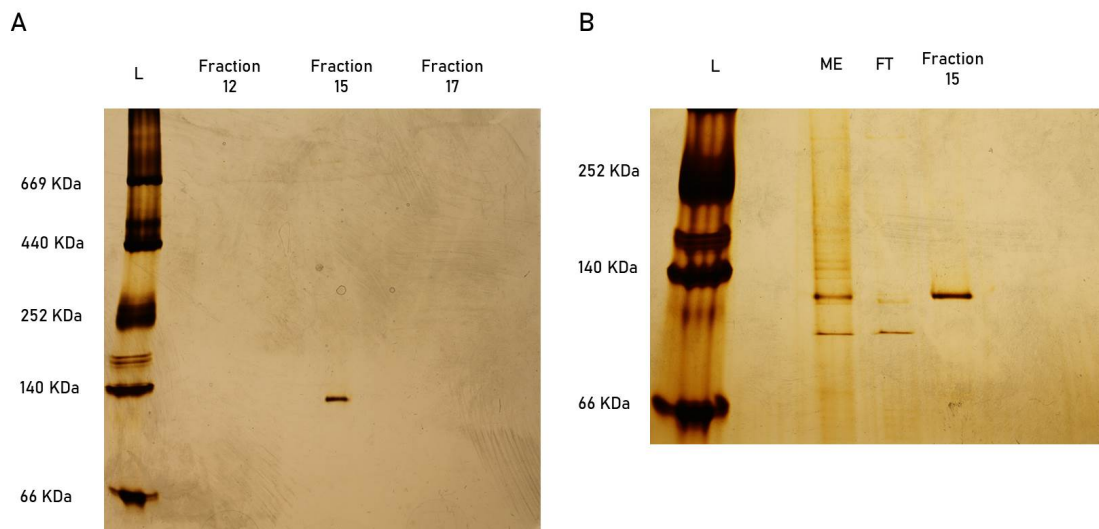


Figure 5.8: CN-PAGE analysis of the fractions obtained from cation exchange chromatography. Panel A) Fractions 12,15 and 17 corresponded to the beginning, the middle and the end of the peak profile observed in the chromatogram, respectively. Panel B) Membrane extract prior to loading on the column (ME), flow-through that did not bind the column (FT) and Fraction 15 showing a neat band at 120 kDa.

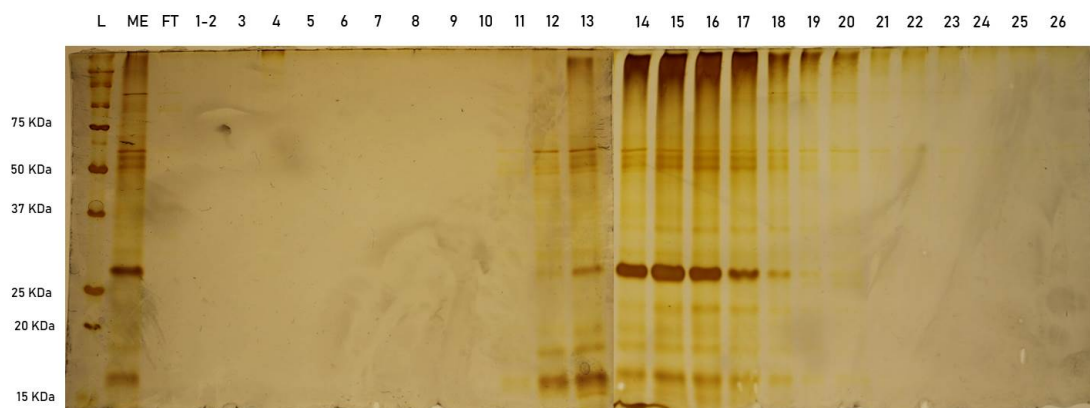


Figure 5.9: SDS-PAGE analysis of the fractions obtained from the cation exchange chromatography. The gel was stained with Silver nitrate.

also observed in earlier CN-PAGE gels where the membrane extract protocol was performed in aerobic conditions (data not shown). This suggests that the exposure to oxygen during sample preparation needed for the chromatography perturbed the RDH complex composition leading to its disassembly. The SDS-PAGE gel showed that the fraction containing the 120 kDa complex was dominated by a protein with a molecular weight of 28 kDa, likely to be Dehre\_1178 corresponding to the homologue of the cytoskeleton protein RodZ of *E.coli*, as defined via MS analysis in an earlier experiment (see **Figure 4.9A** in Chapter 4). Furthermore, the SDS-PAGE gel of the fractions collected throughout the purification revealed that besides the 28 kDa protein, additional proteins were present with lower intensity (**Figure 5.9**).

Overall, these results showed that cation exchange chromatography failed in purifying the RDH complex. However, the aerobic conditions in which the purification step was performed might have been detrimental for the preservation of the physiological state of the RDH complex.

### 5.3.2 Quinol-based PceA enzymatic assay

Earlier studies confirmed the involvement of quinones in the respiratory chain of certain OHRB [46]. However, the mechanism with which electrons from menaquinol, with a midpoint redox potential of  $E^0' = -74$  mV, allow the reduction of PCE via PceA that contains cofactors with midpoint redox potentials of -480 mV (FeS clusters) and -350 mV (cobalamin), remains still unclear. Based on physiological data and sequence information reported for the *pceABCT* operon, a tentative model of the electron transfer chain involved in OHRB harboring this operon has been proposed previously, where PceA, B, and C could form a membrane-bound protein complex [35]. There, PceC was suggested to play a role in electron transfer in agreement with the redox activity of the FMN-binding domain [81]. However, the quantitative proteomics analysis presented in Chapter 3 led to propose a new putative PceA<sub>2</sub>B RDH complex associated with the cytoplasmic membrane, thus likely excluding PceC from the complex [132]. However, a possible role of PceC as a helper protein toward PceA was not precluded, thus not fully excluding its transient participation in the RDH complex. A quinol-based PceA enzymatic assay represented a route to biochemically investigate the electron-transfer chain involved in PCE dechlorination in *D. restrictus* and *D. hafniense* strain TCE1. The assay aimed to evaluate if quinol could transfer electrons to the RDH complex and promote PCE dechlorination. To test this hypothesis, menadiol, a water-soluble analogue of quinol, and PCE were used as electron donor and electron acceptor, respectively. Theoretically, only in the presence of the RDH complex, either in solution as the solubilized membrane extract or from a native gel piece, the electrons should shuttle from menadiol to PCE leading to its reduction to TCE and *cis*-DCE. However, the data from both in-solution and in-gel assay resulted contradictory and it was impossible to draw any conclusion based on these results. The in-solution assay with the membrane extract from *D. hafniense* strain TCE1 revealed a calculated specific activity of 0.30 nkat/mg for PceA, while no activity was observed with the membrane extract previously incubated at 95° C or with the soluble fraction (**Table 5.1**). However, a comparable specific activity value was also observed in this assay when menadiol was replaced by ethanol.

A similar result was also observed with *D. restrictus*. Monitoring of PceA enzymatic activity was also performed via gas chromatography (FID-GC). In anaerobic vials, native gel pieces corresponding to the RDH complex were incubated with menadiol and PCE. Negative controls were included where either the gel piece was omitted or PCE was replaced by ethanol. Taken altogether, no reproducible activity could be observed using this in-gel experimental set-up.

Table 5.1: In-solution quinol-based PceA enzymatic activity assay performed on *D. restrictus* and *D. hafniense* strain TCE1. The asterisk indicates that the analysis was performed in duplicates. ME: membrane extract, ME boiled: membrane extract previously incubated at 95°C, SF: soluble fraction. BDL: below detection limit.

Bacteria	Run	Sample	Sample volume	e-donor	PCE volume	Spec. Act. (nkat/mg)
<i>D. hafniense</i> TCE1	ME	ME	30 $\mu$ l	Menadiol	5 $\mu$ l	*0.30
<i>D. hafniense</i> TCE1	SF	SF	10 $\mu$ l	Menadiol	5 $\mu$ l	*BDL
<i>D. hafniense</i> TCE1	ME boiled	ME	30 $\mu$ l	Menadiol	5 $\mu$ l	*BDL
<i>D. hafniense</i> TCE1	Negative ctrl	ME	30 $\mu$ l	ethanol	5 $\mu$ l	0.30
<i>D. restrictus</i>	ME	ME	30 $\mu$ l	Menadiol	5 $\mu$ l	*0.56 nkat/mg
<i>D. restrictus</i>	SF	SF	30 $\mu$ l	Menadiol	5 $\mu$ l	0.24
<i>D. restrictus</i>	ME boiled	ME	30 $\mu$ l	Menadiol	5 $\mu$ l	0.24
<i>D. restrictus</i>	Negative ctrl	ME	30 $\mu$ l	ethanol	5 $\mu$ l	0.24

Overall, the preliminary data obtained here provide hints that the PceA enzymatic activity observed in membrane extract of the in-solution assay is due to protein as the control with boiled enzyme did not show any activity. However, the slight difference in activity between the soluble and the membrane extract and the presence of activity where menadiol was replaced by ethanol led to carefully consider these results. At this stage, only speculations might be provided to explain these results. Despite that different experiments were performed to evaluate the contribution of the buffer composition in the measured menadiol/menadione absorbance, the complex matrix of the membrane extract, containing glycerol, detergent and dithiothreitol, a strong reducing agent used to preserve the anoxic conditions of the RDH complex, might result in a strong interference with the measurement of quinol oxidation. For this reason, further investigation and optimization of the in-solution assay will be required in the future to undoubtedly assess the quinol-based enzymatic activity of the RDH complex. Alternatively, a robust in-gel GC-based assay also requires further investigation.

### 5.3.3 Cryogenic electron microscopy of the RDH complex

The collaboration with Babatunde Ekundayo and Dongchun Ni from the Laboratory of Biological Electron Microscopy at EPFL was launched in November 2021 in order to try analyzing the RDH complex enriched in the membrane extract of *D. hafniense* strain TCE1 (see **Figure 4.14B** in the previous Chapter) by cryogenic electron microscopy (Cryo-EM). Baba and Dong are kindly acknowledged for the work described in this section.

After replacing DDM by LMNG, the RDH complex was purified by size exclusion chromatography and fractions were analyzed by SDS-PAGE (**Figure 5.10A** and **Figure 5.10B**, respectively). Fractions displaying proteins approximately the size of PceA and PceB were pooled, concen-



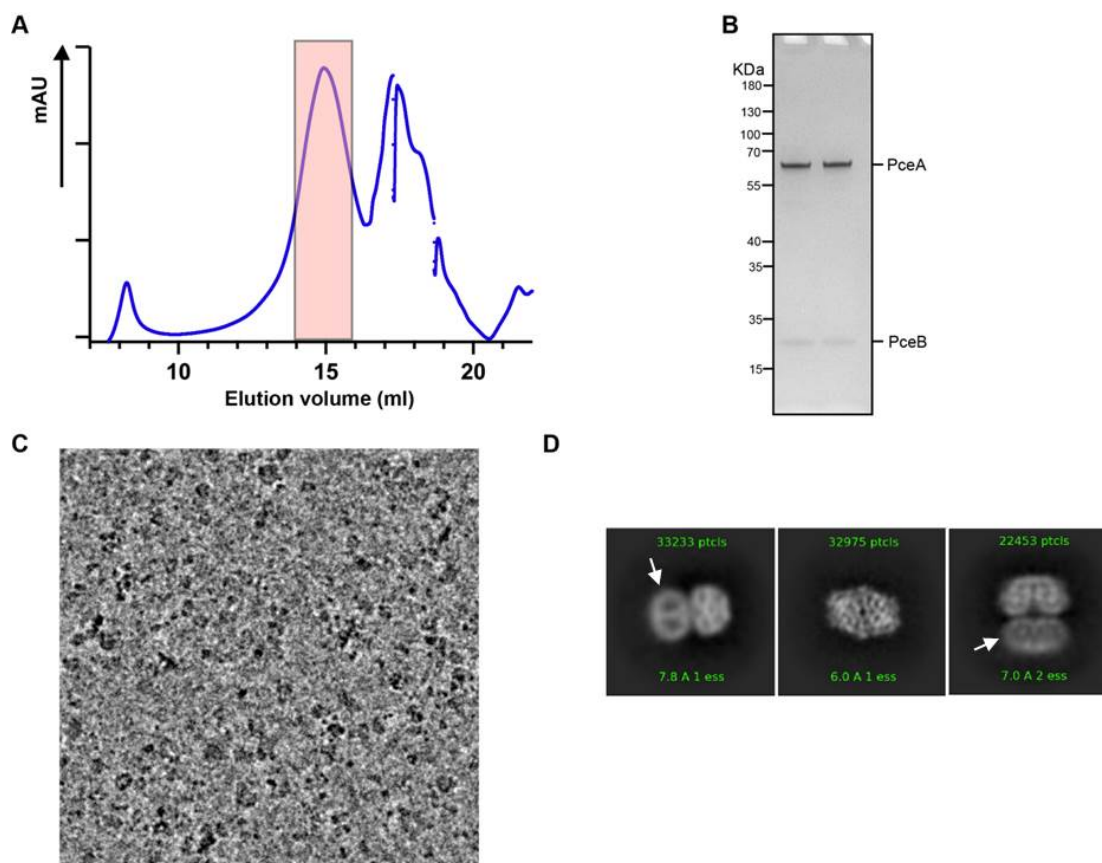


Figure 5.10: Sample preparation and cryo-EM imaging of the RDH complex. A) Size exclusion chromatogram for RDH complex purification, the peak corresponding to the RDH complex is shaded in pink; B) SDS-PAGE analysis of representative fractions of the purified RDH complex; C) Representative cryo-EM micrograph of the purified RDH complex; D) Representative 2D class average of the RDH complex shown in different views (side view, top view and another side view). The box size is 20.4 nm. The white arrows indicate the part of the complex that is covered by the detergent (originally embedded in the cytoplasmic membrane).

trated and analyzed by cryo-EM, from which a representative TEM micrograph is shown in **Figure 5.10C**. The picture indicates a rather heterogeneous population of particles, which is reflected by the final number of particles selected (110'000 out of 5 millions) by 2D classification (**Figure 5.10D**). There, representative particles harbor an overall morphology with a C2 symmetry. Indeed, a vertical mirror symmetry is easily recognized in the third representative particle shown in **Figure 5.10D**. The vertical symmetry in the first particle (rotated by  $\sim 90^\circ$  in comparison to the third particle) is only apparent as the electron density of the two regions are completely different. According to the experts in cryo-EM, the left region of the first particle corresponds to protein domains that are covered with detergent micelles, as indicated by the white arrows in **Figure 5.10D**. The top view of the complex (second particle in **Figure 5.10D**) displays the shape of a flattened hexagon, where a vertical C2 symmetry is also visible.

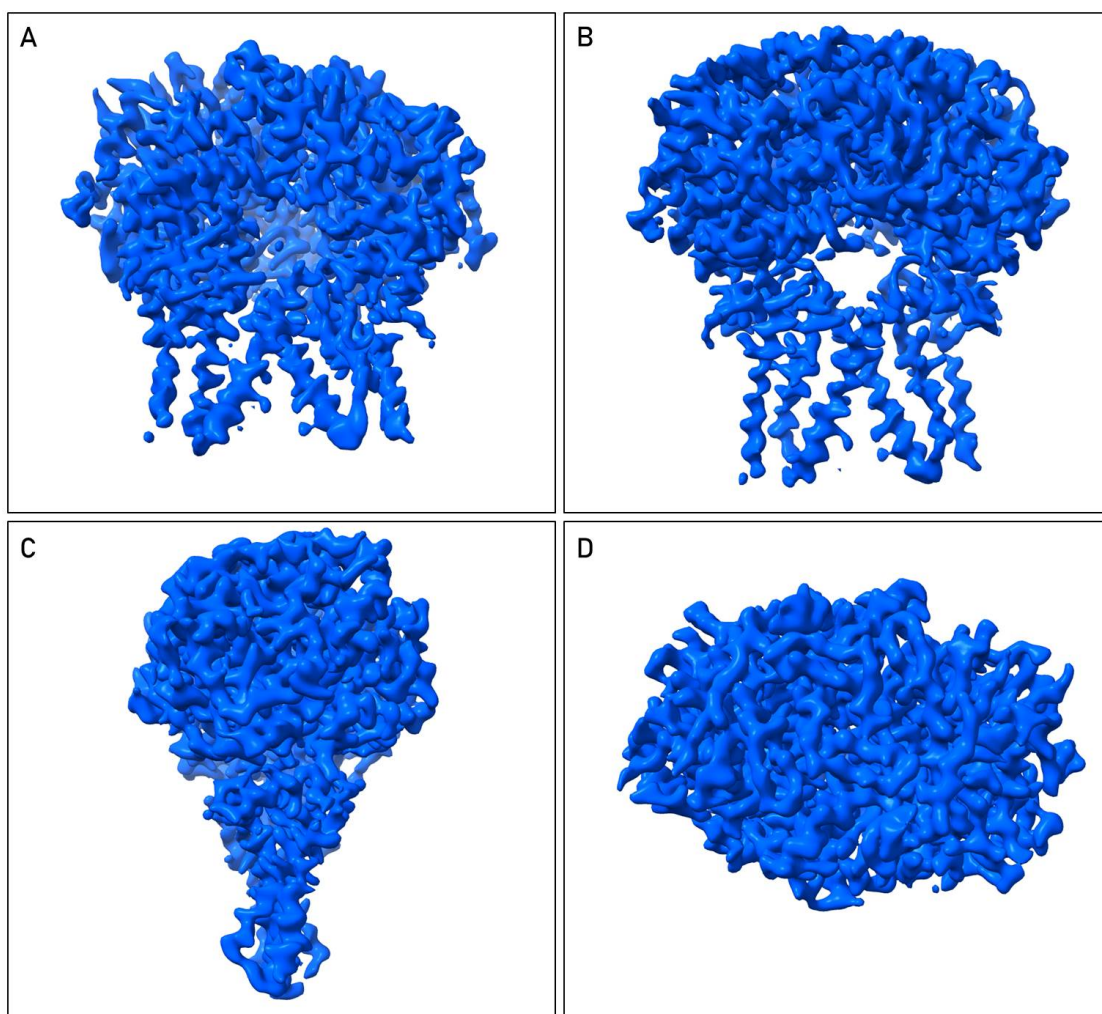


Figure 5.11: 3D Density map reconstruction of the RDH complex using cryo-EM. A) 3/4 bottom view; B) side view; C) side view, rotated by 90°; D) top view of the 3D reconstruction of the RDH complex.

For the first time in the field of OHR, the structure of a reductive dehalogenase complex and the interaction between PceA and PceB in a likely native conformation are being elucidated. The preliminary 3D density map reconstruction of the RDH complex is displayed using the ChimeraX software [134]. From **Figure 5.11**, two subunits of PceB, each one characterized by its typical three  $\alpha$ -helices, can be identified. The two PceB subunits in the complex seem to be oriented so that the trans-membrane helices are tilted in the membrane, possibly crossing each other with their respective N-terminal helix at the center of the complex, in proximity of the P-side of the membrane. If so, the second loop of PceB (between helix 2 and 3) would be positioned in proximity to PceA, as proposed earlier by the topology prediction of PceB from *D. hafniense* strain Y51 [56].

These hypotheses were confirmed with the elucidation of the structure, as shown in **Figure**



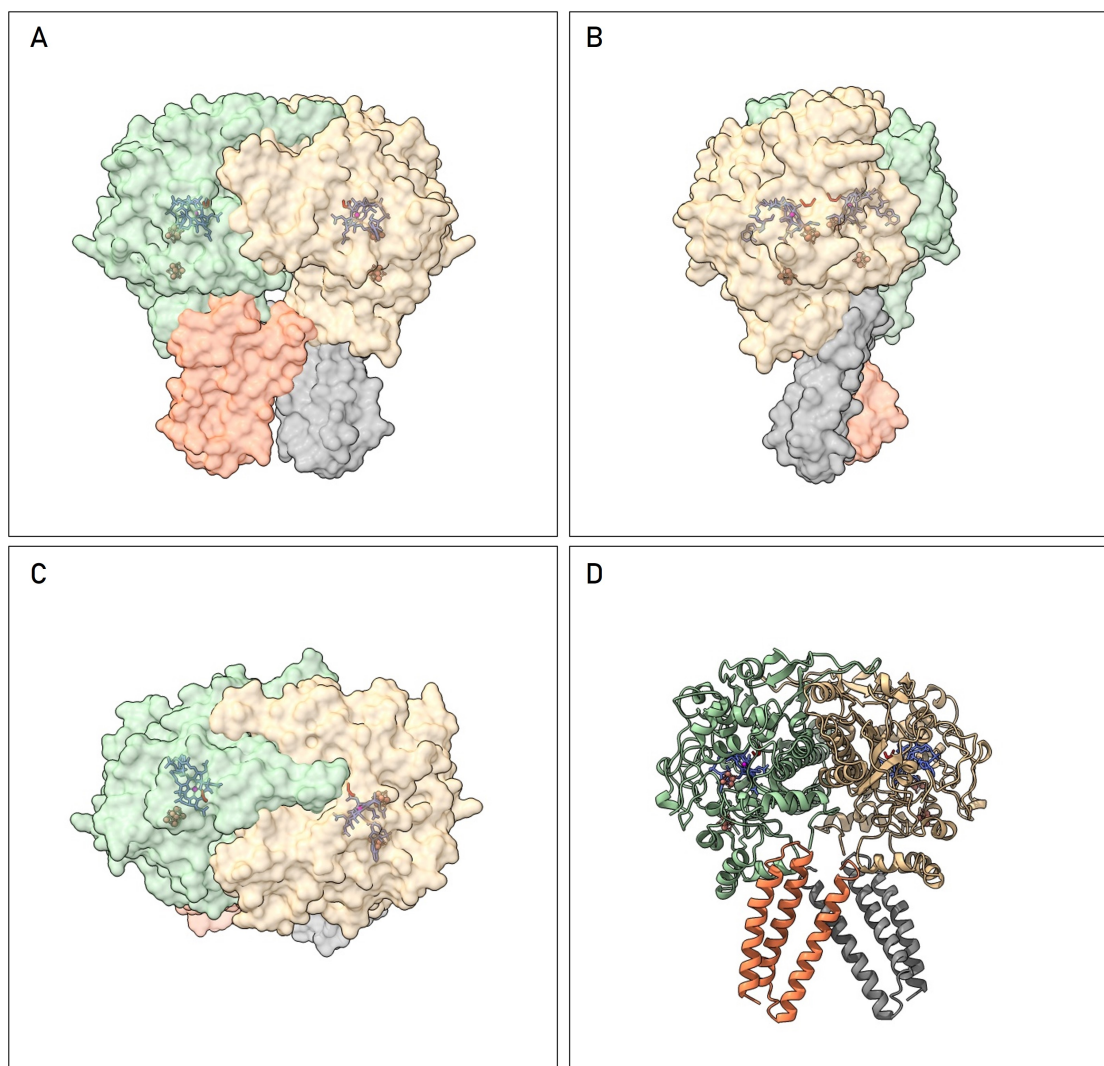


Figure 5.12: 3D reconstruction of the RDH complex using cryo-EM. A) side view; B) side view, rotated by 90°; C) top view of the 3D reconstruction of the RDH complex; D) Side view showing the secondary structures of the different RDH complex subunits. PceA subunits are coloured in green and yellow, while PceB subunits are in orange and grey. For each of the PceA subunits: the cobalamine group is indicated in blue, the two Fe-S clusters in light orange and the substrate *cis*-DCE in red.

**5.12.** Each of the PceA subunits results to be linked to one PceB subunit, forming a Pce(AB)<sub>2</sub> complex with displaying a vertical C2 symmetry. Thus, the final 3D reconstruction of the RDH complex appears in agreement with the homodimeric crystal structure of PceA from *S. multivorans* [106]. Furthermore, the high resolution of the RDH complex structure, approximately at 2.8 ångström (Å), allowed us to identify the two Fe-S clusters and the cobalamin cofactor, characterized by its typical corrin ring which coordinates the atom of cobalt. Moreover, the elucidation of the structure revealed the localization of *cis*-dichloroethene in the active site of each of the PceA subunits at an approximate distance from the cobalt atom of 4.0 Å. The

localization of the dechlorination product will help investigating further the structure of the active site, with the main goal to identify the amino acids responsible for the coordination of the substrate. In addition, a comparison with the crystal structure of PceA from *S. multivorans* [106] should be carried out to evaluate the presence of conserved amino acids that constitute the active site of PceA. Moreover, further investigations on the structure need to be conducted to identify specific amino acids responsible for the interaction between PceA and PceB.

## 5.4 Conclusions

In the present chapter, numerous experiments aiming at characterizing the 180 kDa RDH complex obtained in Chapter 4 were presented. The purification of the RDH complex and the investigation of the electron shuttling mechanism from the quinol pool toward the reduction of PCE constituted the main focus of this chapter. A combination of chromatography and cutting-edge electron microscopy technologies were applied. In collaboration with the Laboratory of Biological Electron Microscopy (LBEM), preliminary results obtained using transmission electron microscopy (TEM) and cryo-EM revealed the presence of a Pce(AB)<sub>2</sub> complex, excluding PceC from the complex. The conformation of the RDH complex in which PceA adopts a dimeric fold is in agreement with the recently proposed X-ray crystal structure of the PceA reductive dehalogenase from *Sulfurospirillum multivorans* [106]. The elucidation of the RDH complex structure including the membrane anchor PceB will constitute an important breakthrough in the field of OHR. Indeed, this result will set the basis for further investigation on the structural features of the RDH complex, namely the access to the catalytic site with regard to the membrane topology and the identification of the amino acid residues relevant for the interaction between the two proteins. Furthermore, the resolution of Pce(AB)<sub>2</sub> complex will also help in the elucidation of the electron transfer mechanism from the quinol pool to the corrinoid redox center of PceA. In this framework, the quinol-based PceA enzymatic assay testing the possible interaction between menadiol and the RDH complex in the membrane extract remains to be clearly addressed. So far, the experiments presented here did not provide a clear answer and the question remains still unanswered. Further investigations on the RDH complex structure will be required to evaluate the presence of a possible quinol binding site in PceB or whether PceB has only a structural role as membrane anchor for the reductive dehalogenase, as it seems to be the case in the quinone-independent complexome elucidated in *D. mccartyi* strain CBDB1 [66, 68].



## 6 Concluding remarks and perspectives

In the recent years, numerous organohalide-respiring bacteria (OHRB) have been characterized at physiological and molecular levels, revealing a large potential of bioremediation, but also pointing out many technological impediments in the study of these microorganisms. So far, OHRB appear as genetically intractable and present several challenges related to their cultivation, which limit biochemical studies concerning their physiology and metabolism. One exemplifying case is represented by the *pceABCT* operon which is shared by *D. restrictus* and *D. hafniense* strain TCE1 with 99% of sequence identity. Since its identification in the early 2000s [79], numerous studies at molecular level have been conducted while only limited information on the role of the gene products from *pceABCT* in the OHR metabolism has been obtained. To date, studies on the *pceABCT* operon defined the function of PceA, the key catalytic enzyme in the process, and PceT, the dedicated molecular chaperone for the maturation of PceA. However, the role of PceB and PceC proteins are still not elucidated and the biochemistry of OHR electron transfer remains elusive.

**Stoichiometry of the *pceABCT* gene products** The assessment of the stoichiometric relationships between the *pce* gene products at RNA and protein levels represented one way to investigate their implication in the OHR respiration chain. To answer this question at protein level, the development of a protocol for quantitative proteomics analysis suitable for the quantification of soluble and membrane-associated proteins, such as PceT and PceA, respectively, as well as of the integral membrane proteins PceB and PceC consisted of the major challenge. Quantitative proteomics was applied to the soluble and membrane fractions resuspended in RapiGest without any additional centrifugation nor physical treatment. As presented in Chapter 2, as a result of the meticulous optimization of sample preparation, up to three reference peptides for each protein were defined via LC-MS/MS analysis. At this stage, the main difficulty was constituted by the identification of peptide(s) for PceB, which is a 105 amino acids long protein predicted to have small regions (loops) exiting outside the lipid environment of the cytoplasmic membrane. The work presented in Chapter 2 led to the identification of only one peptide as target for PceB absolute quantification. According to the

topology prediction published in [56], this peptide is located near the C-terminal part of the protein likely protruding outside the lipid bilayer, thus giving a much better chance for trypsin to access it.

As presented in Chapter 3, the quantification showed a strong relationship between *pceA* and *pceB* gene products, both at RNA and protein levels, thus demonstrating the mutual importance of these two subunits for the OHR metabolism. At RNA level, the transcription pattern of the *pce* genes observed in *D. restrictus* and *D. hafniense* strain TCE1 showed the co-transcription of all four of the gene targets, which led us to consider *pceABCT* as an operon. On the other hand, the quantitative analysis of *pce* individual gene transcripts confirmed the lack of transcriptional regulation of the *pce* gene cluster in *D. hafniense* strain TCE1. However, the higher level of transcription of *pceAB* observed in *D. restrictus*, but not in *D. hafniense* strain TCE1, raises new questions on possible post-transcriptional events occurring in the operon, such as RNA processing and differential RNA stability [114]. Future experiments will be needed to tackle these aspects by using next-generation sequencing technologies for quantification of gene expression, RNA-Seq, with which the mRNA decay rates in genome-wide studies is investigated [135]. Otherwise, mRNA degradation rates have been estimated by blocking transcription through application of specific antibiotics in combination with monitoring the decrease of cellular mRNA levels over time. However, the global inhibition of transcription might result in the loss of transcripts that encode components of the RNA decay machinery, which prevents accurate measurement of mRNA stability because decay pathways are perturbed [136].

The study conducted at protein level represented a strong improvement compared with the latest proteomic analyses performed on Firmicutes OHRB [43]. Despite different methodologies were applied in those studies, the detection of integral membrane proteins always represents the main challenge as their extraction often results in low abundance. Furthermore, among all the studies, only one fourth of them was able to detect both RdhB and RdhC. In the present work, all of the Pce proteins were detected and for the first time with an absolute quantification method using heavy-labelled peptides. The result revealed that the ratio between PceA and PceB from the quantitative data is clearly improved in favour of PceB in comparison to the non-quantitative dataset from the discovery MS analysis. This suggests that the quantitative approach permitted a more accurate estimation, likely closer to the real physiological situation than any classical proteomic analysis performed so far. Furthermore, the unexpected lower abundance of PceC, if compared with PceB, cannot be explained by its hydrophobic nature or limited accessibility, as PceC displays a higher number of tryptic peptides and a substantial peripheral domain that likely protrudes outside of the lipid bilayer. This suggests that PceC is physiologically much less abundant in the membrane compared to PceA and PceB. Interestingly, quantification of Pce proteins applied to sub-cellular compartment highlighted the 1:1 PceA/PceT ratio suggesting that in soluble fraction, the portion of PceA that is not yet associated with the membrane is likely accompanied by PceT. This finding is in agreement with the role of PceT as a molecular chaperone specifically dedicated to the maturation of PceA [82, 83].

**Tentative elucidation of the electron-accepting part of OHR metabolism in *D. restrictus* and *D. hafniense* strain TCE1.** As presented in Chapter 4, the development of protocols for membrane extraction and in-gel PceA enzymatic assay represented fundamental steps for the identification of the RDH complex. The results obtained from the application of these two methods allowed the extraction of the RDH complex from the cytoplasmic membrane and the estimation of its size in native gels. Beside the Pce proteins, the application of the extraction protocol to membranes of *D. restrictus* and *D. hafniense* strain TCE1 coupled with 2D-CN/SDS-PAGE analysis helped also identifying other protein complexes, such as the GroEL maturation complex and the F<sub>0</sub>F<sub>1</sub> ATP synthase. Interestingly, the identification of PceA-containing GroEL maturation complex via immunoblotting opens new questions concerning its physiological localization and its function in transporting the matured PceA protein towards the cytoplasmic membrane [137]. To date GroEL is well-defined in literature as part of the chaperone machinery occurring in the cytosolic compartment [137], however, recent studies revealed the presence of GroEL at the membrane as adaptive response to a toxicity stress [138]. With the present research, first insights on the implication of the GroEL complex in the maturation of PceA have been presented, however, further investigation are required to validate and confirm these findings.

The development of the in-gel PceA enzymatic assay stands out as an important improvement in the identification and localization of active RDH complexes when compared to the existing literature [66, 68]. The in-gel enzymatic assay in CN-PAGE gels as proposed in the present work, is an innovative way to localize the RDH complex in native gels. Its practicality and wide applicability make this method a reference tool for the identification of other RDH protein complexes in the field of OHR.

In chapter 5, the attempts to elucidate the electron-accepting moiety of OHR in *D. restrictus* and *D. hafniense* strain TCE1 are described. The preliminary results obtained using transmission electron microscopy (TEM) and cryo-EM revealed the presence of Pce(AB)<sub>2</sub> complex, excluding PceC from the complex. The structure to come may constitute an important breakthrough in the field of OHR setting the basis for further investigation on the structural features of the RDH complex. Analysis on PceB structure will be performed to elucidate its possible interaction with menaquinol. In this scenario, menaquinol oxidation by PceB could drive electrons to PceA and may be associated with H<sup>+</sup> release to the periplasm, resulting in an electro-neutral process. However, since PceA carries redox centers with low midpoint redox potentials [139], it is possible that the reaction is energy-driven, and may be associated with proton release to the cytoplasm by PceB. This hypothesis would resemble the electron accepting half-loop mechanism proposed for the sulfur reductase SreABC, which is a membrane-bound complex that reduces elemental sulfur to sulfide [140]. However, at this stage the hypothesis of additional protein which can be the link between the menaquinol pool and PceA cannot be excluded. So far, the redox protein PceC was indicated as a possible candidate to carry out this role, however, the quantitative proteomics presented here [132] revealed its much lower abundance compared with PceA and PceB. Furthermore, the 3D structural reconstruction of the Pce(AB)<sub>2</sub> complex raises new questions on the relative abundance of the

Pce proteins at membrane level. The 1:1 stoichiometry between PceA and PceB likely observed by cryo-EM in the RDH complex is in disagreement with the recent calculated ratio of 2:1 in favor of PceA. Beyond possible limitations in the detection of PceB via PRM proteomics that could have biased the quantification, the excess of PceA at the membrane could be explained by the presence of inactive form of PceA associated with the GroEL maturation complex.

This work presents a possible road-map for the identification of new RDH complexes from the biomass of OHRB to the resolution of their 3D-structure and set the basis for the elucidation of the electron-accepting moiety involved in OHR. Moreover, it gives new arguments for a possible catalytic role of PceB in OHR and proposes an electron transfer model to PceA devoid of PceC. In addition, the identification of PceA within the GroEL maturation complex raised new questions about the biosynthetic pathway of PceA and invites to consider the involvement of GroEL, but also PceT and other possible molecular chaperones into the maturation of the key enzyme in organohalide respiration.

# A Supplementary material Chapter 3

## A.1 quantitative PCR analysis

In the present section the parameters and the raw data of the quantitative PCR analysis are shown.

Table A.1: Primers used in the quantitative PCR analysis.

Primer name	Primer sequence (5'-3')	PCR product (bp)
Dre-rpoB-F	GGAAAATCCGTTCTTTATGACG	276
Dre-rpoB-R	TACCACATCATCGGACTTAACG	
Dha-rpoB-F	GACGGGTCAAGACTTATGAAGC	296
Dha-rpoB-R	CTCATCATCAACAGCTTCTTCG	
pceA-F	GACATCGCATCGCCAAAGTC	165
pceA-R	AATCCTCTGGCTGCAGAACC	
pceAB-F	GGCCTGTAAACCCTGATGAAAG	191
pceAB-R	CCAGTGCCATCCAAATCAGC	
pceB-F	ATCTGGCGGTATCTGAAAGG	126
pceB-R	GTATTCACGCTCCGAAAAGC	
pceBC-F	AGGCACGGCACTTATTCCTG	245
pceBC-R	CCTCTTCTATTTTCCAACCTCTGC	
pceC-F	CTGAGGCTGTGAACAAAGGG	196
pceC-R	ACCACGACACTAACCAGCAG	
pceCT-F	GTTGGCGAAATGAGGAGGTAAG	313
pceCT-R	AGGCTTGCTGAATCTCCTCTTC	
pceT-F	TATTCAGCCCGATGCCTTAG	218
pceT-R	GAATATTTGCCTCCCGTTCC	



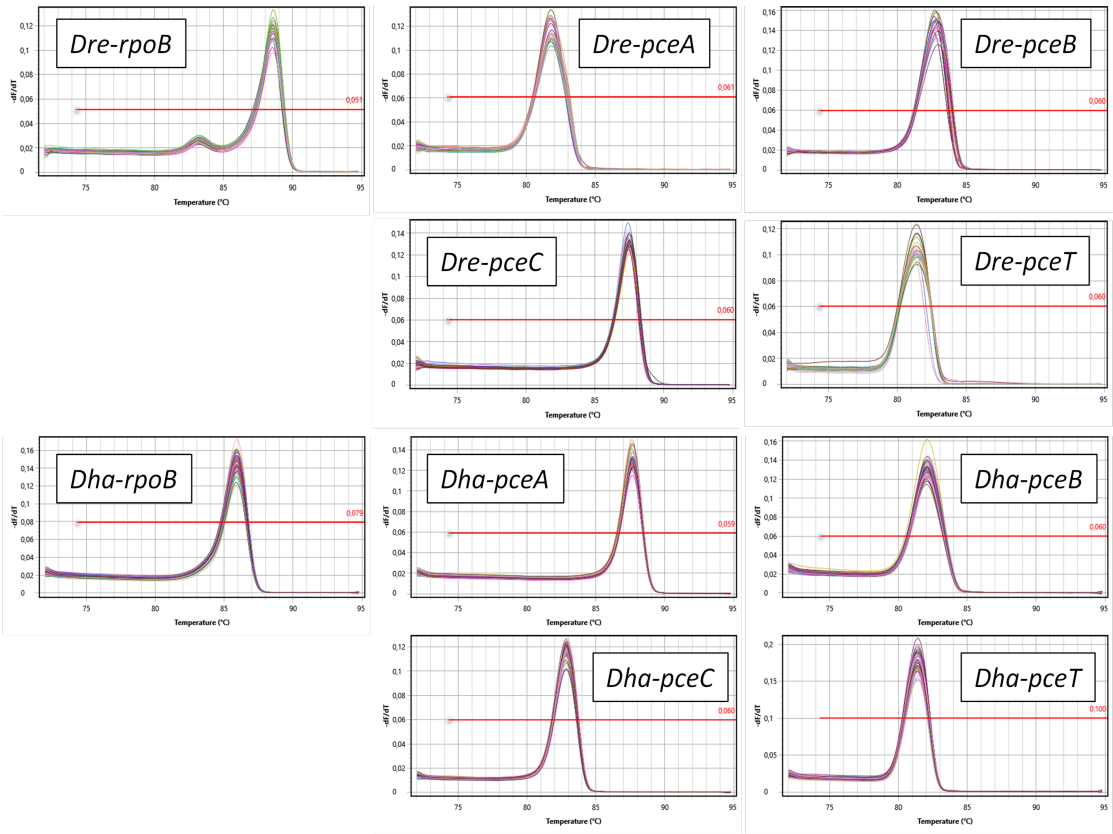


Figure A.1: qPCR reaction melting curves.

Table A.2: Quantitative PCR raw data.

Strain	Sample	Sample name	rpoB Cq	Efficiency	R <sup>2</sup>	pceA Cq	Efficiency	R <sup>2</sup>	pceB Cq	Efficiency	R <sup>2</sup>	pceC Cq	Efficiency	R <sup>2</sup>	pceT Cq	Efficiency	R <sup>2</sup>
<i>D. restrictus</i> strain PER-K23	H2-PCE routine (cDNA)	DreB1c	20.005	0.825	1.000	9.388	0.926	1.000	7.792	0.858	1.000	11.994	0.958	1.000	11.590	0.942	1.000
<i>D. restrictus</i> strain PER-K23	H2-PCE routine (cDNA)	DreB1c	19.580	0.776	1.000	9.215	0.875	1.000	7.650	0.853	1.000	11.799	0.951	1.000	11.579	0.956	1.000
<i>D. restrictus</i> strain PER-K23	H2-PCE routine (cDNA)	DreB2c	19.753	0.814	1.000	9.228	0.936	1.000	7.631	0.870	1.000	11.811	0.954	1.000	11.549	0.950	1.000
<i>D. restrictus</i> strain PER-K23	H2-PCE routine (cDNA)	DreB2c	19.950	0.839	1.000	9.139	0.820	1.000	7.797	0.951	1.000	11.960	0.974	1.000	11.571	0.966	1.000
<i>D. restrictus</i> strain PER-K23	H2-PCE routine (cDNA)	DreD1c	21.092	0.795	1.000	11.183	0.977	1.000	9.273	0.947	1.000	13.216	0.951	1.000	12.773	0.940	1.000
<i>D. restrictus</i> strain PER-K23	H2-PCE routine (cDNA)	DreD1c	21.112	0.841	1.000	11.522	0.942	1.000	9.681	0.950	1.000	13.557	0.965	1.000	13.404	0.962	1.000
<i>D. restrictus</i> strain PER-K23	H2-PCE routine (cDNA)	DreD2c	21.382	0.832	1.000	11.461	0.951	1.000	9.672	0.967	1.000	13.805	0.973	1.000	13.036	0.775	1.000
<i>D. restrictus</i> strain PER-K23	H2-PCE routine (cDNA)	DreD2c	21.442	0.791	1.000	11.259	0.908	1.000	9.678	0.905	1.000	13.549	0.960	1.000	-	-	-
<i>D. restrictus</i> strain PER-K23	H2-PCE routine (DNA)	DreB1d	21.799	0.790	1.000	-	-	-	-	-	-	16.570	0.872	1.000	17.497	0.971	1.000
<i>D. restrictus</i> strain PER-K23	H2-PCE routine (DNA)	DreB1d	21.670	0.795	1.000	19.887	0.918	1.000	19.678	0.922	1.000	18.002	0.966	1.000	17.344	0.983	1.000
<i>D. restrictus</i> strain PER-K23	H2-PCE routine (DNA)	DreB2d	21.676	0.802	1.000	20.017	0.910	1.000	19.777	0.941	1.000	17.861	0.973	1.000	17.363	0.959	1.000
<i>D. restrictus</i> strain PER-K23	H2-PCE routine (DNA)	DreB2d	21.976	0.793	1.000	19.705	0.891	1.000	19.693	0.949	1.000	17.870	0.970	1.000	17.446	0.956	1.000
<i>D. restrictus</i> strain PER-K23	H2-PCE routine (DNA)	DreD1d	22.349	0.774	1.000	19.783	0.892	1.000	19.812	0.940	1.000	18.194	0.985	1.000	17.703	0.945	1.000
<i>D. restrictus</i> strain PER-K23	H2-PCE routine (DNA)	DreD1d	22.447	0.779	1.000	19.800	0.840	1.000	19.683	0.904	1.000	18.286	0.980	1.000	17.744	0.948	1.000
<i>D. restrictus</i> strain PER-K23	H2-PCE routine (DNA)	DreD2d	22.603	0.789	1.000	19.866	0.904	1.000	19.920	0.944	1.000	18.228	0.984	1.000	17.824	0.939	1.000
<i>D. restrictus</i> strain PER-K23	H2-PCE routine (DNA)	DreD2d	22.586	0.792	1.000	20.017	0.946	1.000	19.873	0.956	1.000	18.363	0.969	1.000	17.726	0.983	1.000
<i>D. hafniense</i> strain TCE1	pyruvate (control) (cDNA)	TCE1_Pyr1	26.460	0.855	1.000	17.375	0.964	1.000	16.422	0.936	1.000	19.208	0.899	1.000	17.905	0.957	1.000
<i>D. hafniense</i> strain TCE1	pyruvate (control) (cDNA)	TCE1_Pyr1	26.585	0.869	1.000	17.140	0.960	1.000	16.309	0.903	1.000	19.108	0.902	1.000	18.014	0.971	1.000
<i>D. hafniense</i> strain TCE1	pyruvate (control) (cDNA)	TCE1_Pyr1	26.598	0.902	1.000	17.261	0.944	1.000	16.626	0.910	1.000	19.060	0.922	1.000	17.989	0.955	1.000
<i>D. hafniense</i> strain TCE1	pyruvate (control) (cDNA)	TCE1_Pyr2	20.610	0.872	1.000	11.379	0.911	1.000	11.099	0.958	1.000	12.305	0.877	1.000	11.830	0.982	1.000
<i>D. hafniense</i> strain TCE1	pyruvate (control) (cDNA)	TCE1_Pyr2	20.489	0.861	1.000	11.465	0.930	1.000	11.169	0.980	1.000	12.348	0.899	1.000	11.901	0.967	1.000
<i>D. hafniense</i> strain TCE1	pyruvate (control) (cDNA)	TCE1_Pyr2	20.270	0.866	1.000	11.529	0.942	1.000	11.226	0.969	1.000	12.282	0.920	1.000	11.854	0.933	1.000
<i>D. hafniense</i> strain TCE1	pyruvate (control) (cDNA)	TCE1_Pyr3	24.139	0.857	1.000	14.781	0.944	1.000	14.004	0.941	1.000	16.480	0.893	1.000	15.344	0.973	1.000
<i>D. hafniense</i> strain TCE1	pyruvate (control) (cDNA)	TCE1_Pyr3	24.501	0.829	1.000	14.893	0.959	1.000	13.794	0.936	1.000	16.436	0.884	1.000	15.392	0.940	1.000
<i>D. hafniense</i> strain TCE1	pyruvate (control) (cDNA)	TCE1_Pyr3	24.154	0.851	1.000	14.706	0.948	1.000	14.018	0.937	1.000	16.378	0.927	1.000	15.382	0.924	1.000
<i>D. hafniense</i> strain TCE1	pyruvate (control) (cDNA)	TCE1_Pyr4	20.659	0.835	1.000	11.568	0.964	1.000	10.737	0.943	1.000	12.169	0.882	1.000	11.546	0.890	1.000
<i>D. hafniense</i> strain TCE1	pyruvate (control) (cDNA)	TCE1_Pyr4	20.632	0.860	1.000	11.506	0.955	1.000	11.122	0.981	1.000	12.162	0.896	1.000	11.768	0.941	1.000
<i>D. hafniense</i> strain TCE1	pyruvate (control) (cDNA)	TCE1_Pyr4	20.894	0.830	1.000	11.524	0.966	1.000	10.822	0.910	1.000	12.377	0.947	1.000	11.641	0.935	1.000
<i>D. hafniense</i> strain TCE1	PCE spike (cDNA)	TCE1_Pyr5	23.816	0.856	1.000	14.413	0.959	1.000	13.464	0.893	1.000	15.922	0.927	1.000	14.691	0.939	1.000
<i>D. hafniense</i> strain TCE1	PCE spike (cDNA)	TCE1_Pyr5	23.756	0.841	1.000	14.552	0.948	1.000	13.464	0.938	1.000	15.898	0.926	1.000	15.053	0.934	1.000
<i>D. hafniense</i> strain TCE1	PCE spike (cDNA)	TCE1_Pyr5	23.860	0.848	1.000	14.410	0.951	1.000	13.738	0.927	1.000	15.757	0.905	1.000	14.997	0.927	1.000
<i>D. hafniense</i> strain TCE1	PCE spike (cDNA)	TCE1_Pyr6	22.036	0.820	1.000	12.629	0.899	1.000	12.248	0.935	1.000	13.273	0.850	1.000	12.877	0.947	1.000
<i>D. hafniense</i> strain TCE1	PCE spike (cDNA)	TCE1_Pyr6	21.833	0.839	1.000	12.580	0.958	1.000	12.118	0.971	1.000	13.462	0.967	1.000	12.547	0.939	1.000
<i>D. hafniense</i> strain TCE1	PCE spike (cDNA)	TCE1_Pyr6	22.020	0.821	1.000	12.429	0.968	1.000	12.126	0.925	1.000	13.382	0.953	1.000	12.525	0.912	1.000
<i>D. hafniense</i> strain TCE1	PCE spike (cDNA)	TCE1_Pyr7	25.963	0.870	1.000	16.842	0.951	1.000	16.116	0.948	1.000	17.951	0.889	1.000	17.156	0.937	1.000
<i>D. hafniense</i> strain TCE1	PCE spike (cDNA)	TCE1_Pyr7	26.111	0.850	1.000	16.840	0.955	1.000	16.025	0.888	1.000	17.773	0.891	1.000	17.314	0.941	1.000
<i>D. hafniense</i> strain TCE1	PCE spike (cDNA)	TCE1_Pyr7	25.952	0.857	1.000	16.750	0.967	1.000	16.081	0.950	1.000	18.036	0.928	1.000	17.086	0.981	1.000
<i>D. hafniense</i> strain TCE1	PCE spike (cDNA)	TCE1_Pyr8	22.276	0.835	1.000	12.514	0.959	1.000	12.149	0.964	1.000	13.476	0.955	1.000	12.791	0.973	1.000
<i>D. hafniense</i> strain TCE1	PCE spike (cDNA)	TCE1_Pyr8	22.386	0.845	1.000	12.623	0.959	1.000	12.283	0.933	1.000	13.360	0.955	1.000	13.006	0.984	1.000
<i>D. hafniense</i> strain TCE1	PCE spike (cDNA)	TCE1_Pyr8	22.543	0.819	1.000	12.834	0.955	1.000	12.105	0.919	1.000	13.430	0.900	1.000	13.078	0.940	1.000
<i>D. hafniense</i> strain TCE1	H2-PCE routine (cDNA)	TCE1_HP1	26.911	0.862	1.000	15.081	0.957	1.000	13.408	0.889	1.000	16.585	0.893	1.000	15.583	0.956	1.000
<i>D. hafniense</i> strain TCE1	H2-PCE routine (cDNA)	TCE1_HP1	26.777	0.859	1.000	15.027	0.946	1.000	13.576	0.948	1.000	16.648	0.908	1.000	15.591	0.981	1.000
<i>D. hafniense</i> strain TCE1	H2-PCE routine (cDNA)	TCE1_HP1	27.324	0.849	1.000	15.024	0.958	1.000	13.749	0.947	1.000	16.815	0.918	1.000	15.728	0.956	1.000
<i>D. hafniense</i> strain TCE1	H2-PCE routine (cDNA)	TCE1_HP2	24.174	0.832	1.000	13.612	0.934	1.000	12.757	0.905	1.000	14.454	0.942	1.000	14.098	0.964	1.000
<i>D. hafniense</i> strain TCE1	H2-PCE routine (cDNA)	TCE1_HP2	24.061	0.834	1.000	13.469	0.943	1.000	12.550	0.780	0.999	14.413	0.944	1.000	14.053	0.943	1.000
<i>D. hafniense</i> strain TCE1	H2-PCE routine (cDNA)	TCE1_HP2	24.338	0.840	1.000	13.633	0.956	1.000	12.683	0.898	1.000	14.420	0.936	1.000	14.067	0.967	1.000
<i>D. hafniense</i> strain TCE1	H2-PCE routine (cDNA)	TCE1_HP3	23.542	0.826	1.000	12.820	0.948	1.000	12.097	0.987	1.000	13.533	0.945	1.000	13.294	0.951	1.000
<i>D. hafniense</i> strain TCE1	H2-PCE routine (cDNA)	TCE1_HP3	23.662	0.816	1.000	12.954	0.922	1.000	11.952	0.906	1.000	13.573	0.913	1.000	13.329	0.963	1.000
<i>D. hafniense</i> strain TCE1	H2-PCE routine (cDNA)	TCE1_HP3	23.500	0.828	1.000	12.936	0.955	1.000	11.981	0.976	1.000	13.783	0.980	1.000	13.282	0.938	1.000
<i>D. hafniense</i> strain TCE1	H2-PCE routine (cDNA)	TCE1_HP4	23.929	0.832	1.000	13.798	0.965	1.000	12.359	0.981	1.000	14.270	0.950	1.000	14.376	0.966	1.000
<i>D. hafniense</i> strain TCE1	H2-PCE routine (cDNA)	TCE1_HP4	24.279	0.850	1.000	13.733	0.961	1.000	12.361	0.944	1.000	14.301	0.946	1.000	14.235	0.953	1.000
<i>D. hafniense</i> strain TCE1	H2-PCE routine (cDNA)	TCE1_HP4	23.774	0.798	1.000	13.890	0.973	1.000	12.243	0.941	1.000	14.242	0.938	1.000	14.215	0.966	1.000
<i>D. hafniense</i> strain TCE1	Pyr-PCE routine (cDNA)	TCE1_PP1	25.472	0.829	1.000	15.122	0.971	1.000	13.624	0.914	1.000	16.126	0.938	1.000	16.063	0.921	1.000
<i>D. hafniense</i> strain TCE1	Pyr-PCE routine (cDNA)	TCE1_PP1	25.408	0.837	1.000	15.169	0.958	1.000	13.335	0.885	1.000	16.052	0.958	1.000	16.028	0.975	1.000
<i>D. hafniense</i> strain TCE1	Pyr-PCE routine (cDNA)	TCE1_PP1	25.634	0.856	1.000	15.209	0.956	1.000	13.550	0.900	0.999	16.162	0.922	1.000	16.191	0.957	1.000
<i>D. hafniense</i> strain TCE1	Pyr-PCE routine (cDNA)	TCE1_PP2	24.744	0.831	1.000	14.741	0.971	1.000	13.387	0.852	1.000	15.243	0.922	1.000	15.221	0.950	1.000
<i>D. hafniense</i> strain TCE1	Pyr-PCE routine (cDNA)	TCE1_PP2	24.590	0.870	1.000	14.883	0.929	1.000	13.325	0.949	1.000	15.286	0.933	1.000	15.310	0.966	1.000
<i>D. hafniense</i> strain TCE1	Pyr-PCE routine (cDNA)	TCE1_PP2	24.461	0.834	1.000	14.883	0.927	1.000	13.454	0.927	1.000	15.292	0.937	1.000	15.185	0.963	1.000
<i>D. hafniense</i> strain TCE1	Pyr-PCE routine (cDNA)	TCE1_PP3	22.895	0.840	1.000	13.683	0.957	1.000	12.832	0.951	1.000	14.089	0.930	1.000	13.978	0.963	1.000
<i>D. hafniense</i> strain TCE1	Pyr-PCE routine (cDNA)	TCE1_PP3	22.908	0.814	1.000	13.699	0.956	1.000	12.807	0.837	1.000	14.249	0.917	1.000	13.790	0.965	1.000
<i>D. hafniense</i> strain TCE1	Pyr-PCE routine (cDNA)	TCE1_PP3	23.139	0.828	1.000	13.591	0.950	1.000	12.936	0.883	1.000	14.160	0.939	1.000			

## A.2 PRM-based quantitative proteomics

In the present section the parameters and the raw data of the quantitative proteomics analysis are presented.

Table A.4: Sample list for PRM proteomic analysis.

Strain	Replicate	Sample type
<i>D. restrictus</i> strain PER-K23	1	Cell-free extract (CFE)
<i>D. restrictus</i> strain PER-K23	2	Cell-free extract (CFE)
<i>D. hafniense</i> strain TCE1	1	Cell-free extract (CFE)
<i>D. hafniense</i> strain TCE1	2	Cell-free extract (CFE)
<i>D. restrictus</i> strain PER-K23	1	Soluble fraction (SF)
<i>D. restrictus</i> strain PER-K23	2	Soluble fraction (SF)
<i>D. restrictus</i> strain PER-K23	1	Membrane fraction (MF)
<i>D. restrictus</i> strain PER-K23	2	Membrane fraction (MF)
<i>D. hafniense</i> strain TCE1	1	Soluble fraction (SF)
<i>D. hafniense</i> strain TCE1	2	Soluble fraction (SF)
<i>D. hafniense</i> strain TCE1	1	Membrane fraction (MF)
<i>D. hafniense</i> strain TCE1	2	Membrane fraction (MF)

Table A.5: Raw data of PRM proteomics analysis.

Replicate	PceA peptides			PceB peptide	PceC peptides		PceT peptides			ATP synthase peptides	
	YLPWDLPK	TSPSVISSATVGK	LLGADIVGLIAPYDER	LANHPAK	NVLGVISIEK	QGETPVFFER	DATVPVIR	EVSANLLGK	ELIIGDR	QVAGQLR	
1	14.86	1044.00	1747.84	644.92	44.54	19.94	222.40	314.72	177.90	217.56	
2	11.24	994.48	1781.44	692.40	41.90	21.16	260.22	265.00	228.36	230.48	
3	12.88	1008.12	1970.24	711.06	45.70	20.54	227.82	334.34	202.68	233.58	
1	10.34	704.04	1295.40	487.30	30.94	18.60	194.54	186.98	152.92	168.28	
2	8.66	719.70	1537.98	528.08	36.08	17.78	284.10	221.44	162.20	175.20	
3	8.62	848.20	1546.22	502.76	27.70	15.74	204.10	188.08	164.84	179.04	
1	1205.22	3.44	462.66	297.14	27.02	4.64	42.04	18.04	8.50	36.66	
2	1090.46	20.92	503.62	292.48	26.92	4.92	49.22	34.84	9.10	37.66	
3	1084.52	0.00	498.64	322.70	29.14	5.14	44.56	2263.10	9.24	15.38	
1	950.90	26.70	468.38	275.52	19.36	4.70	33.28	40.42	8.60	18.04	
2	899.40	758.10	510.10	239.90	15.20	3.82	32.84	47.88	9.94	17.82	
3	865.20	60.58	352.30	262.82	38.86	3.72	35.56	15.96	7.94	14.20	
1	6.10	641.12	1025.38	10.94	0.00	0.00	542.00	473.92	105.80	94.06	
2	8.30	497.64	930.58	6.58	0.16	0.06	493.46	536.86	80.18	83.92	
3	5.68	443.78	839.92	7.36	0.06	0.02	501.60	433.08	81.24	93.58	
1	4.44	460.60	906.38	4.56	0.10	0.08	484.58	487.92	80.96	92.18	
2	4.04	439.90	794.10	3.72	0.06	0.02	453.04	515.46	75.48	84.30	
3	3.94	415.84	708.78	3.76	0.06	0.00	558.60	463.52	77.78	83.80	
1	9.16	1201.30	1314.50	671.10	28.26	14.62	66.34	108.30	156.80	161.14	
2	10.02	1395.00	1622.46	941.80	29.12	18.00	83.84	124.26	194.90	241.10	
3	9.60	1510.90	1683.50	875.68	34.28	21.34	106.34	159.66	219.32	211.94	
1	11.68	1372.90	1854.18	920.60	32.22	19.04	62.28	116.78	233.10	200.70	
2	9.38	1344.26	1749.28	884.70	30.12	18.14	30.80	121.50	183.50	187.82	
3	10.36	1275.06	1736.22	874.26	31.98	18.02	71.44	124.70	187.36	201.34	
1	629.08	257.64	416.50	2.38	0.06	0.28	549.14	458.74	22.14	29.84	
2	573.42	190.60	340.40	1.64	0.04	1.18	454.22	363.90	18.46	57.04	
3	528.12	174.32	367.34	1.44	0.00	0.22	484.00	391.88	20.10	37.44	
1	1.18	0.00	0.50	0.16	0.40	0.06	0.00	0.02	0.06	0.00	
2	400.58	151.20	276.40	1.98	0.00	0.40	325.18	340.14	16.28	38.16	
3	480.90	147.12	271.24	2.02	0.02	0.18	385.34	365.70	18.90	45.10	
1	1423.08	650.06	1002.68	582.50	38.12	23.64	45.86	50.26	31.22	61.36	
2	1367.76	619.02	840.78	564.64	37.36	23.22	42.06	45.56	29.14	46.88	
3	1095.36	649.24	811.66	495.72	39.18	22.68	45.10	49.84	29.90	58.64	
1	1289.28	527.24	900.22	485.58	38.68	21.36	37.14	45.16	28.60	56.92	
2	1214.62	395.74	768.20	425.34	35.90	19.74	33.46	37.66	31.82	45.46	
3	1142.38	441.30	697.44	449.10	33.54	19.22	36.44	32.84	31.12	46.32	

Table A.6: Data analysis of PRM quantitative proteomics analysis (avarage and standard deviation).

Sample	Strain	Sample type	PceA		PceB		PceC		PceT		ATP synthase	
			Mean (fmol)	StDev (fmol)	Mean (fmol)	StDev (fmol)	Mean (fmol)	StDev (fmol)	Mean (fmol)	StDev (fmol)	Mean (fmol)	StDev (fmol)
1A	<i>D. restrictus</i> strain PER-K23	Cell-free extract (CFE)	1424.35	454.50	682.79	34.10	32.30	12.94	270.75	45.39	215.09	21.44
1B	<i>D. restrictus</i> strain PER-K23	Cell-free extract (CFE)	1108.59	398.37	506.05	20.59	24.47	8.28	213.21	37.00	167.08	9.38
2A	<i>D. hafniense</i> strain TCE1	Cell-free extract (CFE)	807.52	352.60	304.11	16.27	16.30	12.51	37.74	12.18	19.42	13.97
2B	<i>D. hafniense</i> strain TCE1	Cell-free extract (CFE)	674.38	259.49	259.41	18.05	14.28	13.74	34.32	10.61	12.76	4.56
3A	<i>D. restrictus</i> strain PER-K23	Soluble fraction (SF)	729.74	238.07	8.29	2.33	0.05	0.06	496.82	40.66	89.80	9.89
3B	<i>D. restrictus</i> strain PER-K23	Soluble fraction (SF)	620.93	209.63	4.01	0.47	0.05	0.04	493.85	38.38	82.42	5.87
4A	<i>D. restrictus</i> strain PER-K23	Membrane fraction (MF)	1454.61	184.98	829.53	141.13	24.27	7.49	108.12	32.42	197.53	33.38
4B	<i>D. restrictus</i> strain PER-K23	Membrane fraction (MF)	1555.32	251.41	893.19	24.31	24.92	7.19	87.92	38.74	198.97	18.29
5A	<i>D. hafniense</i> strain TCE1	Soluble fraction (SF)	475.81	117.79	1.82	0.50	0.30	0.45	450.31	66.14	30.84	14.66
5B	<i>D. hafniense</i> strain TCE1	Soluble fraction (SF)	357.28	101.82	2.00	0.03	0.15	0.19	354.09	26.72	29.61	14.21
6A	<i>D. hafniense</i> strain TCE1	Membrane fraction (MF)	1090.22	258.97	547.62	45.83	30.70	8.26	46.45	3.11	42.86	14.83
6B	<i>D. hafniense</i> strain TCE1	Membrane fraction (MF)	1002.02	247.07	453.34	30.34	28.07	8.91	37.12	4.41	40.04	11.24

Table A.7: Data analysis (stoichiometric relationships) obtained via PRM quantitative proteomics analysis.

Sample	Strain	Sample type	PceB/PceA	PceC/PceA	PceT/PceA
1A	<i>D. restrictus</i> strain PER-K23	Cell-free extract (CFE)	0.479	0.023	0.190
1B	<i>D. restrictus</i> strain PER-K23	Cell-free extract (CFE)	0.456	0.022	0.192
2A	<i>D. hafniense</i> strain TCE1	Cell-free extract (CFE)	0.377	0.020	0.047
2B	<i>D. hafniense</i> strain TCE1	Cell-free extract (CFE)	0.385	0.021	0.051
3A	<i>D. restrictus</i> strain PER-K23	Soluble fraction (SF)	0.011	0.000	0.681
3B	<i>D. restrictus</i> strain PER-K23	Soluble fraction (SF)	0.006	0.000	0.795
4A	<i>D. restrictus</i> strain PER-K23	Membrane fraction (MF)	0.570	0.017	0.074
4B	<i>D. restrictus</i> strain PER-K23	Membrane fraction (MF)	0.574	0.016	0.057
5A	<i>D. hafniense</i> strain TCE1	Soluble fraction (SF)	0.004	0.001	0.946
5B	<i>D. hafniense</i> strain TCE1	Soluble fraction (SF)	0.006	0.000	0.991
6A	<i>D. hafniense</i> strain TCE1	Membrane fraction (MF)	0.502	0.028	0.043
6B	<i>D. hafniense</i> strain TCE1	Membrane fraction (MF)	0.452	0.028	0.037

Table A.8: Identification of RdhA, B, C and T proteins from Firmicutes OHRB by proteomic analyses. nr: not relevant as no corresponding gene was reported. FASP: filter aided sample preparation (Wisniewski et al. 2009).

#	Reference	RdhA	RdhB	RdhC	RdhT	Trypsin digestion method
1	(Prat et al., 2011)	yes	no	no	no	in-gel (2D SDS PAGE)
2	(Tang and Edwards, 2013)	yes	yes	nr	nr	in-gel (1D Blue Native PAGE)
3	(Rupakula et al., 2013)	yes	yes	yes	yes	in-ge (11D SDS PAGE)
4	(Kruse et al., 2015)	yes	no	yes	yes	in-gel (1D SDS PAGE)
5	(Rupakula et al., 2015)	yes	yes	yes	yes	in-gel (1D SDS PAGE)
6	(Jugder et al., 2016)	yes	yes	yes	nr	in-solution (FASP)
7	(Alfán-Guzmán et al., 2017)	yes	no	no	no	in-gel (1D Native PAGE)
8	(Kleindienst et al., 2019)	yes	no	nr	nr	in-solution
9	(Low et al., 2019)	yes	no	nr	nr	in-solution
10	(Peng et al., 2020)	yes	no	no	nr	in-gel (1D SDS PAGE)
11	(Liu et al., 2020)	yes	no	no	nr	in-solution
12	(Chen et al., 2021)	yes	no	nr	nr	in-solution
13	This study	yes	yes	yes	yes	in-solution

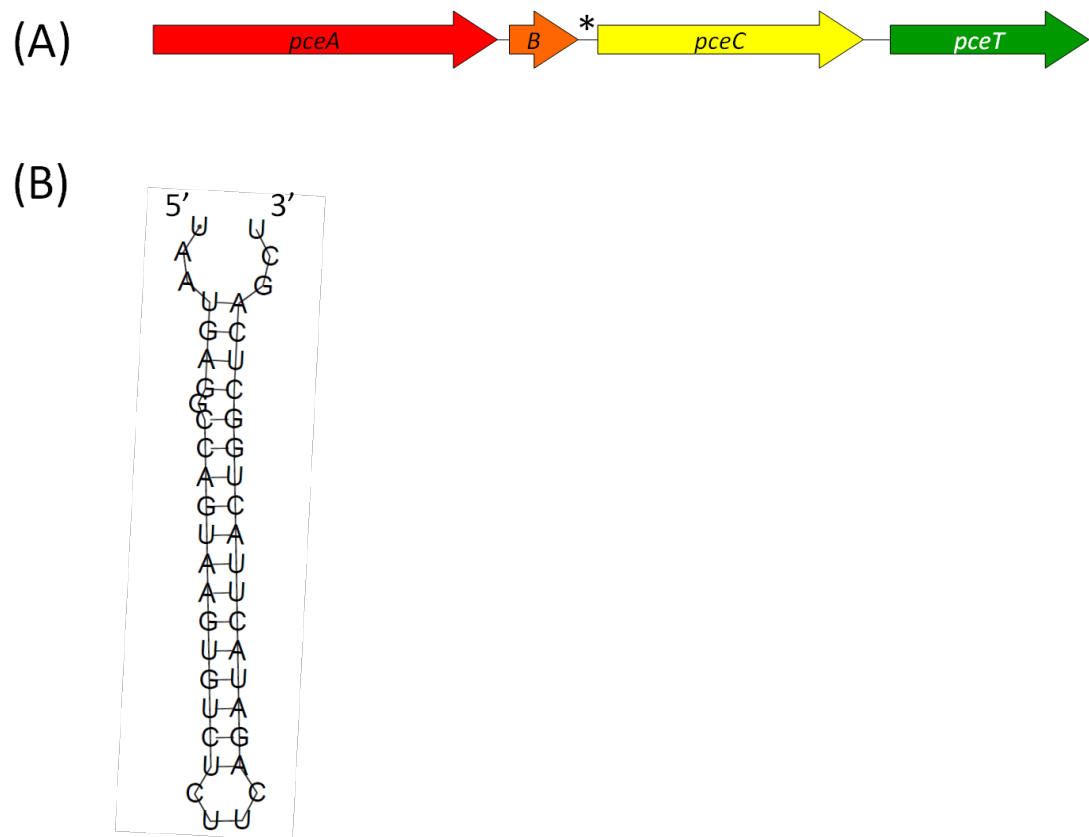


Figure A.2: The *pceABCT* gene cluster of *D. restrictus*. (A) Genetic organization of the gene cluster. (B) Prediction of a putative hairpin loop structure in the *pceBC* intergenic region. The star indicates the position of the hairpin loop in the gene cluster.



## B Supplementary material Chapter 4

Table B.1: CN-PAGE gel preparation. Two different tables were made depending on the spacers used (0.75mm and 1mm). 0.75 mm and 1 mm refer to the space between glass plates used for electrophoresis with Hoefer SE260 Mighty Small II Deluxe Mini Vertical Protein Electrophoresis Unit. AB-mix: Acryl/Bis-Acrylamide solution 49%. Gel Buffer: 15.69 gr of BisTris (MW: 209.2 Da), pH=7.0.

### Amersham Electrophoresis system with 0.75 mm spacer

	Stacking	Resolving	
		5%	15%
H <sub>2</sub> O	1.740 ml	1.592ml	560 $\mu$ l
Gel buffer 3X	1.00 ml	940 $\mu$ l	940 $\mu$ l
AB-mix	250 $\mu$ l	280 $\mu$ l	853 $\mu$ l
Glycerol 87%	-	-	464 $\mu$ l
DDM 10%	4.6 $\mu$ l	8.5 $\mu$ l	8.5 $\mu$ l
APS 10%	26 $\mu$ l	13 $\mu$ l	13 $\mu$ l
Temed	5 $\mu$ l	2.5 $\mu$ l	2.5 $\mu$ l

### Amersham Electrophoresis system with 1 mm spacer

	Stacking	Resolving	
		5%	15%
H <sub>2</sub> O	2.175 ml	1.990 ml	700 $\mu$ l
Gel buffer 3X	1.250 ml	1.175 ml	1.175 ml
AB-mix	312.5 $\mu$ l	350 $\mu$ l	1066 $\mu$ l
Glycerol 87%	-	-	580 $\mu$ l
DDM 10%	5.75 $\mu$ l	8.5 $\mu$ l	10.6 $\mu$ l
APS 10%	32.5 $\mu$ l	16.2 $\mu$ l	16.2 $\mu$ l
Temed	6.25 $\mu$ l	3.2 $\mu$ l	3.2 $\mu$ l



1	<input checked="" type="checkbox"/>	Dehre_2336	chaperonin GroL 2341504:2343138 reverse	NW:57484	57 kDa	★	532
2	<input checked="" type="checkbox"/>	Dehre_2403	Uncharacterized protein related to glutamine synthetase 2416524:2418620 forward	NW:76884	77 kDa		48
3	<input checked="" type="checkbox"/>	Dehre_2398	reductive dehalogenase 2410979:2412634 reverse	NW:61206	61 kDa		44
4	<input checked="" type="checkbox"/>	Dehre_2800	proton translocating ATP synthase, F1 alpha subunit 2836817:2838319 reverse	NW:54762	55 kDa		35
5	<input checked="" type="checkbox"/>	Dehre_2383	glutamate dehydrogenase/leucine dehydrogenase 2393889:2395223 forward	NW:48421	48 kDa		28
6	<input checked="" type="checkbox"/>	Dehre_2178	Coenzyme F390 synthetase 2191523:2192788 reverse	NW:46992	47 kDa		24
7	<input checked="" type="checkbox"/>	Dehre_2798	ATP synthase, F1 beta subunit 2834509:2835912 reverse	NW:50789	51 kDa		29
8	<input checked="" type="checkbox"/>	Dehre_1091	ribosomal protein S2, bacterial type 1102087:1102824 forward	NW:27854	28 kDa		23
9	<input checked="" type="checkbox"/>	Dehre_0153	formyltetrahydrofolate synthetase 148636:150312 reverse	NW:59374	59 kDa		20
10	<input checked="" type="checkbox"/>	Dehre_2598	Putative cell wall-binding domain 2610154:2613528 reverse	NW:113707	114 kDa		20
11	<input checked="" type="checkbox"/>	Dehre_2799	ATP synthase, F1 gamma subunit 2835950:2836798 reverse	NW:31084	31 kDa		18
12	<input checked="" type="checkbox"/>	Dehre_0529	ribosomal protein S4, bacterial/organelle type 515069:515698 forward	NW:23974	24 kDa		20
13	<input checked="" type="checkbox"/>	Dehre_2393	Uncharacterized conserved protein 2406082:2407344 reverse	NW:45997	46 kDa		16
14	<input checked="" type="checkbox"/>	Dehre_2607	Glycosyltransferase 2627265:2628407 reverse	NW:43763	44 kDa		17
15	<input checked="" type="checkbox"/>	Dehre_1584	pyridoxal-phosphate dependent TrpB-like enzyme 1592556:1593926 forward	NW:50024	50 kDa		17
16	<input checked="" type="checkbox"/>	Dehre_1609	L-threonine O-3-phosphate decarboxylase 1619540:1620625 reverse	NW:40900	41 kDa		13
17	<input checked="" type="checkbox"/>	Dehre_0128	pyruvate:ferredoxin (flavodoxin) oxidoreductase, homodimeric 119562:123098 forward	NW:128910	129 kDa		11
18	<input checked="" type="checkbox"/>	Dehre_0492	ribosomal protein L1, bacterial/chloroplast 487417:488109 forward	NW:24556	25 kDa		16
19	<input checked="" type="checkbox"/>	Dehre_0501	translation elongation factor TU 500502:501704 forward	NW:43874	44 kDa		16
20	<input checked="" type="checkbox"/>	Dehre_1157	pilus retraction protein PiliT 1155371:1156441 reverse	NW:39706	40 kDa		14
21	<input checked="" type="checkbox"/>	Dehre_1508	IHP dehydrogenase/GMP reductase 1503637:1505139 reverse	NW:55062	55 kDa		14

Figure B.1: LC-MS/MS analysis of 670 kDa CN-PAGE gel band.

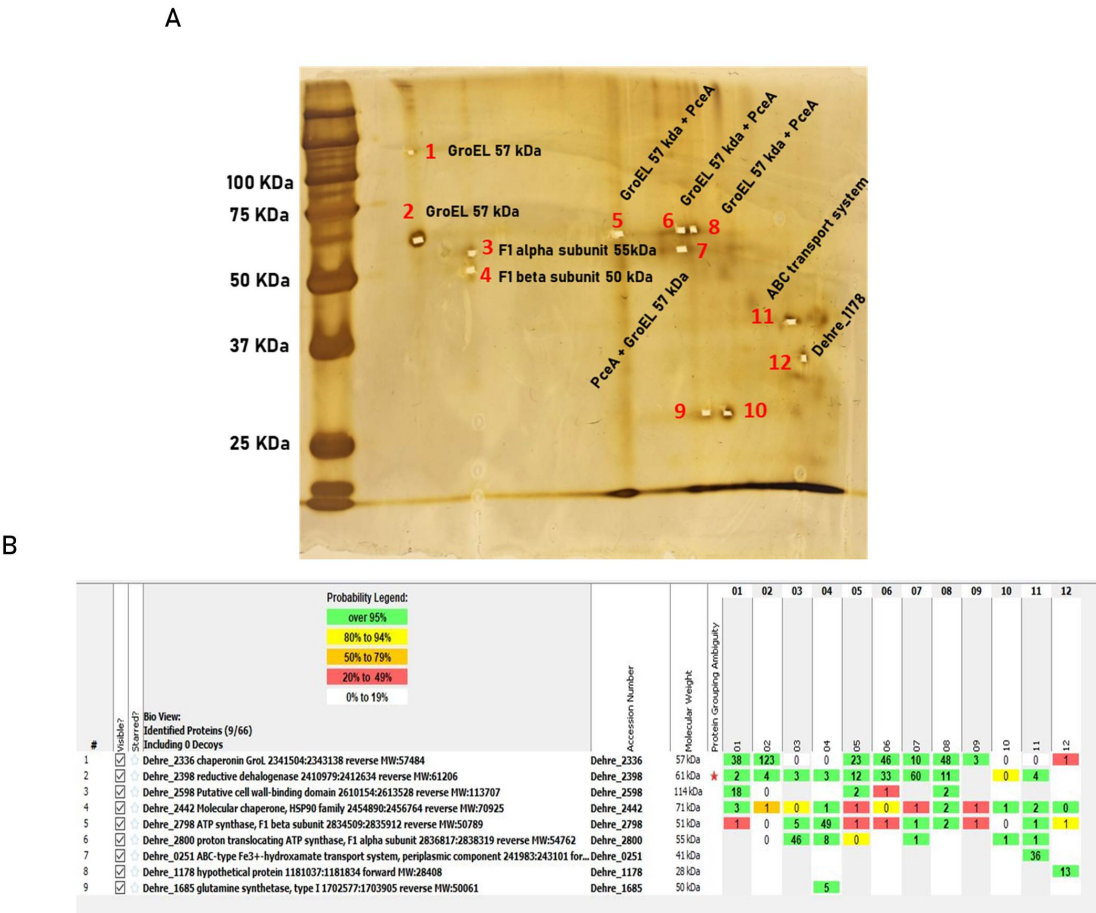


Figure B.2: 2D-Native/SDS-PAGE gel and LC-MS/MS analysis of the gel spots. Panel A) 12 gel pieces were cut from 2D-Native/SDS-PAGE gel and analyzed with LC-MS/MS analysis. In black are noted the most detected proteins per each gel piece analyzed. Panel B) Number of spectra of Pce proteins in the 12 different gel pieces analyzed. PceA and PceT were well detected, while PceB and PceC were never observed.



## Bibliography

- (1) Field, J. A. In *Organohalide-Respiring Bacteria*, Adrian, L., Löffler, F. E., Eds.; Springer Berlin Heidelberg: Berlin, Heidelberg, 2016, pp 7–29.
- (2) Butler, A.; Sandy, M. *Nature* **2009**, 460, Number: 7257 Publisher: Nature Publishing Group, 848–854.
- (3) Abrahamsson, K.; Ekdahl, A.; Collen, J.; Pedersen, M. *Oceanographic Literature Review* **1996**, 7, 670.
- (4) Collén, J.; Ekdahl, A.; Abrahamsson, K.; Pedersén, M. *Phytochemistry* **1994**, 36, 1197–1202.
- (5) Häggblom, M. M.; Bossert, I. D. In *Dehalogenation: Microbial Processes and Environmental Applications*, Häggblom, M. M., Bossert, I. D., Eds.; Springer US: Boston, MA, 2003, pp 3–29.
- (6) Mattes, T. E.; Alexander, A. K.; Coleman, N. V. *FEMS microbiology reviews* **2010**, 34, 445–475.
- (7) Thornton, J.; Campbell, D. *BMJ* **2001**, 322, 497.
- (8) Parthasarathy, A.; Stich, T. A.; Lohner, S. T.; Lesnefsky, A.; Britt, R. D.; Spormann, A. M. *Journal of the American Chemical Society* **2015**, 137, 3525–3532.
- (9) Aulenta, F.; Canosa, A.; Leccese, M.; Petrangeli Papini, M.; Majone, M.; Viotti, P. *Industrial & Engineering Chemistry Research* **2007**, 46, 6812–6819.
- (10) Christ, J. A.; Ramsburg, C. A.; Abriola, L. M.; Pennell, K. D.; Löffler, F. E. *Environmental Health Perspectives* **2005**, 113, 465–477.
- (11) Nijenhuis, I.; Nikolausz, M.; Köth, A.; Felföldi, T.; Weiss, H.; Drangmeister, J.; Grossmann, J.; Kästner, M.; Richnow, H.-H. *Chemosphere* **2007**, 67, 300–311.
- (12) Vogel, T. M.; McCarty, P. L. *Applied and Environmental Microbiology* **1985**, 49, 1080–1083.
- (13) Futagami, T.; Goto, M.; Furukawa, K. *The Chemical Record* **2008**, 8, 1–12.
- (14) Dolinová, I.; Štrojsová, M.; Černík, M.; Němeček, J.; Macháček, J.; Ševců, A. *Environmental Science and Pollution Research* **2017**, 24, 13262–13283.
- (15) Bradley, P. M.; Chapelle, F. H. *Environmental Science & Technology* **1996**, 30, 2084–2086.

- (16) Bradley, P. M.; Landmeyer, J. E.; Dinicola, R. S. *Applied and Environmental Microbiology* **1998**, *64*, 1560–1562.
- (17) Dolfing, J. In *Organohalide-Respiring Bacteria*, Adrian, L., Löffler, F. E., Eds.; Springer Berlin Heidelberg: Berlin, Heidelberg, 2016, pp 31–48.
- (18) Bradley, P. M.; Chapelle, F. H. In *In Situ Remediation of Chlorinated Solvent Plumes*, Stroo, H., Ward, C., Eds.; Springer: 2010, pp 39–67.
- (19) Bradley, P. M.; Chapelle, F. H. *Environmental Science & Technology* **2000**, *34*, Publisher: American Chemical Society, 221–223.
- (20) Holliger, C.; Schumacher, W. *Antonie van Leeuwenhoek* **1994**, *66*, 239–246.
- (21) Holliger, C.; Schraa, G.; Stams, A. J.; Zehnder, A. J. *Applied and Environmental Microbiology* **1993**, Publisher: American Society for Microbiology.
- (22) Oren, A.; Garrity, G. M. *International Journal of Systematic and Evolutionary Microbiology* **2021**, *71*, DOI: 10.1099/ijsem.0.005056.
- (23) Maphosa, F.; de Vos, W. M.; Smidt, H. *Trends in Biotechnology* **2010**, *28*, 308–316.
- (24) DeWeerd, K. A.; Concannon, E.; Suflita, J. M. *Appl. Environ. Microbiol.* **1991**, *57*, 1929–1934.
- (25) Maymó-Gatell, X.; Chien, Y.-t.; Gossett, J. M.; Zinder, S. H. *Science* **1997**, *276*, Publisher: American Association for the Advancement of Science, 1568–1571.
- (26) Krumholz, L. *International Journal of Systematic Bacteriology* **1997**, *47*, 1262–1263.
- (27) Atashgahi, S.; Häggblom, M. M.; Smidt, H. *Environmental Microbiology* **2018**, *20*, 934–948.
- (28) Maphosa, F.; Smidt, H.; de Vos, W. M.; Röling, W. F. M. *Environmental Science & Technology* **2010**, *44*, 4884–4890.
- (29) Futagami, T.; Furukawa, K. In *Organohalide-Respiring Bacteria*, Adrian, L., Löffler, F. E., Eds.; Springer, Berlin Heidelberg: 2016, pp 173–207.
- (30) Ahn, Y.-B.; Kerkhof, L. J.; Häggblom, M. M. *International Journal of Systematic and Evolutionary Microbiology* **2009**, *59*, 2133–2139.
- (31) Boyle, A. W.; Phelps, C. D.; Young, L. Y. *Applied and Environmental Microbiology* **1999**, *65*, 1133–1140.
- (32) Sung, Y.; Fletcher, K. E.; Ritalahti, K. M.; Apkarian, R. P.; Ramos-Hernández, N.; Sanford, R. A.; Mesbah, N. M.; Löffler, F. E. *Applied and Environmental Microbiology* **2006**, *72*, 2775–2782.
- (33) Zhao, J.-S.; Manno, D.; Beaulieu, C.; Paquet, L.; Hawari, J. *International Journal of Systematic and Evolutionary Microbiology* **2005**, *55*, 1511–1520.
- (34) Goris, T.; Schubert, T.; Gadkari, J.; Wubet, T.; Tarkka, M.; Buscot, F.; Adrian, L.; Diekert, G. *Environmental Microbiology* **2014**, *16*, 3562–3580.

- 
- (35) Maillard, J.; Holliger, C. In *Organohalide-Respiring Bacteria*, Adrian, L., Löffler, F. E., Eds.; Springer, Berlin Heidelberg: 2016, pp 153–171.
- (36) Zinder, S. H. In *Organohalide-Respiring Bacteria*, Adrian, L., Löffler, F. E., Eds.; Springer Berlin Heidelberg: Berlin, Heidelberg, 2016, pp 107–136.
- (37) Key, T. A.; Richmond, D. P.; Bowman, K. S.; Cho, Y.-J.; Chun, J.; da Costa, M. S.; Rainey, F. A.; Moe, W. M. *Standards in Genomic Sciences* **2016**, *11*, 44.
- (38) Grostern, A.; Edwards, E. A. *Applied and Environmental Microbiology* **2006**, *72*, 428–436.
- (39) Yoshida, N.; Ye, L.; Baba, D.; Katayama, A. *Microbes and Environments* **2009**, *24*, 343–346.
- (40) Moe, W. M.; Yan, J.; Nobre, M. F.; da Costa, M. S.; Rainey, F. A. *International Journal of Systematic and Evolutionary Microbiology* **2009**, *59*, 2692–2697.
- (41) Maness, A. D.; Bowman, K. S.; Yan, J.; Rainey, F. A.; Moe, W. M. *AMB Express* **2012**, *2*, 54.
- (42) Holliger, C.; Hahn, D.; Harmsen, H.; Ludwig, W.; Schumacher, W.; Tindall, B.; Vazquez, F.; Weiss, N.; Zehnder, A. J. B. *Archives of Microbiology* **1998**, *169*, 313–321.
- (43) Türkowsky, D.; Jehmlich, N.; Diekert, G.; Adrian, L.; von Bergen, M.; Goris, T. *FEMS microbiology ecology* **2018**, *94*, fty013.
- (44) Justicia-Leon, S. D.; Ritalahti, K. M.; Mack, E. E.; Löffler, F. E. *Applied and Environmental Microbiology* **2012**, *78*, 1288–1291.
- (45) Lee, M.; Low, A.; Zemb, O.; Koenig, J.; Michaelsen, A.; Manefield, M. *Environmental Microbiology* **2012**, *14*, 883–894.
- (46) Schumacher, W.; Holliger, C. *Journal of Bacteriology* **1996**, *178*, 2328–33.
- (47) Schumacher, W.; Holliger, C.; Zehnder, A. J. B.; Hagen, W. R. *FEBS Letters* **1997**, *409*, 421–425.
- (48) Maillard, J.; Schumacher, W.; Vazquez, F.; Regeard, C.; Hagen, W. R.; Holliger, C. *Applied and Environmental Microbiology* **2003**, *69*, 4628–4638.
- (49) Rupakula, A.; Kruse, T.; Boeren, S.; Holliger, C.; Smidt, H.; Maillard, J. *Philosophical Transactions of the Royal Society B: Biological Sciences* **2013**, *368*, 20120325.
- (50) Rupakula, A.; Lu, Y.; Kruse, T.; Boeren, S.; Holliger, C.; Smidt, H.; Maillard, J. *Frontiers in Microbiology* **2015**, *5*, 751.
- (51) Kruse, T. et al. *Standards in Genomic Sciences* **2013**, *8*, 375–388.
- (52) Madsen, T.; Licht, D. *Applied and Environmental Microbiology* **1992**, *58*, 2874–2878.
- (53) Gerritse, J.; Drzyzga, O.; Kloetstra, G.; Keijmel, M.; Wiersum, L. P.; Hutson, R.; Collins, M. D.; Gottschal, J. C. *Applied and Environmental Microbiology* **1999**, *65*, 5212–5221.
- (54) Simon, J.; van Spanning, R. J.; Richardson, D. J. *Biochimica et Biophysica Acta (BBA) - Bioenergetics* **2008**, *1777*, 1480–1490.

- (55) Mohn, W. W.; Tiedje, J. M. *Microbiological Reviews* **1992**, *56*, 482–507.
- (56) Schubert, T.; Adrian, L.; Sawers, R. G.; Diekert, G. *FEMS Microbiology Ecology* **2018**, *94*, DOI: 10.1093/femsec/fiy035.
- (57) Thauer, R. K.; Jungermann, K.; Decker, K. *Bacteriological Reviews* **1977**, *41*, 100–180.
- (58) Mitchell, P. *Science* **1979**, *206*, 1148–1159.
- (59) Scholz-Muramatsu, H.; Neumann, A.; Meßmer, M.; Moore, E.; Diekert, G. *Archives of Microbiology* **1995**, *163*, 48–56.
- (60) Van de Pas, B. A.; Jansen, S.; Dijkema, C.; Schraa, G.; de Vos, W. M.; Stams, A. J. *Applied and Environmental Microbiology* **2001**, *67*, 3958–3963.
- (61) Louie, T. M.; Mohn, W. W. *Journal of Bacteriology* **1999**, *181*, 40–46.
- (62) Prat, L. **2009**, DOI: 10.5075/epfl-thesis-4472.
- (63) Vogel, T. M.; Criddle, C. S.; McCarty, P. L. *Environmental Science & Technology* **1987**, *21*, Publisher: American Chemical Society, 722–736.
- (64) Miller, E.; Wohlfarth, G.; Diekert, G. *Archives of Microbiology* **1996**, *166*, 379–387.
- (65) Buckel, W.; Thauer, R. K. *Biochimica et Biophysica Acta (BBA) - Bioenergetics* **2013**, *1827*, 94–113.
- (66) Seidel, K.; Kühnert, J.; Adrian, L. *Frontiers in Microbiology* **2018**, *9*, 1130.
- (67) Jayachandran, G.; Görisch, H.; Adrian, L. *Archives of Microbiology* **2004**, *182*, 498–504.
- (68) Kublik, A.; Deobald, D.; Hartwig, S.; Schiffmann, C. L.; Andrades, A.; von Bergen, M.; Sawers, R. G.; Adrian, L. *Environmental Microbiology* **2016**, *18*, 3044–3056.
- (69) Magnuson, J. K.; Romine, M. F.; Burris, D. R.; Kingsley, M. T. *Appl. Environ. Microbiol.* **2000**, *66*, 5141–5147.
- (70) Hug, L. A.; Maphosa, F.; Leys, D.; Löffler, F. E.; Smidt, H.; Edwards, E. A.; Adrian, L. *Philosophical Transactions of the Royal Society B: Biological Sciences* **2013**, *368*, 20120322.
- (71) Siddaramappa, S. et al. *Standards in Genomic Sciences* **2012**, *6*, 251–264.
- (72) Fincker, M.; Spormann, A. M. *Annual Review of Biochemistry* **2017**, *86*, 357–386.
- (73) Smidt, H.; Leest, M. V.; Oost, J. V. D.; De Vos, W. M. *Journal of Bacteriology* **2000**, *182*, 5683–5691.
- (74) Ni, S.; Fredrickson, J. K.; Xun, L. *Journal of Bacteriology* **1995**, *177*, 5135–5139.
- (75) Müller, J. A.; Rosner, B. M.; Von Abendroth, G.; Meshulam-Simon, G.; McCarty, P. L.; Spormann, A. M. *Applied and Environmental Microbiology* **2004**, *70*, 4880–4888.
- (76) Jugder, B.-E.; Ertan, H.; Bohl, S.; Lee, M.; Marquis, C. P.; Manefield, M. *Frontiers in Microbiology* **2016**, *7*, 249.
- (77) Kruse, T.; Goris, T.; Maillard, J.; Woyke, T.; Lechner, U.; de Vos, W.; Smidt, H. *FEMS Microbiology Ecology* **2017**, *93*, fix135.

- 
- (78) Duret, A.; Holliger, C.; Maillard, J. *Applied and Environmental Microbiology* **2012**, *78*, 6121–6127.
- (79) Maillard, J.; Regeard, C.; Holliger, C. *Environmental Microbiology* **2005**, *7*, 107–117.
- (80) Prat, L.; Maillard, J.; Grimaud, R.; Holliger, C. *Applied Environmental Microbiology* **2011**, *77*, 3853–3859.
- (81) Buttet, G. F.; Willemin, M. S.; Hamelin, R.; Rupakula, A.; Maillard, J. *Frontiers in Microbiology* **2018**, *9*, 755.
- (82) Morita, Y.; Futagami, T.; Goto, M.; Furukawa, K. *Applied Microbiology and Biotechnology* **2009**, *83*, 775–781.
- (83) Maillard, J.; Genevaux, P.; Holliger, C. *Microbiology* **2011**, *157*, 2410–2421.
- (84) Wunsch, P.; Zumft, W. G. *J. Bacteriol.* **2005**, *187*, 10.
- (85) Cuypers, H.; Viebrock-Sambale, A.; Zumft, W. G. *Journal of Bacteriology* **1992**, *174*, 5332–5339.
- (86) Acuña, J. M. B.-d.; Timmis, K. N.; Jahn, M.; Jahn, D. *Microbial Biotechnology* **2017**, *10*, 1523–1534.
- (87) Mac Nelly, A.; Kai, M.; Svatoš, A.; Diekert, G.; Schubert, T. *Applied and Environmental Microbiology* **2014**, *80*, ed. by Spormann, A. M., 4313–4322.
- (88) Picott, K. J.; Flick, R.; Edwards, E. A. *Applied and Environmental Microbiology* **2022**, *88*, Publisher: American Society for Microbiology, e01993–21.
- (89) Buttet, G. F. Properties of Enzymes Involved in Tetrachloroethene Respiration: From Physiology to Protein Function, eng, Ph.D. Thesis, Lausanne: EPFL, 2017.
- (90) Switzar, L.; Giera, M.; Niessen, W. M. A. *Journal of Proteome Research* **2013**, *12*, 1067–1077.
- (91) Keener, J. E.; Zhang, G.; Marty, M. T. *Analytical Chemistry* **2021**, *93*, 583–597.
- (92) Lange, V.; Picotti, P.; Domon, B.; Aebersold, R. *Molecular Systems Biology* **2008**, *4*, 222.
- (93) Picotti, P.; Aebersold, R. *Nature Methods* **2012**, *9*, Number: 6 Publisher: Nature Publishing Group, 555–566.
- (94) Peterson, A. C.; Russell, J. D.; Bailey, D. J.; Westphall, M. S.; Coon, J. J. *Molecular & Cellular Proteomics : MCP* **2012**, *11*, 1475–1488.
- (95) Comensoli, L.; Maillard, J.; Albin, M.; Sandoz, F.; Junier, P.; Joseph, E. *Applied and Environmental Microbiology* **2017**, *83*, e03478–16.
- (96) Wang, P.-H.; Tang, S.; Nemr, K.; Flick, R.; Yan, J.; Mahadevan, R.; Yakunin, A. F.; Löffler, F. E.; Edwards, E. A. *The ISME journal* **2017**, *11*, 626–640.
- (97) Yan, J.; Bi, M.; Bourdon, A. K.; Farmer, A. T.; Wang, P.-H.; Molenda, O.; Quail, A. T.; Jiang, N.; Yang, Y.; Yin, Y.; Şimşir, B.; Campagna, S. R.; Edwards, E. A.; Löffler, F. E. *Nature Chemical Biology* **2018**, *14*, 8–14.



- (98) Schubert, T.; von Reuß, S. H.; Kunze, C.; Paetz, C.; Kruse, S.; Brand-Schön, P.; Nelly, A. M.; Nüske, J.; Diekert, G. *Microbial Biotechnology* **2019**, *12*, 346–359.
- (99) Arachea, B. T.; Sun, Z.; Potente, N.; Malik, R.; Isailovic, D.; Viola, R. E. *Protein Expression and Purification* **2012**, *86*, 12–20.
- (100) Wiśniewski, J. R.; Zougman, A.; Nagaraj, N.; Mann, M. *Nature Methods* **2009**, *6*, 359–362.
- (101) Wagner, D. D.; Hug, L. A.; Hatt, J. K.; Spitzmiller, M. R.; Padilla-Crespo, E.; Ritalahti, K. M.; Edwards, E. A.; Konstantinidis, K. T.; Löffler, F. E. *BMC Genomics* **2012**, *13*, 200.
- (102) Futagami, T.; Yamaguchi, T.; Nakayama, S.-I.; Goto, M.; Furukawa, K. *Applied and Environmental Microbiology* **2006**, *72*, 5998–6003.
- (103) Goris, T.; Schiffmann, C. L.; Gadkari, J.; Schubert, T.; Seifert, J.; Jehmlich, N.; von Bergen, M.; Diekert, G. *Scientific Reports* **2015**, *5*, 13794.
- (104) Neumann, A.; Wohlfarth, G.; Diekert, G. *Journal of Bacteriology* **1998**, *180*, 4140–4145.
- (105) Tsukagoshi, N.; Ezaki, S.; Uenaka, T.; Suzuki, N.; Kurane, R. *Applied Microbiology and Biotechnology* **2006**, *69*, 543–553.
- (106) Bommer, M.; Kunze, C.; Fessler, J.; Schubert, T.; Diekert, G.; Dobbek, H. *Science* **2014**, *346*, 455–458.
- (107) Maillard, J.; Willemin, M. S. In *Advances in Microbial Physiology*, Poole, R. K., Ed.; Academic Press: 2019; Vol. 74, pp 191–238.
- (108) Reinhold, A.; Westermann, M.; Seifert, J. *Applied and Environmental Microbiology* **2012**, *78*, 8025–32.
- (109) Perez-Riverol, Y. et al. *Nucleic Acids Research* **2019**, *47*, D442–D450.
- (110) Padilla-Crespo, E.; Yan, J.; Swift, C.; Wagner, D. D.; Chourey, K.; Hettich, R. L.; Ritalahti, K. M.; Löffler, F. E. *Applied and Environmental Microbiology* **2014**, *80*, 808–818.
- (111) Mukherjee, K.; Bowman, K. S.; Rainey, F. A.; Siddaramappa, S.; Challacombe, J. F.; Moe, W. M. *FEMS Microbiology Letters* **2014**, *354*, 111–118.
- (112) Marzorati, M.; Ferrà, F. d.; Raemdonck, H. V.; Borin, S.; Alliffranchini, E.; Carpani, G.; Serbolisca, L.; Verstraete, W.; Boon, N.; Daffonchio, D. *Applied Environmental Microbiology* **2007**, *73*, 2990–2999.
- (113) Esken, J.; Goris, T.; Gadkari, J.; Bischler, T.; Förstner, K. U.; Sharma, C. M.; Diekert, G.; Schubert, T. *MicrobiologyOpen* **2020**, *9*, e1138.
- (114) Trinquier, A.; Durand, S.; Braun, F.; Condon, C. *Biochimica et Biophysica Acta (BBA) - Gene Regulatory Mechanisms* **2020**, *1863*, 194505.
- (115) Liu, Y.; Beyer, A.; Aebersold, R. *Cell* **2016**, *165*, 535–550.
- (116) Tang, S.; Edwards, E. A. *Philosophical Transactions of the Royal Society B: Biological Sciences* **2013**, *368*, 20120318.

- (117) Kruse, T.; van de Pas, B. A.; Atteia, A.; Krab, K.; Hagen, W. R.; Goodwin, L.; Chain, P.; Boeren, S.; Maphosa, F.; Schraa, G.; de Vos, W. M.; van der Oost, J.; Smidt, H.; Stams, A. J. M. *Journal of Bacteriology* **2015**, 197, ed. by Metcalf, W. W., 893–904.
- (118) Jugder, B.-E.; Ertan, H.; Wong, Y. K.; Braid, N.; Manefield, M.; Marquis, C. P.; Lee, M. *Environmental Microbiology Reports* **2016**, 8, 814–824.
- (119) Alfán-Guzmán, R.; Ertan, H.; Manefield, M.; Lee, M. *Frontiers in Microbiology* **2017**, 8, 558.
- (120) Kleindienst, S.; Chourey, K.; Chen, G.; Murdoch, R. W.; Higgins, S. A.; Iyer, R.; Campagna, S. R.; Mack, E. E.; Seger, E. S.; Hettich, R. L.; Löffler, F. E. *Applied and Environmental Microbiology* **2019**, DOI: 10.1128/AEM.02768-18.
- (121) Low, A.; Zhao, S.; Rogers, M. J.; Zemb, O.; Lee, M.; He, J.; Manefield, M. *FEMS Microbiology Ecology* **2019**, 95, fiz055.
- (122) Peng, P.; Goris, T.; Lu, Y.; Nijssse, B.; Burrichter, A.; Schleheck, D.; Koehorst, J. J.; Liu, J.; Sipkema, D.; Sinninghe Damste, J. S.; Stams, A. J. M.; Häggblom, M. M.; Smidt, H.; Atashgahi, S. *The ISME Journal* **2020**, 14, 815–827.
- (123) Liu, J.; Adrian, L.; Häggblom, M. M. *Applied and Environmental Microbiology* **2019**, DOI: 10.1128/AEM.02146-19.
- (124) Chen, G.; Jiang, N.; Solis, M. I. V.; Murdoch, F. K.; Murdoch, R. W.; Xie, Y.; Swift, C. M.; Hettich, R. L.; Löffler, F. E. *mBio* **2021**, DOI: 10.1128/mBio.00537-21.
- (125) Wang, S.; Qiu, L.; Liu, X.; Xu, G.; Siegert, M.; Lu, Q.; Juneau, P.; Yu, L.; Liang, D.; He, Z.; Qiu, R. *Biotechnology Advances* **2018**, 36, 1194–1206.
- (126) Schagger, H.; von Jagow, G. *Analytical Biochemistry* **1991**, 199, 223–231.
- (127) Nijtmans, L. G. J.; Henderson, N. S.; Holt, I. J. *Methods* **2002**, 26, 327–334.
- (128) Wittig, I.; Braun, H.-P.; Schagger, H. *Nature Protocols* **2006**, 1, 418–428.
- (129) Schagger, H.; Cramer, W. A.; Vonjagow, G. *Analytical Biochemistry* **1994**, 217, 220–230.
- (130) Hjelmeland, L. M. In *Methods in Enzymology*, Deutscher, M. P., Ed.; Guide to Protein Purification, Vol. 182; Academic Press: 1990, pp 253–264.
- (131) Schneider, E.; Altendorf, K. *Microbiol. Rev.* **1987**, 51, 21.
- (132) Cimmino, L.; Schmid, A. W.; Holliger, C.; Maillard, J. *Frontiers in Microbiology* **2022**, 13.
- (133) Buttet, G. F.; Murray, A. M.; Goris, T.; Burion, M.; Jin, B.; Rolle, M.; Holliger, C.; Maillard, J. *FEMS Microbiology Ecology* **2018**, 94, fyy018.
- (134) Goddard, T. D.; Huang, C. C.; Meng, E. C.; Pettersen, E. F.; Couch, G. S.; Morris, J. H.; Ferlin, T. E. *Protein Science* **2018**, 27, eprint: <https://onlinelibrary.wiley.com/doi/pdf/10.1002/pro.3235>, 14–25.
- (135) Kristoffersen, S. M.; Haase, C.; Weil, M. R.; Passalacqua, K. D.; Niazi, F.; Hutchison, S. K.; Desany, B.; Kolstø, A.-B.; Tourasse, N. J.; Read, T. D.; Økstad, O. *Genome Biology* **2012**, 13, R30.

## BIBLIOGRAPHY

---

- (136) Voigt, F.; Gerbracht, J. V.; Boehm, V.; Horvathova, I.; Eglinger, J.; Chao, J. A.; Gehring, N. H. *Nature Protocols* **2019**, *14*, 1603–1633.
- (137) Castanié-Cornet, M.-P.; Bruel, N.; Genevaux, P. *Biochimica et Biophysica Acta (BBA) - Molecular Cell Research* **2014**, *1843*, 1442–1456.
- (138) Seydlová, G.; Halada, P.; Fišer, R.; Toman, O.; Ulrych, A.; Svobodová, J. *Journal of Applied Microbiology* **2012**, *112*, 765–774.
- (139) Schubert, T.; Diekert, G. In *Organohalide-Respiring Bacteria*, Adrian, L., Löffler, F. E., Eds.; Springer Berlin Heidelberg: Berlin, Heidelberg, 2016, pp 397–427.
- (140) Duarte, A.; Barbosa, A.; Ferreira, D.; Manteigas, G.; Domingos, R.; Pereira, I. *Biochimica et Biophysica Acta - Bioenergetics* **2021**, *1862*, DOI: 10.1016/j.bbabi.2021.148416.

## CONTACT ME AT



Ch. des Clochetons 29,  
Lausanne, Switzerland 1004



+41-0779696473



lore.cimmino@gmail.com



/lorenzocimmino88

## TECHNICAL SKILLS

- Microbiology (7 y.)
- Biochemistry (5 y.)
- Molecular biology (5 y.)
- Enzymology (3 y.)
- Microsoft office | Bioinformatics tools
- USP/DSP Bioprocessing (bacteria)

## SOFT SKILLS

Excellent verbal and written communication

Proven ability to collaborate

Flexible and adaptable to changes, willing to accept new and challenging responsibilities

## LANGUAGES

Italian	Mother tongue
English	Level C2
French	Level B2
German	Level A2

## INTERESTS



Outdoor activities



Travel to discover new cultures



Watch movies

## AWARDS & CERTIFICATES



Erasmus scholarship (2013/2014)



Course in Management of Innovation and Technology Transfer (TTO, EPFL, 2020)

## CONFERENCES & RESEARCH VISITS



Visiting Researcher, Inês Cardoso Pereira Lab, ITQB University, Lisbon, (2 months)



7th Swiss Microbial Ecology Meeting (2019 Poster)



DehaloCon III – Conference on Anaerobic Reductive Dehalogenation, Rome, Italy (2021, Oral)



Swiss Proteomics Meeting (2019)



Swiss Society of Microbiology - Annual Meeting (Poster, 2018,2019,2021)

# LORENZO CIMMINO

## BIOTECHNOLOGIST

## WORK EXPERIENCE

### Doctoral researcher

Ecole polytechnique Lausanne (EPFL) | Jan 2018 - May 2022

- Conduct study on expression, & characterization of bacterial enzymes for degradation of groundwater toxic compounds.
- Mentor students/technicians in experimental execution and data analysis.
- Establish and coordinate collaborations with (inter)national laboratories.
- 2 publications (1st author): 1 published & 1 in-process  
<https://doi.org/10.3389/fmicb.2022.838026>

### Research assistant

University of Ghent (Ugent) | Jun 2016 - Dec 2017

- Manage interdisciplinary project from UPS (isolation, bioreactors cultivation and harvest) to DSP bioprocessing (protein characterization) of piezophilic oil-degrading bacteria.
- Author of SOPs, protocols, reports and grant proposals.
- Publication (1st co-author):  
<https://doi.org/10.1093/femsec/fiaa097>

### M. Sc. Intern

Norwegian University Sc. & Tech. (NTNU) | Aug 2013 - Dec 2014

- In vitro molecular screening of 1400 psychrophilic bacteria to identify the genes coding for oil degrading enzymes.
- Publication (co-author):  
<https://doi.org/10.1186/s12864-016-2445-4>

## EDUCATIONAL HISTORY

### Ph.D. in Chemical engineering

Ecole polytechnique Lausanne (EPFL) | Jan 2018 - May 2022

- Major in Biochemistry and Protein science.

### M.Sc., Industrial Biotechnology (with honor)

Tor Vergata University of Rome | Sept 2012 - Jun 2015

- Major in Environmental and Industrial Microbiology.

### B.Sc. Biotechnology

Tor Vergata University of Rome | Sept 2009 - May 2012

- Major in Chemistry, Molecular biology and Biotechnology.